RECOVERY OF VALUES FROM THE RED MUD BY METALLOTHERMIC PROCESS

A THESIS

submitted in fulfilment of the
requirements for the award of the degree
of
DOCTOR OF PHILOSOPHY
in
METALLURGICAL ENGINEERING

By

DEVENDRA PURI

DEPARTMENT OF METALLURGICAL ENGINEERING
UNIVERSITY OF ROORKEE
ROORKEE-247667 (INDIA)

MARCH, 1993

SYNOPSIS

Red mud which is separated from bauxite as clayey waste material from the Bayer process of alumina production furnishes appreciably high quantitative figure of its generation as is evident from the fact that 2.5 tonnes of red mud is generated for every tonne of aluminium metal produced. With the sharply growing demand of aluminium metal, the expected world production estimate of 60 million tonnes per year of alumina upto 2000 AD, is sufficient to prove the future nuiscence regarding the disposal of extremely huge quantities of this solid waste. As a consequence, problems are that of land cost and storage, and pollution in the sense that despite using best available design and operating techniques, the mill water flowing along with it carries polluting substances. Extensive studies have been carried out but no work has been said to be successful regarding its disposal. With this view, in the present investigation, it has been considered that converting it to some useful product by taking the benefit of its mineralogy, will not only solve its disposal problem but will also enable conservation of rapidly depleting mineral resources.

Red muds have been reported to consist of Fe_2O_3, TiO_2 as major constituents along with several minor and trace quantities of oxides of numerous elements. Indian red muds are known for dominant presence of Fe_2O_3 and an appreciable amount of TiO_2 (18-22%). Extraction of titanium alone is difficult due to its highly reactive nature. However its extraction can be

possible in the presence of solvent iron. Titanium forms solid solution with iron thus lowering its own activity. This solid solution can be defined in terms of ferrotitanium. In the present investigation, the same feature has been utilized. The idea is that, the red mud when treated aluminothermically, Fe_2O_3 and TiO_2 both are reduced along with the several other trace constituents and form a ferroalloy which is basically ferrotitanium. Thermodynamic aspects and heat effects of the reduction reaction have been described to be promising for an efficient slag-metal separation.

Reactors of different shapes and sizes have been reported to be used by various investigators. However, no systematic study has been reported about the effect of reactor geometry on the yield or recovery of the alloy. In the present study, this aspect has also been included which may be considered applicable to all aluminothermic reduction processes.

The present st herefore, been made on the possibility of the produc ferroalloy which is basically ferrotitanium by the ope ermic reduction of red mud. The entire thesis has been divided into following seven chapters.

Chapter 1 deals with the basic information about the generation of red mud in Bayer Process and its mineralogy. The problems regarding its disposal and resulting environmental hazards have been briefly taken up followed by brief introduction of the worked up topic.

Chapter 2 deals with a critical review of the work carried out by various investigators and some basic principles

and information, as given in text books relevant to the topic. Starting from the mode and chemistry of red mud generation in Bayer process, discussions have been made about red mud disposal and associated problems, physicochemical and mineralogical details, possible applications etc. To emphasize the aluminothermic application of red mud, the related theory has been discussed with a bit elaboration.

How the selected information from literature led to the present investigation, is the matter of discussion of the chapter 3. Red mud, due to presence of appreciable amounts of Fe_2O_3 and TiO_2, may be considered equivalent to lean illmenite ore and hence it is possible to produce ferrotitanium by the aluminothermic reduction of red mud by creating favourable thermodynamic conditions and heat effects. The basic plan of the study includes the effects of following parameters to be investigated in appropriate couples on the recovery values and composition of the alloy ; (i) Amount of aluminium powder (reductant), (ii) Particle size of aluminium powder, (iii) Particle size of red mud, (iv) Scale of production, (v) Flux additions (Lime,Fluorspar and Magnesia), (vi) Booster addition ($KClO_3$ and KNO_3), (vii) Preheating of the charge (temperature), (viii) Preheating of the charge (time), (ix) Reactor geometry (Defined in terms of h/d ratio)

Chapter 4 deals with the methodology adopted for experimentation as well as basic calculations.

In chapter 5 findings of investigation in respect of recovery and composition of the alloy produced, have been

discussed based on basic principles of aluminothermy, established facts and/or some other possible ways.

Chapter 6 presents the conclusions of this investigation. The present study has shown up the feasibility of production of a metallic button consisting chiefly of Fe,Ti,Si, and Al by the aluminothermic reduction of red mud. The process, suffered inadequate in situ heat liberation which could be compensated partly by preheating and booster additions to the charge and partly by proper fluxing. Excess aluminium powder over stoichiometric amount is necessary which in turn, affects the yield or recovery of the alloy in increasing fashion to a certain maximum value but carries more retained aluminium in the alloy. Good results have been found out when red mud particles are bigger than aluminium particles the difference being not beyond a maximum level.

It is also concluded that for a given reactor geometry, the yield of the alloy increases to a maximum level with the increase in the scale of production. In order to go beyond this maximum level of production maintaining the yield or recovery of alloy, the geometry of the reactor must be changed.

Chapter 7 includes a few suggestions about the more work, that seems could be done as an extension to this work.

CONTENTS

LIST OF TABLES

LIST OF FIGURES

NOMENCLATURE

RM	Red Mud.
OR	Overall Recovery.
PS	Particle Size.
Al	Aluminium Powder,Aluminium.
ΔG^{O}	Standard Free Energy Change.
a	Activity.
h	Height in charge column in the reactor.
d	Top diameter of the charge column in the reactor.
D_1	Bottom diameter (inner) of the reactor.
D_2	Top diameter (inner) of the reactor.
R	A parameter specifying reactor geometry.
K	Equillibrium constant of reaction.
Temp.	Temperature.
Wt.	Weight.

CHAPTER - 1

INTRODUTION

Red mud is an alkaline fine clayish waste residue of the Bayer process of alumina production. The purpose of the Bayer process is to separate the Al_2O_3 content of bauxite from the accompanying contaminants. It consists essentially in digesting the crushed and powdered bauxite with strong caustic soda solution at a temperature upto $240^{o}C$. The reaction is performed in autoclaves under a pressure of 5 to 25 atmospheres. Such an autoclave boiling of bauxite dissolves alumina yielding aluminate liquor and an insoluble residue called 'Red Mud' consisting of iron oxides, silica, and titania along with some insoluble alumina,as major constituents. The red mud is separated from the liquor by precipitation and filteration.

Before disposing of the red mud waste, it is usually treated in a counter-current decantation circuit to recover valuable caustic soda and alumina. The red mud is finally discarded by pumping the under flow of the last mud washer decanter or as a pulped filter cake to an impounded disposal site. Experiences have shown that it is very impossible to have a perfect separation of red mud from the liquor despite using best available design and operating techniques. Consequently, the mill water flowing along with the red mud contains polluting substances.

The red mud contains caustic of the order of 8 to 10 gms per litre and even after subjecting it to hydrothermal

treatment with lime to recover caustic, appreciable amount of caustic remains in the red mud. At present, in Indian aluminium industry, the normal practice done with red mud disposal is impoundment in mud lakes near the plant sites which can pose serious threat to the environment. The caustic of the red mud gets leached by rain water and pollute ground water reservoirs. Moreover, the 'as spread around' red mud is aesthetically unpleasant and possibilities of skin diseases due to dust emission from the disposal sites, can also not be ignored. Some countries, however, followed the practice of dumping this solid pollutant into sea, which has also not been considered advisable keeping in view the marine pollution and damage to marine life.

The red mud as a waste product furnishes an appreciably high quantitative figure of its generation.100 tonnes of bauxite produces nearly 45 tonnes of red mud and nearly 2.5 tonnes of red mud is generated for every tonne of aluminium produced. Obviously the rate of generation of red mud will run parallel 2.5 times to the rate of production of aluminium metal. Due to a sharp increase in the demand the total world production of aluminium metal has grown from less than a million tonne in 1940 to over 16 million tonnes per year now, and it is estimated that it will reach a level of 60 million tonnes per year by 2000 AD, which indicates that extremely huge quantities of red mud have to be disposed of in the future. In India also, with the projected, expansion of alumina production, it has been estimated that over 1.5 million tonnes of red mud has to be disposed of annually in the running decade as compared to 0.5 million tonne per year in

the last decade. In other words, the quantities of red mud generated will keep on increasing in future and will present a tough and challenging task to the environmentalists.

Although the problem of red mud is as old as Bayer process itself, it has been the pin point of R and D activities for the last 2-3 decades to find out its possible applications. In India also this idea was appreciated but in late seventies and now many environmental bodies and aluminium companies are showing interest and looking for its promising results.

A good solution could be the utilization of this solid waste pollutant directly or by converting it to some useful product. Such an endeavour would not only solve its disposal problem but also enable conservation of rapidly depleting mineral resources.

Out of the numerous efforts made in this direction, the extraction of iron from the red mud, has received wide appreciation in the countries which have big alumina refineries but no steel industry to seak of. It is well known that red muds contain a significant amount of iron oxides; hence possibilities of solid state reduction of red muds by carbon or gaseous reducing agents and reduction smelting in blast/electric/low shaft furnace, were established. The former approach, in which after reduction treatment, the iron is separated from the gangue generally by magnetic separation, was not very successful. Smelting technology appeared to have been standardised on a bench to pilot plant scale in several countries including the U.S.A.,USSR, Germany, Yugoslavia, and Hungary. The major break

through in the reduction smelting approach was achieved by McDowell-Wellman Engineering Company (Ohio, USA), who developed the process for the production of steel from red mud, on a semi-industrial scale. The process comprised pelletising the red mud with coal and flux, sintering cum prereduction of pellets in a modified Dwight-Lloyd Sealed Circular Machine,smelting in a submerged arc furnace and finally oxygen blowing of the resulting pig iron in L.D. converter. The steel made in this way was found to be suitable for structural purposes and did not present any rolling problem. The technical and economic aspects of the process have been described to be extremely encouraging to those countries which are poor in iron resources.

Indian red muds are known for the presence of an appreciable amount (15-22%) of titania which presents a promising attraction in the field of the production of ferrotitanium. As is well known that recovery of titanium alone from red mud (titania content) does not bear significant economic as well as commercial viability. The reason is two fold; firstly the red mud is not as rich with respect to titania as it should be, for the easy and economic separation of titania from other constituents of red mud, secondly the production of titanium metal from titania itself is very costly operation due its very high affinity for oxygen, high temperature requirements and a strict device for controlling the reactor atmosphere. An outstanding property of titanium is that it forms solid solution with iron, thus, lowering its activity. This solid solution, in the form of ferro-titanium may be used as a carrier of titanium to steel

melts for deoxidation as well as quality steel making.

In the present work, the above mentioned feature of the titanium has been utilized. Red mud when treated aluminothermically, Fe_2O_3 and TiO_2 both are reduced along with some trace constituents and form a ferro-alloy which is basically ferro-titanium. Thermodynamically and kinetically the reaction is promising and by creating better thermal effects it is possible to produce a large amount of heat necessary for slag-metal separation.

Conducting open aluminothermic reduction of red mud, possibilities have been searched out to produce a ferro alloy which may be basically ferrotitanium by studying those factors which directly or indirectly, may influence the thermodynamics, kinetics, physical chemistry as well as thermochemistry of the process. The major factors which have been studied in this regard include particle size of charge constituents, scale of production, amount of reductant, flux addition, extraneous heating factors etc. Moreover, the role of reactor geometry which signifies design aspect of the reactor has also been taken up and results obtained in this direction are expected to be equally valid for other aluminothermic reduction processes.

It is hoped that the results would provide useful information and add some more steps not only in the area of red mud utilization but in all the cases pertaining to aluminothermal preparation of metals and alloys.

CHAPTER - 2

LITERATURE REVIEW

2.1 BAYER PROCESS

Bayer process is the source process of red mud generation. Virtually all of the commercial production of alumina today is still carried out by this process, although it has been modified over the years for the treatment of specific types of bauxite [1]. The process is based on the fact that the solubility of aluminium hydrate in caustic soda solution varies with temperature and concentration. The process involves digestion of ground and powdered bauxite in caustic soda solution (150-350 gm/litre Na_2O) in the temperature range 150-220^{o}C under a pressure of 5-25 atmosphere. This treatment dissolves most of the alumina. For the trihydrate bauxite the whole process can be represented by the following chemical reaction :

$$Al_2O_3.3H_2O + \text{impurities} + 2NaOH \longrightarrow 2NaAlO_2 + 4H_2O + \text{"red mud"}$$

Solution of monohydrate of European bauxites follow the reaction ;

$$Al_2O_3.H_2O + \text{impurities} + 2NaOH \longrightarrow 2NaAlO_2 + 2HO_2 + \text{"red mud"}$$

The liquor from the Bayer process cooled a little below 100^{o}C [2] and completely depressurised, is next taken to the settling and clarification section where red mud is deposited in settling tanks and is removed. Any remaining red mud in the

liquor is eliminated by a series of washers where it is confronted with a counter-current flow of hot water. In the final stage of clarification, the liquor is filtered through a series of filters. The filterate obtained is a clear solution of sodium aluminate. Residue left behind after filteration consists mainly of ferric hydroxide, silica and alumina.

A lower limit of temperature has been suggested [2] at which the digestion and subsequent processing can be carried out. At the temperature below this limit, aluminium hydroxide may precipitate during clarification leading to a loss of alumina. For efficient operation, the water is maintained at a temperature as close to the boiling point as possible.

In order to precipitate the pure alumina hydrate, the clarified liquor or filterate is cooled below the critical temperature required for precipitation [2]. Very fine freshly prepared aluminium hydroxide is added to the liquor to make available nuclei in order to accelerate the precipitation of $Al(OH)_3$. This mixture is stirred for 30-40 hours [1] to allow the hydrate crystals to grow. Caustic soda meanwhile is regenerated according to the reactions.

$$2NaAlO_2 + 4H_2O \longrightarrow Al_2O_3.3H_2O + 2NaOH$$

$$2NaAlO_2 + 2H_2O \longrightarrow Al_2O_3.\ H_2O + 2NaOH$$

These reactions are reverse of those reactions which caused the solution of impure alumina trihydrate or monohydrate in digestion stage. This process causes about 50-60 % [1] of the alumina

hydrate to dissociate from the soda and precipitate out as crystals. The precipitate is separated from the liquor in a series of thickeners. The product $Al_2O_3.3H_2O$ is finally calcined in a rotary kiln at about 1200^oC to produce anhydrous Al_2O_3.

A simplified flow sheet of the Bayer process as carried out commercially is given in Fig.2.1.

The bauxite used in Bayer process usually contains 40-60 % Al_2O_3. The quality of bauxite is evaluated in terms of Al_2O_3 content and its mineralogical form, gibbsitic bauxite being preferred. Tab.2.1 gives an idea about the chemical compositions and mineralogical forms of Al_2O_3 present in some important world bauxites. Besides, account is taken of silicon module or the ratio of Al_2O_3 and SiO_2 percentage which should be as high as possible. Depending upon the type and origin, bauxite often contains iron oxides, SiO_2, TiO_2 and a large number of impurities in smaller amounts frequently made of oxides of a number of elements like Vanadium, Gallium, Phosphorous etc and organic as well as inorganic compounds. A large part of these undesirable impurities are removed as "red mud" while another part of the impurities goes into solution in digestion process.

2.2 FORMATION OF RED MUD

The insoluble residue of the Bayer process forms 'red mud' so called due to its reddish brown colour which it owes to the dominant presence of iron oxides . Iron oxides fail to react with alkali and remain in the red mud. Geothite (FeO(OH)), however, has been described [1] to be least desirable iron

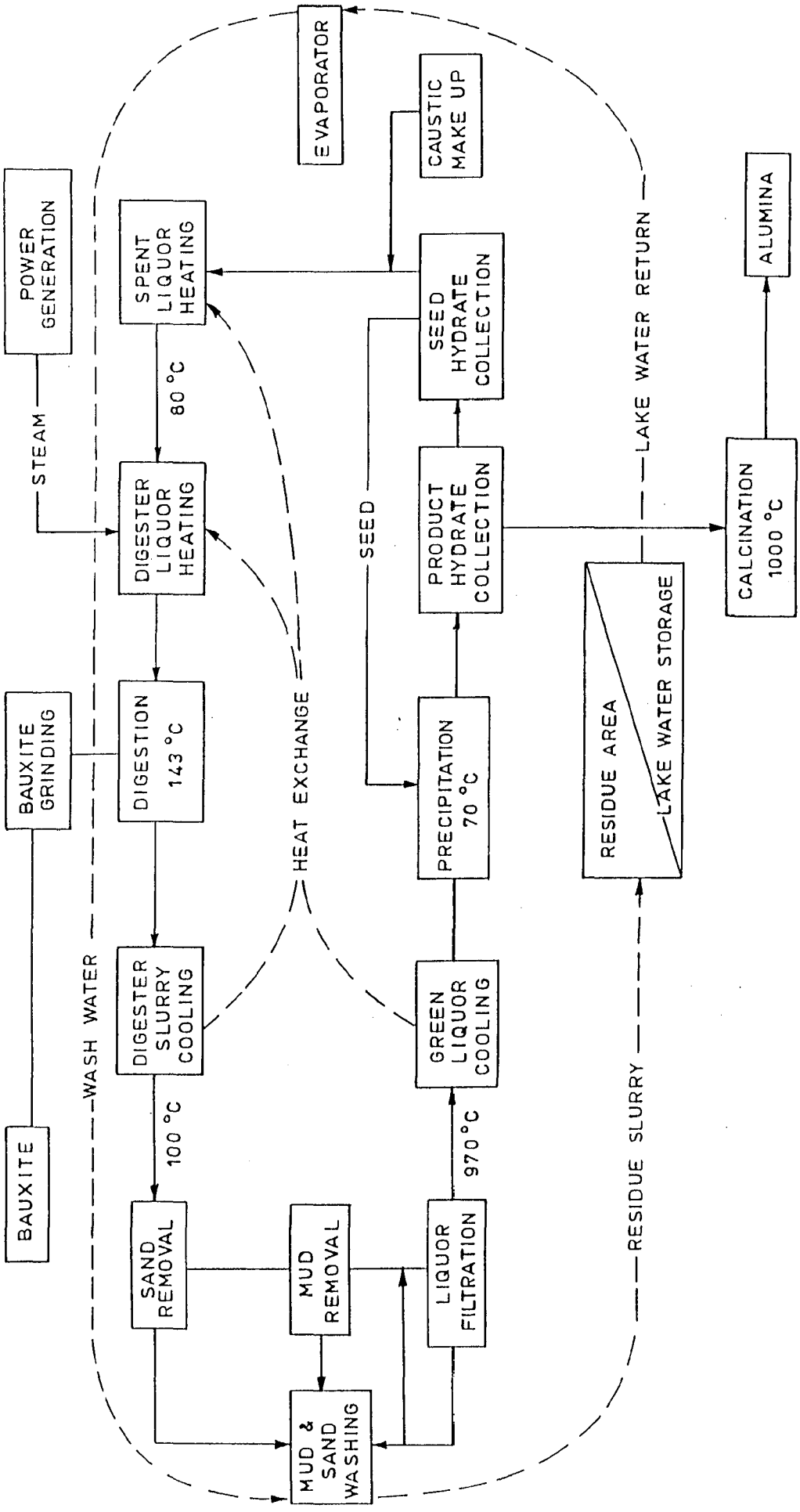

Fig. 2.1 Flow Sheet of the Bayer Process [1]

Table.2.1 Chemical composition and mineralogical forms of Al_2O_3 of some some world bauxite deposits [1].

Country and Location of Deposit	% Al_2O_3	% SiO_2	% Fe_2O_3	% TiO_2	% LOI	Mineral form of Al_2O_3
Australia						Gibbsite(minor boehmite)
(a) Cape York	52-60	2-10	5-13	2.1-3.1	21-29	
(b) Gove	48	3-4	17	3-4	26	
(c) Darling Ranges	30-48	-	-	-	-	
(d) Kimberley.	47-50	2.5-3.5	-	-	-	
Brazil						Gibbsite
(a) Trombetas Nodular	47.1	7.1	8.2	1.3	2.7.9	
(b) Trombetas Massive	49.9	4.8	9.3	1.4	2.8.6	
(c) Minas Gerais	55-59	1.6-5.6	6.9-9.6	1.1-2.0	25-30	
China	50-70	9-15	1-13	2	-	Diaspore/boehmite
France	55-70	3-16	4-25	2-3.5	-	Boehmite (some gibbsite and diaspore)
Ghana						Gibbsite
(a) Awaso	48-61	0.4-2.4	4-22	0.6-2.1	26-33	
(b) Kibi	32-60	0.3-2.9	6-45	2.0-6.2	13-30	
(c) Nyinahin	41-63	0.3-3.1	1.2-30.9	1.5-5.3	20-29	
Guyana	51-61	4-6	1-8	2-3	25-32	Gibbsite
Guinea						Gibbsite
(a) Fria	48	2.5	21	2.2	25	
(b) Sangaredi	60-61	0.3-0.7	2-4	3-5	30	
Hungary	50-60	1-8	15-20	2-3	13-20	Boehmite/Gibbsite/diaspore
India	45-60	1-5	3-20	5-10	22-27	Gibbsite

mineral in favour of Bayer process because of possible loss of aluminium oxide embedded in its lattice.

The silica in bauxite has been described [1,3] to exist in two forms; reactive silica which occurs in combination with silicate minerals (usually clay minerals) and non-reactive silica which is crystalline quartz. The non-reactive silica joins the red mud as such without the losses of alumina and caustic [1] in the course of digestion process. The reactive silica is removed by the formation of insoluble sodium aluminium silicate (desilication) according to the following chemical reactions [1,3];

$$5(Al_2O_3.2SiO_2.2H_2O) + Al_2O_3.3H_2O + 12\ NaOH \longrightarrow 2(3Na_2O.3Al_2O_3.5SiO_2.5H_2O) + 9H_2O$$

$$5(Al_2O_3.2SiO_2.2H_2O) + Al_2O_3.H_2O + 12NaOH \longrightarrow 2(3Na_2O.3Al_2O_3.5SiO_2.5H_2O) + 7H_2O$$

The silica thus passes out in the red mud causing losses of alumina and caustic. Performance calculations tend to indicate that treatment by Bayer process of bauxites with a silicon module less than 8, much alumina and caustic are lost with the red mud [3].

Bauxites often carry calcium and magnesium carbonates [3] which give soda when treated in autoclave -

$$CaCO_3 + 2NaOH \longrightarrow Ca(OH)_2 + Na_2CO_3$$

$$Mg(CO_3) + 2NaOH \longrightarrow Mg(OH)_2 + Na_2CO_3$$

Soda may build up in liquor from the reaction between alkali and atmospheric carbon dioxide. When the liquors are vaporised, soda settles out as monohydrate crystals which are separated, then turned to alkali by heating together with lime water (causticizing) the alkali is recycled.

$$Na_2CO_3 + Ca(OH)_2 \longrightarrow 2NaOH + CaCO_3$$

Titanium oxide content of bauxite is not attacked by caustic soda. However, owing to addition of lime, titanium chiefly remains as calcium metatitanate $Ca_2TiO_2.nH_2O$ [3]. In some recent investigations, titanium minerals have been found to effect the Bayer process depending on their mineralogical form. A 'brief description in this regard shall be taken up in the later sections.

The impurities like V_2O_5, P_2O_5, CaO etc present in bauxite in small quantities, are partially distributed between the solution of sodium aluminate and red mud.

2.3 DISPOSAL OF RED MUD AND ASSOCIATED PROBLEMS

The main problem in the refining of bauxite to alumina is the disposal of the red mud which is a product of refining process. It is separated from the alumina rich caustic liquor, after filteration and washing operation, subsequently reslurried with water and pumped to a disposal site from which the over flow joins a natural stream. The mill water flowing along with red mud carries polluting substances despite using best available design

and operating techniques [4,5].

Recycling of decanted and clarified mill water for reuse in Bayer process, raises capital investment of impoundment and operating costs especially when red mud settles slowly and large volumes must be held in storage.The environmental problems of the classical decanting mudlakes are well known; such impacts are, dike safety, sludge stability, ground water pollution, dusting, reclamation and aesthetic compatibility with the environment.

The quantity of red mud generated by a specific refinery will depend on the tonnage of aluminium produced and grade and composition of bauxite ore. Mc Leod has estimated that in Western Australia the ratio of red mud to alumina produced can be as high as 3.5:1 although 2:1 is typical [1] and 2.5 tonnes of red mud is generated for every tonne of aluminium produced [6]. The annual generation rate of this solid waste in India has nearly crossed the level of 1.5 million tonnes compared to 0.5 million tonnes as reported in 1979 [6,7]. The mud material is finely divided so that even after years of confinement in a disposal site, the solids will vary from 35 to 65 [8]. Such a material has very little bearing strength. The liquid accompanying the solids, even after effective washing, has pH of 12 or higher and therefore cannot be allowed to enter ground water. DSP in red mud will exchange Na^+ for H^+ in contact with water; thus no reasonable amount of washing will make the material inert.

Although some plants dispose of the red muds by dumping

them into sea, pumping of slurry to nearby storage area is more common. The storage areas consist of ponds which are either natural or man made impoundments. Typically a pond is a large basin formed by daming a natural depression and building earth dykes around it. If possible, the ponds are located in areas where the soil has a low natural permeability [1].

The area of the land needed for the red mud ponds is one of the most environmental issues in the siting of alumina refineries since they are considered aesthetically unpleasant and can result in high dust emissions. The land problem becomes aggravated when the quantity of red mud producted is high. The alumina plant at Burntisland built in 1917 with a capacity of 5000 tonnes per annum, adopted the practice of dumping the waste residue to a lagoon adjacent to the factory. With the steady expansion of the plant, the area was exhausted by 1941 [9]. In each specific case the area used will depend on the years of storage desired, the quantity of red mud generated and the depth of the ponds. At Wagerup (Western Australia), the initial disposal pond was planned to cover 25 hectares for the residue depth of 9 to 10 meters and was planned to last for approximately 5 years,with the initial annual production rate of 500,000 tonnes of alumina [1]. At Worsley, where planned initial annual production level was 1 million tonnes (as reported in 1983) of alumina increasing eventually to 2 million tonnes, two ponds were planned which would cover 521 hectares and 439 hectares respectively; the first pond was planned for a life of 31 years while the second one to last for 30 years, giving a potential

filtered mud storage capacity for the production of 126 million tonnes of alumina.

Once in the ponds the solids settle out of the slurry and form a matrix that traps part of the liquid, the remaining liquid is then recycled and raw materials are recovered. When the storage capacity of one pond is reached, a new pond is brought on stream.

2.3.1 Soil Mechanics of Disposal

Keeping in view the basic principles of soil mechanics for the construction and operation of red mud disposal sites, it is shown that environmentally compatible and cost saving disposal is feasible if proper attention is given to [10].

(a) the physical properties of red mud,

(b) conditioning of the red mud for transport and disposal, and

(c) local site conditions and sites operation.

Discussed below some basic principles applicable to the proper disposal of red mud.

2.3.1.1 Water Content of Red Mud

Over a period of time, the water content of red mud in a storage site decreases as the mud consolidates. The change in water content is accompanied by changes in consistency of the mud from liquid to plastic to semi-solid. The condition of mud as it changes from one consistency to another can be defined

quantitatively by using Atterberg limits. These are arbitrarily assigned indices which can be used to establish the water content of mud at its liquid, plastic limits [11].

In soil science, the water content ω is defined as the ratio, expressed as percentage, of water weight (w_w) to dry weight of solids (w_s);

$$w\ (\%) = \frac{w_w}{w_s} \times 100$$

The aluminium industry usually indicates the water content (w') as the ratio expressed as a percentage, of water weight (w_w) to the total weight of the wet sample (w_t).

$$w'\ (\%) = \frac{w_w}{w_t} \times 100$$

Thus the relation between w' and w is

$$w' = \frac{w}{w + 100} \times 100$$

2.3.1.2. Behaviour of Red Mud During Pipeline Transport

The water soluble alkali content of red mud is significantly reduced by filteration prior to transport of the mud from alumina plant to the disposal site. The water content of the red mud filter cake is usually in the region of W =80%(w'=45%),corresponding to a solids concentration of approximately 870 g/1 [10]. In this condition the red mud, as reported can be pumped up to 2 km. without liquifying additives.

However, mud viscosity must be reduced if it is to be pumped over longer distance. Mud viscosity can be lowered either by adding liquifiers [11,12] or water, the later being more cost saving. Pump efficiency and mud pumpability increases as mud viscosity decreases. The addition of 10% of transport water to filter cake virtually halves the yield value for viscous mud flow (the reference value for describing the viscosity behaviour of red mud). The correlation between yield value and water content, as investigated for a typical Australian red mud, is given in Tab. 2.2.

Table.2.2 Effect of water content on red mud yield value [10].

Water added to red mud cake	Red Mud	
%	Water content(W') %	Yield value N/m^2
0	45	171
10	50	80
20	54	68
30	58	51
40	61	46
50	63	40

These relationships are useful in determining the water content of the red mud slurry to be pumped to a known distance of disposal site.

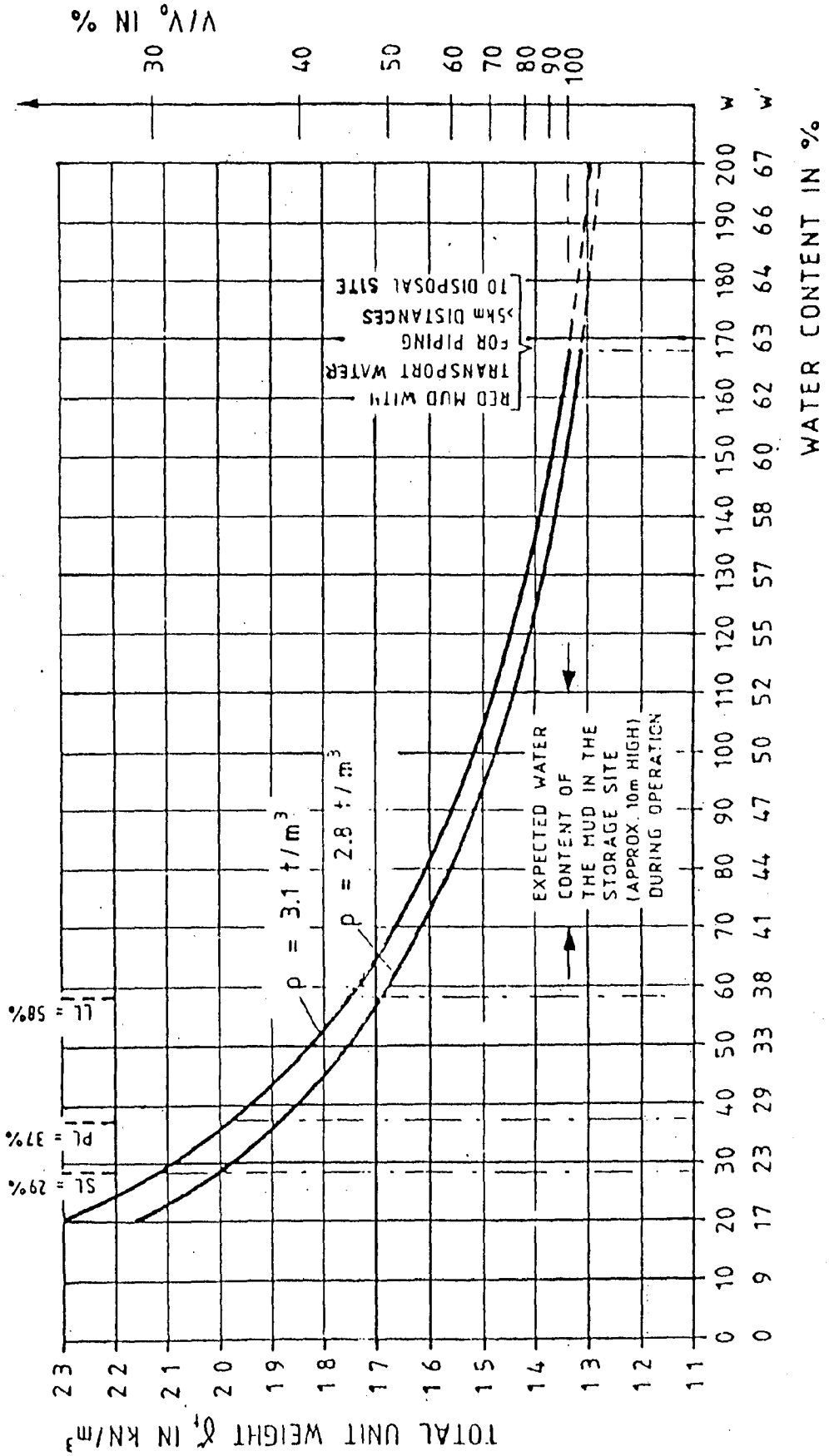

Fig.2.2 Relationship between total unit weight 'γ_t' of red mud and its water content [10]

2.3.1.3. Dewatering and Consolidation Behaviour of Red Mud At Disposal Site

Thorough dewatering and compaction of red mud are the most important factors, since the cost of disposing of red mud is much dependent on the water content of the mud which in turn affects the storage area requirements. Dewatering is carried out in the following fractions [10].

(a) Recovery of surplus transport water and rain water at the disposal site.

(b) Consolidation of red mud under its own weight.

(c) Air-drying of the mud over a prolonged period.

The relationship between total unit weigh γ_t of a red mud mixture and its water content [10] is given in Fig. 2.2 assuming that a red mud suspension of relatively high water content w = 165-170%, is fed to the disposal site. This water content corresponds of a solids concentration of approximately 490 g/l, so that mud can be satisfactorily pumped over a distance of several kilometers.

The figure shows removal of surplus water taking place during transportation of red mud, accounts for a considerable reduction in the mud volume. At the disposal site also, dewatering of red mud continues as it consolidates under its own weight, thereby increasing total unit weight of red mud and decreasing its volume. Such a consolidation accounts for a further reduction in water content of the red mud, irrespective of the transport water content as it arrives at the site. At a water content of 70% the mud remains above its liquid limit

(LL58%). Provided a dam is of adequate stability, a shear resistance value almost zero for the mud is not necessarily a disadvantage [10].

Use of drainage towers, and filter beds below the dam base, raising the height of the disposal site in conjunction with air drying of exposed surface of the mud, have been found to be helpful in accelerating the dewatering and consolidation of red mud, the later being due to the accompanying increase in consolidation stress.

With the application of dewatering principles, VAW [10] were successful in keeping down the water content of the red mud to a value of approximately 40% from a level of 80% (as pumped from the plant) approaching the plastic limit of red mud. The volume in the storage reduced by almost 35% the total unit weight increasing from 16 to 19 KN/m^2 respectively.

Final consolidation stage accounts for a value close to the shrinkage limit which is achieved by the further removal of residual moisture. This stage is characterised by further reduction in volume. This stage,however, is reached after decades.

2.3.1.4 Geo-Technical Behaviour of Red Mud [10,13]

Red mud can be considered as a highly cohessive soil of silt/clay which it owes to its particle size distribution and defined by a water content 'w' at its plastic limit between 20-40% and a plasticity index PI = 10-19. As a result of high degree of cohessiveness, red muds posses low permeability which

enables it to be used as a suitable soil sealant material. Use of permeability coefficient 'k' in Darcy's law has been suggested to characterise the red muds on the basis of permeability. 'k' may be determined by the following expression of Darcy's low

$$Q = K.i.A \ (m^2/s)$$

where Q = Rate of flow

k = Coefficient of permeability

i = Hydraulic gradient $i = \Delta h/L$

Δh = Pressure head

L = Length of the sample

A = Cross sectional area of sample

Lower values of 'k' can be obtained by reducing the water content of the red mud slurry. Thus, consolidated red mud can be used directly as a soil sealant provided 'k' lies within the acceptable range of soil sealants.

In addition to this, red mud starts gaining material strength on further dewatering to lower side. Practically this behaviour has been shown by the red mud, whose water content has been sufficiently reduced by consolidation and/or air drying. These effects, however, can also be achieved by minor lime additions.

The strength of a soil material is best represented by its shear strength which is given by the friction angle ϕ and by cohession C. The shear strength increase steeply with the decrease in water content. Cohession C of the red mud also increases sharply with the lowering of the water content as given

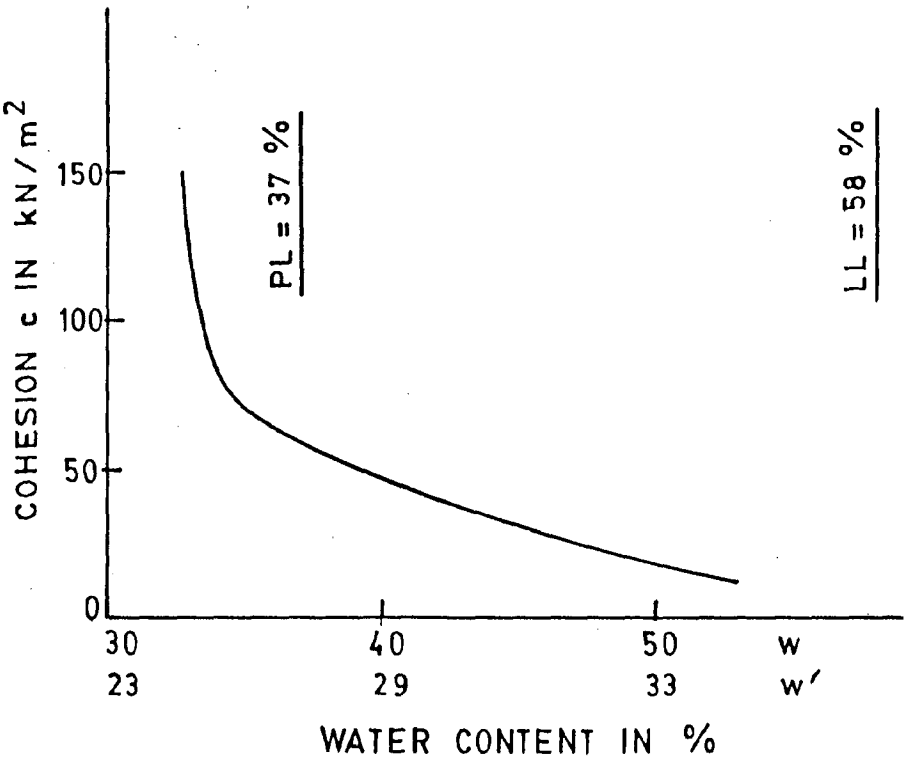

Fig.2.3 : Relationship between cohesion 'C' and water content of red mud [10]

in Fig. 2.3.

2.3.2 Disposal Techniques

Although the problem of disposal of red mud is as old as Bayer process itself, it received far less attention than other type of polluting emissions, in aluminium industries. With a steady and sharp growth in the aluminium production capacity all over the world, the problem was realised worldwide and now many aluminium companies and government agencies are looking worried to search out an economic and environmentally compatible solution for the disposal of large quantities of this solid pollutant. It is only in last 2-3 decades that efforts have been made in this direction and there has been a significant spurt in such R and D activities. Investigations [10] have shown that the acceptability of red mud disposal methods to environmentalists should be evaluated independently of the water content of the red mud disposal. Important factor is the rate of dewatering and consolidation of muds both of which should be as rapid as possible. In other words, the most appropriate disposal technique varies according to local conditions and site operation.

The general way to treat red mud has been to dewater it to the possible extent which generally meant 35-50% solids depending upon the bauxite concerned and pump it to a pond near the plant. After settling and consolidation, the supernatant liquid could be returned to the plant or possibly, giving correct climatic conditions, lost by evaporation. In a number of cases like Alcan in Jamaica, after the capacity of the pond was

exhausted, top soil was added and vegetation was grown. For the red muds with as high as 60% solid content, Guilini [1] developed a 'filtered mud' process for its Ludwigshafen plant in Germany and also used by Martin Marietta in its Virgin Island plant and at the San Ciprian refinery in Spain. The weight of solids is reduced only to 20-40%. The main advantage stated with the filtered mud process is that the mud solidifies and compacts quickly so that within a few days it can be walked on and in a few weeks will bear the weight of heavy earth works equipments. Moreover, with the process the resulting residue has a relatively high resistance to chemical leaching. It can be deposited in small discrete contained areas. The process has been said to be successful in reducing the mud storage requirements compared with the conventional disposal systems.

In the areas where the land was not appropriate, disposal at sea practiced. The British Aluminium company Limited adopted the same practice for its smelter on the Bristol channel at Newport in Wales [14,15]. In this case a ship was loaded at high tide from holding tanks or ponds at plant. The ship then moved downstream with the ebb tide, to a dredged cut, and discharged the slurry. Pechiney [14] are discharging approximately one million tonnes of this sediment per year into the Mediterranean sea. The discharge was into a submarine canyon named cussidaigne (near Marseilles). They investigated that the red mud spread into the deeper part of the canyon and no intoxication of the marine biots was found.

Discussed below some disposal techniques and possible remedies which have been suggested time to time by various investigators working on this issue.

2.3.2.1 Bottom Sealing and Daming the Red Mud Ponds

Use of synthetic membrane layers of compacted clayey soil, or installation of positive cut-off diaphragm walls to bedrock levels, have been suggested to avoid any seepage [1,4,5,10], Most modern systems also include a series of underdrains to collect any seepage and to recycle liquid for reclaimation of raw materials; An observation system of bores may be included to allow for the monitoring of chemical composition of ground water and to check ground water levels.

The physical properties of red mud like particle size distribution, high degree of cohessivity, enable it to be used, under certain conditions, as storage site building material. To prevent alkali contamination of ground water, red mud due to its high clay fraction can also be used as a suitable material for bottom sealing in place of conventional materials like clay and bentonite. To ascertain a desired level of permeability in red mud as suitable for a soil sealant material, the water content of the slurry is reduced to a limit of proper consolidation. Consolidated red mud may directly be used as a sealent provided it possesses the desired level of permeability. Freshly pumped mud, however, has a higher water content and must be stabilised before it can be used as bottom sealing material. VAW and some soil laboratories [10] report to have developed a method in

which small additions of lime (CaO or Ca $(OH)_2$) accounted for the rapid solidification of the mud and an increase in its cohession. They investigated that when red mud from the plant was deposited on the lime-stabilised mud layer, self sealing took place as the mud consolidated. The achievable permeability coefficient for lime stabilized red mud, has been said to be at least 50 times lower than the limits stipulated by the authorities for natural soil sealing materials. A compression load of 75 KN/m^2 obtained in their laboratory tests corresponded in practice to a red mud layer approximately 5 meter thick, the water content of test samples 'w' being 35-40%. Due to inexpensive lime additions, the construction costs were significantly less than the other sealants.

The use of red mud for daming the disposal ponds has also been reported by VAMI. Land requirement is reduced significantly and cost is saved as no other material would be needed. They have estimated that, for a disposal site of 10 meter height with a working volume of 10 million m^3, more than 10% of external building material could be saved by the application of a dam construction system, they developed. The salient features of their dam construction system were, stage by stage building of dam as they are filled, use of consolidated air dried mud from within the site and construction of filter beds at the bottom of all dams. The author, however, suggests that local conditions allow for the better choice of building material but normally choice is made from consolidated red mud, lime stabilised red mud and/or waste material from coal mines.

The above mentioned system for the formation of embankment from the red mud itself could, however, not find success at the Burntisland Alumina plant (now a part of British Alcan Aluminium company) as it suffered from extensive errosion due to damage of storm water. As a remedy, they [9] investigated, that the use of a natural depression in the topography and the utilization of burnt oil shale to form retaining embankments together with a controlled dumping procedure could be possible solution from the technical and economic point of view. Such a system has been reported quite suitable for the local conditions pertaining at Burntisland. The plant adopted the same system and all new embankments, as reported, were constructed of spent oil shale with a 3 meter blanket of sand laid across the face of shale which was in contact with the mud. The embankments were some 6 meter high to the west and 14 meter high to the east.

In Germany some residue impoundments with portions of dikes made permeable, thus allowing the residue to drain and the drainage is channelled to water treatment facilities before discharge to the surroundings [8]. An American design [8] lines the impoundment with clay and sometimes with a polymeric membrane, then place drainage tile in a sand bed on top of the lining. Most of the dilute solution used to suspend the residue for pumping is decanted, but a significant fraction drains through deposit. The sand bed is so permeable that there is virtually no hydraulic head on the pond bottom; hence chance of leakage is slight. Drainage also compacts the residue so that more can be deposited on the same pond volume.

In Germany from its Martinswerke plant, Alusuisse is pumping the red mud slurry into a mined out brown coal mine for land reclaimation [14].

2.3.2.2 " Dry Stacking" of Red Mud [4,5,8]

The 'Dry Stacking' of 'Dry Disposal' which has now become a competing technology in the area of red mud disposal, has been adopted by six alumina plants in West Germany, since its conception in Ludwigshafen, West Germany.

The dry Disposal system can be successfully applied when the red mud waste has thixotropic properties and economically acceptable filteration rate. In certain Bayer alumina plants where the red mud is deposited as dewatered filter cake, filteration rate of red mud may vary from a low of 80 $kg/m^2/hr$ to a high of about 200 $kg/m^2/hr$. The drum or disc filter is placed at the end of the existing chain of mud-decanter washers which results in a greater pulp washing efficiency, hence, valuable chemicals can be recovered to a greater extent. Filteration concentrates the residue to perhaps 50% solid, thus imparting it thixotropic characteristics.

Thixotropic filter cake is made free flowing by heavy vibrations and agitations in a reactor. Minor additions of chemicals may be desirable depending on the characteristics of red mud. The aim of this operation is to transform the filter cake into pumpable sludge. The reactor treatment offers a very high drop in apparent viscosity. Generally the red mud has an initial apparent viscosity between 200,000 and 90,000

Water in 1) Precipitation
2) Surface run off
3) Ground water

Water out 4) Evaporation
5) Percolation
6) Seepage

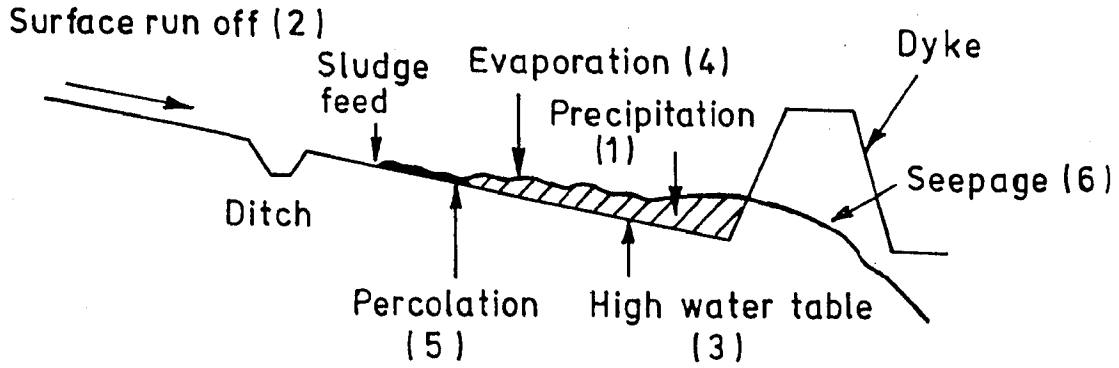

Fig.2.4 : Water balance for a dry waste disposal site.

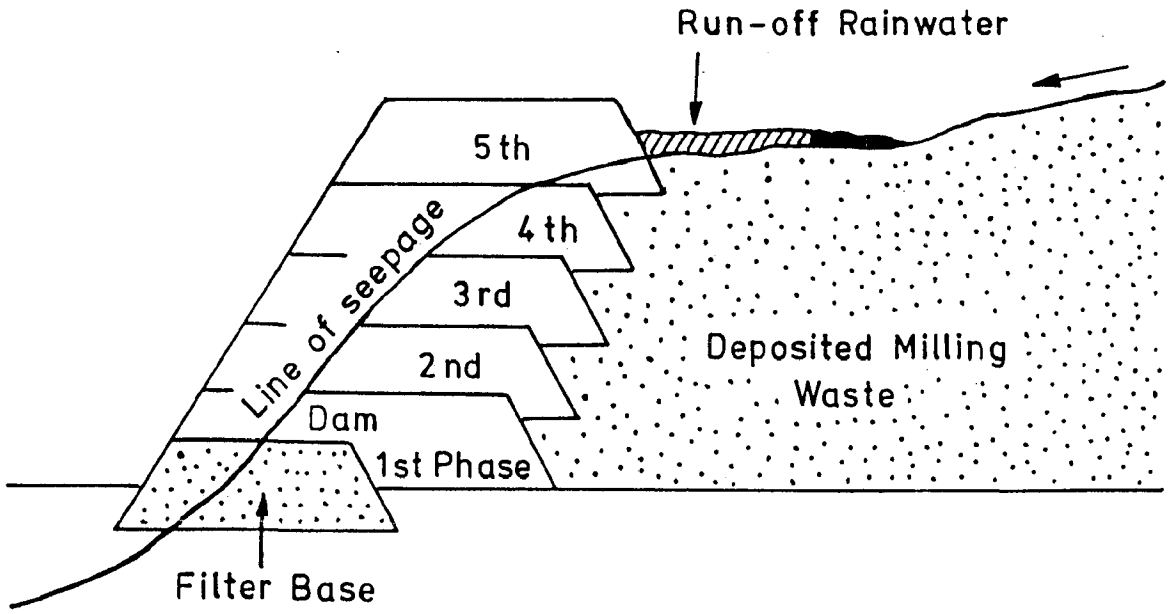

Fig.2.5 : A typical method of removal of precipitation from a dry waste disposal site.

centipoises. The agitation reduces the viscosity by the two orders of magnitude. When the filter reached a desired viscosity, it can be pumped to a disposal site in the agitated state.

Since drum filters are used, no decantation will take place at the disposal site and possibility of percolation of chemicals is largely eliminated. Under these conditions the water balance given in the Fig.2.4 for a dry waste disposal site, shows that only uncontrolled precipitation causes ground water pollution. Use of catchall ditches have been suggested, if the surface run-off is significant. Hence assuming, the location of dry waste disposal site has been properly selected, only uncontrolled rain water can cause the ground water pollution.

Due to extremely low permeability of red mud to water, the treated red mud has ideal soil sealant characteristics, hence precipitation will not penetrate orrepulp the deposited sludge layer and will remain on top free flowing to the lowest area of the impoundment.

Quick removal of rain water is suggested from the surface of the deposited sludge, during heavy and long existing rains to minimise the possibility of any diffusion of chemicals from the surface of deposited sludge into the supernatant rain water.Appropriate rain water removal also promotes deposited sludge to dry out and harden in a relatively short period of time.

In order to remove precipitation from the dry waste disposal site, dike is constructed in parts of permeable material which are not subject to saturation or shear. The Fig.2.5 shows a

typical method of removal of precipitation. The author claims that the seepage of rain water through the permeable dikes does not contain any contaminants under the normal European weather conditions. The ground water samples taken from the immediate vicinity of the existing disposal sites were all non-turbid, colourless and showed a pH value of the ground water taken at some distance from the dry waste disposal site.

As has already been said that heavy and long existing rains may extract, to limited degree, caustic soda from the surface of the deposited sludge. Such a ground water pollution due to surface run-off can be prevented by prompt removal of rain water and using filter base for dam construction, having cation absorption properties. In the regions where heavy tropical rains occur and also when sludge retaining dike is small in relation to a large disposal area, rain-water interceptional ditches have been suggested.

Heavy precipitation from the disposal site can be removed by the use of vertical flood control towers located in the lowest area of the disposal site. The collected rain water if required, may be piped back to the plant C.C.D. circuit.

To keep the dusting under control, the author suggests subdivision of waste impoundment in smaller areas. The mini dikes built for this purpose may consist of dried mud. This also offers stability to the disposal site. By alternatively feeding the smaller impoundment areas, the deposited filter cake sluge dries out and harden in relatively short period of time. For a typical Bayer process red mud, the author reports that the stability of

the dry waste increased markedly after about 30 days and after 4-5 month it became worthwhile for the passage of heavy vehicles without danger.The Tab.2.3 below furnishes some operating data as observed by author for several Bayers dry waste disposal systms. The main advantages as cited by the author [4] are listed as follows -

(i) The minimum quantities of chemicals will be discarded with the washed and filterred mud cake.

(ii) Minimum contact exists between red mud and supporting soil.

(iii) As the treated red mud filter cake has usually excellent soil sealing characteristic, seepage of chemicals into ground water can practically be eliminated.

(iv) The chemicals diffused into supernatant rain water, can be trapped by specific dam design features or where required, by flood control towers, permitting excess rain water to be collected and returned to plant site.

Table.2.3 Typical Operating Data for Several Waste Disposal Systems [4]

Process data	
Solid content of filter feed	20-40% (by wt.)
Filter feed tempr	55-65 ^{o}C
Percent solid in filter cake	55-65% (by wt.)
Waste discarded in tonnes/day	500-1000 tons (dry basis)
Filter capacity kg/m^{2}/hr	80-200
Chemical remnanti in filter cake	0.8% Na_2O (dry basis)
Discharge pressure of disposal pump	max. 100 Bar.
Angle of repose of filter cake material	2-8 degress

2.3.2.3 Red Mud Neutralization

One more way reported [16] to minimize the intensity of pollution of this solid effluent, is to meet the environmental regulation limit of pH as stipulated by the environmental authorities. Such a limit generally lies between 6.5 to 8.5. The investigation showed that it was technically feasible to bring down the pH of red mud slurry from a level of 12 (as pumped) to the limit of environmental regulations by neutralizing red mud slurry with flue gases. Neutralization with oil fired boiler flue gases was tested. The principle is based on the fact that CO_2 makes up 14% of its volume and there is also some SO_2 present. In the course of neutralization the following reactions have been outlined to take place.

$$2\ NaOH + CO_2 \longrightarrow Na_2CO_3 + H_2O$$

$$Na_2\ CO_3 + CO_2 + H_2O \longrightarrow 2NaHCO_3$$

$$2NaOH + SO_2 \longrightarrow Na_2SO_3 + H_2O$$

$$NaOH + SO_2 \longrightarrow NaHSO_3$$

The neutralization was conducted on a pilot plant using a bubbler and a floatation cell. Excerpts from the author's study indicated that neutralization was possible both ways. However, decision to use a bubbler or a floatation cell would be based on the gas availability. If gas generation exceeds the amount required, the bubbler would be preferred. On the other hand use of floatation cell has been suggested if the gas generation rate is close to the requirements for neutralization. In his study on

the Saramenha alumina plant red mud, the author interpreted on the basis of post neutralization pH variation of red mud slurry, that a red mud of pH 12, if neutralized to a pH of 7.5 by this manner, would maintain its pH value within the range 6.5 to 8.5 after disposal to the pond.

2.3.2.4 Rehabilitation of the Disposal Areas

Rehabilitation programmes which are meant to release the land from the useless occupation of mud lakes, have now become an important part of refinery operations parallel to a 'search out' for an improved disposal technique. The success of vegetation, however, is the subject of considerable controversy . Alcoa tried to justify this concept in 1947 with restoration work of one pond, and now as reported [1], the area is able to support pastures, sheep have been grazed and a variety of cereal crops have been established; an older residue site is now used to grow a variety of vegetables. The study was intensified in 1973 at Alcoa's Kwinana refinery and a detailed geotechnical programme [17] was undertaken to investigate the engineering aspects for a long term rehabilitation in the background engineering properties of red mud with respect to strength, permeability, grading and consolidation characteristics. Followings were the major points of study.

(i) allowable bearing pressures for building foundations,

(ii) total and differential settlements beneath structures, road pavements, etc.

(iii) removal of the caustic liquor retained in the lakes.

(iv) earthworks for contouring the site.

The investigations established that the basic engineering parameters of the residue were quite consistent with those accepted for naturally occuring soils. Conventional techniques might be used to determine the in-situ characteristics of red mud, like soil type, shear strength, consolidation characteristics and permeability. Once these parameters established, might be used to provide a preliminary appraisal of the development potential of mud lakes, taking into account foundation bearing pressures, total and differential settlement and the requirement removing caustic liquors stored within the lakes. This work established the feasibility of developing the mud lakes for industrial use without major constraints being placed on development due to the properties of the red mud.

Though numerous methods are being developed in this direction, the success still lies under a question mark. Solymar [18] accepts that the up-to-date storing and complex processing of red mud is still a challenging task. Despite going through an extensive literature on this problem, McGeer [14] has to say "we know that all work has been unsuccessful".

2.4 PHYSICAL AND PHYSICOCHEMICAL PROPERTIES OF RED MUD

2.4.1 Particle Size

Red muds have been described [1,6,19] as fine dispersed systems which are distinctly alkaline with pH varying from 11.5 to 12.5 and composed of a fine fraction (mud) and a relatively coarse fraction (sand). The percentage of these fractions,

Table.2.4 Typical compositions of Australian and Guinean Red Muds [10].

Soil Classification	mm.	% by wt.of red mud	
		Average	variation
Fine Sand	0.06-0.2	4	3.5
Silt	0.002-0.06	42	36-48
Clay	Less than		
	0.002	54	47-60

Table.2.5 Particle size distribution of a Red Mud obtained from Jamaican bauxites [20,21].

Mesh Size	wt.%	Size	Micron	Wt.%
+28	Nil	-35	+23	1.0
-28 + 48	0.1	-23	+12	4.9
-48 + 100	0.4	-12	+ 6	13.1
-100 + 200	1.2	-6	+ 3	39.5
-200 + 270	0.6	-3	+1.5	32.2
-270 + 325	0.4	-1.5	+0.9	5.8
-325 + 35μm	0.8	-	-	-

however, depends on the mineralogy of the processed bauxite. Bauxites with nonreactive silica (quartz) content account for the sandy fraction of red mud. To some extent this also depends on the crushing and grinding operations carried out on processd bauxite. Monohydrate ores, especially with significant amount of diaspore are more difficult to crush and grind because of their high hardness values (diaspore, 6.5 - 7 mhos). The monohydrate bauxites (boehmite and diaspore) have also been observed to posses higher percentage of nonreactive silica than trihydrate bauxites which is indicated in Tab.2.1 On the other hand, the clay content of the red mud depends, to a significant extent, on the mineralogy of iron-oxides and presence of clay minerals (like kaolinite) in the concerned bauxite. Tab.2.4 shows a typical composition of Australian (Wiepa) and Guinean (Boke) red muds with respect to sand and clay fractions, as reported by Lotze [10].

Alcoa's Kwinana Works [17] produces the red mud which is half fine mud (clayey silt) and half sand size material which is indicated on the grading curve given in Fig.2.6, Tab.2.5 presents the particle size distribution [20,21] of red mud obtained from Jamaican bauxites.

The Indian red muds have been found [6,7] to be very fine sized material, bulk of particles being of - 325 mesh size (i.e less than 44 micron size) and a high proportion of these are in colloidal range. Prasad et al.[7] have determined the particle size distribution of HINDALCO red mud (uncausticised) which is presented in Fig. 2.7.

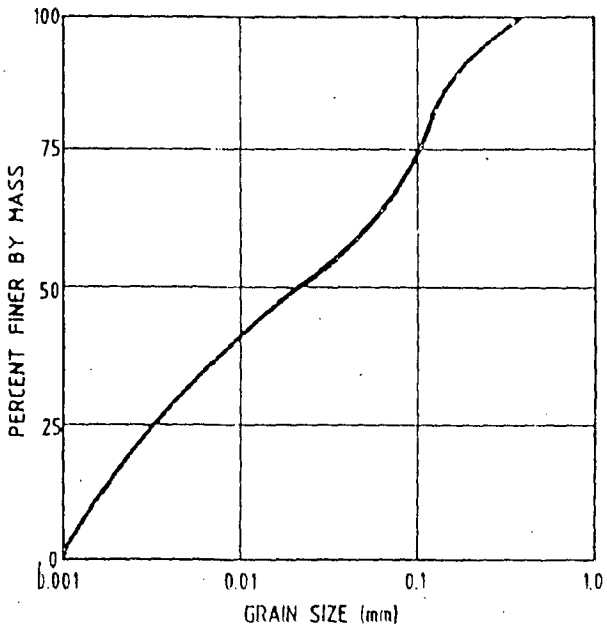

Fig.2.6 Typical grading curve
for red mud [17]

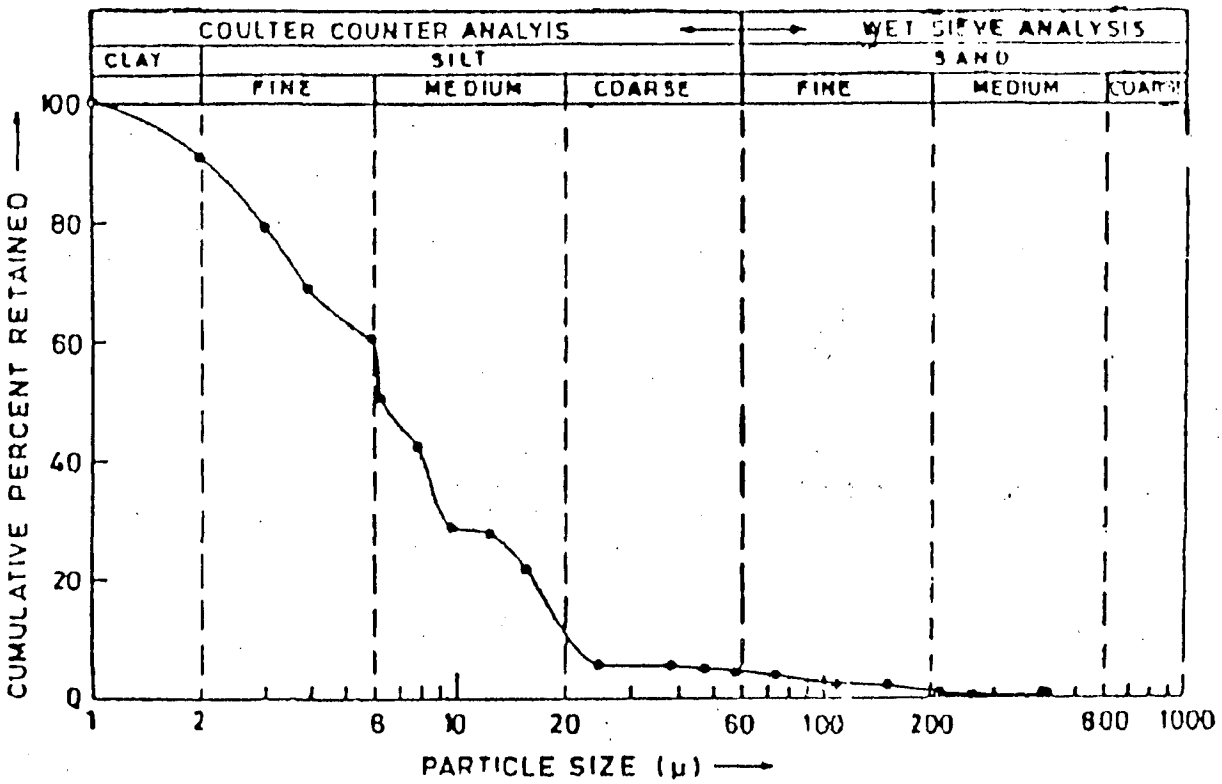

Fig.2.7 : Particle size distribution of uncausticised HINDALCO red mud [7]

2.4.2 Texture

Solymar [22] studied the texture of Soviet and Hungarian red muds using scanning electron microscope. The micrographs helped in recognising the texture of sodium aluminium silicates. However, the effect of mineralogical composition, surface area, crystallinity, goethite and hematite respectively, could not directly be observed although great differences existed from case to case from the technological view point. Author's study revealed that morphology of different sodium aluminium silicates differed at least in part. It has been pointed out that the practical utility of the results may be expected only by means of systematic scanning electron microscope studies.

2.4.3 Specific Surface Area

The knowledge of specific surface area is important in the sense that it leads to helpful conclusions concerning digestibility and suitable particle size to be obtained in grinding, since a relatively high specific surface area that is fairly independent of particle size indicates [22] that grinding finness does not affect or slightly affects the digestibility.

Solymar [22] on his investigation on Soviet and Hungarian bauxites observed that the specific surface area of the red mud formed depended on the temperature of digestion of bauxite, and a decrease in the specific surface area of the red mud was reported with increase in the temperature of digestion. He found the maximum specific surface of area of red muds from

Hungarian bauxites at a digestion temperature of 210^{o}C.

The specific gravity of red muds have been reported to vary between 2.6 to 3.2 depending on composition. Most of the Indian red muds have been characterised [4,5,6,9] to be very fine sized with poor settling characteristics, thixotropic and crack on drying. Prasad and Sharma [7] carried out extensive studies to determine the physical and geotechical properties of HINDALCO red mud. The results of this investigation are summarised on Tab.2.6. Properties of some American red muds [20,21] are shown in Tab.2.7.

Red muds are distinctly alkaline with pH varying from 11.5 to 12.5. Walker et al. [17] carried out in-situ determination of alkalinity of Alcoa's Kwinana refinery mud. The results showed that total alkalinity varied between 10 and 30 g/l over a depth of 16 meters. Since the total alkalinity of the mud at the time of deposition falled in the same range, the authors concluded that no change in concentration or alkalinity occured with time.

On the basis of consolidation behaviour,red muds can be characterised by using Atterberg Limits. Lotze [10] reported the characterisation of Australian and Guinean red muds using Atterberg Limits which is shown in Tab.2.8.In the same investigation, the author observed that the permeability of the red mud slurry which can be expressed by the permeability cofficient 'k' in the Darcy's law, depended on the water content and lower values were obtainable by reducing water content. The study revealed that lime addition prompts lowering of the

Table.2.6 Soil characteristics and geotechnical properties of HINDALCO Red Mud [7].

Property/Test	
1. Specific Gravity (G)	2.88
2. pH	10.60
3. Atterberg's Limits	
(a) Liquid limit %	33.70
(b) Plastic limit %	27.90
(c) Shrinkage limit %	27.90
(d) Plasticity index (P.I.)	5.80
4. Grain Size Distribution (%)	
(a) Clay sizes (<2μm)	9.10
(b) Silt sizes (2-60μm)	85.10
(c) Sand sizes (>60μm)	5.10
5. Compaction And Consolidation Tests	
(a) Optimum Moisture Content (% OMC)	25.60
(b) Max, Dry Density (gm/cc)	1.62
(c) Permeability (K) X 10^{8} cm/sec	3.23
(d) Void Ratio (e) at OMC	1.78
(e) Compression index (C_c)	0.33
(f) Swelling index (C_s) X 10^{2}	2.10
6. Unconfined Compression Test	
(a) Unconfined Compressive Strength (kg/cm^2)	1.95
(b) Shear Strength (Kg/cm^2)	0.98
(c) Consistency	Stiff
7. Triaxial Shear Test	
(a) Cohesion, C(Kg/cm^2)	0.80
(b) Angle of internal friction, ϕ(degree)	25.64
8. California Bearing Ratio Test (soaked)	4.30

Table.2.7 Physical characteristics of some American Red Muds [20,21].

Specific gravity	2.6 - 3.1
pH Value	11.7 - 12.3
Pulp density, gms/cc	1.1 - 1.3
Initial percent solids in mud slurry	7.8 - 35.9
Settling rate cm/hr.	0.05 - 2.96
Percent solids after 24 hrs,settling	25.6 - 55.5

Table.2.8 Characterisation of Red Mud using Atterberg Limit [10].

State depending on water content		Atterberg Limits	Sym-bol	Water Contemt 'ω'of red mud at Atterberg Limit %
Decre-asing water con-tent	Liquid	Liquid Limit	LL	58 ± 8
	Plastic	Plastic Limit	PL	37 ± 7
	Semi-solid	Shrinkage Limit	SL	29 ± 2

permeability due to rapid solidification of the mud and an increase in its cohesion. By this method it was possible to obtain a permeability cofficient as low as 9-10X 10^{-10} m/s. The dependence of the cohesion of red mud on water content, as studied by the author, is indicated in Fig.2.3.

2.4.4 Surface Properties

The stability of red muds suspensions and methods of its upsetting, basically depends on such characteristics as specific surface area dispersion and hydrophilic character.Zavaritskaya et al. [19] studied those characteristics for red muds obtained by degestion of bauxites of different mineralogical and chemical compositions. Since red muds are fine dispersed systems, an electron microscope was used. Degree of polydispersion was found to be different, the gibbsitic bauxite red mud being less polydispersed compared to others.The bulk of red muds obtained from diasporic and boehmitic bauxites, consisted of fine particles of indefinite shape, at the same time there were distinct separate crystals having the shape of regular and irregular quadrangle, and particles of sodium alumino silicate of a relatively equiaxial shape. For crystals of red mud of gibbisitic bauxite, the equiaxial shape of particles was characteristic which corresponded to the shape of sodium alumino silicate crystals formed in alkali-aluminate liquor.

The above investigators also conducted microscopic study of red muds in process of decantation as a function of time to define their structure and ability to aggregate. Red mud of

diasporic bauxite, was more dense and consisted of big aggregates and for the boehmitic bauxite the red mud particle size did not exceed 1 to 1.5 microns and was less dense. For gibbsitic bauxite red muds, presence of separate group of particles was found to be characteristic, as well as chains of different length formed by the particles.

It is known that red mud obtained after treatment of bauxite forms a solvatised rather stable structured system with the dispersion media (aluminate liquor). The fact that the dispersion substance is strong electrolyte as well as lyophilic character of red mud particles and their interaction bring forth different difficulties in the process of thickening. Stability of this system depends on many factors one of which is the hydrophilic character. The measure of the hydrophilic character of the solid matter is the quantity of bonded water. Zavaritskaya and co-workers [19] determined the hydrophilic character of washed red mud in terms of bonded water. The data obtained allowed to some extent to characterise a relation of red mud to water in aluminate liquors. To determine the quantity of bonded water in red muds the refractometric method was used and 10% sacchorose solution was given as indicator.

2.4.5 Washing Characteristics

Red mud washing is necessary to recover the part of caustic which remains adhering with the red mud. In practice counter-current flow system is used for washing of red mud in the settler tank unit. Counter-current flow system is advantageous as

compared to the multistage unidirectional washing system [23].

Washing characteristics of red mud depends on the composition of bauxite and digestion conditions under which the red mud is formed. Difficulties have been observed with red mud obtained from the Indian bauxites in separation and washing. Zambo and Kovacs [24] examined the washability of red mud obtained from Indian bauxites. They encountered difficulties in washing which was attributed to the presence of $TiO_2.H_2O$ gelly. They proposed the formation of $NaHTiO_3$ during the digestion. This compound was reported to be in the form of gelly. This gelatinous precipitate goes into red mud and creates difficulties in separation. In OH^- rich or OH^- ion active solution, $NaHTiO_3$ is quite stable but with decrease in OH^- ion concentration during washing, it hydrolyses as follows :

$$NaHTiO_3 + H_2O \longrightarrow TiO_2.H_2O + NaoH$$

This end product of hydrolysis $TiO_2.H_2O$ is also surface active gelly like precipitate and so can absorb large amount of aluminate solution which indicates use of large amount of water for washing.

Kovacs [25] studied the effect of digestion conditions on the washability of red mud obtained from Indian bauxite. The red mud from lower temperature of digestion was found to fix more Na_2O during washing. It has been attributed to the fact that in digestion at 180^oC with molar ratio of about 2 whereas for higher temperature 210^oC digestion molar ratio was 1.8 and extent of

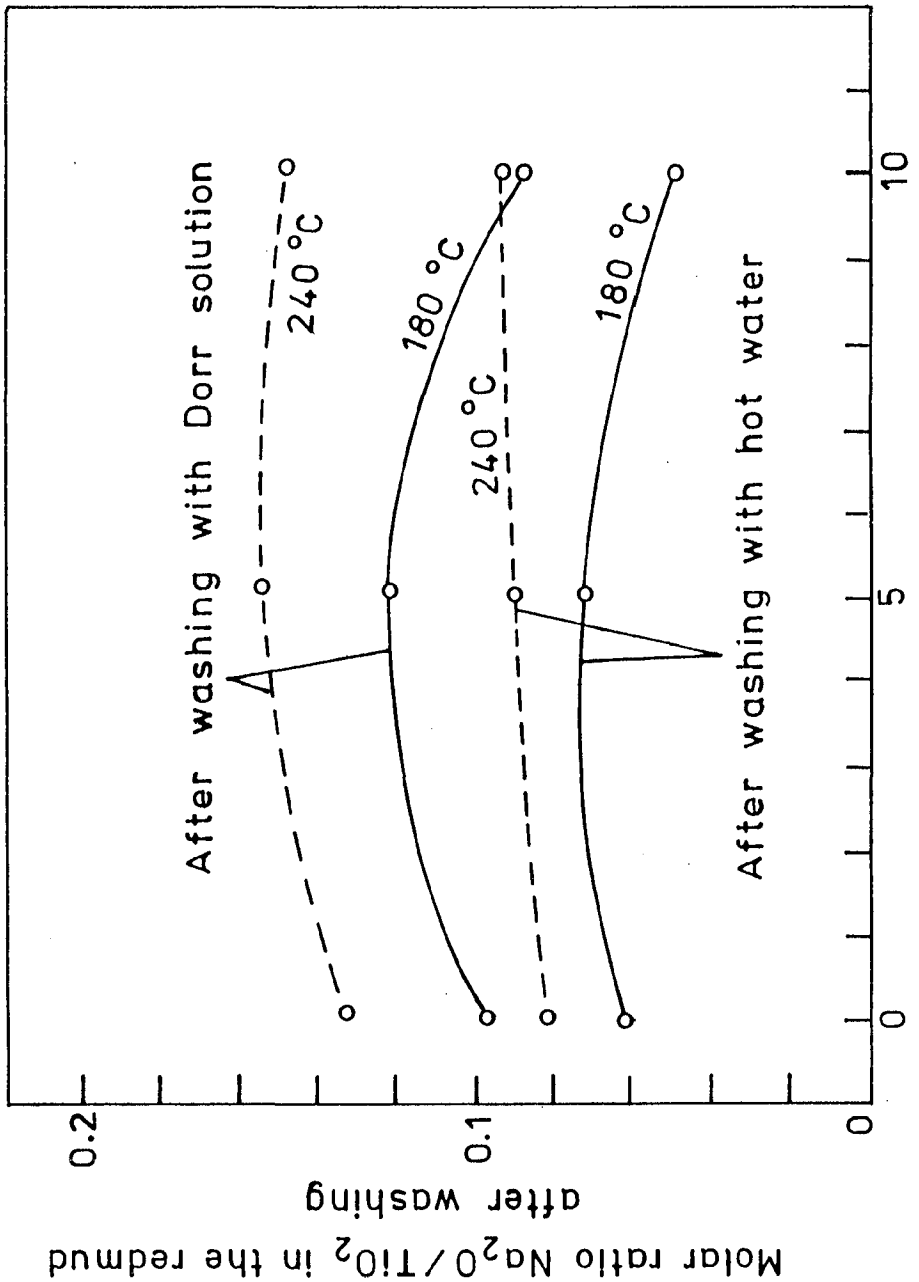

Fig.2.8 : Relationship between Na_2O/TiO_2 molar ratio in the red mud after washing and TiO_2 content during the digestion of an Indian bauxite [26]

digestion of anataze was proportional not only to the digestion temperature but also to the free caustic concentration or the end molar ratio. They concluded that with repeated washing, Na_2O content of red mud can be decreased appreciably.

Solymar et al. [26] investigated the Dorr type washing of red mud from an Indian bauxite. Washing was done in six steps with sodium aluminate solution having composition similar to those existing in actual Dorr type washing practice in alumina plants. Fig.2.8 shows the Na_2O/TiO_2 molar ratio plotted against TiO_2 contents of bauxite for the red muds obtained by digestion at 180°C and 240°C respectively and washing with hot water and also separate washing by the Door type sodium aluminate solution. They observed that the red mud obtained by digestion at 240°C after Dorr type washing, Na_2O/TiO_2 molar ratio was 0.13-0.16 whereas in case of washing with hot water this ratio was 0.08-0.09. It can also be seen that with increase in temperature of digestion the sodium fixed in sodalite also increases.

Mariassy et al. [27] examined the use of dilute liquors for bauxite digestion and concluded that with the use of dilute liquor for digestion, water requirement for washing of red mud is considerably reduced. Solymar et al [28] have proposed a mechanism of washing of red mud and sodalites. They observed that in first stage washing, adhering liquor is removed and hydrolysis takes places partly, and in second stage unchanged sodalite starts dissolving.

Prakash and Horvath [29] conducted studies on washing of red mud with alcohol, 2% Na_2O solution and distilled water at

$90^{o}C$. The washing was kept continued till the pH of wash water was less than 8. They observed increase in specific surface area of red mud with increase in TiO_2 (anataze form) content of bauxite. It was concluded that with increase in TiO_2, TiO_2 content larger amounts of sodium aluminate liquor would adhere on the surface of red mud which necessitated requirements of larger amounts of wash water.

2.4.6 Settling Characteristics

In the Bayer process, settling has been said to be one of the most important steps in the separation of liquor and red mud. The selecting of the method of separation depends on the quantity of red mud in the slurry. In case of large red mud content of slurry, settlers are used before filteration to decrease the load on filteration unit.

Settling of the red mud is governed by factors like [30] (i) origin, geological age and chemical and mineralogical composition of bauxite (ii) method of ore dressing (iii) digestion conditions (iv) conditions after digestion. Recent studies [22] indicated that the specific surface area of red muds was inversely proportional to the settling properties. It has therefore, been proposed that settling and washing properties may be estimated directly from specific surface area of red mud which can be measured with the BET method.

Bauxites contain lot of impurities namely silica, iron sulfide, hematite, magnetite, minerals of titanium like anataze, rutile, brookite and illmenite. As a rule [31] it is not

possible to predict exactly how muds will be settled by material composition of bauxite. However, a preliminary opinion about the character of mud settling ability can often be prepared by material composition of bauxite. In the following paragraphs, the role of various factors affecting the settling ability of produced red mud,has been briefly discussed.

2.4.6.1 Role of Titanium Minerals

Titanium minerals are found to occur in all the bauxites in varying amount from negligible in Brazilian bauxites to above 17% in Indian bauxites. Titanium minerals have been observed to affect the settling characteristics of red mud. Zambo and Kovacs [24] examined the settling characteristics of red mud from Indian bauxites. As a result of their study they concluded that settling rate and compaction was unsatisfactory. They also tried to find out the effect of addition of CaO during digestion and concluded that settling rate of red mud was improved when percentage of CaO was more than the percentage of TiO_2 whereas lesser amount of CaO led to decrease in settling rate. Schepers [32] has also found that addition of 2% CaO in digestion charge improved the settling rate which is attributed to the formation of calcium titanates or calcium silico titanates etc. thereby binding TiO_2 content and avoiding its effect on the settling rate.

The adverse effect of TiO_2 has been reported to be due to formation of $NaHTiO_3$ gelatinous precipitate which passes into red mud and creates difficulties in separation. Kovacs [25] in

the detailed study on a pilot plant scale on settling characteristics of Indian bauxites red mud observed that settling rate of red mud from Indian bauxite was lower as compared to red mud obtained under similar digestion conditions from Hungarian bauxite. Poor settling ability was attributed to High TiO_2 content of bauxite which is in anataze form and transforms during digestion into amorphous gelly like precipitate which makes separation of red mud difficult.

Prakash and Horvath [30] arrived at the same conclusion on the basis of specific surface area measurements of red muds, obtained by digestion of bauxites with 12% and 18% TiO_2 in anataze form. The increase in specific surface area was attributed to the formation of higher amount of amorphous sodium titanates and dispersed TiO_2 as observed from X-ray diffractometry of red muds.

2.4.6.2. Role of Iron Minerals

Settling properties of red muds are affected by the form of iron minerals present in the system. The two forms of iron minerals generally found in bauxites are aluminous goethite, α-(Fe, Al), OOH and hematite, α $-Fe_2O_3$. A general observation [31,33] is that in case iron is present as hydrates of oxides (goethite etc), the settling of mud becomes worse. On the contrary, the availability of oxide forms of ferrous minerals (hematite etc) promotes the settling ability. Basu [34] undertook a detailed investigation in this regard and confirmed the relation of settling rate to the type of iron mineral. Model

systems comprising of systhetic goethite and hematite in pure sodium aluminate solutions were used to study reactions representative of those occuring in Bayer process by the study of relative settling rates as function of particle size and surface area. For goethite and hematite, the author observed that for a given particle size and surface area,hematite exhibited considerably faster settling rates than goethite. He interpreted that the agglomeration tendency of the α-FeOOH particles was much lower than that of hematite due to difference in their surface properties. The surface properties of goethite has been reported to be such that they do not allow for the strong particle-particle interaction necessary for flocculation.

Leitenzen et al. [31,35] have shown that if a considerable part of iron oxide is bound to siderite, the process of settling of low quality bauxites of gibbsite type becomes considerably worse. In so doing it was determined that siderite by itself does not effect the settling ability of red mud, because it completely decomposes with reaction. of magnetic ferrous oxide during digestion. But if a considerable part of iron oxide, present in bauxite is bound to siderite, the ratio of hemitite to silicon oxide therewith is sharply reduced which according to author's opinion, represents the main reason of deterioration of mud settling ability.

Degree of dispersion of iron oxides has also been stated [36] to be responsible for settling characteristics of red mud. Geothite type of bauxites generally result in a red mud found to have higher dispersion which adversely affects the

settling rate. In case of Ghanian bauxite having crystallised goethite, rate of settling is higher as compared to Jamaican bauxite having highly dispersed hematite.

2.4.6.3. Role of Silica Minerals

The presence of SiO_2 minerals adversely affect the settling rate. Silica in quartz form during settling behaves in two ways; the solution may set to a gel, or the particles have such a size that they settle slowly in solution forming a cake or an aggregated mass on the bottom of the container. The later tends to occur if the size of the individual particle exceeds 150 to 200 microns. It has been reported that the rate of formation of gel increases with concentration of SiO_2. Silica however, in kaolinite form has been considered [37,38] to have most unfavourable effects on settling behaviour of red mud.

2.4.6.4. Role of Other Inpurities

Effects of other impurities present in bauxite on settling rate of red mud has also been established. Presence of sulfide minerals (pyrites and marcasite) adversely affect the settling of red mud because if the sulfur content [39] is more than 2% then colloidal iron-sulfide particles are formed. Presence of magnesium and calcium carbonates in slightly higher amounts may produce some problems in washing line and red mud separation [40]. Higher amounts of calcium and magnesium carbonates may entail loss of caustic. There may be high solid containing foam which may float and accumulate on the surface

thereby leading to break down in settling and washing line. Role of phosphorous has also been investigated and it has been reported [41] that P_2O_5 concentration of 10 gm/l or less has no negative effect on the technological index. Now it has also been well established that the availability of kaolinite, pyrite, limonite, dolomite and some minerals can essentially deteriorate the settling ability of red muds [42].

The content of organic material, expressed as carbon, may vary from 0.05% to 0.4% which partly goes into thethe digestion liquor while the non-dissolved part is removed from the process with the red mud. Pohland and Tielens [43] have revealed that organic material present in bauxite also hamper the process of settling of red mud by making the process liquor more viscous. They pointed out sodium oxalate and sodium humate as most harmful organic compounds which are formed during the digestion process. On studying the Ludwigshafen refinery (Germany), they observed that when the concentration of sodium humate compounds increased above a critical level, red mud settling rate was decreased drastically resulting in muddy overflows. Authors have suggested an improved method to avoid difficulties caused by organic impurities.

2.4.6.5 Role of Settling Agents

Settling agents are organic or synthetic materials added to digested liquor to improve properties of red mud by way of coagulating and flocculating the fine particles of red mud thereby making the settling fast. Kovacs and Solymar [44]

investigated the use of ryeflour and riceflour on red mud obtained from an Indian bauxite. They reported that the rate of settling was not found to improve with increase in amount of rice-flour added. They also observed that red mud obtained by digestion at 240^{o}C had better settling characteristics as compared to red mud obtained at a lower temperature of 220^{o}C . This has been attributed to incomplete digestion of bauxite. According to them, use of settling agents is not necessary in case of Indian bauxites considering the speed with which red mud and aluminate liquor move in the industrial Dorr-settlers.

Generally it has been found that the small addition of settling agent enhances the settling rate to great extent. It has been shown [45] that the mode of preparation of solution and water used for making solution of settling agents affects the settling rate. For efficient settling a flour solution containing 8 to 10 g/l of distilled water should be made and before its addition to settling tank, it should be boiled. Plant water has not been suggested for the preparation of flour solution as it contains materials which may affect the settling rate adversely.

Use of synthetic flocculants which are polyelectrolytes having sufficiently high molecular weight, have also been suggested to improve the settling charactristics of red mud. Flocculation has been considered to occur due to bridging of suspended particles by the long chains of these polymers. Synfloc flocculating agents have been reported [46] being used in recent practices.

2.4.6.6 Role of Process Parameters

The relationship between the digestion temperature of bauxite and sedimentation behaviour of red mud was studied by various researchers [25,32,47,48] in detail and it was found that settling characteristics of red mud improved with increase in digestion temperature. Dunay [47] established that in general digestion at temperatures above 250^{o}C improved the sedimentation of red mud. Basu [34] investigated that the hydrothermal transformation of goethite into hematite during digestion led to an alteration of the FeOOH surface properties and resulted in considerable increase in settling rate. Such a transformation gets accelerated with the increase in temperature of digestion. Hydrothermal transformation, can also be achieved by prior calcination of bauxite. However, this does not always improve the sedimentation behaviour [37]. Some times it may even be harmful because of resulting disintegration.

In a tube digestion system suggested by Lanyi [49], red mud contained magnetite and settled satisfactorily.

Digestion of bauxite carried out with the use of catalysing additives [50] prompts hydrothermal transformation of goethite to hematite and hence improvement in sedimentation of red mud. The method, said to have been patented world-wide, gives safe transformation of goethite to hematite even for bauxites (e.g from Guina) containing extremely stable goethite.

The conditions of mud preparation also influence the settling ability of the mud [31]. It has been demonstrated that factors like digestion temperature, period of holding before and

after digestion, method of pulp cooling influence considerably the speed of settling in the zone of free falling and period of solution clarification.

2.5 CHEMICAL AND MINERALOGICAL CONSTITUTION OF RED MUD

The chemical composition of red mud depends on the chemical and mineralogical characteristics of the bauxite treated and Bayer process variables. Tab.2.9 gives an idea about the chemical composition of red muds produced in the alumina refineries of different countries. This indicates that the major constituents present in red muds are Fe_2O_3 and Al_2O_3 whereas TiO_2, Na_2O, SiO_2, and CaO are present in minor quantities. Besides, the trace quantities of several other elements such as the oxides of [6] V, Ca, Cr, Zr, V, th, Sc, La, Y, Sr, Ba, Hf, K, Pb, Mn, Mg, Ca, Ni, Zn, Bi, Co, Li etc are also present.

Although the exact chemical composition of red muds varies over a wide range depending on the actual bauxite source from which it has originated, major mineral phases identified (Tab.2.10) include hematite α-Fe_2O_3, boehmite (α-$Al_2O_3.H_2O$), gibbsite, (α-$Al_2O_3.3H_2O$), goethite (α-$Fe_2O_3.H_2O$), calcite ($CaCO_3$)and the sodalites group of minerals. Based on X-ray diffraction, Infra Red and Derivatogrhphic studies, Prasad and Sharma [7] identified 15 mineral phases in an Indian red mud from HINDALCO which is shown in (Tab.2.11).

The chemical and phase composition of red mud depend to a great extent on digestion temperature of bauxite. Solymar and Kovacs [51] on examining the red muds formed at 180 and

Table.2.9 Chemical composition of red muds [6,18]

Country	Constituent %						
	Fe_2O_3	Al_2O_3	TiO_2	SiO_2	Na_2O	CaO	LOI
Jamaica	51-52	14-15	6-7	2-3	1-3	5-7	9-11
Surinam	25-28	19-29	12-13	11-12	1-9	4-6	13
USA							
(a)ALCOA, Mobile Plant	30-40	16-20	10-11	11-14	6-8	5-6	11
(b)Reynolds Arkanas Plant	55-60	12-15	4-5	4-5	2	5-10	5-10
(c)Reynolds Sherwin Plant	50-54	11-13	trace	3-6	2-5	7-9	10-13
Hungary	33-41	14-19	4-7	11-14	3-10	1-22	10-14
Yugoslavia							
(a)Skokaj (red)	45	37	7	4	-	-	19
(b)Krupa (red)	21	51	3	14	-	-	9
India							
(a)HINDALCO Renukoot	35-38	18-20	19-20	7-8	5-6	1-2	10-11
(b)INDAL, Muri	19	33	24	7	4	2	11
(c)INDAL, Belgaum	18-21	30-40	17-19	6-8	4-5	1-3	10-12
(d)BALCO, Korba	24-26	22-25	16-19	7-9	5-7	3-6	11-12
(e)ALUCOIN, J.K.Nagar	24	27	20	8	8	-	12
(f)MALCO, Methur Dam	54	16	3	8	1	-	3
(g)NALCO, Damanjodi	60-68	13-13.8	3-3.8	5-6.5	3.5-4.85	-	-
Guinea	57.7	15.8	7.1	7.1	5.3	0.2	5.0
Australia	41.3	18.2	7.9	14.9	11.3	0.3	5.6

Table. 2.10 Mineral phases in red muds [6]

Gibbsite	Hematite	Quartz
Boehmite	Goethite	Anataze
Diaspore	Maghmemite	Rutile
Chamosite	Calcium aluminate	Calcium titanate
Sodalites	Calcium aluminosilicate	Cancrinites

Table.2.11 Mineral phases in uncausticised HINDALCO Red Mud [7]

Major	Minor	Very Minor
Hematite	Boehmite	Quartz
Goethite	Diaspore	Sodium titanate
Gibbsite	Rutile	Kaolinite
Sodalites	Calcium titanate	
Cancrinite	Calcite	
Anataze	Calcium alumino silicate	

240°C found that red mud obtained at a digestion temperature of 180°C contained sodium aluminium silicate predominantly in the form of sodalite while at a temperature of 240°C only cancrinite could equivocally be identified. It was also found that increase of the cancrinite phase of red mud affected the Na_2O content of the mud and hence reduction in consticizability. Authors' observations on the chemical and phase composition of the muds on this investigation are shown in (Tab.2.12).

Transformation of goethite into hematite with increasing temperature of digestion has also been well established. Basu [34] on studying the kinetics and mechanism of this tranformation revealed that tranformation proceeded via a dissolution, reprecipitation mechanism. Factors found to affect this tranformation reaction included temperature, liquor composition and presence of hematite seed.

Solymar and Kovacs [51] on their studies on phase transformation taking place during digestion, revealed the following information regarding the interaction of TiO_2 modifications and liquor.

(i) Reactivity of anataze with respect to the digesting liquor is significantly higher than that of rutile.

(ii) Na_2O binding, that is the degree of conversion of anataze and rutile increases with the increase in digestion temperature until the equillibrium state is achieved.

(iii) The conversion rate is determined by the activity of OH^- ion of the digesting liquor and also by the reaction temperature.

(iv) The maximum possible degree of conversion depends on the free caustic content of the liquor i.e. on the difference between the actual and equillibrium molor ratio TiO_2 in practice does not react with a liquor of a composition corresponding to equillibrium molar ratio.

(v) The sodium-containing titanium compound formed during digestion does not hydrolyse completely in practice; after washing with hot water,the Na_2O remaining in red mud corresponds to a molar ratio of Na_2O: TiO_2= 1.5.

The results of authors experiments on digestion of a gibbsitic bauxite are given in Tab.2.13.

The composition of mineral phases present in red mud, has also been reported to be influenced by the addition of CaO and using additives [18] like Iron-hydrogarnet during the digestion of bauxite.

2.6 QUANTITATIVE EVALUATION OF RED MUD

2.6.1 Determination of Composition

X-ray diffractometry was thought to be the fundamental method in the determination mineralogical composition of bauxites and red muds until the development of ICP-AES techniques. Systematic methodological research continued for several years, allowed to select among phase analysis methods described in literature, the procedure that best suited for bauxite studies. This was then modified and improved with regard to mineralogical particularities of bauxites. The method was described in journal "Kohaszati Lapok" in 1966 and in Soviet journal 'Litologiya'

Table.2.12 Chemical and phase composition of red muds of digestion temperature of 180°C and 240°C [51]

Components	Percentage at	
	180°C	240°C
Ignition loss	6.4	5.3
Al_2O_3	14.3	12.0
Fe_2O_3	50.3	52.3
SiO_2	11.3	12.2
TiO_2	5.0	5.4
Na_2O	9.2	10.1
Others	3.5	2.7
sodalite	30.4	Traces
Cancrinite	6.0	38.5
Hematite	41.8	43.4
Goethite	9.3	9.8
Anataze	4.3	4.6
Rutile	0.7	0.8
Boehmite	3.6	Traces
Others	3.9	2.9

Table.2.13 Chemical and phase compositions of Red Muds at 140°C and 160°c [51]

Components	Percentage at 140°C	Percentage at 160°C
Ignition Lossos	12.0	12.2
Al_2O_3	11.5	11.2
Fe_2O_3	17.6	13.2
SiO_2	1.6	1.8
TiO_2	53.2	47.0
Na_2O	1.7	13.3
Others	3.4	1.3
Hematite	13.0	9.2
Goethite	5.1	4.4
Gibbsite	13.2	11.3
Sodalite	5.7	6.1
Anataze	43.7	20.0
Rutile	9.5	9.0
Amorphous Na_2O -bearing titanium Compound	Traces	34.0
Others	9.4	6.0

Polesnye Iskopayemye' [52] and got world-wide appreciation. The technique was again refined with the application of an AMR Norelco graphite crystal monochromator, allowing to filter all diffuse radiation and thus the use of a copper anticathode.Later modification was the introduction of 1500 W copper anticathode x-ray tubes which lowered the limit of detection of individual minerals. Also the method was suggested to remove the so called 'mineralogical error' said to be the main source of error.

R. Tertian [53,54] has suggested x-ray flourscence spectrometry as quick analytical method for industrial analysis of bauxites which can be carried out on the spot or in the mining area for the convenient evaluation of the quality and approximate composition of bauxite. It was shown on theoretical and practical background that accurate analyses appropriate to widely different materials (bauxites of diverse origins and compositions, red muds etc) could only be carried out by fusion methods using a mixture of $B_4O_7Li_2$ and Li_2O_3 as fluxing material. Bryan and Wright [55] have carried out the analysis of Jamaican bauxites and red muds using x-ray fluorscence spectrometry and applied a method for the calculation of influence coefficients for matrix correction. They compared the results obtained for aluminium, silica, phosphorus, titanium and iron to those obtained by wet method.

To promote automation of alumina production by Bayer process, Farkas and co-workers [56] reported the instrumented determination of the chemical composition of aluminate liquors. To develop the suitable method, they studied conductivity and

specific gravity as a function of composition. It was found that besides conductivity and specific gravity, a third parameter K_{max} was also felt to be measured at constant temperature. The concept of K_{max} represented the value of maximum conduction measured in the solution to be tested during isothermal dilution at a constant molar ratio. This value was found to be dependent only on the molar ratio and varied proportionately with the reciprocal value of this parameter in the investigated region. The latest development authors claim, to have determined the composition of synthetic liquors by conductivity measurement with a precision similar to that of chemical analysis. They designed a high frequency conductivity measuring instrument with inductive measuring cell. Based on the same principle, Klug and Tajnafoi [57] determined the solid content of red mud slurries by oscillometer and studied the application of a measuring instrument for the Al_2O_3 industry to measure the composition of wash water. An oscillometer type cond-meter OK-105 has been reported to be used for the analysis of synthetic sodium aluminate solutions.

Kwat [58] developed and applied ICP-AES techniques for the analysis of raw materials including bauxites, red muds and finished products in the aluminium industry. After suitable dissolution, the samples were analysed for the major and minor elements using La and Y as their respective internal standards in matrix matched calibration solutions prepared from synthetic standard solutions or from dissolution of a standard reference material. The technique has been said to be capable of achieving

sensitivity and accuracy as good as obtained by the conventional methods. Bitto and co-workers [59] have used AAS system for serial determination of aluminium, iron, silica, titanium, calcium and magnesium and flame emission spectrometry for the sodium in bauxite and red mud. The data were evaluated by using a computer programme. Ajlec and Stupar [60] employed AAS for the rapid and routine analysis of aluminium and iron in red mud from the alumina production plant. The suspension was prepared by mixing 0.5 gm of sample with 10 ml. hydrochloric acid for 10 minutes, diluted to 100 ml. and then iron and aluminium were measured in an air-N_2O-C_2H_2 flame at 386 nm. and a N_2O-C_2H_2 flame at 392.2 nm. respectively.

2.6.2. Phase Analysis

Three methods are in prevalent use for phase analysis, namely, x-ray diffraction, derivatography and IR-spectroscopy. All three methods are separately suitable for determining the phase composition of red mud. However, if only one single method was to be applied, X-ray diffraction is undoubtedly the one that yields most information [61] since it allows the detection of largest number of constituents at highest speed and with the exception of one or two phases, the limit of detection is lowest. The absolute values of limits of detection can best be determined by this method, so that it is suitable for determining the causes of undigested losses resulting under differing technological conditions . Such absolute values are less defined in case of IR-spectroscopy [61], firstly because the extinction greatly

depends on the degree of crystallinity of the constituent in question and secondly the percentage and nature of foreign ions incorporated by isomorphous substitution substantially affect extinction. However, for the very reason that band width depends on crystallinity to a larger extent, IR-spectroscopy, though less suited for exact quantitative determination, yields highly valuable information in case when red muds obtained in the same technological process for bauxites of different origins are being compared. IR-Spectroscopy yields reliable quantitative information only when applied together with x-ray diffractometry [61].

Orban et al. [61] successfully determined the phase composition of Soviet and Hungarian red muds applying x-ray diffractometry, derivatiography and IR-spectrophotometry. According to this study the method was found to be well suited for the determination gibbsite present even in traces. The authors were successful in identifying boehmite by means of both OH-Valency vibrations (3100-3300 cm^{-1}). Both sodalite and cancrinite could readily be determined by IR-spectrophotometer. For quantitative determination of the crystalline phase , they used peak heights or peak areas of 100-intensity (relative) reflections. In case of coincidences, the effect of interfering phases was accounted for, on the basis of their relative intensities. They developed a method and suggested formula for the quantitative determination of iron minerals based on the proportions of peak heights or peak areas. This method has been said to be applicable for red muds obtained under any digestion

conditions and proved satisfactory in practice. Gado and Orban [62] carried out automated quantitative mineralogical phase analysis of bauxites and red muds by X-ray diffraction, X-ray fluorescence and Atomic Absorption spectrometer.

Kontopoulos et al.[63] studied physical, chemical and mineralogical characteristics of Grecian red mud containing Al_2O_3 15.26% ,Fe_2O_3 39.11% , SiO_2 6.05% ,TiO_2 5.22% ,CaO 18.72% and Na_2O 2.07% . The major phase including hematite, magnetite, calcite, diaspore, SiO_2, Ca-Al compounds, complex compounds of Si-Na-Mg-Ca-Al were identified using X-ray diffraction, DTA, TGA, IR, electron probe and optical microscopic studies.

Bertoti et al. [64]by transmission and Fourier transform IR-spectroscopy carried out studies on acid treated red mud. Red mud was leached with sulfuric acid and hydrochloric acid and adjusted to different pH values. IR-studies showed the phase transitions occuring. Grachey and coworkers [65] determined the different forms of sulfur in sodium hydroaluminosilicates.

2.7 UTILIZATION OF RED MUD

As a result of continuous efforts the possible applications searched out [6,7,20] are enlisted in (Tab.2.14). As the present work is concerned with the recovery of titaninm value in form of a ferro-alloy via aluminothermic route,the aluminothermy and aluminothermic production of ferro-alloy as studied by various investigators shall be discussed below with a bit elaboration.

Table.2.14 Possible applications for red mud [6]

Category of application	Illustrative list
Recovery of major constituents	Production of iron and steel Recovery of alumina Recovery of alkali Production of titania (from such red muds where TiO_2 is a major constituent)
Recovery of minor constituents	Recovery of V and Ga Recovery of Zr,U,Th,Nb,etc.
Direct uses for Production of building materials and ceramics	Bricks or constructional blocks Low density (foamed) bricks and other shapes special tiles Fireproof insulation Light weight aggregates Special cements or additive to cement Prefab structures Highway road bed stabiliser Special ceramics and glasses Pottery and sanitary ware
Miscellaneous direct applications	Plastic,rubber and resin filler Pigment Corrosion inhibitive primer Catalyst Insecticide/pesticide Production of special fertilisers Waste gas adsorbent Flocculating agent Cation exchanger Sewage treatment Cleansing of industrial waste waters

2.7.1 Aluminothermic Ferro-Titanium Production

2.7.1.1 Principles

Aluminothermic reduction reactions come under the catagory of metallothermic reduction processes where a metal is used to reduce the oxide of another metal.This unit operation is concerned with the preparation of metals and alloys by reduction of their oxides or halides with metals. These reactions can be expressed in general, by the following equation.

$$AX + B \longrightarrow A + BX$$

where X is oxygen, chlorine or flourine and A and B are two metals.

Metallothermic reductions are batch processes [66]in which both the reactants are solids and characterised by the facts that (i)the reducing metal is converted to a solid or liquid product and not to gas as in other reduction processes and (ii) as associated with high negative free energy change, these reactions are highly exothermic thereby permitting self-sustaining reaction .In fact this method is used when reduction by carbon or hydrogen or by electrowinning from aquous solution is not possible due to either high thermodynamic stability of oxides or halides or too reactive nature of reduced metal to permit isolation in pureform. The most common example of metallothermic reduction is the use of aluminium as reducing metal in thermit welding of rails and repair of steel casting. The application of this process has now become most prevalent in

the extraction of many technologically important metals and alloys particularly from the class of less common metals and considerable interest has been shown in developing extraction flowsheets of some rare and refractory metals and alloys based on aluminothermic process. It has been possible to produce [67,68] niobium, tantalum vanadium, molybdenum and tungsten in adequately pure form by the aluminothermic reduction of their oxides, followed by one or a combination of purification processes namely vacuum arc melting, electron beam melting, pyrovacuum treatment, and fused salt electrowinning.

2.7.1.1.1 Choice of Reducer Metals

The most commonly used reducing metals are Al, Ca, Si (in the form Fe-Si), Mg etc. and accordingly these reduction reactions are named as aluminothermic, calciothermic, silico thermic or magnesiothermic reductions. Our main emphasis, however, shall be on aluminothermic reduction reactions for oxides for further discussion. The choice of a reducing agent for a metallothermic reduction reaction is governed by the following considerations;

(i)Thermodynamic Consideration

The reduction reactions are characterised first of all by the stability of oxides at high temperatures. For a comparative characterization of the stability of various oxides, standard values of free energy of oxide formation as a function of temperature are shown in Fig.2.9. It follows from these

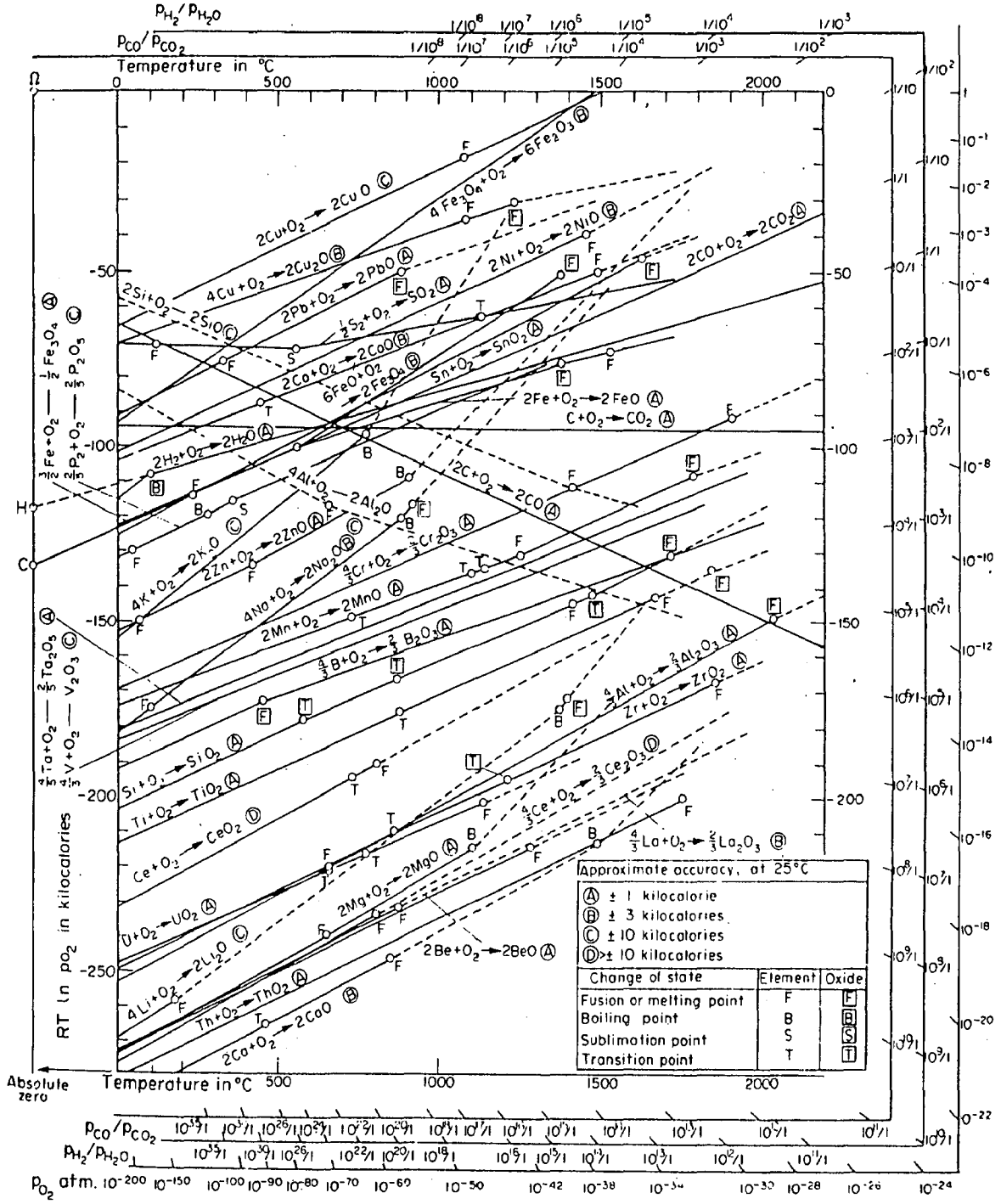

Fig.2.9 : Free energies of formation of some oxides [70]

diagrams that the lower oxides are more stable than the higher ones and are therefore more difficult to reduce. Theoretically, any element forming a more stable oxide may be used as reducing agent for a less stable oxide but for the practical realization of a reduction reaction, it is necessary that the difference between the values of the energy of the oxides of the element to be reduced and that of reducing agent should be of a considerable magnitude. If this difference is small, the reduction reaction does not proceed completely, and the alloy obtained has an increased concentration of reducing element [69]. In practice, if the reaction has a small value ΔG^{o}, favourable conditions for its realization in the desired direction should be created [69,70].

(ii) Heat of Reaction :

The heat of reaction should be sufficient to form fluid products in order to facilitate the separation of slag and metal. If heat of reaction is very high so as to give higher temperature than required , some coolant (usually the iron scrap) is incorporated in the change. In case, the heat of reaction is not sufficient to give molten products the charge may be preheated before igniting. Some chargiser or booster is usually added to increase the heat of reaction e.g. some higher oxides such as CrO_3 or some O_2-rich salts. Flux is included to lower down the melting point of slag.

(iii) Availability and Cost :

The reducing agent of desired purity should be available in adequate quantities at economic rate.

(iv) Alloying Tendency :

In order to achieve highest reduction efficiency, the reducing metal should posses minimum tendency to form alloy with metal/alloy. The resulting metal/alloy should not get contaminated by the reducing metal beyond the desired limit,especially by way of formation of intermetallic compounds with the metal produced [66].

(v) *Other factors* :

In addition to the above mentioned factors, the reductant selected should posses low vapour pressure (high B.P.) at the reaction temperature so that there is less vaporization loss of reductant and less pressure build up. As far as possible, the slag produced by the reductant should be easily melting. Despite all these factors, the handling of reductant enevitably incorporates its importance. Sodium metal has not been used as a reducing agent to any great extent due to difficulties encountered in handling [71]. The similar thing is also with calcium though its cost factor also being important.

In the preparation of IV group metals (Titanium, Zirconium, Hafnium etc.), use of carbon and silicon are discounted as they lead to the formation of stable carbides and silicides. Despite being the strongest reducing agent, calcium

and magnesium can not be used due to their low boiling points and their use in the preparation of these metals from their oxides requires air tight reactors if the products are to be separated as liquid phase. The high melting points of their oxides i.e. 2580^{o}C for CaO and 2800 for MgO require that the reaction products should be raised above these temperatures to achieve the efficient slag-metal separation.These reductants are costly also. Aluminium on the other hand has a number of desirable properties like low melting point (660^{o}C) and high boiling point (2467^{o}C),high heat of formation (-400 Kcal/mole) and low melting point of its oxide (2045^{o}C). The other advantages are low cost, ease of handling, availability in high purity and lower equivalent weight for reduction as compared to calcium or magnesium. These attributes make aluminium a very useful reductant for a variety of metal oxides.

2.7.1.1.2 Thermodynamics, Kinetics and Equillibrium Aspects:

For a reaction proceeding at constant temperature and pressure, the motive force behind is characterised by change in free energy-

$$\Delta G = \Delta H - T\Delta S$$

Where ΔH is the change in enthalpy and ΔS is the change of entropy. The direct reaction is only possible when ΔG has a negative value and state of equillibrium is established when $\Delta G = 0$.

At low temperatures or when change in entropy ΔS is negligible, the chemical affinity between substances may be

characterised approximately by the heat effect of the reaction at the considered temperature [69]. This occurs mainly in condensed systems in which substances interact in solid or liquid state and in which the gaseous phase is absent. The alumino and silico-thermal processes of reduction of oxides of manganese, chromium, molybdenum, zirconium, vanadium, boron and columbium are the examples. For reaction in which gaseous phase participates (carbon-reduction), free energy should be used since the heat effect may differ considerably from it.

The reaction of a metallothermic reduction

$$MX + M' \longrightarrow M'X + M$$

proceeds from left to right on condition [72] that $\Delta G_{M'X} > \Delta G_{MX}$ and hence $\Delta G = \Delta G_{M'X} - \Delta G_{MX}$ is negative, Now two conditions may arise-

(i) If the reaction takes place in a solid or liquid phase without the formation of a solid or liquid solution, the reaction proceeds in the forward or reverse direction (depending on the sign of thermodynamic potential) until one of the reactants disappears, since in this case both the equation terms and the total thermodynamic potential, incur no change in the course of reaction.

(ii) If the reaction takes place in melt with the formation of solutions (e.g.metal and slag) , the concentrations or activities of the metals and oxides in melt, the thermodynamic potential of the reaction, all change in the course of reaction. In this case the reaction is

not completed as an equillibium sets in as soon as ΔG for the reaction becomes equal to zero.

$$(MX) + [M'] \rightleftharpoons (M'X) + [M]$$

The equillibrium constant is written as

$$K = \frac{a_{M'X} \cdot a_{M}}{a_{MX} \cdot a_{M'}}$$

For the initial state

$$K' = \frac{a_{M'X} \cdot a'_{M}}{a'_{MX} \cdot a'_{M'}}$$

where 'a' denotes the activities of respective components

$$\Delta G = RT \ln K' - RT \ln K$$

For success of the reaction $K' < K$

The value of equillibirum constant can be determined with the aid of the equation -

$$\ln K = - \frac{\Delta G^{O}}{RT}$$

Where ΔG^{O} is the standard free energy change

The values of $\Delta G^{O}_{M'X}$ and ΔG^{O}_{MX} can be roughly calculated from the ΔG_{MX} Vs. temperature diagrams. It is obvious that, the value of the equillibrium constant K should be very large and that of ΔG^{O} should be big negative, in order to cause the reaction.

When the standard affinity M' for X is less than that of M for X or a has a small value of ΔG^{O} in favourable direction, the reaction between MX and M' still may occur under

the following conditions [72].

(i) If M dissolves M'; The particular feature of the production of ferro-alloys is that the reduction of oxides is realised in the persense of solvent iron or its oxides, which faciliates to a large extent the reduction processes. This is explained by the following reasons [69].

(a) Iron oxides are reduced considerably easier than most other oxides and as a result of this fact more favourable energy conditions are created in the system (the total value of (ΔG^{o}) decreases).

(b) By dissolving the reduced elements iron lowers their activities, which in accordance with the equllibrium constant of the reactions, is followed by the displacement of equillibrium in the direction of reduction. Sometimes the process is accompanied by a considerable decrease in free energy (Fe-Si, etc) and therefore the reduction of oxides is facilituted even to a greater extent.

(c) By dissolving the reduced element, iron removes it from the reaction site facilitating the reaction in forward direction and impending the development of secondary reactions (oxidations) as well as volatilisation of element.

(d) As a rule, iron lowers the melting temperature of metal phase and permits the smelting process to be conducted at lower temperature.

Considering the metallothermic reduction of an oxide –

$$(MO) + [M'] \longrightarrow (M'O) + [M]$$

At equillibrium, the standard free energy of reaction is related to the activities of the reactants and products as follows –

$$\Delta G^{o} = -RT \ln \frac{a_{(M'O)} \cdot a_{(M)}}{a_{(MO)} \cdot a_{(M')}}$$

Where

$$K = \frac{a_{(M'O)} \cdot a_{(M)}}{a_{(MO)} \cdot a_{(M')}}$$

and

$$\frac{a_{M'}}{a_{M}} = \frac{\exp\ (\Delta \bar{G}^{o}/RT)}{a_{MO}/\ a_{M'o}}$$

This expression decides about the contamination of the reduced metal M by the reducing metal M'. By manipulating different activities, it is possible to obtain either a high metal purity or a high recovery or a compromise between the two. In general an excess of reducer is invariably used for obtaining high reduction yields, but an excess over an experimentally established value would result in an increased residual concentration of the reducing agent in the metal or alloy [67,68]. Also an increase in M'/M ratio might mean lowering its density and increasing its chances of entrapment in the slag.This point has wide significance in aluminothermics of low density refractory metals.

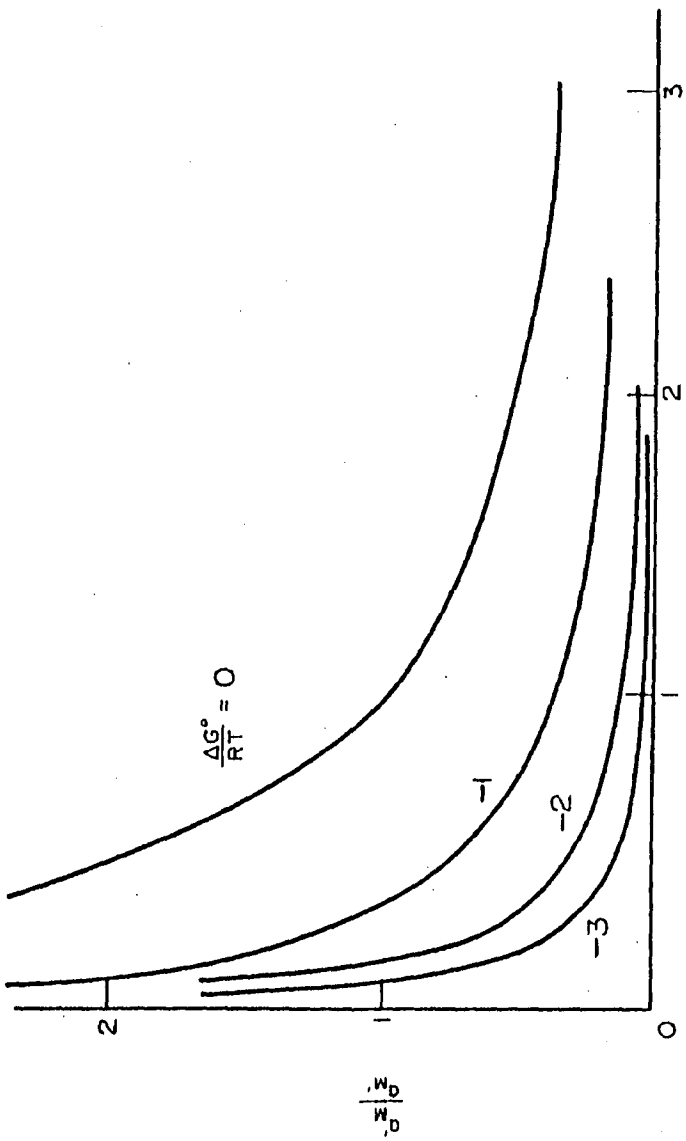

Fig. 2.10 Relationship between the activity ratios of oxides and metals [70]

In addition to free energy considerations, the following two parameters are equally important in order to reduce the contamination, [70].

(a) the temperature is as low as possible, subject to the metal and slag being sufficiently fluid and separate efficiently

(b) The ratio $a_{Mo}/a_{M'o}$ is large. The losses of oxide MO in slag are allowable because they increase its activity and decrease the activity of M'O.

The Fig.2.10 illustrates the relationship between the activity ratios of oxides and metals

In practice, however, it is an advantage to add to the slag an oxide that forms stable compounds with M'O. In the production of pure manganese by metallothermic reduction, aluminium must be used in place of silicon [70] and it is necessary to operate at the lowest possible temperature, to allow for some losses of mangnese oxide in the slag and to decrease the activity of aluminium oxide formed by slagging with CaO. In this way, aluminium is at a very low residual level in the metal.

(ii) When M or M'X or both in vapour state -

The equillibrium constants in these are given by [72].

$$K_1 = \frac{P_{M'X} \cdot P_M}{a_{MX} \cdot a_{M'}}$$

$$K_2 = \frac{a_{M'X} \cdot P_{Me}}{a_{MX} \cdot a_{M'}}$$

$$K_3 = \frac{P_{M'X} \cdot a_M}{a_{MX} \cdot a_{M'}}$$

The reaction proceeds in the forward direction, until the equillibrium pressures of M and M'X vapours are attained. When vapours are removed, the reaction may proceed sufficiently completely.

As the reaction proceeds, the equillibrium vapour pressures P_M ,$P_{M'X}$ or the product $P_M \cdot P_{M'X}$ remain constant, provided MX and M' form no solutions [72].

In case, no saturated solutions are formed , the above equillibrium vapour pressures are given by –

$$P_M = \frac{K\, a_{MX} \cdot a_{M'}}{a_{M'X}}$$

$$P_{M'X} = \frac{K \cdot a_{MX} \cdot a_{M'}}{a_M}$$

$$P_M\, P_{M'X} = K\, a_{MX} \cdot a_{M'}$$

which are the function of concentrations. In this case, therefore, the equillibrium vapour pressures, decrease in the course of reaction, since the activities of the substances on the left of reaction equation also decrease.

The order of reactivity of oxides can be changed by applay vacuum. Under vacuum silicon can reduce MgO and aluminium can reduce CaO, although the reverse is expected under standard conditions. The chemical potential of MgO is reduced by 17.5

Kcal/mole at 1000^{0}C by operating at about 0.001 atm and at the same temperature and pressure the free energy change for the reduction of MgO by silicon is reduced negative[2,72].

2.7.1.1.3 Factors Influencing Kinetics of Reaction [68]

Aluminothermic reduction reactions are accompanied with high reaction rates. The reaction rate is controlled by following factors,

(i) Particle sizes of the reactants involved.

(ii) Degree of mixing of all above constituents in the reactor assembly.

A charge consisting of coarse particles will have slower reaction than the charge consisting of fine particles. Fine particles of reducer metal (e.g.Aluminium) produce a high peak temperature which disappears within a short period of time. For coarse particles the reaction is slow and it is difficult to attain a high temperature. A good compromise however, can be made with medium particle size range, between the peak temperature and time of its existence.

2.7.1.1.4 Thermochemistry

A metallothermic reduction is usually accompained by the evolution of heat $Q = Q_{M'X} - Q_{MX}$ where $Q_{M'X}$ and Q_{MX} are respectively the heats of formation of M'X and MX, from the elements. The heat of reactions of some important reduction processes are given in (Tab.2.15) and (Tab.2.16).Although the thermodynamic potential of a metallothermic reaction at low

Table. 2.15 Heat of Reactions for some aluminothermic reactions of oxide systems [117]

Metallothermic Reaction	$-\Delta H^{o}_{298}$ Kcal./ mole of oxygen	$-\Delta H^{o}_{298}$ Kcal./kg. of reactants	Remarks
1. $2ZnO+4/3Al=2/3Al_2O_3+2Zn$	1300.0	504.8	Reaction heat is adequate
2. $SnO_2+4/3\ Al=2/3Al_2O_3+Sn$	128.0	686.0	Reaction heat is adequate
3. $2MgO+4/3Al=2/3Al_2O_3+2Mg$	-19.4	-167.5	Endothermic reaction
4. $2/3Fe_2O_3+4/3Al=2/3Al_2O_3+4/3Fe$	136.0	953.3	Excess heat
5. $2/5V_2O_5+4/3Al=2/3Al_2O_3+4/5\ V^2O_3$	117.7	1083.8	Excess heat
6. $1/2Mn_3O_4+4/3Al=2/3Al_2O_3+3/2Mn^2O_3$	101.0	671.4	Reaction heat is adequate
7. $1/3Mn_2O_3+4/3Al=2/3Al_2O_3+4/3Mn^2O_3$	114.2	808.6	Excess heat
8. $MnO_2+4/3Al=2/3Al_2O_3+Mn$	142.4	1158.3	Excess heat
9. $2/3Cr_2O_3+4/3Al=2/3Al_2O_3+4/3Cr^2O_3$	86.6	631.2	Reaction heat is adequate
10. $SiO_2+4/3Al=2/3Al_2O_3+Si$	49.7	517.0	Reaction heat is adequate
11. $2CuO+4/3Al=2/3Al_2O_3+2Cu$	192.4	986.7	Excess heat
12. $2Cu_2O+4/3Al=2/3Al_2O_3+4Cu$	186.5	579.5	Reaction heat is adequate
13. $TiO_2+4/3Al=2/3Al_2O_3+Ti$	44.13	380.5	Reaction heat is not adequate
14. $MoO_2+4/3Al=2/3Al_2O_3+Mo$	155.9	950.6	Excess heat
15. $2/3MoO_3+4/3Al=2/3Al_2O_3+2/3Mo$	146.5	1110.0	Excess heat
16. $2/3WO_3+4/3Al=2/3Al_2O_3+2/3W$	133.0	697.9	Reaction heat is adequate

Table.2.16 Heat of reactions of some heat boosters [78]

Reactants	ΔH°_{298K} Kcal/mole of Metal
Al + $KClO_3$	204.97
Al + I_2	72.80
Al + Cl_2	163.80
Al + BaO_2	170.79
Ca + $KClO_3$	155.32
Ca + I_2	128.49
Ca + Cl_2	190.60
Ca + BaO_2	132.20
Ca + S	114.30
Mg + $KClO_3$	147.56
Mg + I_2	86.80
Mg + Cl_2	155.22
Mg + BaO_2	124.34

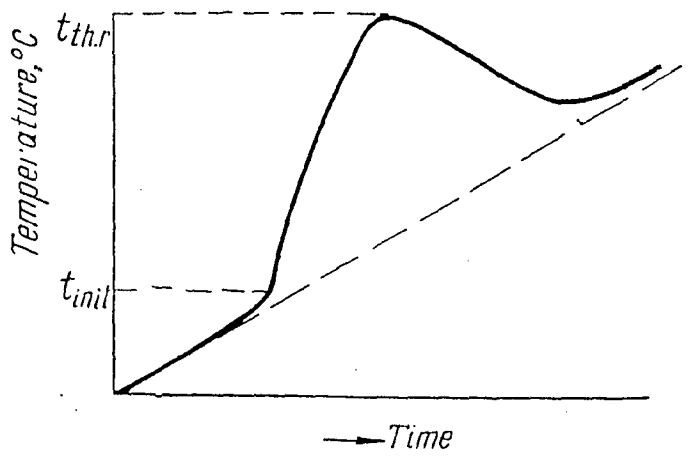

Fig.2.11 : Curve illustrating rise of temperature in metallothermic reduction [70]

temperature is negative, and therefore, the reaction can take place, the process is very slow and the liberated heat dissipates without raising the temperature of the system; hence a certain minimum temperature is necessary for the reaction to proceed vigorously, the reaction rate and amount of heat evolving in a unit time then becoming sufficiently large to ensure an appreciable rise in temperature of the system [72] as shown in Fig.2.11.

The reactants are heated by the heat of reaction, chiefly, through the agency of vapour or liquid products and then by the gas medium which fills the pores of the metallothermic compounds [72]. The maximum temperature attained in the course of reduction process is called 'reaction temperature'. The reaction temperature can be distinguished from theoretical temperature where the reaction is conducted under adiabatic condition. The theoretical temperature can be determined by calculation of heat balance being struck for the temperature under consideration.

2.7.1.1.4.1 Heat Losses

Practically the reaction temperature is determined by the heat losses accompanying the reaction. In heating the reactor, radiation into surrounding medium, heat removed by the discharged gases and vapours, are the main factors responsible for heat losses. Therefore, heat losses depend on the design of reactor, the reaction rate and other factors. Larger the heat (i.e. batch of material melted) the lesser both the specific volume of the burden and volume of the reactor. For high reaction

rate, the heat losses are less and actual temperature is found closer to theoretical temperature.

2.7.1.1.4.2 Thermal Boosters

When the heat effect of the reaction is low, thermit additions are used to provide extra heat. These additions are composed of substances which interact with the evolution of large amount of heat. A frequent practice is to compose these thermit additions either of a reducer metal and a compound which reacts with reducer metal with the liberation of heat or of high valency compound of metal to be reduced. Table 2.16 gives an idea about the heat of reaction of some boosters.

2.7.1.1.4.3 Coolents

If metallothermic reaction liberates excessively large amount of heat and proceeds vigorously, the reaction products are superheated, volatile matter vaporises in considerable amounts and both the burden and reaction products are projected out of the reaction vessel. In this case use is made of some cooling agents which are composed of remelted slag of fluxes, commonly salts which do not react with the reducer but form easy melting and less vigorous melt, with the slag. Use of iron scrap has also been suggested in this direction [73].

2.7.1.1.4.4 Parameters Controlling Heat Effects

Following parameters control the heat effects of metallothermic reduction process.

(i) Coefficient of Thermicity [72]

Various parameters have been suggested about the sufficiency of heat effects of a metallothermic reduction process. One of these is 'coefficient of thermicity'which is expressed as the quantity of heat liberated per gram of the burden or per gram of the reaction products.

(ii) Choice of Reducer Metal

This takes into account -

(a) The difference in heat values and free energies of formation of compounds of the reducer and the metal to be reduced; This difference should be sufficiently high to ensure the possibility of greater reduction of metal and its efficient separation from the slag. Rigorous thermochemical calculations have to be carried out for this purpose. Nevertheless, certain generalisations may be made with respect to the thermal effects of these reactions. Perfect [74] specified that for reactions releasing less than about 2510 joules per gm. of total charge, the heat of reaction is insufficient for melting and separation of the slag and metal and external heat supply is required. Reactions releasing heat above 4600 joules per gm, the reaction is violent or even may be explosive in extreme cases and the use of inert material or coolent in the charge is necessary. Reaction proceeds in a controlled manner without any additions when heat released is between 2510 joules and 4600 joules per gm. The heat generated

Table. 2.17 Standard free energy of formation of some oxides at 298K [75]

Oxides	Standard free energy of formation at 298°K (kJ/mole of oxygen)
MoO_3	-445.5
FeO	-486.6
Fe_2O_3	-493.2
WO_3	-508.9
V_2O_5	-571.5
SrO_2	-578.2
Cr_2O_3	-706.1
Nb_2O_3	-707.8
MnO	-725.8
Ta_2O_5	-764.1
SiO_2	-823.4
TiO_2	-889.3
ZrO_2	-1036.6
Al_2O_3	-154.6
MgO	-1138.7
CaO	-1208.3

per unit mass of the charge is some times called the specific heat or specific enthalpy of the charge mixture.

(b) The solubility of reducer metal in the reduced metal under the reduction conditions.

(c) The fusibility of the slag obtained ; the slag should have low melting point and wet but slightly the reduced metal.

Thermodynamically, aluminium is the best commercial reductant. It has been extensively used as a reductant for the production of carbon free ferro-alloys [75] such as ferro-chrome, ferro-vanadium, ferro-tungsten and ferro-titanium, metals such as chromium and manganese ,alloys such as aluminium-chromium, aluminium- titanium etc, refractory metals such as molybdenum, tungsten,vanadium etc, and rare metals like tantalum and niobium. In all these cases the free energy of formation of the metal oxides involved have a big difference from that of alumina, as shown in (Tab.2.17). Zirconia (ZrO_2) and Titania (TiO_2) are, however, very close to alumina. The driving force for reduction in these cases is therefore low and these reduction reactions can only be possible by providing extra driving force by way of decreasing the activity of the products formed [75]. Calcium on the other hand has been used for the reduction of zirconia (ZrO_2) due to the larger difference betweenthefree energy of formation of zirconia and CaO. The use of calcium and magnesium however, has been restricted to a few cases due to high costs, low boiling points and formation of

oxides of high melting temperature [71,75]. Aluminium, though, thermodynamically less suitable than both calcium and magnesium, does not have these difficulties and is therefore, commercially more acceptable.

2.7.1.1.5 Solubility and Chemical Affinity

The solubility and chemical affinity of the metals and compounds involved in a metallothermic reduction with other metals and compounds have significant effect on the reduction reaction. When reductant and the reduced metals have high mutual solubility or chemical affinity,the production of the pure reduced metal will not be possible as it will be contaminated by the reductant [70,71,75]. This is the case with most of the metallothermic reductions when aluminium, silicon, calcium or magnesium etc are used as reductants.

The chemical affinity and solubility aspect between the reductant and reduced metal may sometimes be used to decrease the thermodynamic activity of the reduced metal [75] in such a way as to provide extra driving force for reaction in the forward direction. This is what happens in the case of reduction of titanium dioxide (TiO_2) by aluminium.

A reaction between the compound to be reduced and the compound formed in reduction reaction will affect the reduction itself in an adverse way due to undesirable interaction between the two compounds [75].

The presence of a compound which will react with the product compound in reduction reaction, will facilitate the

reaction in the forward direction by decreasing activity of the product compound.

2.7.1.1.6 Distribution of Impurities Between Metal and Slag [72]

The reduced metal, in particularly when liquid, dissolves to a greater or lesser degree the many metal impurities contained in the initial substances or reducer. If the metal impurities posses a lesser affinity for the metalloid than the base metal, these contaminants are almost entirely reduced in process and pass over to the base metal. When the contaminating metals have a greater affinity for the metalloid than the base metal, these are partly reduced and reverted to the base metal.As a result, an equillibrium sets in with the metal impurities being distributed between metal and slag in accordance with the equation -

$$\frac{(M)_m}{K\ (MX)_s} = \frac{(M')_m}{K_1\ (M'X)_s} = \frac{(M'')_m}{K_2\ (M''X)_s} = \text{etc.}$$

2.7.1.1.7 Slag Metal Separation

2.7.1.1.7.1 Factors Influencing Slag-Metal Separation

The success of reduction process requires a proper slag-metal separation which can be achieved when taking into account the following.

(i) Sufficient heat of reaction for melting and consolidation of the metal and slag.

(ii) Wide difference between the densities of the metal and slag

[75,76].

(iii) Use of thermal boosters such as sulfur and iodine to improve slag-metal separation [77].

(iv) Sulfur has also been employed in aluminothermic reduction to yield a lower melting slag phase and thus facilitate the slag-metal separation [77].

(v) The separation of metal and slag phases can also be promoted by lowering the solidification temperature of metal phase through the formation of a selected alloy.

2.7.1.1.7.2 Role of Fluxes

The fluxes that are used in any pyrometallurgical operation may serve one or more of the following functions by way of changing composition of the existing slag with the formation of low melting phases or compounds to keep the slag in molten and well fluid condition for adequate time.

(i) decreasing the melting point of the slag thus making the whole mass molten at low temperature.

(ii) increasing the fluidity by weakening the interionic bonds and reducing the ionic sizes.

(iii) decreasing the activity of constituents of slag which will, therefore, favour the forward reaction to proceed.

Lime (CaO), Magnesia (MgO) and Fluorspar (CaF_2) are the fluxes which are frequently used in a metallothermic especially, aluminothermic reduction process. Most of the aluminates are not only high melting but very viscous when liquid. However, many aluminates such as calcium oxide aluminate have a very low

viscosity. CaO forms four chemical compounds with Al_2O_3 [72]; $3CaO.Al_2O_3$ (decomposes at 1535°C), $5CaO.3Al_2O_3$ (melting point 1455°C), $CaO.Al_2O_3$ (melting point 1600°C), $3CaO.5Al_2O_3$ (melting point 1715°c), forming a number of eutectics, the most low melting ones having the melting points 1395°C (49.8% Al_2O_3), and 1400°C (53% Al_2O_3). Therefore, lime is added to decrease the melting point of alumina slag and keep it molten for a longer time which helps in settling of metal droplets. Addition of lime also shows beneficial effects when added to Al_2O_3-SiO_2 system of slag forming low melting eutectics ranging from 1165 to 1380°C. Besides, the addition of CaO will decrease the activity of Al_2O_3 [68,70,78] and hence equillibrium is shifted to favourable direction.

Addition of magnesia in the presence of lime, though does not decrease the melting point to an appreciable extent, it certainly helps in increasing the fluidity of the melt [78].

Effect of flourspar addition, as studied by Behera and Mohanty [78], in an investigation on aluminothermic production of ferro + titanium, showed remarkable results with regard to alloy yield and titanium recovery. This was attributed partly due to high increase of fluidity and partly due to the fact that fluorspar like lime decreases the activity of alumina thus releasing TiO_2 for further reduction and formation of titanium.

2.7.1.2 Applications

Many elements like silicon, manganese, chromium, calcium,magnesium, titanium, molybdenum, vanadium, zirconium,

boron, columbium etc alloyed with iron go under the general name Ferro Alloys and are used in the production of carbon steel, alloy, tool and stainless steels. The natural source of these elements is in the form of oxides from which they are reduced to their metallic state. The heats of formation of these oxides are generally very high and hence their reduction to metals normally calls for very high energy requirements. Aluminium has been determined to be the most suitable reducing agent for the successful reduction of these oxides to produce carbon-free ferro alloys.

In practice, aluminothermic reductions are generally performed [67,68] in refractory lined reactors which may be either close bomb type or open type. In some cases, the reactions are carried out in presence of electric arc to meet additional heat requirement. The reduction reaction is triggered either by local priming with an electric fuse or magnesium ribbon or by externally heating the reactor in a furnace. On completion of reaction, the reactor is allowed to cool sufficiently prior to separation of reaction products. Simple physical or mechanical methods are generally applicable for separation of the consolidated metal from slag.

The production of chromium metal has now been established in commercial scale by adopting Goldsmiths process. In the process, chromium oxide and aluminium powder turnings are put in a refractory lined vessel and the reaction initiated by placing a small amount of the mixture of barium peroxide powder and magnesium in the charge and the charge is preheated before

initiating the reaction. In this process, chromium metal of about 97-99% purity is possible to be obtained.

In the last few years, a large number of R & D work in India and abroad on the thermit process for extracting some rare and refractory metals have been carried out [67,79]. As early as 1907 Von Bolton [80] and later Mondolfo have prepared niobium metal by aluminothermic reduction of its pentoxide . Later Wilheim et al. [81] have been able to get massive niobium metal by aluminium reduction of its pentoxide by externally heating around 1000^{o}C putting the charge contained in a sealed bomb. The yield was more than 90% and the metal contained around 2.2% aluminium. Jena and Gupta [82] obtained a similar result by detonating the reaction at a relatively lower temperature of 450^{o}C by using a mixture of calcium and sulfur for triggering the reaction. Processes have also been developed [83,84] for the production of massive tantalum from its pentoxide by reduction with aluminium. Use of calcium oxide (lime) and sulfur has been proved to be beneficial in producing low melting slag and as high as 90% yield of metal. Jena and Bose [85] obtained massive vanadium metal with an yield around 91% on 200 gm. scale of the oxide and using stoichiomtric amount of aluminium with the incorporation of sulfur in the charge to facilitate formation of low melting slag. Gupta and others [86] produced vanadium by open reduction of vanadium pentoxide on 200 gm V_2O_5 scale using 30% excess of aluminium and some lime to form lower melting eutectic of CaO and Al_2O_3. Jena and others [87] have been able

to make molybdenum metal by aluminothermic reduction of molybdenite concentrate in a vacuum induction furnace.

The production of low carbon and extra low carbon ferroalloys by aluminothermic process has got wide acceptance in the last few decades. Extensive work has been carried out in this direction and now the production of some ferro-alloys has become possible on commercially viable scale.Khodorovosky and Riss [88] established the method of successful production of carbon free ferro-chrome. Ferro-niobium has been produced by Mehra and co-workers [89,90] both from Indian columbite-tantalite ore and niobium oxide concentrate (obtained as byproduct from tantalum separation) using closed bomb and open reactor techniques. In the closed bomb test the scale of production was kept to be 1 kg with the incorporation of chemical triggers like Ca-S, Al-BaO_2 and Mg-$KClO_3$. The reaction was initiated by external heating to a temperature of about 900^{o}C. The open aluminothermic reduction was tested upto 10 kg scale using Mg-BaO_2 without the supply of external heat. In both the cases the alloys have been reported with high yields (over 85%), well consolidated and with clear separation from slag.

Aluminothermic ferrotitanium production has also been reported in literature. The technique was first introduced in Germany by Dautzenberg and Gissen [78] in which they confined the work to beach sand illmenite. In India the pioneering work in this field has been done in National Metallurgical Laboratory [91] where the investigators have produced ferrotitanium from

Kerala beach sand illmenite and obtained a maximum yield of 60% of alloy. Paretkar et al.established the effect of excess aluminium on the distribution coefficient and recovery of titanium. Behera and co-workers [92] made an attempt to produce ferrotitanium from massive illmenite rocks using lime as fluxing material and mixture of BaO_2 + $KClO_3$ as booster. In this regard they studied a few parameters such as preheat temperature of charge mixture, amount of aluminium as percentage of theoretical, particle size of aluminium and concentrate. The authors observed 83% yield with 36 mesh B.S.S. concentrate. They also studied the effect of fluxes on the yield of the alloy.

Possibilities have been searched out to recover the TiO_2 value of red mud in the form of ferrotitanium. Prasad and co-workers [6,20] have established that aluminothermic reduction of red mud is possible by raising the thermal potential of the charge to compensate for the inadequate insitu heat liberation.

2.7. 2 Recovery of Major Constituents

As noted earlier, since iron oxide, alumina and titania are present in red muds from high to moderate amounts, these muds have been considered as a source for recovery of these constituents.

2.7.2.1 Recovery of Iron

Due to dominant presence of Fe_2O_3 in several red muds, recovery of iron from these muds has been the point of attraction

of several investigators who considered it as a possible source material for the production of iron and steel for the countries having big alumina refineries but lacking in iron resources. Two main approaches investigated include solid state reduction of red mud by carbon or gaseous reducing agents and reduction smelting in a blast/electric/low shaft furnace to produce pig iron. McDowell-wellman Engg. Company (Ohio,U.S.A.) [93] have been successful in achieving a major break through in reduction smelting approach for the production of steel from red mud on a semi-industrial scale. The process comprises pelletising the red mud with coal and flux, sintering cum prereduction of pellets in a modified Dwight-Lloyd sealed circular machine, smelting of the prereduced pellets in a submerged arc electric furnace and finally oxygen blowing of the resulting pig iron in L.D.converter to produce steel. A method for briquetting of red mud in order to make it more suitable for smelting was worked out at the Research Institute for Non-ferrous Metals, Hungary [94] involving the addition of quick lime and homogenization. Optimum smelting conditions were obtained with a moisture content of 15-25% and a CaO content 10-20% .A method of thermal processing of red mud has also been reported [95] which is based on the recognition of the facts that dried alkaline red mud treated at a temperature of 400-700^{o}C and leached with dilute alkali may be converted into "secondary mud" which is considerably poorer in Al_2O_3 and Na_2O and can be easily filtered and washed. By smelting such a secondary mud in an electric furnace or low shaft kiln, slag containing pig iron and 18-20% of titanium oxide can be obtained

without additivies.

Dobos has reported [96]that pilot plant investigations at Almasfuzito proved the possibility of the continuous processing of red mud by the Krupp agglomeration process. Commerical scale experiments proved the possibility of obtaining from red mud a Krupp-slag similar to acid slags. The reducibility of Krupp process agglomerated red mud has been described to be extremely favourable with low dust losses. In the last stage of the experiment, an iron recovery of 81.5-83.0% was obtained with an average Fe content of 77-81% in the agglomerates.

Kontopoulos et al. [97] treated the Grecian red mud containing 39.11% Fe_2O_3 with prereduction, roasting and smelting for the recovery of iron. It has been shown that recovery of iron by magnetic separation was not feasible. Pellets prereduced at 1200^{o}C were compact, strong and highly metallized which could be smelted to produce a pig iron with almost 95% iron recovery. Farkas and co-workers [98] removed iron from red mud and prepared $Fe(CO)_5$ by treating in an autoclave with hydrogen or hydrogen containing gases at 0.1-100 bar and 150-800^{o}C. After removing $Fe(CO)_5$ from the autoclave, the residue contained 24.3% Al_2O_3 and the iron removal was 72.8%

2.7.2.2 Recovery of Alumina and Alkali :

Numerous attempts have been made to recover alumina from red mud with the simultaneous recovery of alkali. The approaches followed include [96,99] recovery of Al_2O_3 and Na_2O directly from the red mud, from the slag produced in the

reduction smelting for red mud and from the nonmagnetic portion left behind after removal of iron powder from reduced red mud.

Soda ash sintering and lime sintering followed by hot water leach have been among the favoured methods for recovery of alumina and alkali [6]. The recovery of alkali alone has been possible by treatment with lime under suitable conditions. Fursman and coworkers [6] devised an approach for the simultaneous recovery of not only alumina and alkali but also iron applying carbon-soda-lime sintering process. The process consisted of pelletising red mud with adequate quantities of carbon, soda ash,and limestone, sintering of these pellets in a shaft furnace, wet grinding of the reduced mass and its hot water leaching to produce sodium aluminate liquor which may be recycled to Bayer process circuit for alumina and caustic recovery. Subsequent wet magnetic separation of the leach residue results in an iron rich product which on melting yields pig iron.

Ziegenbalg and coworkers [100] attained the complete recovery of alkali metals from red mud by reduction smelting in an electric furnace with the addition of coke, lime and SiO_2 for the formation of pig iron and a slag containing not less than 20% $2CaO.SiO_2$. The Na_2O was sublimed during smelting and recovered as flue dust which was leached with alkali for the recovery of 85-95% of Na_2O. The self disintegrating slag was leached with alkali for the recovery of 78-82% of Al_2O_3 and recovery of pig iron was 99.6% . Recoveries of iron and aluminium were carried out by Yoshii Ishimura [101] from red mud after removing Na_2O.

The metallic iron has been produced by heating the leached red mud at 1450°C under reducing conditions. Al_2O_3 was recovered as $NaAlO_2$ by sintering the slag with CaO and $CaSO_4$ and leaching.

Ejima and coworkers [102] reported more than 80% recovery of aluminium from red mud using a pH control process. Aluminium was removed along with iron as $NH_4\ Al(SO_4)_2$. The leached solutions were freed from iron by control of pH.

Extensive and noteworthy investigations in this area have been carried out in Hungary by the Hungarian Aluminium corporation and Non Ferrous Metals Research Institute at Budapest.

2.7.2.3 Recovery of Titania

Titania is a major constituent of Indian and Surinam muds. Numerous investigations have been carried out to recover titania directly from the red muds, from the TiO_2-rich slag produced by the reduction smelting of red muds and non magnetic tailing of reduced red muds made by solid state reduction methods. The approaches include gravity concentration [103], chlorination [104], sulphuric acid digestion [105] and SO_2-treatment [106]. Sulphuric acid digestion has been described to be most successful which results in the dissolution of not only TiO_2 but also Fe_2O_3,Al_2O_3, Na_2O and some trance elements to form their respective sulphates. From leach solution, after reduction of ferric ion to ferrous state, hydrated titania is selectively precipitated out and recovered.

2.7.3 *Recovery of Trace Constituents*

Most of the trace elements like V,Ga,Zr,U, Th,Nb etc. present in bauxite get accumulated in the red mud thereby making it a raw material for the production of these elements. Logomerac [107,108] developed an approach consisting of reduction smelting of red mud followed by sulphuric acid leaching of resultant slag. Individual metals and trace elements are then recovered. From the leach solution by selective D2EHPA solvent extraction and stripping at controlled pH values. The process has been said to be of special interest to Yugoslavia. Cegledi [109] revealed the possibilities of recovery of rare metals from bauxite containing an average V_2O_5 0.4%, rare metal oxides 0.12%, Ga_2O_3 0.007%,TiO_2 2.9%, Mo_2O_3 0.003%, Nb_2O_3 0.005% and Sc_2O_3 0.002%.

Thakur and coworkers [110] reported the recovery of vanadium as sodium vanadate. Red mud roasted with sodium chloride and sodium carbonate at 850^{o}C, was quenched in water thereby obtaining vanadium in the form of alkaline solution containing $NaVO_3$, $NaAlO_2$ and $NaCrO_2$ free of titanium and iron.

2.7.4 Direct Applications of Red Mud

The presence of alkali and iron oxide in red mud lowers its fusion point and Na_2O may confer bonding properties to it [6]. With this view, possibilities have been searched out of producing self bonded bricks,building blocks and light weight aggregates. Such applications, however, have been described economically viable for the transportation radius not exceeding a few hundred kilometers.

Bricks may be made with the red mud alone or red mud with varying amounts of clay and proprietary binder. Such bricks have been reported [20] to posses sufficient strength, 100-500 kg/cm^2 depending upon the nature and quality of additives and firing temperature. Although the compression strength of such bricks have been experienced to be lower than those of fire clay bricks fired at same temperature, these are acceptable for building trade which generally requires the crushing strength not exceeding over 150 kg/cm^2. In India, the Central Building Research Institute, Roorkee has developed the technology for the production of constructional bricks [111,112] containing 50% red mud and 50% clay, but no commercial use has been reported. Prasad [113] has been successful in improving the soil mechanical properties of red mud by diluting the red mud with fly ash or lime. The modified red mud with fly ash additive has been said to have a definite potential for use in brick production and construction of dams, pavaments etc. As a result of his bench scale investigation, the another reveals that good quality bricks can be produced from the red mud diluted with 10-25% fly ash. Such bricks have been claimed superior to A-grade constructional clay bricks.

Red mud in admixture with shales or nonbloating clays would bloat on heating to yield light weight aggregates. One of the most prominent studies in this regard concerns the production of light weight structural products by very small additions of proprietary foaming agents, mud deflocculants and foam stabilisers. Nakamura et al [113] have demonstrated the

production of light weight building materials with densities ranging from 30 to 70 lbs/ft^2 and compressive strengths from 150 roof checking and floor slabs, interior partition, wall and ceiling tiles, fire-proof insulation materials, building blocks etc.

Red mud, due to its alkaline character with good cation exchange properties and a large surface area, may be used as a coagulant or flocculating agent for cleansing municipal industrial waste waters containing even poisonous species [114]. Red mud can be an effective absorbent for waste gases like H_2S and SO_2. It has been tested as an effective scrubber for the removal of S, H_2S and SO_2 from town/household gases [115].

Red mud has been shown to be a good raw material for making pigment for some applications. Efforts have been made by Satapathy and co-workers [116] to utilise the NALCO red mud for making red oxide pigment and paint of IS : 446 shade. The process includes hot water leaching of red mud to lower the alkalinity followed by filteration and drying at 378 K. The paint was prepared by treating this product with linseed oil, mineral turpentine oil and required amount of cobalt nickel napthanate in tumbler containing ceramic pebbles for a period of 48 hours. Formation of red oxide paint and pigment, however, is possible from the red muds with high-amounts of iron oxides.

the order of 400 KCal/kg. Although the heat is not sufficient to provide the thermal effects as established by perfect (74) for the proper running of the reaction and efficient slag-metal separation, it may be compensated by a combination of the booster addition and preheating the charge.

As the yield or recovery of the alloy is governed by the thermodynamic, kinetic, and physicochemical conditions of the melt, the factors directly or indirectly influencing those aspects may be undertaken for investigation.

In the reactor, radiation into surrounding medium, heat removed by the discharged gases and vapours are the main factors responsible for heat losses. Therefore, heat losses depend on the design of reactor, reaction rate and other factors (72). Reactors of different shapes and sizes have been reported to be used by various investigators. However, no systematic study has been reported about the effect of reactor geometry (signifying the design aspect) on the yield or the recovery of the alloy. In the present work, this aspect is also included which may be considered applicable to all the processes pertaining to aluminothermic preparation of alloys and metals.

The effects of the following parameters were investigated on the recovery values (overall Recovery, Ti-Recovery and Si-Recovery) and composition of the alloy produced by open aluminothermic reduction of Red Mud.

(i) Amount of reductant (Al, powder)

(ii) Scale of production (amount of Red Mud)

(iii) Particle size of reductant (Al, powder)

(iv) Particle size of Red Mud

(v) Geometry of Reactor

(vi) Flux Addition (Lime, Magnesia and Fluorspar)

(vii) Thermal Booster Addition ($KClO_3$, KNO_3)

(viii) Preheating temperature

(ix) Preheating time.

Most of these parameters were studied in couples in order have an idea about the better compromise between the coupled factors in producing improved recovery values . The following combinations have been undertaken for the present investigation with the expectation that their mutual influence on the thermodynamic, kinetic and physicochemical conditions of the melt, would provide useful information about the recovery of metallic values into the alloy.

(i) Amount and Particle Size of Reductant

(ii) Scale of Production and Reactor Geometry

(iii) Particle Size of Reductant and Red Mud

(iv) Booster Addition and Preheating Temperature

(v) Preheating Temperature and Time

(vi) Flux Addition (Amount and Type of flux)

CHAPTER - 4

EXPERIMENTAL

4.1 MATERIALS

The Red Mud was received from Hindustan Aluminium Company (HINDALCO), Renukoot (Dist. Mirzapur), India. The Materials used in this investigation along with their grade and make are listed in Tab. 4.1 below.

Table 4.1 List of Materials used.

Materials	Grade and make.
(i) Red mud	Received from HINDALCO, India.
(ii) Aluminium Powder	97.76% Al, as analysed (make not known)
(iii)Lime (CaO)	87.40% CaO as analysed, Burgoyne Urbidges & Co.
(iv) Fluorspar (CaF_2)	Extrapure 99%, CDH.
(v) Magnesia (MgO)	90.65% MgO as analysed, Fine Chem. India
(vi) Potassium Chlorate ($KClO_3$)	99.5% (AR), CDH.
(vii)Potassium Nitrate (KNO_3)	99% (AR), Samir Tech.

4.2 DETERMINATION OF CHEMICAL COMPOSITION OF RED MUD

The red mud was chemically analysed for Fe_2O_3, SiO_2, Al_2O_3, TiO_2, Na_2O and Loss of Ignition, by the gravimetric/ volumetric methods [119,120]. Discussed below the basic

principles.

4.2.1 Loss of Ignition

Bauxite mineral components transform to stable modifications at 1100^{o}C. The decrease in weight on ignition after deduction of adhering moisture gives loss of ignition.

4.2.2 Determination of SiO_2 Content

The red mud is dissolved in mixture of hydrochloric acid, nitric acid and sulfuric acid. The material left after acid digestion is in the form of silica gelly which is fumigated in presence of H_2SO_4 with hydrogen fluoride and left overs are ignited. The loss in weight is equal to SiO_2 content.

4.2.3 Determination of Fe_2O_3

The powdered red mud sample is digested with potassium hydroxide and acidified with sulfuric acid and then oxidised with potassium permanganate. The permanganate excess is decomposed by hydrochloric acid. Fe^{3+} is reduced to Fe^{2+} by $SnCl_2$. The iron is determined by chromatometric titration in presence of $HgCl_2$ and phosphoric acid.

4.2.4 Determination of Al_2O_3 Content.

The solution obtained from acid digestion of red mud is treated with 10 N NaOH to separate aluminium oxide in the form of sodium aluminate. Aluminium is determined by complexometric method.

4.2.5 Determination of TiO_2 Content

The TiO_2 in the acid solution leads to the formation of yellow coloured perexo-complexes with H_2O_2. The colour intensity of the solution is proportional of concentration of TiO_2. Colour intensity is measured by spectrophotometer. The evaluation of TiO_2 concentration is done with use of calibration curves.

4.2.6 Determination of Na_2O Content

The Na_2O content of the red mud is dessolved in nitric acid in presence of ammonium nitrate. The R_2O_3 group ions are removed by ammonium hydroxide and calcium is separated by ammonium carbonate and Na_2O content of the filterate is measured by the flame photometer. The evaluation of Na_2O content is done by the use of calibration curves.

Table 4.2 gives out the results of chemical analysis of the considered red mud.

Table 4.2 Chemical composition of Red Mud

Fe_2O_3	TiO_2	SiO_2	Al_2O_3	Na_2O	LOI
38.80%	18.80%	9.64%	17.28%	6.86%	7.34%

4.3 PHASES PRESENT IN RED MUD

The mineral phases present in red mud as identified by X-Ray Diffractometry described in [121], are listed below in Table 4.3.

Table 4.3 Mineral phases present in Red Mud

Hematite	Maghemite	Quartz
Alumohematite Anataze	Pseudo-rutile ($Fe_2 Ti_3 O_9$)	Kaolinite
Boehmite	Calcium Titanate	
Gibbsite	Calcium alumine silicate	

4.4 CHEMICAL ANALYSIS OF ALLOY BUTTON

4.4.1 Determination of Iron

1.0 gm powdered sample of reduced button was taken in a beaker and dissolved in conc HNO_3 and evaporated to dryness. Now 5 ml of H_2SO_4 was added covered with watch glass and heated to white fumes. Now beaker was cooled and 15ml of conc HCl was added and boiled, then diluted with water and filtered: The residue of filter paper was washed four or five times with hot water until free from iron. The filterate was taken in a measuring flask of 250 ml and made upto the mark with distilled water. Then 25ml. of the above solution was taken into a conical flask and heated to boiling. Then stannous chloride was added drop by drop till the red colour in ferric iron was completely discharged. A few drops of more $SnCl_2$ were added and cooled quickly to room temperature by putting the flask under running tap water. Then four drops of $HgCl_2$ solution were added to the above reduced solution, which is followed by the addition of 2 drops of indicator. This solution is then titrated with standard $K_2Cr_2O_7$ solution. When indicator

gave a violet colour the oxidation of Fe^{++} to Fe^{+++} is completed; Reading corresponding to this end point was noted down from buratte; percentage of iron is calculated by

$$\% \text{ Fe} = \frac{0.56 \times \text{volume of soln. prepared X Burette Reading}}{\text{vol. of solution taken for titration}}$$

4.4.2 Determination of Silicon

The filter paper used for the filteration of the above solution was transferred to a silica crucible alongwith the residue in it. The silica crucible with the residue was ignited in a muffle furnace to $900^{o}C$ and then cooled and weighed. the percentage of silicon is given by -

% Si = Weight of ignited mass X 46.7

4.4.3 Determination of Titanium

4.4.3.1 Preparation of sample solution

1.0 gm of powdered sample of metal (alloy) was taken in a beaker and dissolved in conc. H_2SO_4 and then filtered. Filtered solution was made upto 250 ml. by adding water. 20 ml of this solution was taken in a flask and about 20 ml of H_3PO_4 was added to the flask to remove iron followed by the addition of H_2O_2 solution to get yellow colour.

4.4.3.2 Preparation of standard solution

0.82 gm of potassium titanium oxalate, 2 gm of ammonium sulfate and 25 c.c. of conc H_2SO_4 were mixed upto dissolution.

Then it was made 250 cc by adding water. 20 ml of this solution was taken and added to it some H_3PO_4 and H_2O_2 as added in sample solution.

4.4.3.3 Preparation of reference solution

2 gm of $(NH_4)_2SO_4$ is dissolved in 25 cc of conc. H_2SO_4 and made 250 cc; After preparation of all three solution firstly reference solution was taken in cubette tube which was then put in the required space in spectronic-20 colorimeter, so that scale was adjusted to 100 and 0 respectively.Then standard solution was taken in the tube and standardised the apparatus. Readings are noted for different concentrations. Then for 1:10 conc. of sample solution all readings were taken. The above readings are plotted together in the graph. Then Ti is calculated as follows-

Since 1cc = 0.5 mg of Ti. Reading of vertical line which cut the x-axis at different concentration -

$$\% \text{ Ti} = \frac{\text{Concentration} \times 0.5 \times 100}{1000} = \text{Concentration} \times 0.05$$

4.4.4 Determination of Aluminium

The Al content of the alloy was determined by applying principle of precipitation by cupferron from a cold formic acid solution [119].

4.5 DRESSING OF RED MUD

The as received red mud was in the form of solid lumpy masses. The dressing operation was done in the following steps.

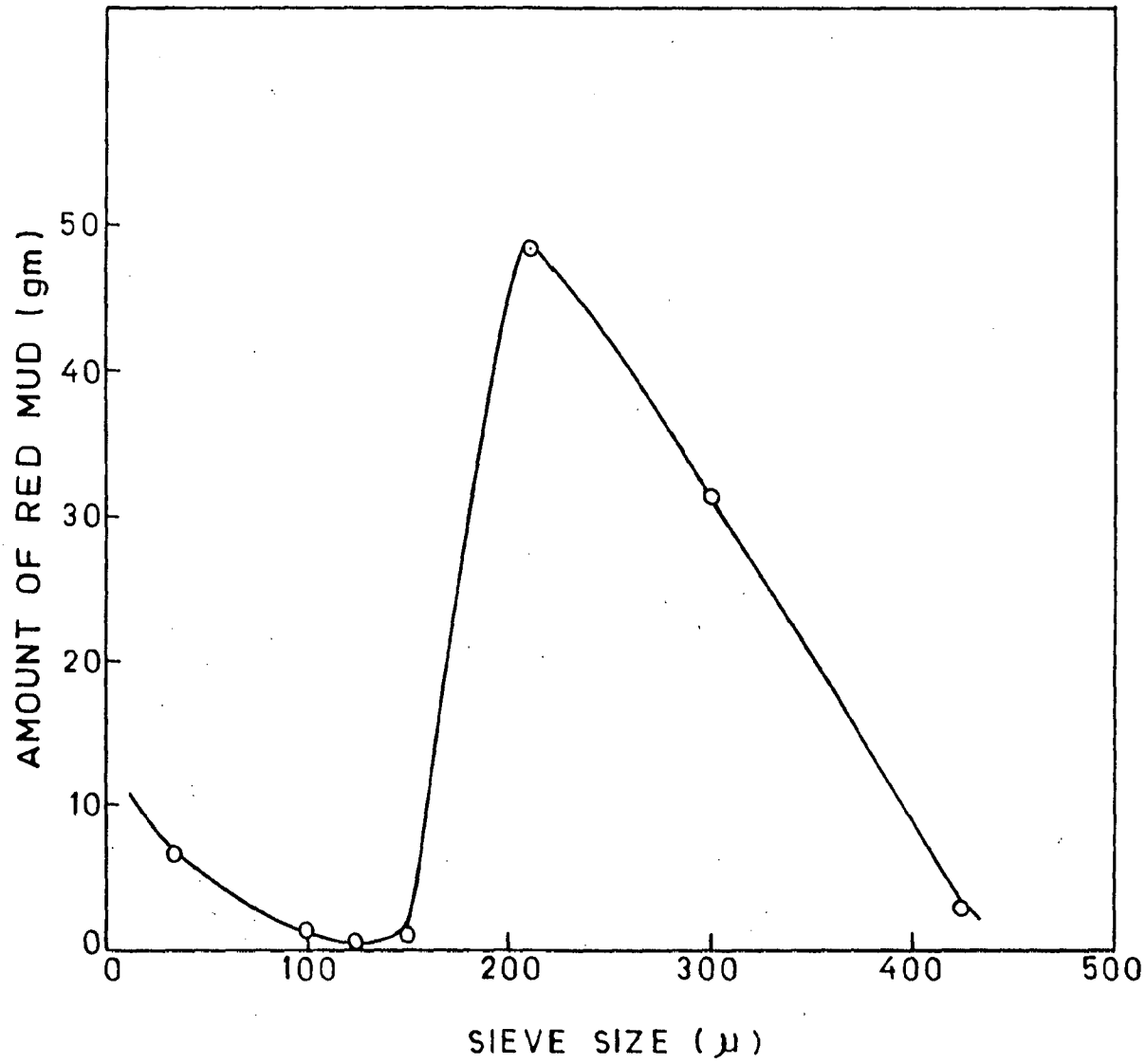

Fig.4.1 Particle size distribution of Red Mud.

(i) Ball Mill Grinding

(ii) Sizing

4.5.1 Grinding in Ball Mill

To make the red mud in powder form it was ground in Ball Mill. 10 kg of red mud was ground at a time using 25 balls of different sizes. The Ball mill was operated for 5 hrs.

4.5.2 Sizing of Red Mud

The red mud powder from Ball mill was subsequently divided into three sizes namely; -425+300, -300+212 and -150+125 microns in a Rotap Sieve Shaker. The sieves were kept in the following order of sizes from top to bottom; 425, 300 212, 150 and 125 microns. At one time nearly 200 gms of red mud was taken for sizing by operating the shaker nearly for 10 minutes. The size distribution of red mud is shown in Fig. 4.1.

4.6 Sizing of Aluminium Powder

The aluminium powder was also sized in the same manner as red mud. It was divided into the following sizes; -425+300, -300+212, -300+150, -150+125 , -106+63, -63+53 and -53+45 microns. The setting of the sieves was carried out according particle size requirements.

4.7 PROCESS SET UP FOR ALUMINOTHERMIC REDUCTION OF RED MUD

The reduction reaction was conducted in graphite crucible (Reactors). The crucibles were not lined with the view

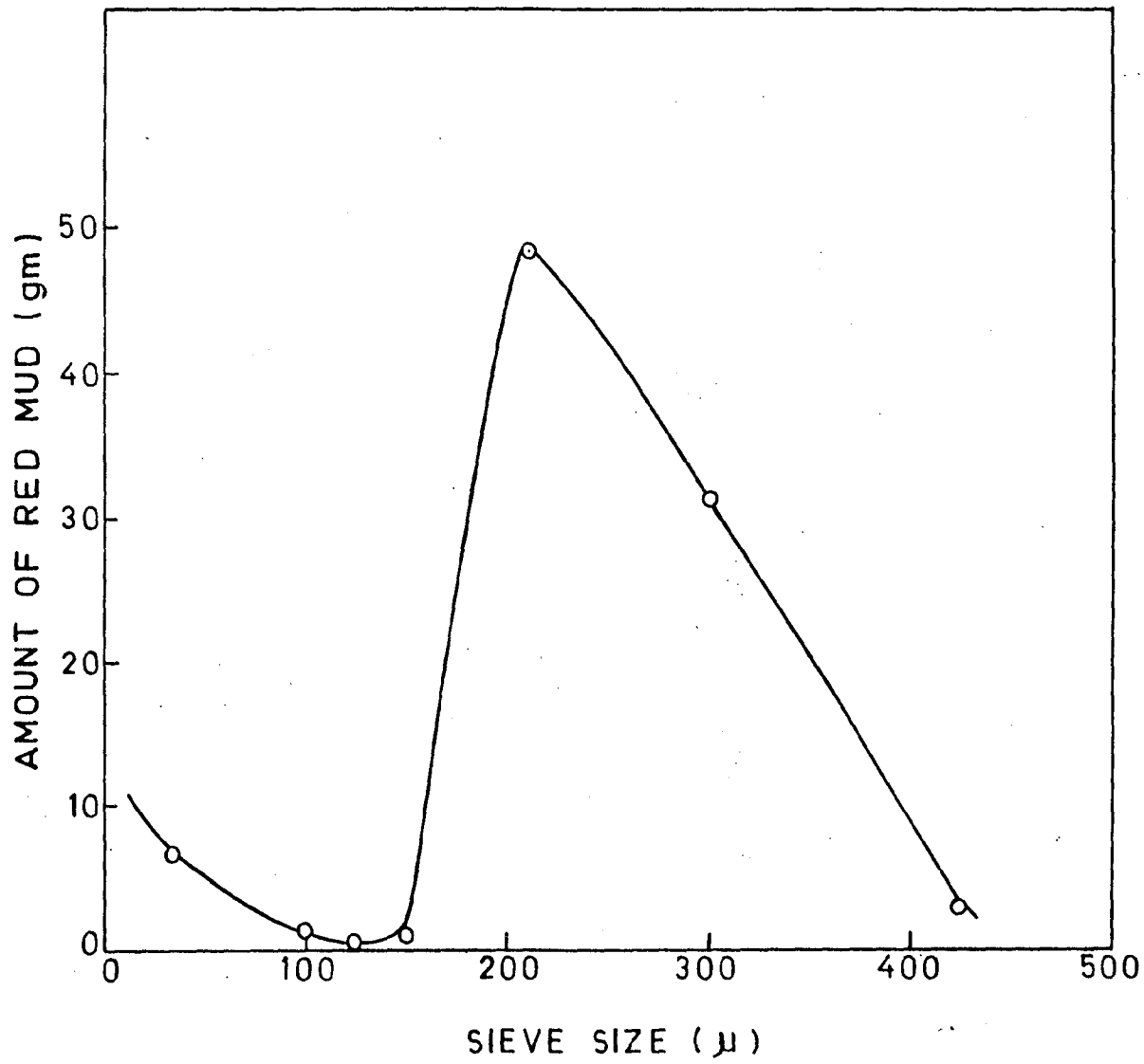

Fig.4.1 Particle size distribution of Red Mud.

(i) Ball Mill Grinding

(ii) Sizing

4.5.1 Grinding in Ball Mill

To make the red mud in powder form it was ground in Ball Mill. 10 kg of red mud was ground at a time using 25 balls of different sizes. The Ball mill was operated for 5 hrs.

4.5.2 Sizing of Red Mud

The red mud powder from Ball mill was subsequently divided into three sizes namely; -425+300, -300+212 and -150+125 microns in a Rotap Sieve Shaker. The sieves were kept in the following order of sizes from top to bottom; 425, 300 212, 150 and 125 microns. At one time nearly 200 gms of red mud was taken for sizing by operating the shaker nearly for 10 minutes. The size distribution of red mud is shown in Fig. 4.1.

4.6 Sizing of Aluminium Powder

The aluminium powder was also sized in the same manner as red mud. It was divided into the following sizes; -425+300, -300+212, -300+150, -150+125 , -106+63, -63+53 and -53+45 microns. The setting of the sieves was carried out according particle size requirements.

4.7 PROCESS SET UP FOR ALUMINOTHERMIC REDUCTION OF RED MUD

The reduction reaction was conducted in graphite crucible (Reactors). The crucibles were not lined with the view

that carbon pick up would not interfere with the recovery values of the reduced metallics into the alloy. Five crucibles namely A,B,C,D and E of different shapes and sizes (specifications given in Table 4.4) were used according to our experimental requirements. Crucibles A,B and C belong to same shape (bucket shape) but differ in sizes in the order A < B < C. Reactor 'D' was formed by adjoining the open ends of the two 'A' crucibles with the fire clay paste at the joint. The joint is more secured by tightening a steel ring around it. To create the open end of this reactor, the bottom of the upper crucible was removed by cutting it at an appropriate height. Reactor 'E' belongs to the

Table 4.4 Details of Reactors' specifications

Reactor	Height H (cm)		Inner diameter (cm)		Thickness of wall (cm)	$R = \frac{H(inner)}{D_2 - D_1}$
	Inner	outer	Bottom D_1	Top D_2		
'A'	14.50	16.50	7.50	11.30	1.50	3.816
'B'	18.50	20.50	9.00	13.00	1.50	4.625
'C'	20.50	22.50	11.00	15.00	1.50	5.125
'D'	26.00	28.00	7.50	9.00	1.50	A-A Assembly, Refer Fig.4.4 and Fig.4.5
'E'	18.50	20.50	12.50	12.50	1.50	∞

cylindrical shape which was prepared by hollowing a graphite electrode. Fig. 4.2, Fig. 4.3 and Fig 4.4 illustrate the

sectional views of these reactors whereas Fig. 4.5 shows their graphical representations in terms of height and diameter.

The Reactors can also be represented by a geometrical factor 'R' given as

$$R = \frac{H}{D_2 - D_1}$$

where H = Height of the reactor

D_2 = Inner diameter of the open end (top).

D_1 = Inner diameter of bottom

In case of Reactor 'D' it can be represented graphically as shown in Fig. 4.5.

4.8 SEQUENCE OF PROCEDURES

4.8.1 Charge Preparation

Weighed amounts of Red Mud, Aluminium Powder, Thermal Booster ($KClO_3$ or KNO_3) and Flux (Lime or Magnesia and Fluorspar) were transferred to a horizontally rotating ceramic mixer containing ceramic balls. The mixing was carried out by adding the ingradients in two stages. In the first stage Red Mud, Al, powder and thermal booster are added to the mixer. Flux is added in the second stage after 15 minutes of mixing the above ingradients. This was done to ensure the maximum possible interfacial contacts between the reductant and the reducibles. The mixer was operated for another 5 minutes after flux addition. The prepared charge was now transferred to graphite reactors (crucibles) for preheating and subsequent operations.

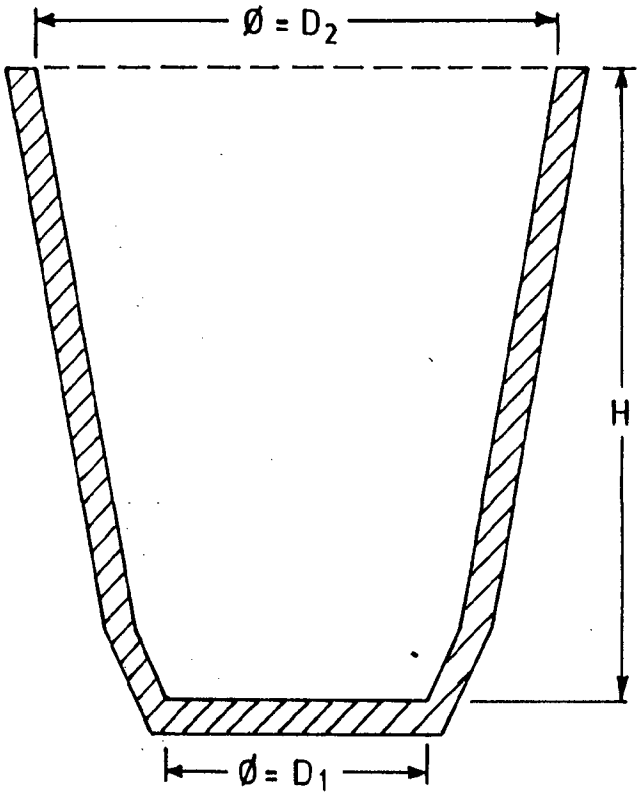

Fig.4.2 : Shape of Reactor A,B, and C.

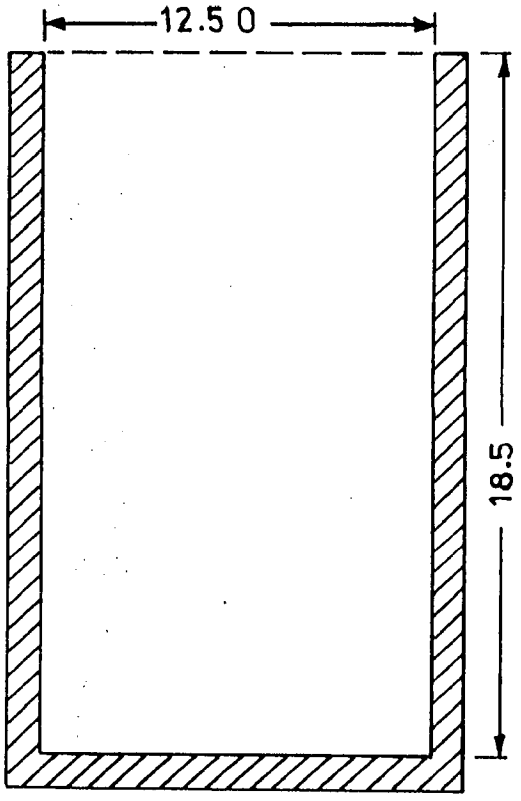

Dimensions in cm

Fig.4.3 Sectional view of Reactor E.

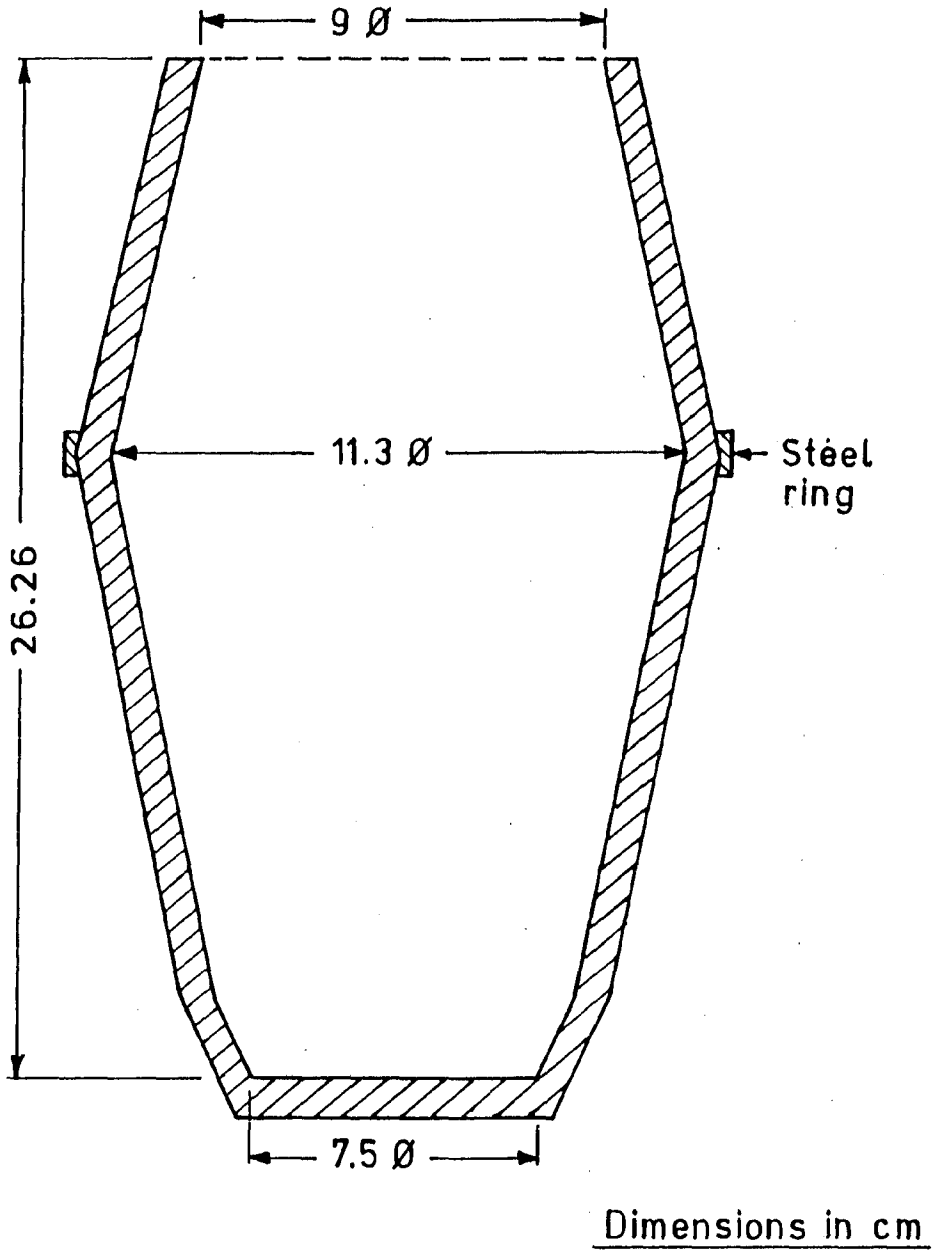

Fig.4.4 : Sectional view of Reactor D.

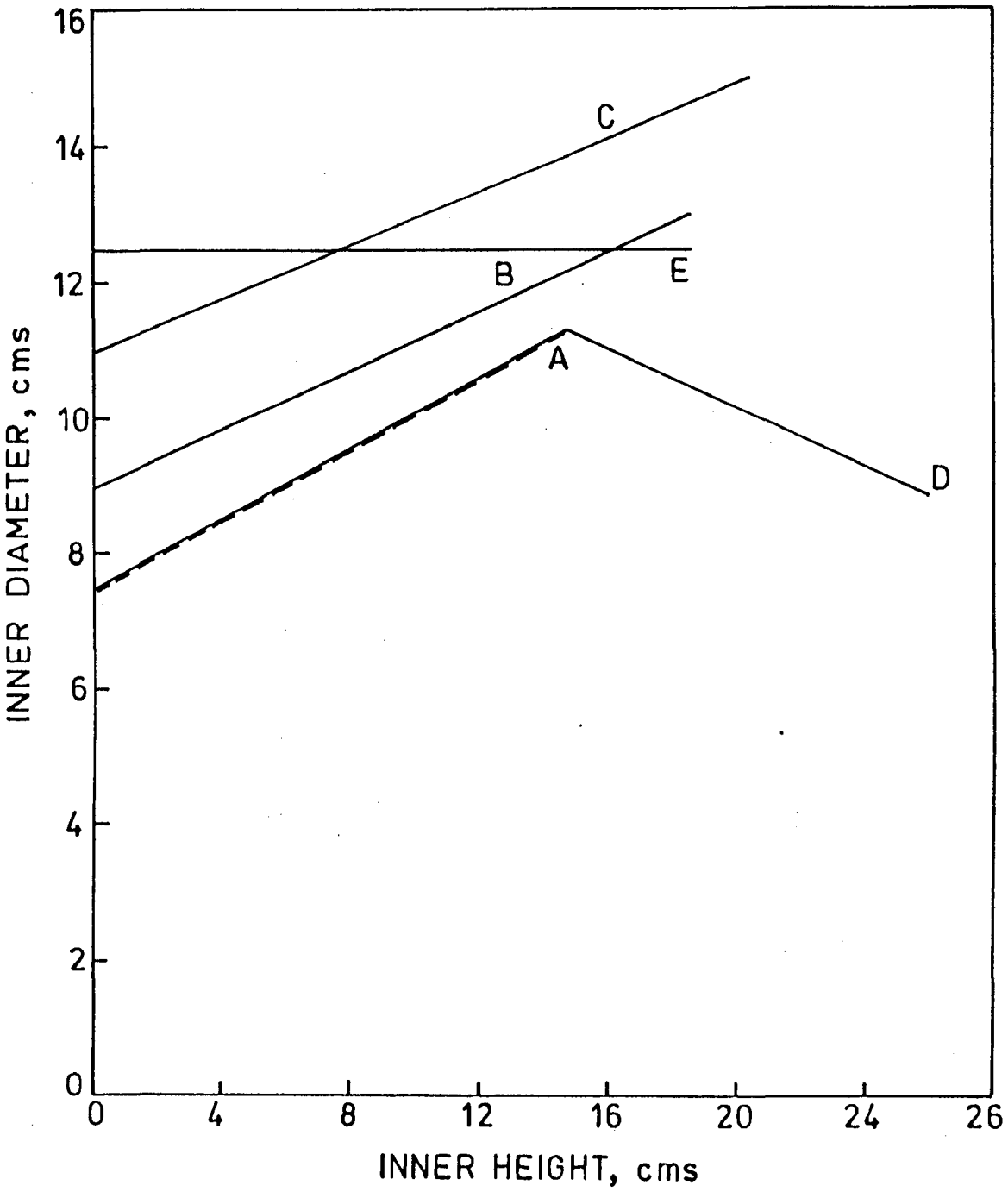

Fig. 4.5 Graphical representation of Reactors A,B,C,D and E in terms of height and diameter.

4.8.2 Preheating of the Charge

The charge filled reactor was placed in a Resistance Pit Furnace for preheating. The time of preheating was counted after the indicator started showing the applied preheating temperature.

4.8.3 Ignition of the Charge

The crucible was taken out of the furnace to the open space where the reaction was triggered by touching a burning sparkler on the surface of the charge.

4.8.4 Separation of Alloy Button

After sufficient air cooling of the reaction products, the alloy button was separated from the slag by simple mechanical operations.

Fig. 4.6 presents a simplified Flow Sheet of the procedures followed in conducting the aluminothermic reduction.

4.9 CHARGE CALCULATION

The stoichiometric amount of aluminium (reductant) was determined with the presumption that Fe_2O_3, TiO_2 and SiO_2 are completely reduced in the course of reduction process. The reactions can be expressed by the following chemical equations.

$$Fe_2O_3 + 2Al \longrightarrow 2\,Fe + Al_2O_3$$

$$3\,TiO_2 + 4Al \longrightarrow 3\,Ti + 2\,Al_2O_3$$

$$3\,SiO_2 + 4Al \longrightarrow 3\,Si + 2\,Al_2O_3$$

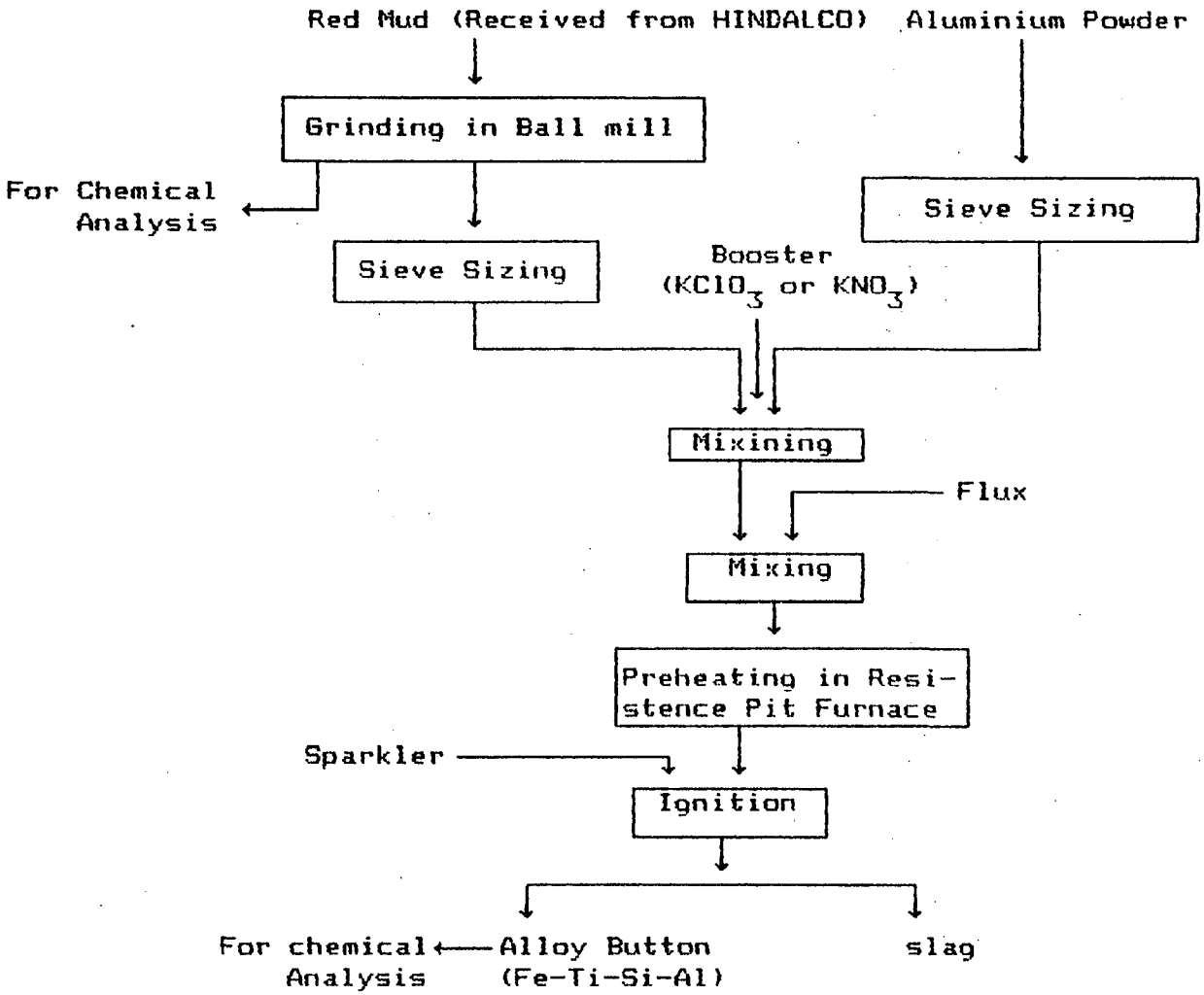

Fig.4.6 Flow Sheet of Aluminothermic Reduction of Red Mud

For the reduction of 100 gms of Red Mud, the stoichiometric requirement of Al was calculated as follows.

(i) Amount of Al to reduce Fe_2O_3,

$$= \frac{54}{160} \times 38.80 = 13.095 \text{ gms}$$

(ii) Amount of Al to reduce TiO_2,

$$= \frac{108}{240} \times 18.80 = 8.46 \text{ gms}$$

(iii)Amount of Al to reduce SiO_2,

$$= \frac{108}{180} \times 9.64 = 5.784 \text{ gms}$$

The total amount of Al,

$$= 13.095 + 8.46 + 5.784 = 27.34 \text{ gms}$$

4.10 Thermicity of the Charge

The heat librated in reaction was computed on the basis of the data presented in Table 2.15 which furnishes following amounts of heat produced by the reduction of reducible components-

$$Fe_2O_3 + 2Al \longrightarrow 2\,Fe + Al_2O_3,\ \Delta H_{298}{}^{o}{}_{k} = -204 \text{ Kcal}$$

$$3\,TiO_2 + 4Al \longrightarrow 3\,Ti + 2\,Al_2O_3,\ \Delta H_{298}{}^{o}{}_{k} = -132.40 \text{ Kcal}$$

$$3\,SiO_2 + 4Al \longrightarrow 3\,Si + 2\,Al_2O_3,\ \Delta H_{298}{}^{o}{}_{k} = -149.10 \text{ Kcal}$$

Heat liberated by the reduction of 100 gms of Red Mud -

$$= \frac{204}{160} \times 38.80 + \frac{132.40}{240} \times 18.80 + \frac{149.10}{180} \times 9.64 = 67.80 \text{ Kcal}$$

Thermicity of the charge (Kcal/kg) was calculated by

the following expression

$$\text{Thermicity (Kcal/kg)} = \frac{\text{Heat liberated by the charge during reaction}}{\text{Total weight of the charge (kg)}}$$

The charge represents the total of the amounts of Red Mud, Al powder, Flux and Thermal Booster.

4.11 CALCULATION OF RECOVERY VALUES OF THE ALLOY

(a) Overall Recovery (OR)

The Overall Recovery was calculated with the consideration that the alloy contained only Fe,Ti,Si and Al. It can be defined as percentage of total amount of reducible metallics (Fe+Si+Ti) of red mud which passed into the alloy. The following expression was used to calculate the Overall Recovery;

$$OR\ (\%) = \frac{W_A - \frac{W_A . P_{Al}}{100}}{W_{RM}} \times 100$$

where

W_A ; Weight of alloy button

W_{RM} ; total amount of Fe+Ti+Si in the considered lot of Red mud.

P_{Al} ; Percentage of Al in the alloy

(b) Individual Recovery of Constituents of the Alloy

The recovery of the constituent metal was calculated as follows.

$$\% \text{ Recovery of constituent metal} = \frac{W_A \cdot m}{M}$$

where

W_A ; weight of the alloy

m ; percentage of the considered metal in the alloy

M ; amount of the same metal value in the Red Mud.

CHAPTER - 5

RESULTS AND DISCUSSION

5.1 EFFECT OF AMOUNT AND PARTICLE SIZE OF REDUCTANT

The effect of amount of reductant (Al, powder) was investigated in terms of the percentage excess over stoichiometric amount. The amount of reductant was varied as 0, 20, 40, 60, 80 and 100% excess over stoichiometric requirement. The study was made for three different sizes of reductant namely; -63+53, -106+63 and -300+150 microns (sieve size). The charge make up is given in Table 5.1 whereas Table 5.5 presents the charge balance of heat taken for this investigation.

5.1.1 Effect of Amount of Reductant (Al) of Particle Size, -63+53 Microns.

The results pertaining to the recovery values and compositions of the alloys are reported in Table 5.2 and respectively plotted in relation to the amount of reductant in Fig. 5.1 and Fig. 5.2.

Fig. 5.1 indicates that the overall recovery increased sharply for upto 40% excess amount of reductant. Beyond this mark the increase in overall recovery slowed down and tended to assume a constant value. It can also be observed that upto 40% excess reductant, the overall recovery was dominantly contributed by the recovery of Fe.

The recovery of Ti which was marginal for upto 20% excess reductant, increased significantly beyond it upto the mark

Table 5.1 Details of charge composition and parameters of the process. (amount and particle size of reductant)

(a) Constant Parameters-	
(i) Amount of Red mud (scale of production)	500 gms.
(ii) Amount of CaO	50% of Al-powder (reductant)
(iii) Amount of fluorspar (CaF_2)	10% of CaO
(iv) Amount of heat booster ($KClO_3$).	15% by wt. of (R.M.+ Al powder + CaO + CaF_2)*
(v) Particle size of red mud.	-300 + 212 microns.
(vi) Particle size of lime (CaO).	-63 microns.
(vii) Particle size of fluorspar.	-63 microns.
(viii) Temperature of preheating.	400^{o}C
(ix) time of preheating.	2 hrs.
(x) Geometrical parameters of reactor	Reactor'B' (as specified in section 4.7)
(b) Variables-	
(i) Amount of Reductant (Al).	0,20,40,80, and 100 percent excess over stoichiometric amount.
(ii) Particle size of reductant (Al).	-63+53, -106+63 and -300 +150 microns.

* described as total charge.

representing 80% excess reductant (Fig. 5.1). Above 80% excess reductant, however, the magnitude of increase in recovery of Ti narrowed down. The recovery profile of Si also showed the similar trend but with appreciably lower recovery values. Fe was recovered to the maximum extent with same trend as exhibited by Ti and Si. Regarding the composition of the alloy, which can be observed from the Fig. 5.2, the Ti and Si content of the alloy increased with the increase in the amount of reductant (i.e. Al powder) almost proportionately to their recovery values. The Al content of the alloy first decreased for upto 40% excess reductant and then started increasing significantly beyond it.

5.1.2 Effect of Amount of Reductant of Particle Size, -106+63 Microns.

Recovery figures and compositions of the alloys are given in Table5.3 and plotted in relation to amount of reductant in Fig. 5.3 and Fig. 5.4 respectively. In this case also, the amount of reductant affected the recovery values as well as their reduced metallic content in the same way as experienced with the reductant of particle size, -63+53 microns. Comparing with the previous case this is noteworthy in this case that while the recovery levels of Ti increased, a significant drop was noticed in respect of Si recovery. The maximum Ti recovery 48.00% (for 100% excess reductant) was obtained as against 45.92% in the preceding case. Maximum 14.43% Si was recovered in this case which was 24.78% (for 100% excess reductant) in the previous case. Besides this, the alloys obtained for the amount of

reductant beyond 60% excess, possesed higher Ti content than the last case. The trend of variation of Al content also remained unaffected but the alloys contained higher percentage of Al (Fig. 5.4).

5.1.3 Effect of Amount of Reductant of Particle Size, -300+150 Microns

Results are reported in Table 5.4. Fig. 5.5 and Fig. 5.6 indicate that recovery values of the reduced metallic constituents as well as their contents in the alloy followed the similar trend of variation by increasing the amount of reductant. No significant variation was observed on the recovery values of Ti and Si as well as their content in the alloy compared to previous case.

Fig. 5.6 indicates that the Al content of the alloy showed an increasing trend with increasing amount of reductant. Upto 60% excess reducer the increase remained marginal and rather sharp beyond it.

5.1.4 A General Observation and Discussion of Results

This investigation which led to the formation of an alloy containing as high as 16.26% Ti revealed the following facts :

(i) The metal can only be recovered by using excess amount of reductant (Al) over stoichiometric requirement.

(ii) Recovery values as well as the reduced metallic content can be significantly improved by increasing the amount of

reductant upto 80% excess over stoichiometric amount beyond which the magnitude of increase in recovery values starts diminishing.

(iii) An increase in the particle size of reductant (Al) though does not disturb the relationship of its amount with recovery values of the alloy, the numerical magnitudes of recovery values may vary. According to observations, the recovery levels shifted towards higher side for the reductant of particle size -106+63 microns beyond which they tended to assume almost constant values.

(iv) A decreasing tendency upto 40% excess reductant followed by an increasing tendency beyond it has been exhibited by the Al content of the alloy for the reductant particle sizes -63+53 microns, -106+63 microns. However, with the reductant of particle size, -300+150 microns, the Al content of the alloy has shown an increasing tendency by increasing the amount of reductant.

This study makes an hint that an alloy with lower Si and Al content is possible to produce by using the reductant amounting 40% excess over stoichiometric amount, provided a heavy sacrifice has to be made in respect of Ti content of the alloy. In order to get higher Ti recovery and hence its content in the alloy, the passage of Si and Al into the alloy is unavoidable. It follows from the examination of the equilibrium constant of the reaction of reduction of TiO_2 by aluminium, TiO_2+4/3 Al $\longrightarrow$Ti+ 2/3 Al_2O_3 that increasing the concentration of Al in the alloy

$$K = \frac{a_{Ti} . a^{2/3}_{Al_2O_3}}{a_{TiO_2} . a^{4/3}_{Al}}$$

displaces the equilibrium towards the formation of titanium i.e increase in its recovery in the alloy [69]. The equilibrium constants of Fe_2O_3, and SiO_2 are also shifted towards the formation of respective elements. This increased recovery of Ti is obtained with the simultaneous increase in the Al content of the charge. Increasing the Al content of the charge beyond a certain maximum level may not result in any material increase in the titanium yield because the excess Al which passes into the additional loss of alloy in the form of metal droplets entrapped additional loss of alloy in the form of metal droplets entrapped in the slag. The amount of heat liberated in the process (Table 5.1 for charge composition) has been calculated to be around 946.38 kcal/kg (discussed in section 5.5) out of which 384.84 kcal/kg is contributed by the exothormicity of reducible components of red mud. Therefore, the presence of excess amount of reductant in the charge, not only provides better thermodynamic conditions for the smooth running of reduction but also ensures the availability of the in-situ heat liberation thus maintaining the heat effects of the process during the course of reduction (discussed in section 5.4 and 5.5).

Considering Fe_2O_3, TiO_2 and SiO_2 as fully reducible components in red mud, the constitution of red mud in other way, may be presented as containing 67.24% reducibles (Table 4.2) and

rest 32.76% non-reducibles. When practicing the stoichiometric amount of Al (i.e 0% excess), which was made on the basis of reducible components, it may not be possible to have stoichiometric concentration available at the sites of reducibles in the bulk of charge because of its dilution by the non reducible fraction (32.76%). This may account for the reaction to proceed sluggishly without any metal being recovered.

The particle size of reductant may influence the reduction process in two ways ; firstly by changing the number of reaction interfaces and secondly by affecting the kinetics. Though very fine particles of Al may provide increased number of reaction interfaces, they disappear quickly from the sites of reduction reaction and hence the peak temperature is not maintained for the time adequate for the proper slag-metal separation [68]. On the contrary too coarse particles not only reduce the number of reaction interfaces but also lower the peak temperature. In other words, a proper selection of particle size of reductant is very necessary.

The charge being in the solid form, it may not always be necessary, that the amount of reductant with view point of stoichiometry provides the sound thermodynamic condition at the sites of reducibles. The finer the reductant, the better will be the chances of getting desired concentration of reductant at the sites of reducibles. Therefore, besides the stoichiometric consideration, it may also be important to take into account the aspect of reaction interfaces in the sense that the amount and particle size of reductant should be such that it may provide the

maximum possible number of reaction interfaces. The maximum number of reaction interfaces to be created, however, will depend upon the amount and particle size of reducibles provided the degree of mixing is ideally maximum. Our observation regarding a sudden drop in Al content of the alloy at 40% excess reducer (Fig. 5.2 and Fig 5.4) may be attributed due to this reason. At this mark, the concentration of Al in the red mud was calculated to be 54.68 gms/100 gms of red mud which is more than the stoichiometric concentration (45 gms/100 gms of red mud). In addition to this, the maximum availability of reaction interfaces ensuring the reduction of a higher fraction of reducibles, may be the reason behind the higher consumption of Al in actual reduction process and hence lower Al content in the alloy.

5.2 EFFECT OF SCALE OF PRODUCTION (AMOUNT OF RED MUD) AND REACTOR GEOMETRY

The effect of scale of production i.e. amount of Red Mud was investigated by varying it as 100,200,300, 400,500 and 600 gms (depending on the capacity of the reactor). Five reactor namely A,B,C,D and E (specified in section 4.7) were selected to conduct this investigation. Out of these reactors, A,B, and C are similar in geometry (shape) but differ in sizes whereas reactors D and E differ in geometry also. The composition of the charge prepared is given in Table 5.6. The Table 5.12 presents the charge balance of heats associated with this study.

Table 5.6 Details of charge composition and parameters of the process.(Scale of production and reactor geometry).

(a) Constant Parameters-	
(i) Amount of reductant (Al).	80% excess over stoichiometric amount
(ii) Amount of CaO	50% of reductant (Al)
(iii) Amount of fluorspar (CaF_2)	10% of CaO
(iv) Amount of heat booster ($KClO_3$).	15% by wt. of (R.M. + Al, powder + CaO + CaF_2).
(v) Particle size of red mud.	-300 + 212 microns.
(vi) Particle size of reductant (Al)	-106+63 microns.
(vii) Particle size of lime (CaO).	-63 microns.
(viii) Particle size of fluorspar (CaF_2).	-63 microns.
(ix) Temperature of preheating.	400^{o}C.
(x) Time of preheating.	2 hrs.
(b) Variables-	
(i) Scale of production (amount of red mud)	100,200,300,400,500 and 600 gms.
(ii) Reactor geometry.	-Reactors A,B,C,D, and E as specified in section 4.7

5.2.1 Effect of Scale of Production in Reactors A, B, and C

The data regarding the recovery values and compositional details of the alloys produced in these reactors, which differ in size (capacity) in the order A<B<C, are given in Table 5.7, Table 5.8 and Table 5.9 for reactors A,B, and C respectively. These Tables also include the geometrical details received by the charge column in the associated reactor.

The observed relationships of recovery value as well as the composition of the alloy with the scale of production are shown respectively in Fig.5.7 and Fig.5.8 (for Reactor 'A'), Fig.5.9 and Fig.5.10 (for Reactor 'B') and Fig.5.11 and Fig.5.12 (for Reactor 'C'). It is evident that overall recovery increased significantly by increasing the scale of production to a certain maximum level.Reactor 'A' observed the increase in overall recovery for the scale of production upto 300 gms beyond which is started droping. For reactors 'B' and 'C' the increase in overall recovery could be observed on going upto 500 gms although the alloy could not be recovered for 100 gms production scale. This can also be noted that the overall recovery was dominantly contributed by Fe recovery for upto 200 gms production levels.

The recovery of Ti increased with the similar trend in the all the reactors (A,B,C) by increasing scale of production. Making a comparison among the reactors A,B and C in respect to Ti recovery values obtained for upto 400 gms production levels, it can be observed that by increasing the size of reactor, the Ti recovery first increased on going from reactor 'A' to reactor 'B' and then decreased on going to reactor 'C'. The recovery of Ti

i.e. 31.57% as obtained in reactor 'A' at 400 gms scale of production was enhanced substantially to the level of 41.5% in reactor 'B' and it droped to 29.33% in reactor 'C'. Now on comparing reactor 'B' and 'C', for above 400 gms scale of production reactor 'C' can be observed to furnish higher recovery of Ti than reactor 'B'.

The Si recovery also increased with the increase in scale of production as well as the size of the reactor. The trend of increase remained almost same in reactor 'A' and reactor 'B'. However, reactor 'C' showed an increasing trend for upto 300 gms scale of production and a decreasing trend leading to constant recovery level, beyond 300 gms (Fig.5.11).

The Ti and Si contents of the alloy varied almost proportionately to their respective recovery values (Fig.5.8, Fig.5.10, Fig.5.12). The maximum Ti content of the alloy as received in reactors A,B and C are 13.19%, 16.12% and 16.81% respectively. The Al content of the alloy decreased by increasing scale of production. A bit sharp decrease, however, was observed upto a certain limit of scale of production. This limit, however, was observed to be shifting towards higher side of scale of production by increasing the size of reactor. It can be seen that reactor A gives out appreciable decrease in Al content for upto 200 gms production level, whereas 300 gms and 400 gms represent such limit for reactors 'B' and 'C' respectively. This is also noteworthy that while the Al content of the alloy was not much affected by the size of reactor towards the higher side of scale of production (300-600 gms), alloys received at lower production

levels, were found to have increased Al content with the increasing reactor size. This can be noted at 200 gms scale of production at which the Al content of the alloys produced in reactors A,,B and C are 9.62%,9.74%, and 11.21% respectively.

5.2.2 Effect of Scale of Production in Reactor 'D'

The reactor 'D' was formed by adjoining the open ends (mouths) of two 'A' reactors with the view of achieving a new shape (geometry). The geometrical details have been described in section 4.7. The data about the recovery values and compositions of the alloys and geometrical details received by the charge column, are reported in Table 5.10. The observed relationships of recovery values and compositions of the alloys with scale of production are shown in Fig.5.13 and Fig.5.14 respectively.

As this reactor was formed by a composition of A-A reactors, a comparison of its results with the results of reactor 'A', may provide useful information.

An important observation in this regard is that this reactor furnished better results than reactor 'A' in respect of overall recovery of the alloy as well as the individual recovery of its constituent metals. The trend of variation of recovery values and composition of alloy with increasing scale of production remained almost same as experienced in previous cases.

It can be seen that for the scales of production upto 400 gms, the recovery of Ti slightly went up compared to reactor 'A'. However, for higher scale of production, the extent of Ti recovered could be as high as realised with reactor 'B'. The

maximum recovery 46.36% noticed in this reactor was obtained at 500 gms scale of production. In addition to this, the recovery values of Si were also increased as compared to reactor 'A'.

This is also noteworthy (Figs.5.8,5.10,5.12,5.14) that despite the recovery values being quite comparable to reactors A,B and C, the Ti content of the alloy decreased in this reactor (i.e.D) being appreciable for production scales above 300 gms (i.e.400,500 and 600 gms) which is due to the higher amount of Si recovered as well as an increasing trend of Al content of the alloy in this region. Fig.5.14 indicates a decreasing trend of Al content for upto 400 gms scale of production and increasing trend beyond it. However, it can also be observed that a decreased Al content of the alloy resulted for upto 400 gms scale of production as compared to reactors A,B and C, whereas an increased Al content resulted for the alloys produced for above 400 gms scale of production.

5.2.3 Effect of Scale of Production in Reactor 'E'

Reactor 'E' is cylindrical in shape its dimension being described is section 4.7. The results regarding the recovery values and compositional details of the alloys along with the dimensions of the charge column, are reported in Table 5.11. Recovery values and compositions of the alloys are plotted as a function of scale of production in Fig. 5.15. The figure indicates that Fe was recovered to the maximum extent in this reactor throughout the range studied. Not much variation was observed in overall recovery with scale of production. The

overall recovery, due to dominant contribution of Fe, varied almost in the same way as Fe recovery.

The trend of variation of Ti and Si recovery with increasing scale of production adopted the same profile as in the previously studied cases. However, the magnitude of their recovery values and contents (Fig. 5.16) in the alloy were found to have decreased in this reactor compared to 'B' 'C' and 'D'. Fig. 5.16 also indicates that Al content of the alloy remained almost unaffected (at an average 8.50%) by increasing scale of production upto 500 gms. Beyond this, it decreased to 7.33%. This is just a reverse phenomenon of what observed with reactor 'D'.

5.2.4 A General Observation and Discussion of Results

This investigation, which established the possibility of production of an alloy with as high as 16.81% Ti content recovered with a considerably high recovery margins (45 to 50%) along with appreciably lower Al contents, revealed the importance of the design aspects of the reactor in the form of its shape and size factor. The results obtained can be outlined in the following sentences.

(i) As the recovery of the alloy in respects of its valuable metallics (i.e Ti) depended not only on the scale of production but also on the size factor of the reactor, the selection of reactor should be made on the basis of the size of the charge (scale of production). Small batch of charge practiced in large reactors (and vice-versa) will not furnish good results regarding the recovery values.

Moreover, with a particular reactor, the increase in recovery of metallics can be realised upto a certain max. level of scale of production.

In order to practice still more production size, reactor of higher capacity (size) must be preferred to achieve the improved recovery of metallics in the alloy. Reviewing the results in reference of Ti recovery it is clear that while the reactor 'A' could produce the alloy for 100gms batch, reactor 'B' gave out improved recovery (41.51%) at 400gms production level. On the other hand, reactor 'C' produced poor recovery value at 400 gms whereas for higher scales, this reactor generated higher recovery values than reactor 'B'.

(ii) Higher recovery of Ti can also be achieved by changing the shape (geometry) of reactor. Considering the capacity of reactor 'B' and 'D' (made of A-A Assembly) almost same, the recovery levels achieved in both reactors were quite comparable. However, the superiority of reactor 'B' over reactor 'D' can be proved with the fact that reactor 'D' not only produced the alloys with lower Ti content but with higher passage undesirable Si in it. Therefore, the application of a pear shaped reactor cannot be suggested for the aluminothermic reduction of red mud. The cylindrical reactor ('E') which too is almost similar in capacity as 'B' (section 4.7), although produced a bit lower recovery of Ti and consequently a bit lower Ti content of the alloy, the quality of alloy, especially for higher scale of production, improved appreciably due to lower Si and Al contents. Listed

below some typical features of this investigation.

(a) Maximum recovery of Ti ; 50.60% (Reactor 'C', 500gms production level).

(b) Maximum Ti content of the alloy ; 16.81% (Reactor 'C', 600gms production level).

(c) Minimum Al content of the alloy ; 7.33% (Reactor 'E', 600gms production level).

(d) Maximum Ti:Si ratio of the alloy ; 15.42/1.42 (Reactor 'D', 600gms production level).

The combined effect of scale of production and reactor dimensions on the yield (recovery) of alloy, leads to the fact that the geometrical dimensions of the charge column (in the reactor) may also influence the physicochemical parameters, heat effects and hence the extent of either reduction to metal or separation of metal from the slag phase. The reactor imparts its own geometrical details (inner) to the charge column kept inside. The geometrical influence of the charge column (and hence the reactor) can be represented by h/d ratio where h is the height of the charge column in the reactor and d is the top diameter (open to environment). Fig. 5.17 indicates the variation of h/d ratio with the scale of production for studied reactors. Now considering the scale of production as a function h/d ratio of the charge column, it can be set forth that by increasing the h/d ratio, the recovery of Ti (and others) increased. Moreover, by locating the points of maximum extraction of Ti (from A,B,C and E) in the Fig. 5.17, it may also be possible to find out an h/d ratio which gives out maximum possible recovery. These points are

400gms (Reactor 'A'), 500gm (reactor 'B') 500gms (reactor'C') and 500gms (reactor 'E'). From the Fig.5.17 it can be noted that these points correspond to an h/d ratio between 0.70-0.80. This means that a certain combination of height and diameter of reactor (or the charge column) provides the best possible conditions for the reduction reaction to proceed.

Our results showing increasing trend of Ti recovery into the alloy with increasing scale of production are well supported by the findings of Elyutin [69] regarding the extraction of Fe-Ti from the illmenite concentrate.

Since the success of an aluminothermic reduction not only depended on the extent of reduction of the concentrate but also on the physical state of the reaction products, the magnitude of maximum temperature attained in the process as well as the provision made to sustain it for the maximum possible duration, are equally important to consider in order to achieve the favourable conditions in the melt.

Practically, the reaction temperature is determined by the heat losses accompanying the reaction, i.e in heating the reactor, radiation into surrounding medium, heat removal by discharged gases and therefore, depends on design of the reactor, the reaction rate etc. It is clear that larger the size of heat (batch of material), the less both the specific volume of the burden and the volume of the reactor and greater the reaction rate, the relatively less are the heat losses. With the lower scales of production, there are extended possibilities of quick dissipation of heat to the environment and reactor walls.

Not only this, due to aluminothermic reactions being vigorous in nature, lower volume of melt may undergo severe splashing, and violent movement lending to still further exposure to the environment. Table 5.12 (charge balance) indicates that higher losses of charge were resulted for lower production scales. To some extent, slag layer formed also protects the melt from the environment. The thickness of slag layer, however, will depend on the volume of the melt as well as the area of its exposed surface, which, in turn, will depend on the size of the charge and the geometry of the reactor. By increasing the amount of charge, the heat losses caused by violent movement of the melt are significantly reduced. On the other hand, by increasing the scale of production the height of the charge column also increases which beyond a certain extent may create the difficulty in the propagation of reaction front from top to bottom or in other words, the generation of total heat can not be realised simultaneously.

5.3 EFFECT OF PARTICLE SIZE OF REDUCTANT (Al) AND RED MUD

The particle size of reductant (Al) was varied as -53+45, -106+63, -150+125, -300+212 and -425+300 microns. This study was carried out on the red mud with three different particle sizes namely; -150+125, -300+212, -425+300 microns. The charge make up and process parameters of this investigation are reported in Table 5.13 whereas Table 5.17 presents the charge balance of heats included.

Table 5.13 Details of charge composition and parameters of the process.(Particle size of reductant and red mud).

(a) Constant Parameters-	
(i) Amount of red mud (Scale of production.	500 gms
(ii) Amount of reductant (Al-powder)	246 gms (80% excess over stoichiometric amount)
(iii) Amount of CaO	123 gms (50% of the Al)
(iv) Amount of fluorspar (CaF_2)	12.30 gms (10% of CaO).
(v) Amount of heat booster ($KClO_3$)	15% of total charge.
(vi) Particle size of lime (CaO)	-63 microns.
(vii) Particle size of fluorspar.	-63 microns.
(viii) Temperature of preheating.	400^{o}C.
(ix) Time of preheating	2 hrs.
(x) Geometrical parameters of reactor.	Reactor 'B' (as specified in section 4.7
(b) Variables-	
(i) Particle size of reductant (Al)	-53+45, -106+63,-150+125, -300+212 and -425+300 microns.
(ii) Particle size of red mud	-150+125, -300+212 and -425+300 microns.

5.3.1 Effect of Particle Size of Reductant Al, (Red Mud Particle Size, -150+125 Microns)

The recovery values and compositions of the alloys are given in Table 5.14. Fig. 5.18 and Fig. 5.19 illustrate the observed relationships of recovery values and composition with particle size of reductant.

Fig. 5.18 indicates that by increasing the particle size of reductant, the recovery of the reduced metallic values (Ti and Si) decreased slowly with similar trend resulting in a consequent decrease in the overall recovery of the alloy. However, recovery of Ti, observed a relatively sharp drop by increasing the reductant particle size above -150+125 microns. This can also be seen form Fig. 5.18 that recovery values were least affected within the particle size range -106+63 microns to -150+125 microns. The maximum recovery values of metallics which were received for reductant particle size, -53+45 microns include ; Ti, 48.74%; Si, 16.13% and Fe 83.81%.

The Ti and Si contents of the alloy (Fig. 5.19) exhibited the same trend as their respective recovery values the maximum Ti and Si contents being 16.51% and 2.18% (for -53+45 microns). A steep drop in Ti content of the alloy from 16.12% to 9.64% was observed by increasing the reductant particle size from -150+125 microns to -425+300 microns. The Al content of the alloy increased by increasing the particle size of reductant as shown in Fig. 5.19, the minimum being received for -53+45 micron particle size of reductant and maximum for -425+300 microns.

5.3.2 Effect of Particle Size of Reductant Al, (Red Mud Particle Size, -300+212 Microns)

The details of the alloys produced, are given in Table 5.15. Recovery values and composition of the alloys as plotted against the particle size of reductant, are shown respectively in Fig. 5.20 and Fig. 5.21.

In this case, the recovery of Ti first increased by increasing particle size of reductant upto -106+63 microns beyond which it started decreasing slowly. The recovery of Si increased for upto -300+212 microns particle size of reductant and then droped beyond it. Differentiating this case with the previous one, the maximum recovery of Ti (45.16%) could be obtained in this case for -106+63 micron particle size but with a decreased magnitude. Si recovery also increased from 10.44% to 15.05% by increasing reductant particle size upto -300+212 microns beyond which a decrease was observed. Upto -106+63 particle size of reductant, the Ti content of the alloy was found to be maximum (16.12%) and remained almost unaffected. However, beyond this mark a decrease was observed (Fig. 5.21). Si content varied almost proportionately to its recovery values, the maximum (2.28%) being obtained for -300+212 microns. The Al content of the alloy showed a very similar behaviour as in the previous case. It can also been seen that there was not significant variation in the Al content of the alloy compared to the previous case.

5.3.3 Effect of Particle Size of Reductant Al, (Red Mud Particle Size, -425+300 Microns)

Recovery values and compositions of the alloys, are reported in Table 5.16. The observed relationship of recovery values and compositions of the alloy are illustrated respectively in Fig. 5.22 and Fig. 5.23.

As can be seen from Fig. 5.22 that the trend of variation of recovery values remained same as in previous cases. The maximum recovery peak (40.56%) of Ti, not only shifted towards the larger particle size of reductant (i.e -150+125 microns), but also lowered in magnitude as compared to the previously studied case. This is notable that the lowest recovery of Ti (26.04%) was observed for -53+45 microns particle size of reductant whereas in the earlier cases it was observed for -425+300 microns. The same thing was also observed with Si recovery which attains its maximum level (12.72%) for the reductant particle size, -150+125 microns.

Fig. 5.23 indicates that the Ti as well as the Si content of the alloy varied almost proportionately to their respective recovery values. The maximum Ti content 15.83% and maximum Si content 1.98% were observed for the reductant particle size,-150+125 microns. The Al content of the alloy, however, did not show significant variation with increasing particle size of reductant. In comparison to the preceding case, the Al content shifted towards lower magnitude.

5.3.4 A General Observation and Discussion of Results.

In this investigation, an alloy with the maximum Ti content 16.51% was possible to produce with the maximum recovery of 48.74% (for reductant particle size, -53+45 micron and red mud particle size, -150+125 microns). The following are the broadlines :

(i) The recovery values of the metallics as well as their respective content in the alloy firstly increased to a maximum level and then started decreasing, on increasing the particle size of reductant. Increased particle size of red mud also resulted in a decrease in the recovery values.

(ii) Increased particle size of red mud, not only resulted lower recovery of Ti, but also shifted the maximum recovery peak towards higher particle size of reductant. It can be observed from the Fig. 5.18, Fig. 5.20 and Fig.5.22 that the magnitude of steepness of the decreasing profile of Ti recovery (with increasing particle size of reductant), lowered down by increasing the particle size of red mud. These facts lead to the following (iii) observation.

(iii) Recovery of Ti, (and to some extent Si also) depended on the particle size difference between red mud and reductant. In Fig. 5.24, the recovery of Ti is plotted in relation to the particle size difference of mud and reductant. This Figure reveals a few more important information as described below.

(iv) It can be seen form the Fig. 5.24 that higher recovery values were obtained near the zero difference line whereas the points far from this line indicate poor recovery values. This can also be observed that negative particle size difference (reductant particles being coarser than red mud) also resulted poor recovery of Ti. On the basis of these facts, it can be said that in order to achieve the improved recovery of Ti, the reductant particle size should be less than the particle size of red mud, the difference not exceeding beyond a certain optimum limit.

(v) This is also noteworthy from Fig. 5.24 that the maximum recovery peaks were exhibited by the reductant of particle sizes -53+45 microns followed by -106+63 microns and -150+125 microns. Therefore, an important inference which can be drawn is that by using the finer range of particle sizes of reductant and red mud, better recovery of Ti is possible. At the maximum recovery point (Fig. 5.24), the reductant (Al) particle size has been calculated to be 65% less than the red mud particle size.

The obtained results are also well compromised with the established fact (68) that a charge consisting of coarse particles will have a slower reaction compared with another composed of fine particles.A Particular difference between the particle sizes of reductant and red mud may provide a sound conditions for their mutual packing in the charge which, in turn, provides extended number of interfacial contacts between them.

5.4 EFFECT OF FLUX ADDITION

Effect of Lime, Magnesia and Fluorspar were investigated in terms of their respective CaO, MgO and CaF_2 contents (Table 4.1). The details of charge make up and process parameters are given in Table 5.18. The charge balance of the heats taken is indicated in Table 5.20 for Lime and Magnesia addition and in Table 5.23 for Fluorspar addition.

5.4.1 Effect of Lime (CaO) Addition

The amount of CaO taken in terms percentage by wt. of (Red mud + Al, powder), was varied as 0,10,20,30 and 40 percent. The details regarding the recovery values of the alloys obtained and their respective compositions, are reported in Table 5.19. The recovery values and the composition of alloy as plotted in relation to the amount of CaO are shown in Fig. 5.25 and Fig. 5.26 respectively.

Fig. 5.25 indicates that recovery of the alloy, though dominantly contributed by the iron, was possible even without the addition of CaO or flux. It can also be seen that on increasing the amount of CaO in the charge upto 20% produced a marked increase in the recovery of titanium, achieving a maximum level of 47.69%. Silicon recovery suffered an appreciable drop from a level of 19.33% to a level of 14.96% while iron recovery increased significantly after going through a slight decrease for up to 10% CaO addition. As can be noted from the Fig. 5.26 that in this region (i.e up to 20% CaO), while the Ti content of the alloy received a sharp increase from a level of 2.25% to a

Table 5.18 Details of charge composition and parameters of the process (Flux Addition).

(a) Constant Parameters-	
(i) Amount of red mud (Scale of production.	500 gms
(ii) Amount of reductant (Al-powder)	246 gms (80% excess over stoichiometric amount)
(iii) Amount of heat booster($KClO_3$)	15% by wt.of [R.M.+Al;powder+ Flux]
(iv) Particle size of red mud.	-300+212 microns.
(v) Particle size of reductant (Al)	-106+63 microns.
(vi) Particle size of flux.	-63 microns.
(vii) Tmperature of preheating.	$300^{o}C$.
(viii) Time of preheating.	2 hrs.
(ix) Geometrical parameters of reactor.	Reactor'B' as specified in section 4.7
(b) Variables-	
CaO Addition;	
(i) Amount of CaO.	0,10,20,30,and 40% by wt.of (R.M + Al,powder).
MgO addition;	
(a) Constant parameters	Same as above.
(b) Variables;	
(i) Amount of MgO	5,10,20 and 30% by wt.of (R.M.+Al,powder)
CaF_2 addition;	
(a) Constant parameters.	
(i) Amount of CaO	74.60 gms.(10% by wt of (R.M.+Al,powder).
(ii) Amount of booster($KClO_3$)	15% by wt.of (R.M.+Al,powder+ CaO + CaF_2)
(b) Variables	rest parameters are same as above.
Amount of CaF_2	5,10,15,20 and 25% of CaO(by wt.)

level of 16.30%, the silicon content of the alloy was significantly decreased. Above 20% CaO addition, however, was not proved to be beneficial in the sense that recovery of titanium as well as iron started decreasing slowly. This is important to note that silicon recovery variation exhibited the opposite trend to that observed with titanium and iron.

The Al content of the alloy, as can be seen from the Fig. 5.26, was observed to be decreasing with the increase in the amount of CaO in the charge.

The marked effect of lime addition on the recovery values are certainly due to its interaction with the produced slag resulting in substantial alteration in thermodynamic as well as physicochemical parameters of the process. Though our concentration was not on the slags which are complex systems [69], aluminothermic reduction of red mud is expected to produce a slag with high amount of alumina with some unreduced amount of titanium oxide (may be in the form of TiO_2, TiO, Ti_2O_3), iron oxides (possibly in the form of FeO), silica (SiO_2) and little calcium oxide which enter the slag from red mud, such a slag with high alumina content will have a melting point around 1900^{o}C to 1950^{o}C [78]. The heat evolved during the process may not be sufficient to keep this high melting slag molten for an optimum period of separation of suspended alloy particles from slag. Lime addition affects the process of reduction, separation as well as consolidation of metallic value from the slag in the following ways -

(i) Melting point of the slag is decreased which not only improves the heat effects of the process but also the physicochemical characteristics of the melt (fluidity is increased) resulting in better settling and consolidation of metal droplets. Four eutectics reported [72] to have existed in the system $CaO-Al_2O_3-SiO_2$ have the melting points, 1165°C (CaO, 23.25%, Al_2O_3, 14.75%, and SiO_2, 62.0%), 1265°C (CaO, 38%, Al_2O_3, 20%, and SiO_2, 42.0%), 1310°C (CaO,47.8%, Al_2O_3, 11%, and SiO_2,41.2%), and 1380°C (CaO, 29.5,Al_2O_3, 38.5%, and SiO_2, 32.0%)

(ii) It has been well established by Elyutin [69] that TiO_2 during its reduction by Al may form lower oxides, Ti_2O_3 and TiO which are difficult to reduce. In this case the final results of the process will be determined by the stability of the lowest oxide i.e TiO. The reduction of TiO_2 to Ti is characterised by the following free energy equations in high temperature range :-

$$TiO_2 + Al \longrightarrow TiO + Al_2O_3. \quad \Delta G^\circ = -89640 + 3.41\,T$$

$$TiO + Al \longrightarrow Ti + Al_2O_3. \quad \Delta G^\circ = -7720 + 2.59\,T$$

The plots [69] showing the numerical magnitude of free energy, indicate that reduction of TiO by Al develop well and equilibrium is established when there is a high concentration of Al in the alloy and of TiO in the slag. TiO being rather a strong base may combine with alumina making the reduction of Ti from TiO even more difficult. The CaO being a stronger base than TiO, weakens the $TiO-Al_2O_3$ bonds and improves the conditions of reduction. In addition, by diluting the slag, CaO promotes the precipitation of

metal reguli and consequently increases the recovery of Ti into the alloy. Lime addition also improves effectiveness of the reduction process by lowering the activity of Al_2O_3, as described in Filippov enequality [122]. A decreasing trend of Al content of the alloy (Fig. 5.26) supports this fact implying more utilisation of Al in the reduction process.

The above stated facts might have been responsible for the rise in recovery values of Ti and Fe for upto 20% lime addition. Silica on the other hand being acidic in nature, may partly join CaO and is lost in the slag. Our results regarding more than 20% lime addition are also in agreement with the facts as stated by Elyutin [69] that introduction of more CaO increases frequency of slag formation and for this reason despite low concentration of oxides of principal element, the absolute losses of extracted element may become considerable. Apart from this, lime addition more than 20% may adversely influence the heat effects of the process in the following ways -

(i) Fusion of added flux requires additional amount of heat.

(ii) As the heat effects of the reaction of interaction between silica (alumina) and CaO related to 1 mole of CaO decreases with the increase in CaO content in the slag [69] , the specific heat effect of the process of solution of CaO in SiO_2 (Al_2O_3) is decreased by increasing the quantity of flux resulting in a higher amount of heat to be supplied for smelting the flux.

(iii) Higher CaO addition may impair the fluidity of the melt by increasing the its viscosity [122].

The anomalous drop in Fe recovery from 0-10% CaO addition (Fig. 5.25) may either be due to a comparatively low content of Fe_2O_3 in that particular bulk of red mud or to the possibility of formation of iron calcium silicates [72] causing loss of some FeO into the slag system. The increasing trend of Si recovery beyond 20% lime addition though remained unexplained, a rigorous examination of the slag compositions associated with different temperatures may reveal the possible facts.

The results are also supported by the data presented in Table 5.20 revealing pronounced losses of the charge and hence some fraction of metallic values beyond 20% lime addition.

5.4.2 Effect of Magnesia (MgO) Addition

The amount of MgO was varied as 5,10,20 and 30% by wt. of (RM + Al, powder). The results about the recovery values and compositions of the alloys are presented in Table 5.21. In Fig. 5.27 and Fig. 5.28 the recovery values and composition of the alloy are respectively plotted against the amount of MgO. The charge balance of the heats taken is presented in Table 5.20.

Fig. 5.27 shows that upto 10% MgO addition, recovery of Fe as well as Ti increased. The trend of Ti-recovery variation as well as the magnitudes of recovery levels achieved were almost similar to that observed with the equivalent amount of lime addition (Fig. 5.25). The recovery of Si, however, remained unaffected. The Ti content of the alloy increased but to a lesser extent than that observed with lime (Fig. 5.28). MgO addition above 10%, resulted in a decrease in the recovery values of all

the metallic constituents of the alloy (Fig. 5.27). A significant decrease in the Ti content of the alloy, however, was observed above 20% MgO addition.

It is noticeable from the Fig. 5.28 that throughout the range studied, while the Si content of the alloy displayed a decreasing trend, Al content of the alloy increased with the increase in amount of MgO.

The most simple slag systems which can be studied in this regard could be $MgO-SiO_2$ and $MgO-Al_2O_3-SiO_2$. Such slag have been reported to posses high refractoriness. $MgO-SiO_2$ system forms two chemical compounds [72] ; $2MgO.SiO_2$-forsterite (melting point 1890) and $MgO.SiO_2$-clinoestatite which decomposes at 1557°C (below its melting point). The most low melting eutectic found in the system contains 34% MgO and melts at 1543°C. The refractoriness of the $MgO-Al_2O_3-SiO_2$ system increases with the increase in the amount of MgO [69]. These facts lead to the idea that the pronounced recovery levels, achievable in case of lime addition, cannot become possible with MgO addition, in the sense that physicochemical characteristics (fluidity) and heat effects of and process as desired for the favourable reduction and consolidation of metal, are adversely affected. The existence of the viscous melt due to MgO addition may also be confirmed to some extent from the charge balance of heat taken for MgO addition (Table. 5.20) showing reduced losses of the charge. The increasing level of Al content of the alloy (Fig. 5.28) along with the reduced recovery values also indicates that the reduction reaction did not progress well.

5.4.3 Fluorspar (CaF_2) Addition :

The Fluorspar (CaF_2) was taken in terms of percentage by wt. of CaO added. The amount of CaF_2 was varied as 5,10,15,20 and 25% by wt. of CaO added to the charge. The recovery values as well as the compositions of the alloys obtained are presented in Table 5.22. Table 5.23 gives an account of the charge balance of the heats taken. The results were studied by plotting the recovery values and compositions of the alloys obtained in relation to the amount of fluorspar as shown in Fig. 5.29 and Fig. 5.30.

As can be seen from Fig. 5.29 that Fluorspar addition upto 15%, increased the overall recovery from a level of 55.2% to 60.06%, whereas above 15% Fluorspar addition resulted in slowly decreasing trend of the same.

It is also apparent from the Fig. 5.29 that upto 15% Fluorspar, increased the recovery of Ti, however, the major increase was observed above 10% whereas below 10% the recovery of Ti remained almost unaffected. Above 15% Fluorspar addition, no marked effect was observed on the recovery of Ti. The recovery of Fe increased steadily with the addition of Fluorspar amounting upto 15%. Further increase, however, resulted in a drop. Similar results were observed with the recovery of Si also.

No major variations were observed in respect of the content of the metallics in the alloy as shown in Fig. 5.30.

As the lime (CaO) incorporated in the charge during this investigation was 10% by wt. of (RM + Al, powder) i.e. 74.60

gms. (Table 5.18), the improvement in recovery values can well be assessed by comparing the results to that obtained by 10% lime (CaO) addition only (Fig. 5.25). It can be inferred that the Ti recovery level of 22.35% as achieved by adding 10% CaO only, was further improved appreciably to a level of 36.18% by the addition of Fluorspar amounting 15% of CaO. Similar results were also observed with Fe and Si.

The positive effects of Fluorspar addition on the recovery values may be attributed partly due to high increase in fluidity of the slag [123,124] and partly due to the fact [78] that Fluorspar like lime decreases the activity of alumina thus releasing TiO_2 for further reduction. The higher losses of charge noted for 15% Fluorspar addition (Table 5.23) indicates the existence of highly fluid slag at this mark providing best conditions in favour of reduction as well as the consolidation of the alloy.

5.5 EFFECT OF THERMAL BOOSTER ADDITION, AND PREHEATING TEMPERATURE

Thermal boosters are meant to supply additional heat to the charge to compensate for inadequate insitu heat liberation. The boosters studied are Potassium Chlorate ($KClO_3$) and Potassium Nitrate (KNO_3). To rationalise a proper combination of extraneous heating factors, effect of preheating was also studied together with that of booster addition. The amount of booster was taken as the percentage by weight of (RM + Al, powder + CaO + CaF_2) which has been termed as total charge. The composition of the charge

prepared and parameters of the process are reported in Table 5.24. The thermcity of this charge (without booster and preheating) was calculated to be 384.84 Kcal/kg of charge. Table 5.30 presents the charge balance of all the heats involved in this investigation.

5.5.1 Effect of Potassium Chlorate ($KClO_3$)

The effect of $KClO_3$ addition was studied at preheating temperatures 100^o, 200^o and 300^oC by varying the amount of $KClO_3$ as 0,5,10,15 and 20%.

5.5.1.1 $KClO_3$ Addition at 100^oC preheating :

Table 5.25 presents the recovery values and the compositional details of the alloys produced. The recovery values of the alloy as studied in relation to the amount of $KClO_3$ is given in Fig. 5.31 while Fig. 5.32 indicates the observed variations in the contents by the alloy.

It can be inferred from the Fig. 5.31 that the alloy could not be recovered without $KClO_3$ (booster) addition. The overall recovery increased sharply on increasing the amount of $KClO_3$. The recovery values of all the metallic constituents of the alloy increased with similar trend. Upto 10% $KClO_3$ addition, the overall recovery was mostly contributed by Fe recovery, because Ti and Si recovery values remained marginal upto this level. Major increase in the recovery values of the metallic constituents of alloy was obtained for above 10% $KClO_3$ in the charge. Ti recovery was enhanced from 4.88% (for 10% $KClO_3$) to

Table 5.24 Details of charge composition and parameters of the process.(Boostor addition and preheating temperature).

(a) Constant Parameters-	
(i) Amount of red mud (Scale of production.	500 gms
(ii) Amount of reductant (Al-powder)	246 gms (80% excess over stoichiometric amount)
(iii) Amount of CaO	123 gms (50% of Al)
(iv) Amount of fluorspar (CaF_2)	12.30 gms (10% of CaO).
(v) Particle size of red mud	-300 + 212 microns.
(vi) Particle size of reductant (Al)	-106 + 63 microns.
(vii) Particle size of lime.	-63 microns.
(viii) Particle size of fluorspar.	-63 microns.
(ix) Time of preheating	2 hrs.
(x) Geometrical parameters of reactor.	Reactor 'B' (as specified in section 4.7)
(b) Variables-	
(i) Type of booster	$KClO_3$ and KNO_3
(ii) Amount of booster	$KClO_3$;0,5,10,15 and 20% by wt. of (R.M.+Al,powder+ CaO+CAF_2).
	KNO_3;0,5,10,15 and 20% by wt. of (R.M.+Al,powder+ CaO+CuF_2).
(iii) Preheating Tempr.	$KClO_3$; 100°,200° and 300°C
	KNO_3; 300°C

31.76% (20% $KClO_3$). Moreover, the Ti content of the alloy, as shown in Fig. 5.32 was also increased sharply from 3.88% (10% $KClO_3$) to 12.44% (20% $KClO_3$).

The Al content of the alloy (Fig. 5.32) decreased with increasing $KClO_3$ amount in the charge. However, the Al content of the alloys obtained by $KClO_3$ addition upto 15%, remained quite higher than the Ti content indicating higher Al:Ti ratio (more than 1) of such alloys. The Ti content of the alloy and could dominate the Al content of the alloy only for more than 15% $KClO_3$ addition.

5.5.1.2 $KClO_3$ Addition at 200°C Preheating.

The data about the recovery values and composition of the alloys are reported in Table 5.26 and plotted graphically as a function of the amount of $KClO_3$ in Fig. 5.33. The Figure indicates that recovery values of the alloy increased by increasing the amount of $KClO_3$ though small recoveries of metallics were observed to be possible without $KClO_3$ (or any booster) addition. The trend of variation of recovery values remained almost same as in the previous case but towards higher recovery levels.

This is important to note that a marked increase in the recovery of Ti which was observed beyond 10% $KClO_3$ in the previous case (Fig. 5.31) has now been attained above 5% $KClO_3$ addition .

Fig. 5.34 indicates that by increasing $KClO_3$ content of the charge, the Ti and Si contents of the alloy increased.

Comparing with the previous case, the alloys produced in this case were richer in respect of their Ti and Si contents. The Al content of the alloy did not show any significant variation. However, the alloys produced were observed to have received appreciably lower Al content than the previous case, and hence the alloy with Al : Ti ratio less than 1 might be produced for $KClO_3$ addition above 10%.

5.5.1.3 $KClO_3$ Addition at 300°C preheating :

Recovery values and compositions of the alloys produced are reported in Table 5.27. Fig 5.35 and Fig. 5.36 respectively indicate the variation in recovery values and composition of the alloy as a function of the amount of $KClO_3$.

It is apparent from Fig. 5.35 that overall recovery of the alloy increased almost linearly (proportionately), the absolute magnitude being still towards higher side than the previously studied cases. Recoveries of all the metallics in the alloy increased by increasing the amount of $KClO_3$. Fe-recovery increased linearly upto 15% $KClO_3$ whereas Ti and Si recoveries tended to become linear in respect of the amount of $KClO_3$ added. It can also be seen that the magnitude of recoveries of Fe and Ti raised considerably compared to previous cases. The maximum Ti recovery 41.07% achieved in this case was quite higher than the previously studied case (32.46%).

The Ti content of the alloy also tended to have a linear relationship with the amount of $KClO_3$ whereas the

countable increase in Si content was observed above 5% $KClO_3$ addition (Fig. 5.36). Al content increased slightly by $KClO_3$ addition up to 10% and then started decreasing reasonably beyond it.

5.5.2 Effect of Potassium Nitrate (KNO_3)

The effect of KNO_3 addition was studied only at 300°C preheating by varying its amount as 0,5,10,15 and 20% by weight of (RM + Al, powder + CaO + CaF_2). Recovery values and compositions of the alloys produced are reported in Table 5.28 whereas Fig. 5.37 and Fig. 5.38 show their relationship with respect to the amount to KNO_3.

As can be noted from the Fig. 5.37 that overall recovery increased with the increase in the amount of KNO_3 the trend being similar to that observed with $KClO_3$ addition at 300°C. However, the recovery levels (Overall Recovery)remained towards higher side which was apparently due to the higher recovery values of Fe. Recovery of Ti also increased but to a lesser extent than that experienced with $KClO_3$. The maximum Ti recovery 32.63% (for 20% KNO_3) was achieved in this case as against 41.07% observed for 20% $KClO_3$ addition. Si recovery, though, exhibited the same trend of variation as with $KClO_3$ (at 300°C), the recovery levels were not much affected.

Fig. 5.38 reveals that Si content of the alloy increased by increasing the amount of KNO_3. It is noticeable that Ti and Al content of the alloy showed just opposite trend of variation below 10% KNO_3 addition whereas they varied in similar

manner above this mark. However, within our experimental confines, the Al : Ti ratio less than 1 was found by KNO_3 addition above 15%. The abnormal behaviour of Ti content variation (Fig. 5.38) is certainly due to the mutual quantitative influence of other ingredients of the alloy because of their pronounced recovery levels and almost unchanged recovery levels of Ti in that particular range (e.g.0-5% KNO_3).

5.5.3 A General Observation and Discussion of Results

This study revealed the following facts :

(i) Booster addition increased the recovery of all the metallic ingredients (Fe, Ti and Si) of the alloy and hence the overall recovery.No recovery, however was possible without booster at lower temperatures of preheating which is 100°C in our case.

(ii) Preheating alone upto 300°C could not produce any marked effect on the recovery of the alloy. However, if coupled with booster addition, recovery levels were pronounced considerably.

(iii)$KClO_3$ furnished far better results than KNO_3 in respect of Ti and Si recoveries as well as their percentage in the alloy. $KClO_3$ addition studied in association with preheating temperature, revealed that by increasing preheating temperature, the numerical magnitude of recovery values as achieved by $KClO_3$ addition, shifted towards higher side, consequently higher recovery was possible even at lower amount of $KClO_3$ addition practiced at higher temperature of

preheating. Apart from this, $KClO_3$ addition Vs Recovery relationship tended to become linear by increasing preheating temperature.

(iv) The Al content of the alloy decreased with the increase in the amount of $KClO_3$ and temperature of preheating. The magnitude of decrease, however, narrowed down on proceeding towards higher $KClO_3$ amount and preheating temperatures.

(v) As a consequence of increase in Ti content and decrease in Al content, (by increasing $KClO_3$ addition and preheating temperature). the Al : Ti ratio of the alloy lowered down.

This investigation confirms that selection a proper booster material and an optimum preheating temperature is very necessary in order to get improved recovery of metallics in the alloy. These two parameters invariably influence the thermodynamic, kinetic and physicochemcial conditions of the process by mounting their own thermal effects. Table 5.29 furnishes the details about the thermicity levels of the charge for the investigated range of $KClO_3$ and preheating temperature.

Table 5.29 Thermicity levels of the charge by $KClO_3$ addition at different preheating temperatures.

Preheat Tempr ^oC	Amount of booster, % of (RM+Al,+CaO+CaF_2)				
	0	5	10	15	20
100	414.84	562.02	709.20	856.38	1003.56
200	444.84	592.02	739.20	886.38	1033.56
300	474.84	622.02	769.20	916.38	1063.50

The thermicity (specific heat of the charge) was calculated on the basis of Table 2.15 and Table 2.16 and the fact

[68] that for every 100°C preheat the amount of heat released by the charge is 30 Kcal/kg. Thermicity levels presented in Table 5.29 indicate that our results are in agreement with the Perfect's [74] criteria which establish the range of thermicity between 600 to 1200 Kcal/kg for the successful running of a metallothermic reaction. Discussed below are more reasons which might have contributed to the results of this investigation -

(i) Lower thermicity (due to lower amount $KClO_3$ and preheat temperature results in slow and incomplete reduction of the reducible components in the charge because the temperature attained by the charge in not adequate for keeping the melt in sufficiently fluid condition as desired for proper slag-metal separation. As the product is not removed from reaction site, progress of the reaction is hampered. Due to partial reduction, the Al content of the reduced alloy becomes high beacuse of low consumption. Apart from the partial reduction, lime is not activated to the extent of joining the slag phase to produce its own effects. Fe_2O_3, however, can be reduced to some extent because of its thermodynamic simplicity. At this stage the recovery of Ti and Si may remain feeble on account of the fact that it requires a simultaneous influences of heat effects and lime addition to provide proper thermodynamic and physicochemical conditions.

(ii) Preheating may play supporting role with booster addition in two ways. Better initiation as well as propagation of reaction front (i.e. rate of reaction) and hence

achievement of high temperature and secondly prolonging the period of persistence of high temperature. Higher charge losses for higher booster addition and preheating temperature (Table 5.30) confirms to some extent the increased rate of reaction.

(iii) KNO_3 possibly due its less oxidizing power [125] than $KClO_3$ cannot produce better results.

5.6 EFFECT OF PREHEATING TEMPERATURE AND TIME

The preheating temperature was varied as 100^{o},200^{o}, 300^{o}, 400^{o} and 500^{o}C. The study was conducted for the preheating time 1,2 and 3 hrs. Table 5.31 gives the details of charge composition and process parameters. The results regarding recovery values and compositional details of the alloys are presented in Table 5.32 (for 1 hr. preheating), Table 5.33 (for 2 hrs. preheating) and Table 5.34 (for 3 hrs. preheating). Table 5.35 presents the charge balance of heats taken.

Recovery values and compositions of the alloys are respectively plotted in relation to preheating temperature in Fig. 5.39 and Fig. 5.40 (for 1 hr. preheating time), Fig 5.41 and Fig. 5.42 (for 2 hrs.) and Fig. 5.43 and Fig 5.44 (for 3 hrs). It can be seen that recovery values of the alloy increased with the increase in preheating temperature. By increasing the duration of preheating, the recovery values increased but the trend of preheating temperature-recovery relationship remained almost unaffected.

Table 5.31 Details of charge composition and process parameters (Preheating Temperature and time).

(a) Constant Parameters-	
(i) Amount of red mud (Scale of production)	500 gms
(ii) Amount of reductant (Al-powder)	246 gms (80% excess over stoichiometric amount)
(iii) Amount of CaO	123 gms (50% of CaO)
(iv) Amount of fluorspar (CaF_2)	12.30 gms (10% of CaO).
(v) Amount of booster ($KClO_3$)	15% by wt. of (R.M.+Al, powder+CaO+CaF_2).
(vi) Particle size of red-mud	-300 + 212 microns.
(vii) Particle size of reductant (Al)	-106 + 63 microns.
(viii) Particle size of lime (CaO)	-63 microns.
(ix) Particle size of fluospar (CaF_2)	-63 microns.
(x) Geometrical parameters of reactor.	Reactor 'B' (as specified in section 4.7)
(b) Variables-	
(i) Preheating tempr.	No preheating, 100^{o},200^{o}, 300^{o},400^{o} and 500^{o}C.
(ii) Preheating Time.	1,2 and 3 hrs.

It can also be observed that the magnitude of increase in recovery narrowed down as the preheating temperature increased and it may be expected that after a certain limit of preheating temperature (it may be beyond our experimental confines) there may not be any further increase in recovery value. As can be noted that the preheating temperature upto $400^{o}C$ gives out a significant increase in the recovery of Ti and Si. The unpredictable decrease of Si recovery at $400^{o}C$ (for 2 hrs. preheating duration) may be due to inhomogeinity of that particular lot of red mud carrying less amount of SiO_2. The preheating time affected the recovery values in a similar way. Taking the example of Ti recovery, the maximum recovery of 38.05% (at $500^{o}C$) obtained for 1 hr. duration was raised to 44.45% for 2 hrs. duration of preheating. Further increase in preheating duration, (i.e. 3 hrs.), however, enhanced the maximum recovery of Ti only to 45.74% with the expectation that further increase in preheating time may not cause any reasonable increase in recovery values.

The Ti content of the alloy increased proportionately to its recovery value (Fig.5.40, Fig.5.42, Fig.5.44) by increasing the preheating temperature that is, a sharp increase upto $400^{o}C$. The preheating duration also affected the Ti content in similar manner exhibiting significant increase for the preheating duration upto 2 hrs and marginal beyond it. Raising the preheating duration from 1 hrs. to 2 hrs. improved the maximum Ti content (at $500^{o}C$) from 14.60% to 16.44% whereas a further increase in time duration to 3 hrs, resulted 16.38% Ti

content in the alloy pointing out that further prolonging of the duration of preheating would not result in any material increase in the Ti content of the alloy. The Si content of the alloy observed higher values at higher preheating temperature and time, almost parallel to its recovery values.

A general trend of the Al content of the alloy is that it decreased with the increase in temperature and time of preheating. Prolonging the preheating duration, not only resulted in lowering the Al content of the alloy but also in a rather sharp drop in its content on increasing the temperature of preheating (Fig. 5.44).

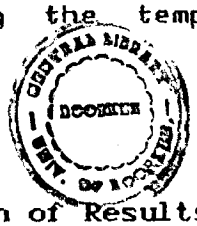

5.6.1 A General Observation and Discussion of Results

This investigation established the necessity of proper selection of preheating temperature and its duration because an increase in these parameters upto a certain limit led to a significant increase in the recovery values as well as the reduced metallic contents of the alloy along with a marked decrease in its Al content. A preheating of 400^{o}C for 2 hrs may be considered reasonable in our case.

The influencive role of preheating can be explained on the basis of the fact that it contributes to the total heat effect of the process in the sense that every 100^{o}C preheating increases the heat content of the charge by a margin of 30 kcal/kg [68]. Effect of preheating on thermodynamic, kinetic and physicochemical factors of the process has already been discussed in section 5.5.4. Our results are also to the

satisfaction of the fact [69] that excessive increase in temperature may not inhance the recovery of the alloy due to undesirable losses caused by volatilization and splashing as well. Table 5.35 also gives an indication of increased losses of charge at higher temperature. Apart from this, the preheating temperature at which the recovery values get saturated, may represent that limit where the melt attains its maximum possible fluidility to drive the kinetic and thermodynamic forces towards the maximum possible extraction. On having a look on all the previously studied cases it seems that around 55 to 60% should mark the maximum possible limit of titanium extraction for the considered lot of red mud and within our experimental confines. The necessity of a proper preheating duration is realised in the sense that the charge requires a certain period of time to pickup the applied preheating temperature and get homogenised with respect to it. This enevitably will depend on the factors like time, temperature, thickness of the charge column and its conductivity.

CHAPTER - 6

CONCLUSIONS

The present investigation has established the feasibility of production of an alloy consisting of Fe, Ti, Si and Al by open aluminothermic reduction of red mud conducted under favourable thermodynamic conditions and heat effects. Since the factors like amount of reductant, amount of red mud, particle sizes of reductant and red mud, amount and type of flux, preheating temperature, preheating time, amount and kind of thermal booster and reactor geometry all found to affect the recovery of Ti into the alloy, a proper co-ordination among all these factors is quite necessary in order to achieve the improved recovery of Ti. The increase in Ti recovery, however, is realised with a simultaneous and unavoidable increase in the recovery of Si in the alloy. The following conclusions may be drawn as a result of this investigation.

(i) The alloy can only be recovered by using excess amount of reductant (Al, powder) over stoichiometric requirement.

(ii) A significant increase in the recovery of Ti can be observed by increasing the amount of reductant upto the mark representing 80% excess over stoichiometric amount and also by increasing the particle size of reductant upto -106+63 microns. The Si-recovery, however, was found to be decreasing by increasing the particle size of reductant within our experimental confines.

(iii) The Al content of the alloy produced with the reductant (Al) of finer particle size (-63+53 and -106+63 microns), has shown a decreasing tendency by increasing the amount of reductant upto 40% excess and increasing tendency beyond it whereas for larger particle size (-300+150 microns) of reductant almost an increasing tendency has been observed throughout the studied range of amount of reductant.

(iv) The recovery of the alloy in respect of its valuable metallic constituent (i.e Ti) depends not only on the scale of production but also on the size and geometry of the reactors. Small batch of charge practiced in large reactors would not furnish good results regarding recovery values. In a particular reactor the increase in the recovery of the alloy (recovery of Ti) can be realised upto a certain maximum level of scale of production. For practising still higher scale of production, improved recovery values can be achieved either by increasing the size of reactor or by making some favourable changes in the geometry of the reactor. The geometry of reactor should be such as to provide a suitable combination of the height of the charge column and the diameter of its exposed surface. The h/d ratio (signifying this aspect) between 0.70-0.80 has been found suitable for getting imporved recovery of Ti.

(v) Recovery of Ti has also been found to be dependent on the difference of particle sizes between the red mud and reductant. Improved recovery can be achieved with the conditions; (a) reductant particles are smaller than the red mud (b) the difference between them not exceeding beyond a certain extent which is around 65% in our case and (c) red mud and reductant belong to finer particle size range.

(vi) Recovery of Ti can also be increased by Lime addition amounting upto 20% of (Red Mud + Al, powder i.e. reductant). The beneficial effect of Lime can further be improved by the addition Fluorspar amounting upto 15% of the CaO content of Lime. Use of the Magnesia (MgO), however, cannot be suggested as fluxing agent because it does not create any marked effects in improving the recovery values.

(vii) It is not possible to recover the alloy without providing external thermal effects to the process i.e. Thermal Booster Addition and preheating the charge.

(viii) Preheating alone upto $300^{o}C$ cannot produce any significant influence on the recovery of the alloy. However, if coupled with thermal booster addition, recovery levels of all the reduced constituents of the alloy, are pronounced considerably.

(ix) $KClO_3$ has been proved to be beneficial in comparison to KNO_3. However, the major inhancement in the recovery of Ti

is experienced when the $KClO_3$ addition amounts to more than 10% of total charge i.e (Red Mud + Al, powder + CaO + CaF_2).

(x) The duration of preheating is also important to consider for achieving the maximum possible beneficial effects of preheating temperature. Proper selection of preheating temperature and duration of preheating is necessary because an increase in these parameters upto a certain limit leads to significant increase in the recovery values as well as the reduced metallic contents of the alloy along with a marked decrease in its Al content.

(xi) In order to get higher Ti recovery and hence its content in the alloy, the passage of Al and Si into the alloy is unavoidable.

CHAPTER-7

SUGGESTIONS FOR FUTURE WORK

1. Study can be made on the assessment of the utility of the alloy as complex deoxidiser to steel melts.
2. Taking into account all the variables investigated in this work, a modelling study of the process can be carried out in order to predict an optimised condition for achieving improved recovery levels.
3. To minimise the passage of Si into the alloy as well as to reduce the volume of the slag formed, trials can be made to remove SiO_2 and Al_2O_3 fraction of Red Mud before treating it metallothermically.
4. Economic aspect of the process can be examined to find out its feasibility on the industrial scale. Pilot plant sudies are also advisable.

REFERENCES

1. Aluminium, Vol.1, Australian Mineral Economics, Pty. Ltd. (1981),5-7,18-20,46-51,110-112;
2. Ray,H.S.,Sridhar,R. and Abraham,K.P.; Extraction of Nonferrous Metals (1985), East - West Press Put Ltd.
3. Sevrukov,H.;Nonferrous Metallurgy, Mir Publishers, Moscow,330-360.
4. Tielens,A.J.; INCAL-1985,Vol.2, New Delhi (India),411.
5. Tielens,A.J.; Eng. Min. J. (1977), 84 .
6. Prasad,P. M.; Proc. Intl. Conf. Metal Sciences ; The Emerging Frontiers (ICMS-77), IIM. Calcutta,India, (1979), 461.
7. Prasad,P.M. and Sharma, J.M.; Proc. Sym. on Electro-metallurgy, CERI Karaikudi, India, (1966),12.
8. Hudson,L.K.; Production of Aluminium and Alumina, A Critical Report on Applied Chemistry.
9. Purnell, B.G.; Light Metals (1986), Met. Soc. AIME,157.
10. Lotze, J.;Light Metals (1983),Met.Soc.AIME,1159.
11. Lambe,T.W. and Whiteman,R. W.; Soil Mechanics, John Wiley and Sons. Inc., New York, 1969.
12. Dams,R. and Feige,H.; Verfehren Zur Herstellung eines spruhgranulates aus Rotschlamm,DBP 24,25,234 (1980).
13. Bolling,W.H.; Bodenkennziffern und Klassifizierung von Boden, Springer-Verlag Wien,New York (1971).

14. Mc Geer,J.P.; Environmental control in our Industry ; An Historical Overview, Hall - Heroult Centennial, Met. Soc.AIME,169.

15. Davies,V.E.; Experience in the Disposal of Red mud in the Sea, Sym. Protection of Environment, Stuttgart (1972).

16. Versiani,F.; Light Metals (1983), Met.Soc. of AIME,337.

17. Walker,L. K., Parker,R.J. and Gibson,S.J.; Light Metal (1986),Met.Soc. AIME, 1047.

18. Solymar,K; Proc.Sym. Light Metals : Science and Technology; BHU, Varanasi,India (1985),1.

19. Zavaritskaya,T.A., Kraus,I.P. and Narushevich,L.P.; Proc. 2nd Conf. of VAMI and FKI experts: Mineralogical and Technological Evaluation of Bauxites, Leningrad (1972),189.

20. Prasad,P.M.,Kachhawaha,J.S.,Gupta,R.C., Mankhand, T.R. and Sharma,J.M.; Proc. Light Metals : Science and Technology, BHU Varanasi, India (1985),31.

21. Parekh, B. K. and Goldberger,W. M.; EPA Report, 600 (1976), US Environ. Prot.Agency, Ohio (USA), 276.

22. Solymar,K.; Proc. 2nd Conf. of VAMI and FKI experts: Mineralogical and Technological Evaluation of Bauxites, Jan.18-21,Leningrad (1972),229.

23. Horvath,Z.; Elmeleti Kohaszattan,Tankonyvkiado, Budapest, Hungary (1974),227.

24. Zambo,J. and Kovacs, B.; Femipari Kutato Intezet Kozlemenyei, VII,Budapest (1964),17.

25. Kovacs,B.;Femipari Kutato Intezet. 511, sz.megbizasa, (1965),Budapest.

26. Solymar,K. and Hazaine, Borsiczky Veronika; Banyaszati es kohaszati Lapok, Kohaszat, 101,5, (1968),187.

27. Mariassy,M.; Femipari Kutato Intezet Kozl, IV, Konyvkiado, Budapest (1960),37.

28. Solymar,K., Steiner,J. and Huszar,L,; Femipari Kutato Intezet Kozlemenyei, VII, (1964),Budapest,47.

29. Prakash,S.;Behaviour of Titanium Minerals in the Titanium Rich Indian Bauxite during its Treatment by Bayer's Process, Ph.D.Thesis, Technical Univ. of HeavyIndustries, Miskole, Hungary (1978).

30. Prakash,S. and Horvath,Z.; Acta Technica Acad. Scientiarum Hungaricae, Tomus 90 (1-2) (1980),15.

31. Tikhonov, N.N.; and Lapin,A.A.; Proc. 2nd Conf. of VAMI and FKI experts; Mineralogial and Technological Evaluation of Bauxites, Jan.18-21,1972, Leningrad (1972),204.

32. Schepers,B.; Aufschluss van Bauxiten, Erzmetall., 29, (1976),61.

33. Bernshtein,V.A.; Trudi VAMI, 44 (1960),17

34. Basu,P.; Light Metals (1983),Met.Soc.AIME,83.

35. Leitenzen,M.G., Lapin,A.A. et al.; Trudi VAMI, 64 (1968),31.

36. Szabo,Z. and Solymar, K.; Femipari Kutato Intezet, Budapest, Ideszaki Jelentes. Temaszam, 11-10.

37. Mariassy, M.; FKI Kozl. 3, (1959),51.

38. Papp,E.; Proc. Res.Inst. Nonferrous Metals, IX, Publ. House of Hung. Acad. of Sc.(1971), Budapest,43.

39. Napokryth,T.A.; Kuznetsov, S.F. and Fedyaev,F.F.; Izv. Vyssh Ucheb, Zaved.Tsvet. Metall. 5 (1974),42.

40. Zambo,J., Orban-Kelemen, M.; Acta Technica Acad. Scientiarum Hungariae, 82 (3-4), (1976),333.

41. Romanov, L.G.,Rovazhnyi, B.S.and Dzhumbaev, B.S.; Tr. Inst. Met. Obogasch. Akad. Nauk. Kaz.SSR (44),(1972), 102.

42. Novojonov,V.A., Kuznetsov, C.I. and Derevjankin,V.A.; Khimija i tekhnologija glinozema. Novosibirsk (1971), 445.

43. Pohland,H.H. and Tielens,A.J.; Light Metals (1983) Met. Soc. of AIME, 211.

44. Kovacs, B. and Solymar, K.; Femipari Kutato Intezet (1969), Budapest, 511.

45. Bogavadi,E.; Kohasz. Lapok, 141 (1954),172.

46. Brassinga,R.D. and Fulford,G.D.; Light Metals (1986), Met. Soc. AIME, 51.

47. Dunay, S.; FKI Kozl., 1 (1956),29.

48. Beilfeldt,K.; J. of Metals, 20, 9, (1968),48.

49. Lanyi,B.; FKI Kozl., 1 (1956),5.

50. Solymer,K.; Trends of Technological Development in Alumina Production, 4th Yugoslav Intl. Sym. on Aluminium, Titograd, April 21-25, 1982.

51. Solymar,K. and Kovacs,B.; Proc. Res. Inst. Nonferrous Metals IX, Publ.House of Hungarian Acad. of Sciences (1971), Budapest, 79.

52. Bardossy, Gy.; Proc. 2nd Conf. of YAMI-FKi experts : Mineralogial and Technological Evaluation of Bauxites, Jan.18-21,(1972), Leningrad ,27.

53. Tertian,R.; Proc.Res. Inst. for Nonferrous Metals IX, Hungarian Acad. of Sciences, Budapest (1971), 167.

54. Tertian,R.; Proc.Res. Inst. for Nonferrous Metals IX, Publ. House of the Hungarian Acad. of Sc. Budapest (1971), 179.

55. Wallen-Bryan,W. and Wright, G.; Light Metals (1986), Met. Soc. AIME, 1101.

56. Frakas,F., Skuteczky, E. and Gombos, M.; Proc. Res.Inst.for Nonferrous Metals IX, Hungarian Acad. of Sc. Budapest (1971), 179.

57. Klug,O. and Tajnafoi, M.; Hung. Sci. Instrum. 42, 1978, 31, C.A.; 89; 203694 q

58. The Kwat, I.; Light Metals (1986), Met. Soc. AIME, 43.

59. Bitto,A., Borsodi, M. and Tomcsanyi, L.; Magy. Kem. Foly. 87(6), 1981, 283, CA 95:90490 Y.

60. Ajlec, R. and Stupar, J.; Vestn. Slov. Kem. Drus., 29(4), 1982, CA 98 : 190849 C.

61. Orban-Kelemen, M., Kotsis, T. and Sajo-Feszl, M.; Proc. 2nd Conf. of VAMI and FKi experts: Miner. and Tech. Evaluation of Bauxites, Jan.18-21, 1972, Leningrad. Ed. Res.Inst. Nonferrous Metals, Budapest (1975),267.

62. Gado,P. and Orban,M.; Light Metals (1979), 59, CA. 94 : 184981 r.

63. Kontopoulos, A. et al.; Intl. Congr. Study Bauxites, Alumine Alum.,3,1978, CA. 90:58149 e.

64. Bertoti, I., Mink, G., Szekely, T. and Zelei, B.; Trav. Com. Intl. Etude Bauxites, Alumine Alum., 17, 1982, 231, CA 99 : 108558 W.

65. Grachev, V.V., Shevchenko, N.V. and Severukhina, T.N.; Tsv. Metallurgiya, 1, 1986, 30, C.A. 105 : 182-951 C.

66. Habashi,F.; Principles of Extractive Metallurgy, Vol.3, Gordon & Breach Sc. Publish.

67. Gupta, C.K.; Proc. Silver Jub. Symp: Recent Developments in Metallurgical Science and Technology, IIM New Delhi (1972),515.

68. Suri, A.K. and Gupta,C.K.; Proc. Sem; Physical Chemistry of Extractive Metallurgy, Univ. of Roorkee (India), March 29 (1979), 71.

69. Elyutin,V.P.et al.; Production of Ferro Alloys, The State Scientific and Technical Publ. House, Moscow (1957).

70. Coudurier,L., Hopkins, D.W., and Wilkomirsky, I.; Fundamentals of Metallurgical Processes, 2nd Ed, Pergamon Press, (1978), 2-21, 319-343.

71. Juneja,J.M., Vijay,P.L., and Sehra,J.C.; Proc. Symp. : Metallothermic Processes in Metal and Alloy Extraction Dec. 28-30 (1983), Nagpur (India), 127.

72. Volsky, A. and Sergievskaya,E.; Theory of Metall- urgical Processes, Mir Publishers,Moscow,252-290.

73. Kumar,D., Bugga, P.S. and Jain,S.K.; Proc. All India Semr. Recent Trends in Ferro-Alloy Technology, Instn. of Engrs. Nagpur, Dec. 17-18 (1977), VRCE Nagpur (India),168.

74. Perfect, P.H.; Trans. Met. Soc. AIME, 239 (1967), 1282.

75. Mohanty,A.K.; Proc. Symp.; Metallothermic Processes in Metal and Alloy Extraction, Dec. 28-30 (1983),Nagpur (India),21.

76. Jena,P.K.; Proc. All India Sem. : Ferro Alloys Technology, Dec.17-18 (1977), VRCE Nagpur, 125.

77. Wilhelm, H.A., Bergman, R.M. and Schmidt, F.A.; J. of Metals, 22(1), (1970).

78. Behera,R.C. and Mohanty, A.K.; Proc. All Ind.Sem. : Ferro Alloys Technology, Dec. 17-18 (1977),VRCE Nagpur,119.

79. Rao,G.S.,Singh,A.J.and Ranganathan,T.N.; Proc. Symp : Metallothermic Processes in Metal and Alloy Extraction, Dec.28-30 (1983) Nagpur, India, 179.

80. Bolton,V.; W.Z. Elektvochem, (1907) Vol.13, 145.

81. Wilhelm, H.A., Schmidt, F.A. and Ellis,T.G.; J. Metals (1966), 1303.

82. Gupta,C.K. and Jena, P.K.; Trans. Metal, Dec. 1969, 51.

83. Gupta,C.K. and Jena, P.K.; Jour. of Metals, May 1968, 25.

84. Nayar, K.U., Mukherjee, T.K. and Gupta, C.K.; Jour. Less Common Metals, Vol.41, 1975, 87.

85. Bose,D.K., and Jena, P.K.; Trans. IIM, March 1970,56.

86. Gupta,C.K. et al., Trans. IIM, Vol.26, No.6, Dec.1973,24.

87. Mehra, O.K.,Gupta,C.K. and Jena,, P.K., Trans. IIM, March 1968, 45.

88. Riss, M. and Khodorovosky, Y.; Production of Ferro Alloys, Foreign Language Publishing House, Moscow (1971),174.

89. Mehra,O.K., Taneja, A.K., Gupta, C.K. and Jena, P.K.; Trans. IIM, March 1971, 66.

90. Mehra,O.K., Bose,D.K. and Gupta, C.K. Trans. IIM, April,1973, 24.

91. Bhatnagar, P.P. and Nijhawan,B.R.; Ferroalloys Industry in

India, Proc. Symp. N.M.L. India, 1662,83.

92. Behera, R.C., Mohanty, A.K. and Misra,S.; Trans. IIM, Vol.31(3), June 1978, 201.

93. Guccione, E.; Engg. Min. J., 172(9), 1971, 136.

94. Magyarosy,I. and Skuteczky, E.; Preparation of Alumina Plant Red Mud for Smelting (Hungarian), FKI, K021. 1962,6,91.

95. Lanyi,B., Method for Utilization of Bayer Process Muds (Hungarian), Koh.Lapok, 1950,83,40.

96. Dobos,Gy.; Proc.Res. Inst. Nonferrous Metals, IX, Publ. of Hung.Acad. of Sc. (1971), Budapest.61.

97. Kontopoulos, A., Sideris, J. and Moropulou,A.; Trans.Com. Int. Etude Bauxites,Alumine Alum.16, 315, 1981, C.A.96: 166201 Y.

98. Farkas,I., Csikos,R.and Bathory,J., Teljes, HU 34, 713 (C1.001 G49/16),29 Apr. 1985, Appl. 83/2,763,04 Aug. 1983,11 pp., CA. 103 : 127032 n.

99. Zambo,J.; Proc. INCAL-91, Aluminium Association of India, Banglore, 1991,163.

100. Ziegenbalg et al. Ger. (East), DD 200, 896 (C 1. C 22 B7/00), 22 Jun. 1983 Appl. 233, 521, 24 Sep. 1981, 16 pp. CA.99 : 142437 r.

101. Yoshii, C. and Ishimura, K.; Hokkaido Daigaku Kogakabu Kenkyu Hokoku, 89, 1(1978). C.A. 91 : 77336 a.

102. Ijima,T., Shimakage, K. and Hoshi,M.; Keikinzoku, 27(10), 465 (1977(. C.A. 90 : 155072 g.

103. Rumke, S.R. and Meare,R.G.; AIME Tech. Bull. No.1698, Chem. Abs. 1944, 38, 5176.

104. Baetz, H.B. and Lightbourne, R.C.; US Pat.3, 1972,690,828.

105. Udy, J.M. US Pat 2, 1958, 830,892.

106. Nishimoto,Y.; Tech. Rev. Mitsubishi Heavy Ind. 31(1) 59; 1966, Chem Abs. 1968, 68 116031 u.

107. Logomerac, V.G.; Verhandelingen Kon.Ned. Geol. Mijnbouwk Gen 1969,27,155.

108. Logomerac,V.G.; Proc. 2nd Intl. Symp. ICSOBA 1971,3,383.

109. Cegledi,B.; Banyasz,Kohasz. Lapols, Kohak,114(4), 180, 1981, C.A.95: 100965 Y.

110. Thakur,R.S., Muralidhar, J. and Ram Krishna Sant, B.; 17 June 1974, Chem. Abs. 92: 62481 r.

111. Prasad, P.M. et al., Intl. Conf. Prog.Met. Res.; Fundamental and Applied Aspects, Feb. 11-15, 1985, IIT Kanpur,India,383.

112. Anon, Project Proposal No.42, CBRI Roorkee,India, 1975.

113. Nakamura,H.H., Bortz,S.A. and Schwartz, M.A.; J.Amer. Cer. Soc. Bull.50(3), 1971, 248.

114. Chowdhry,N.A., Water Pollution Control, 113(2), 1975,17.

115. Shultz,F.G. and Berber,J.S., J.Air Pollution Centr. ASS. 20(2), 1970, 93.

116. Satapathy,B.K., Patnaik,S.C. and Vidyasagar, P; Proc. INCAL-91, July 31-Aug.2(1991), Bangalore,India, 159.

117. Kumar,D.and Jain,S.K.; Proc. Symposium on Metallothermic Process in Metal and Alloy Extraction, Dec. 28-30,1983, Nagpur (India),17.

118. Taggart,F.; Hand Book of Mineral Dressing , John Wiley and sons. Inc. New York (1953).

119. Aggarwal,B.C. and Jain,S.P.; Metallurgical Analysis, Khanna Publishers, New Delhi.

120. Bassett, Denney and Jeffery.; Vogel's Text Book of Quantitative Analysis, ELBS and Longman (1978).

121 Index (Inorganic) to the Powder Diffraction File,1971, Joint Committee on Powder Diffraction Standards.

122. Filippov,S.; The Theory of Metallurgical Processes, Mir Publisher Moscow, 168-171, 198-216.

123. Baak,T.; Proc.Conf.'Physical Chemistry of Iron and Steel Making,Endicott House, Dedham, Massachussetts (1956),48.

124. Gupta,V.K, and Seshadri,V.; Trans.IIM, 29,(1976),103.

125. Partington,J.R.; A Text Book of Inorganic Chemistry, 6th Ed., ELBS,703.

Table 5.2 Details of recovery values and composition of alloy as influenced by variation in the amount of reductant i.e. Al-powder (particle size of Al-powder, -63+ 53 microns)

Sl. No.	Amount of Al-powder (gms)	% excess over stoch Amount.	wt.of alloy (gms)	OR %	Chemical Analysis of alloy %				Recovery of constituent metals %		
					Fe	Ti	Si	Al	Fe	Ti	Si
1.	136.70	0	-	-	-	-	-	-	-	-	-
2.	164.00	20	58	24.93	84.80	1.87	0.3	7.72	36.22	1.92	0.77
3.	191.40	40	131	57.60	79.88	6.67	0.75	5.60	77.06	15.49	4.3
4.	218.70	60	144.50	62.80	75.23	10.74	1.68	6.69	80.05	27.52	10.79
5.	246.00	80	148.50	63.02	66.90	15.66	2.96	8.89	73.16	41.23	19.54
6.	273.40	100	163	68.43	65.38	15.89	3.42	9.87	78.45	45.92	24.78

Table 5.3 Details of recovery values and composition of alloy as influenced by variation in the amount of reductant i.e. Al- powder (particle size of Al-powder, -106+63 microns)

Sl. No.	Amount of Al-powder (gms)	% excess over stoch. Amt.	wt.of alloy (gms)	OR %	Chemical Analysis of alloy %				Recovery of constituent-metals %		
					Fe	Ti	Si	Al	Fe	Ti	Si
1.	136.70	0	-	-	-	-	-	-	-	-	-
2.	164.00	20	32	13.76	86.52	1.27	0.43	7.91	20.39	0.72	0.61
3.	191.40	40	142	61.68	78.92	7.16	1.21	6.73	82.52	18.03	7.64
4.	218.70	60	138.50	59.85	75.08	10.79	1.81	7.22	76.57	26.50	11.14
5.	246.00	80	158	66.81	68.15	16.12	2.01	9.21	79.29	45.16	14.11
6.	273.40	100	166.50	69.88	65.90	16.26	1.95	9.89	80.80	48.00	14.43

Table 5.4 Details of recovery values and composition of alloy as influenced by variation in the amount of reductant i.e. Al= powder (particle size of Al-powder, -300+150 microns)

Sl. No.	Amount of Al-powder (gms)	% excess over stoch. Amt.	wt.of alloy (gms)	OR %	Chemical Analysis % alloy				Recovery of constituent metals %		
					Fe	Ti	Si	Al	Fe	Ti	Si
1.	136.70	0	-	-	-	-	-	-	-	-	-
2.	164.04	20	47.50	20.44	86.24	1.20	0.38	7.62	30.16	1.01	0.81
3.	191.38	40	134.50	57.82	79.77	7.82	1.16	7.71	79.01	18.64	6.93
4.	218.72	60	148	63.34	75.21	9.87	1.78	8.11	81.97	25.90	11.71
5.	246.06	80	155.50	65.47	68.42	15.93	1.98	9.61	78.35	43.92	13.68
6.	273.40	100	173	72.33	67.27	16.02	2.05	10.24	85.68	49.14	15.76

Table 5.5 Charge balance of the heats taken (amount and perticle size of reductant)

S N	Charge Weight (gms)					Total weight of charge (gms)	Weight of alloy +Slag (gms) Al-Particle size (μ)			%Loss of Charge Al-Particle size (μ)		
	RM	Al	Lime	CaF_2	$KClO_3$		-63+53	-106 +63	-300 +125	-63 +53	-106 +63	-300 +150
1	500	136.70	78.20	6.80	106.80	828.50	764.60	765.20	766.70	7.71	7.64	7.46
2	500	164.00	93.80	8.20	113.10	879.10	803.25	807.00	807.55	8.63	8.20	8.14
3	500	191.40	109.50	9.60	120.00	930.50	829.25	834.50	834.75	10.88	10.32	10.29
4	500	218.70	125.00	10.90	126.00	980.60	847.45	855.90	859.40	13.58	12.72	12.36
5	500	246.00	140.70	12.30	132.00	1031.0	884.50	888.20	896.15	14.21	13.85	13.08
6	500	273.40	156.40	13.70	136.60	1080.1	926.95	929.10	938.40	14.18	13.98	13.12

Table.5.7 Recovery values, composition of alloys and geometrical details of charge column as obtained by the variation of scale of production in Reactor 'A'

Sl No	Scale of Prodn (gms)	Geometrical Details as received by charge column in reactor			Wt.of alloy (gms)	OR %	Chemical Analysis of alloy %				Recovery of constituents %		
		h (cm)	d (cm)	h/d			Fe	Ti	Si	Al	Fe	Ti	Si
1.	100	4.80	9.50	0.51	21.50	45.25	83.88	3.45	0.91	9.62	66.39	6.58	4.35
2	200	7.50	10.00	0.75	58.50	61.96	84.21	3.70	1.08	9.04	90.69	9.60	7.02
3.	300	10.00	10.60	0.94	90	63.82	78.22	6.32	1.12	8.94	86.40	16.81	7.47
4.	400	12.70	11.00	1.15	108	57.28	67.31	13.19	1.41	8.91	66.91	31.57	8.46

Table.5.8 Recovery values, compositions of alloy and geometrical details of charge column as obtained by the variation of scale of production in Reactor 'B'

Sl No	Scale of Prodn (gms)	Geometrical Details as received by charge column in reactor			Wt.of alloy (gms)	OR %	Chemical Analysis of alloy %				Recovery of constituents %		
		h (cm)	d (cm)	h/d			Fe	Ti	Si	Al	Fe	Ti	Si
1.	100	4.00	11.00	0.36	-	-	-	-	-	-	-	-	-
2	200	6.00	12.70	0.47	55	57.81	79.14	4.43	0.85	9.74	80.13	10.85	5.19
3.	300	7.80	12.90	0.60	73.50	51.89	72.29	8.21	1.22	9.18	65.21	17.83	6.64
4.	400	10.50	13.00	0.81	117.5	62.02	67.66	15.94	1.31	9.34	73.17	41.51	8.55
5.	500	12.70	13.10	0.97	158	66.81	68.15	16.12	2.01	9.21	79.29	45.16	14.11
6.	600	12.90	13.30	0.97	194	68.53	68.21	16.04	2.38	8.98	81.20	45.98	17.10

Table.5.9 Recovery values, compositions of alloy and geometrical details of charge column as obtained by the variation of scale of production in Reactor 'C'

Sl No	Scale of Prodn (gms)	Geometrical Details as received by charge column in reactor			Wt.of alloy (gms)	OR %	Chemical Analysis of alloy %				Recovery of constituents %		
		h (cm)	d (cm)	h/d			Fe	Ti	Si	Al	Fe	Ti	Si
1.	100	3.50	11.50	0.30	-	-	-	-	-	-	-	-	-
2	200	5.10	13.50	0.41	63	65.13	74.64	5.10	2.14	11.21	86.57	14.24	14.98
3.	300	7.00	13.50	0.51	96	68.64	76.33	5.42	2.50	9.98	89.93	15.38	17.78
4.	400	8.50	13.90	0.61	119	63.16	73.00	11.12	2.08	8.84	79.96	29.33	13.75
5.	500	10.50	14.10	0.74	171.5	72.45	65.08	16.64	1.87	9.30	82.19	50.60	14.25
6.	600	11.50	14.30	0.80	192	67.85	62.73	16.81	2.10	8.95	73.90	47.69	14.93

Table 5.12 Charge balance (Scale of production and reactor geometry

SN	Scale of production (gms)	Charge Weight (gms)					Total weight of charge (gms)	Weight of alloy +Slag (gms)					% Loss of Charge				
		RM	Al	Lime	CaF_2	$KClO_3$		Reactor 'A'	Reactor 'B'	Reactor 'C'	Reactor 'D'	Reactor 'E'	Reactor 'A'	Reactor 'B'	Reactor 'C'	Reactor 'D'	Reactor 'E'
1	100	100.00	49.00	28.00	2.45	26.40	205.85	177.30	168.39	170.98	178.90	178.79	13.87	18.20	16.94	13.09	13.15
2	200	200.00	98.00	56.00	4.90	52.80	411.70	357.27	351.96	350.81	357.19	355.34	13.22	14.51	14.79	13.24	13.69
3	300	300.00	147.00	84.00	7.35	79.20	617.55	538.87	530.41	529.12	550.10	532.88	12.74	14.11	14.32	10.92	13.71
4	400	400.00	196.00	112.00	9.80	105.60	823.40	707.14	714.30	719.82	731.10	714.29	14.12	13.25	12.58	11.21	13.25
5	500	500.00	246.00	140.70	12.30	132.00	1031.0	–	888.20	900.48	916.00	887.18	–	13.85	12.66	11.16	13.95
6	600	600.00	294.00	168.00	14.70	158.40	1225.1	–	1037.6	1030.5	1061.92	1051.38	–	15.30	15.88	13.32	14.18

Table. 5.14 Recovery values and compositions of alloy obtained by varying the particle size of reductant (Al) for red mud particle size, -150+125 micron.

Sl. No.	Particle size ofAl, Micron	Av.particle size difference of red mud & Al, Micron	Wt.of alloy (gms)	OR %	Chemical Analysis of alloy %				Recovery of constituents metal %		
					Fe	Ti	Si	Al	Fe	Ti	Si
1.	-53+45	88.50	166.50	71.28	68.36	16.51	2.18	8.08	83.81	48.74	16.13
2	-106+63	53	154	65.84	69.51	16.36	2.12	8.20	78.83	44.67	14.51
3.	-150+125	0.00	158	67.03	68.54	16.12	2.10	8.92	79.74	45.16	14.75
4.	-300+212	-118.50	145.50	61.38	68.30	12.92	1.78	9.43	73.18	33.33	11.51
5.	-425+300	-225	133	55.37	70.32	9.64	1.69	10.62	68.87	22.73	9.99

Table. 5.15 Recovery values and compositions of alloys obtained by varying particle size of reductant (Al) for red particle size, -300+212 microns.

Sl. No.	Particle size ofAl, Micron	Av.particle size difference of red mud & Al, Micron	Wt.of alloy (gms)	OR , %	Chemical Analysis of alloy %				Recovery of constituents metals%		
					Fe	Ti	Si	Al	Fe	Ti	Si
1.	-53+45	207.00	132	56.08	70.24	16.10	1.78	8.59	68.27	37.68	10.44
2	-106+63	171.50	158	66.81	68.15	16.12	2.01	9.21	79.29	45.16	14.11
3.	-150+125	118.50	145	61.21	69.90	15.76	2.22	9.36	74.64	40.52	14.31
4.	-300+212	00.00	148.50	62.72	68.32	15.38	2.28	9.32	74.71	40.50	15.05
5.	-425+300	-106.50	141	59.09	68.82	14.98	1.97	10.03	71.45	37.45	12.34

Table 5.16 Recovery values and compositions of alloys obtained by varying the particle size of reductant (Al) for red mud particle size, -425+300 Micron.

Sl No	Particle size (sieve) of Al (μ)	Average p.s of Al (μ)	Av.particle size difference of RM and Al Micron	wt. of alloy (gms)	OR %	Chemical Analysis of alloy %				Recovery of constituent metals %		
						Fe	Ti	Si	Al	Fe	Ti	Si
1.	-53+45	49.0	313.5	135	57.27	70.34	10.88	1.51	8.92	69.92	26.04	9.06
2.	-106+63	84.5	278.0	148	62.82	68.07	13.91	1.47	8.86	74.19	36.50	9.67
3.	-150+125	137.5	225.0	144.5	61.41	70.71	15.83	1.98	8.75	75.24	40.56	12.72
4.	-300+212	256.0	106.5	151.5	64.23	68.12	14.61	1.70	8.98	76.00	39.25	11.45
5.	-425+300	362.5	0.0	144	60.91	71.87	14.46	1.36	9.18	76.20	36.92	8.70

Table 5.17 Charge Balance of the Heats Taken (Particle Size of Reductant and Red Mud)

S N	Charge Weight (gms)					Total weight of charge (gms)	Weight of alloy +Slag (gms)			%Loss of Charge		
							Red Mud Particle size (μ)			Red Mud Particle size (μ)		
	RM	Al	Lime	CaF_2	$KClO_3$		-150 +125	-300 +212	-425 +300	-150 +125	-300 +212	-425 +300
1	500	246.00	140.70	12.30	132.00	1031.0	882.44	885.12	887.28	14.41	14.15	13.94
2	500	246.00	140.70	12.30	132.00	1031.0	886.45	888.20	889.14	14.02	13.85	13.76
3	500	246.00	140.70	12.30	132.00	1031.0	886.97	891.61	892.33	13.97	13.52	13.45
4	500	246.00	140.70	12.30	132.00	1031.0	891.00	892.44	891.60	13.58	13.44	13.52
5	500	246.00	140.70	12.30	132.00	1031.0	899.90	894.91	902.54	12.62	13.20	12.46

Table. 5.19 Recovery values and Compositions alloys obtained by Lime (CaO) addition

Sl No	Amount of CaO (gms)	% of (RM+ Al)	Wt.of alloy (gms)	OR %	% Chemical Analysis of alloy				% Recovery of constituents		
					Fe	Ti	Si	Al	Fe	Ti	Si
1.	0	0	104	43.19	68.85	7.25	4.18	10.83	52.73	13.37	19.33
2	74.60	10	102	42.92	62.03	12.36	3.90	9.66	46.59	22.35	17.68
3.	149.20	20	165	69.69	64.10	16.30	2.04	9.32	77.88	47.69	14.96
4.	223.80	30	158.5	67.28	63.78	16.89	2.63	8.85	74.44	47.47	18.56
5.	298.40	40	138	58.63	61.45	16.47	3.56	8.78	62.45	40.30	21.84

Table 5.20 Change balance (CaO and MgO addition)

SN	Amount of flux as% of(RM+Al	Charge weight (gms)				Total wt. of the charge (gms)		Wt. of alloy +Slag (gms)		% Loss of Charge	
		Flux			Booster	Lime addition	Magnesia Addition	Lime addition	Magnesia addition	Lime addition	Magnesia addition
		RM+Al Powde	Lime	Magnesia	$KClO_3$						
1	0	746.00	0.00	0.00	112.00	858.0	858.00	740.00	740.00	13.75	13.75
2	5	746.00	-	41.15	119.00	-	906.15	-	785.65	-	13.30
3	10	746.00	85.35	82.30	125.00	956.35	953.30	816.75	821.30	14.60	13.85
4	20	746.00	170.70	164.60	138.00	1054.7	1048.6	904.30	898.65	14.26	14.30
5	30	746.00	256.00	246.90	150.00	1152.0	1142.9	977.80	965.50	15.12	15.52
6	40	746.00	341.40	-	164.00	1251.4	-	1055.5	-	15.65	-

Table 5.21 Recovery values and compositions of the alloys obtained by magnesia (MgO) addition.

Sl. No.	Amount of MgO (gms)	% of (RM+ Al)	Wt.of alloy (gms)	OR %	Chemical Analysis of alloy %				Recovery constituents %		
					Fe	Ti	Si	Al	Fe	Ti	Si
1.	37.30	5	112	47.43	70.60	8.95	4.63	9.07	58.23	17.77	23.06
2	74.60	10	119	50.07	69.25	10.14	4.40	9.67	60.68	21.39	23.28
3.	149.20	20	94	39.37	70.22	10.55	3.90	10.08	48.60	17.58	16.30
4.	223.80	30	90	37.42	71.32	8.27	3.12	10.73	47.27	13.19	12.49

Table.5.22 Recovery values and compositions of the alloys obtained by Fluorspar (CaF_2) addition

Sl. No.	Amount of CaF_2 (gms)	CaF_2 as % of CaO	Wt.of alloy (gms)	OR %	Chemical Analysis of alloy %				Recovery of constituents %		
					Fe	Ti	Si	Al	Fe	Ti	Si
1.	3.73	5	132	55.21	70.12	14.18	3.28	10.20	68.16	33.19	19.25
2	7.46	10	138	57.93	68.25	13.21	3.09	9.87	69.36	32.32	18.96
3.	11.19	15	143.50	60.06	68.32	14.22	3.45	10.14	72.19	36.18	22.01
4.	14.92	20	141	59.16	64.34	14.06	2.88	9.92	66.80	35.15	18.06
5.	18.65	25	134.50	56.60	66.28	14.28	3.73	9.65	65.65	34.05	22.31

Table - 5.23 Charge balance (CaF_2 addition)

S. No	weight of charge (gms)				$KClO_3$	Total weight of charge (gms)	Total weight of alloy + slag (gms)	% Loss of charge
	Red mud	Al	Lime	CaF_2				
1.	500	246.00	85.35	3.73	125.30	960.38	827.92	13.79
2.	500	246.00	85.35	7.46	125.80	964.61	834.30	13.51
3.	500	246.00	85.35	11.19	126.40	968.94	827.48	14.60
4.	500	246.00	85.35	14.92	126.90	973.17	844.23	13.25
5.	500	246.00	85.35	18.65	127.50	977.50	852.78	12.76

Table.5.25 Recovery values and compositions of the alloys obtained by $KClO_3$ addition at 100°C preheating.

Sl No	Amount of $KClO_3$ (gms)	% of total charge	Wt.of alloy (gms)	OR %	Chemical Analysis of alloy %				Recovery of constituents %		
					Fe	Ti	Si	Al	Fe	Ti	Si
1.	0	0	–	–	–	–	–	–	–	–	–
2	44.00	5	67	27.20	78.20	4.26	1.01	12.85	38.58	5.06	3.00
3.	88.00	10	71	29.20	78.82	3.88	1.29	11.70	41.20	4.88	4.07
4.	132.00	15	110	45.33	72.02	7.80	1.16	11.52	58.34	15.21	5.67
5.	176.00	20	144	59.87	67.34	12.44	2.60	10.74	71.41	31.76	16.65

Table. 5.26 Recovery values and compositions of the alloys obtained by $KClO_3$ addition at 200°C preheating.

Sl No	Amount of $KClO_3$ (gms)	% of total charge	Wt.of alloy (gms)	OR %	Chemical Analysis of alloy %				Recovery of constituents %		
					Fe	Ti	Si	Al	Fe	Ti	Si
1.	0.00	0	45.00	19.30	82.15	2.88	2.63	7.91	27.22	2.30	5.26
2	44.00	5	70.50	30.20	79.06	3.60	1.85	8.02	41.04	4.50	5.80
3.	88.00	10	78.50	33.56	73.82	8.26	2.89	8.22	42.67	11.50	10.08
4.	132.00	15	109.00	46.78	75.26	8.89	3.84	7.86	60.40	17.18	17.64
5.	176.00	20	131.50	56.36	72.18	13.92	3.44	7.98	69.89	32.46	20.11

Table.5.27 Recovery values and compositions of the alloys obtained by $KClO_3$ addition at 300°C preheating.

Sl No	Amount of $KClO_3$	% of total charge	Wt.of alloy (gms)	OR %	Chemical Analysis of alloy %				Recovery of constituents %		
					Fe	Ti	Si	Al	Fe	Ti	Si
1.	0.00	0	68.00	28.73	80.15	3.57	1.24	9.27	40.13	4.30	3.75
2	44.00	5	94.00	39.68	74.91	4.61	1.21	9.38	51.85	7.68	5.05
3.	88.00	10	116.50	48.91	70.23	7.94	2.46	9.86	60.25	16.40	12.74
4.	132.00	15	140.00	59.63	68.82	10.22	2.93	8.56	70.94	25.37	18.24
5.	176.00	20	152.00	64.96	64.24	15.24	3.19	8.24	71.90	41.07	21.56

Table.5.28 Recovery values and compositions of the alloys obtained by KNO_3 addition (Preheating , 300°C)

Sl No	Amount of KNO_3 (gms)	% of total charge	Wt.of alloy (gms)	OR %	Chemical Analysis of alloy %				Recovery of constituents %		
					Fe	Ti	Si	Al	Fe	Ti	Si
1.	0.00	0	68.00	28.73	80.15	3.57	1.24	9.27	40.13	4.30	3.75
2	44.00	5	104.50	43.60	81.20	2.57	2.21	10.41	62.48	4.76	10.26
3.	88.00	10	126.50	52.95	73.34	8.20	2.52	10.13	68.32	18.39	14.17
4.	132.00	15	144.50	61.11	72.64	7.72	2.89	9.20	77.29	19.78	18.57
5.	176.00	20	161.00	67.85	67.69	11.43	3.23	9.52	80.25	32.63	23.23

Table 5.30 Charge balance of the heats booster addition and preheating temperature

S N	Charge Weight (gms)					Total weight of charge (gms)	Weight of alloy +Slag (gms)				% Loss of Charge			
							$KClO_3$			KNO_3	$KClO_3$			KNO_3
	RM	Al	Lime	CaF_2	Booster		100°C	200°C	300°C	300°C	100°C	200°C	300°C	300°C
1	500	246.00	140.70	12.30	0.00	899.00	819.25	811.00	794.90	794.90	9.87	9.78	11.58	11.58
2	500	246.00	140.70	12.30	44.00	943.00	849.85	823.00	800.90	790.25	9.88	12.72	15.07	16.20
3	500	246.00	140.70	12.30	88.00	987.00	858.40	845.65	841.10	824.55	13.03	14.32	14.78	16.46
4	500	246.00	140.70	12.30	132.00	1031.0	913.25	902.10	889.55	856.45	11.42	12.50	13.72	16.93
5	500	246.00	140.70	12.30	176.00	1075.0	924.30	904.50	898.60	889.10	14.02	15.86	16.41	17.29

Table 5.32 Details of alloy recoveries and compositions as affected by preheating temperature for 1 hr preheating time.

Sl. No.	Tempr. of pre-heating ^{o}C	wt.of alloy (gms)	OR %	Chemical Analysis of alloy %				Recov. of constitu-ent metals %		
				Fe	Ti	Si	Al	Fe	Ti	Si
1.	No pre-heating	-	-	-	-	-	-	-	-	-
2.	100	76	31.76	81.15	3.17	0.66	10.27	45.42	4.27	2.23
3.	200	97.50	40.95	78.62	5.25	0.84	9.82	56.44	9.08	3.64
4.	300	128	54.12	78.30	7.98	0.89	9.22	73.80	18.11	5.06
5.	400	138.50	58.40	68.72	13.96	1.08	9.47	70.09	34.28	6.65
6.	500	147	62.20	67.78	14.60	1.68	9.16	73.37	38.05	11.03

Table 5.33 Details of alloy recoveries and compositions as affected by preheating temperature for 2 hrs preheating time.

Sl. No.	Tempr. of pre-heating °C	wt.of alloy (gms)	OR %	Chemical Analysis of alloy %				Recov. of constitu-ent metals %		
				Fe	Ti	Si	Al	Fe	Ti	Si
1.	No pre-heating	–	–	–	–	–	–	–	–	–
2.	100	110	45.33	72.02	7.80	1.16	11.52	58.34	15.21	5.67
3.	200	109	46.78	75.26	8.89	3.84	7.86	60.40	17.18	17.64
4.	300	140	59.63	68.82	10.22	2.93	8.56	70.94	25.37	18.24
5.	400	158	66.81	68.15	16.12	2.01	9.21	79.29	45.16	14.11
6.	500	152.50	65.32	65.85	16.44	3.06	8.04	73.95	44.45	20.74

Table 5.34 Details of alloy recoveries and compositions as affected by preheating temperature for 3 hrs preheating time.

Sl. No.	Tempr. of pre-heating °C	wt.of alloy (gms)	OR %	Chemical Analysis of alloy %				Recovery of constituent metals %		
				Fe	Ti	Si	Al	Fe	Ti	Si
1.	No pre-heating	-	-	-	-	-	-	-	-	-
2.	100	116.50	48.88	76.56	7.69	1.21	9.91	65.68	15.88	6.27
3.	200	124	52.32	73.55	8.85	2.75	9.41	67.16	19.46	15.16
4.	300	144	61.39	73.21	10.66	3.54	8.74	77.63	27.22	22.66
5.	400	161.50	68.86	68.08	16.26	3.71	8.46	80.96	46.56	26.30
6.	500	157.50	67.72	68.32	16.38	3.51	7.68	79.24	45.74	24.57

Table 5.35 Charge balance (preheating temperature and time)

S N	Charge Weight (gms)					Total weight of charge (gms)	Weight of alloy +Slag (gms)			%Loss of Charge		
	RM	Al	Lime	CaF_2	$KClO_3$		1 hr. pr.ht.	2 hr. pr.ht.	3 hr. pr.ht.	1 hr. pr.ht	2 hr. pr.ht	3 hr. pr.ht
1	500	246.00	140.70	12.30	132.00	1031.0	928.62	928.62	928.62	9.93	9.93	9.93
2	500	246.00	140.70	12.30	132.00	1031.0	927.50	925.63	923.26	10.04	10.22	10.45
3	500	246.00	140.70	12.30	132.00	1031.0	924.90	894.10	888.93	10.29	13.28	13.78
4	500	246.00	140.70	12.30	132.00	1031.0	920.89	889.65	888.62	10.68	13.71	13.81
5	500	246.00	140.70	12.30	132.00	1031.0	912.95	888.20	887.28	11.45	13.85	13.94
6	500	246.00	140.70	12.30	132.00	1031.0	904.40	887.07	884.40	12.28	13.96	14.22

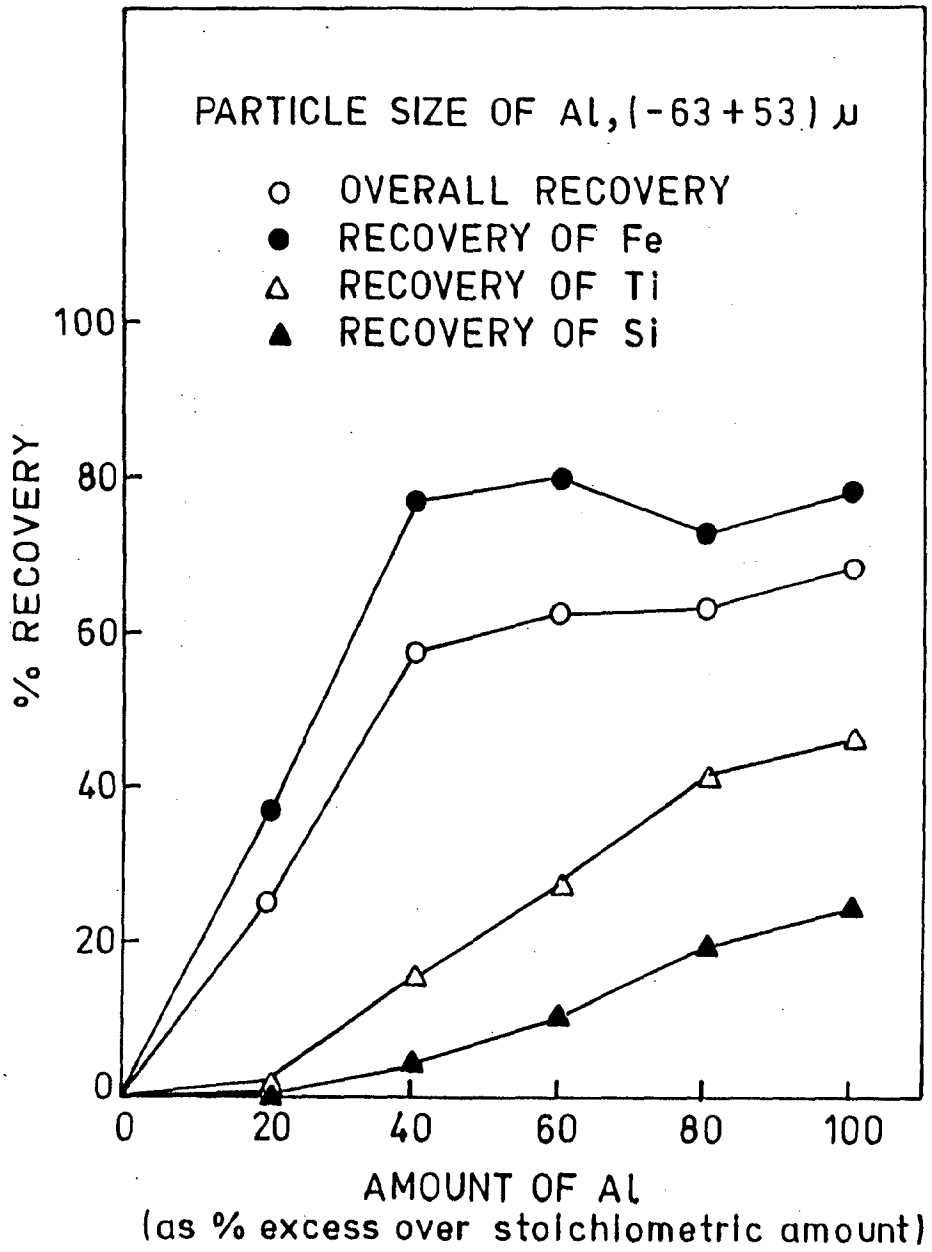

Fig.5.1 : Effect of amount of reductant (Al), on recovery values of the alloy (particle size of Al, -63+53 microns).

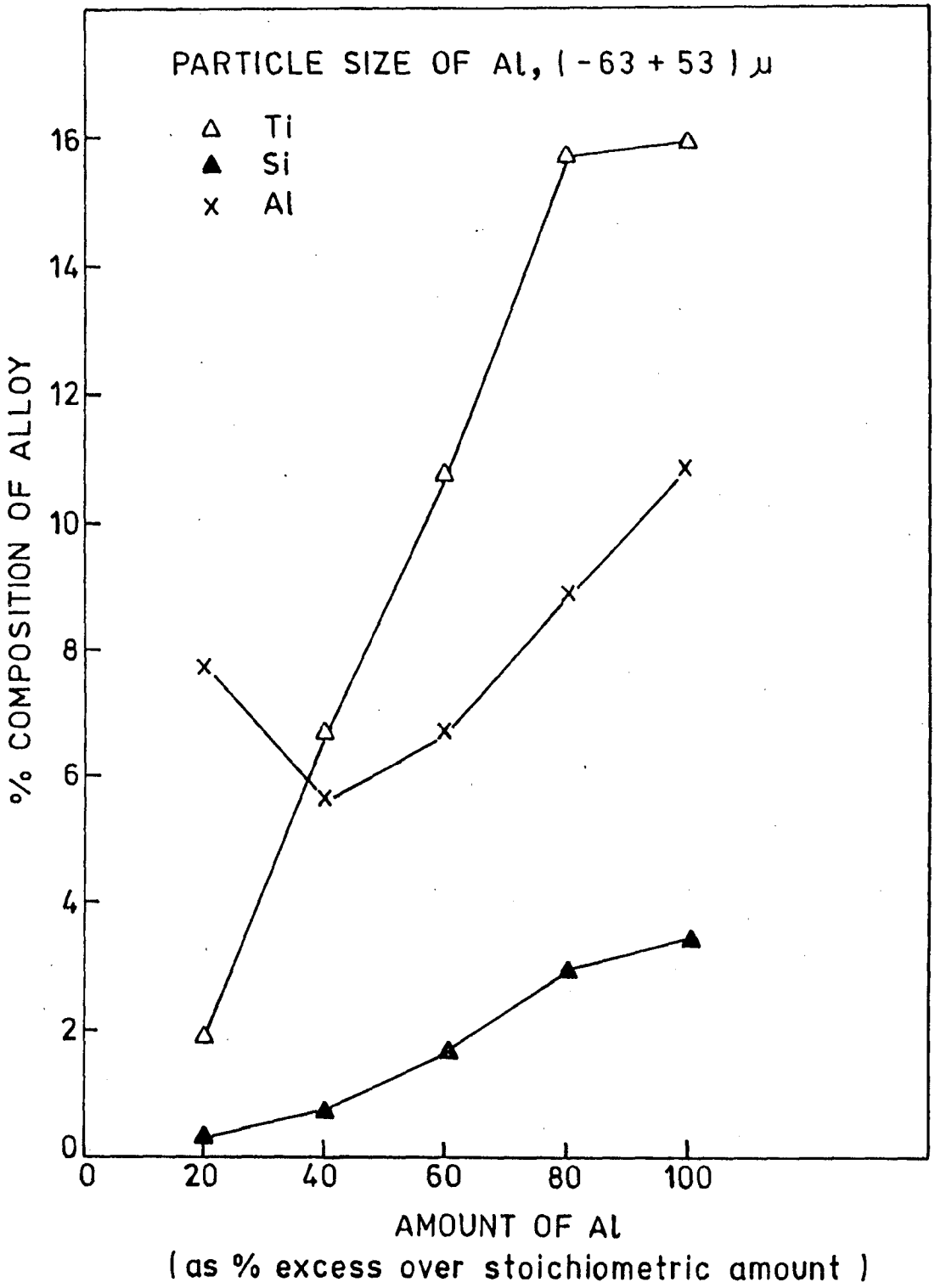

Fig.5.2 : Effect of amount of reductant (Al), on the composition of the alloy (particle size of Al, -63+53 microns).

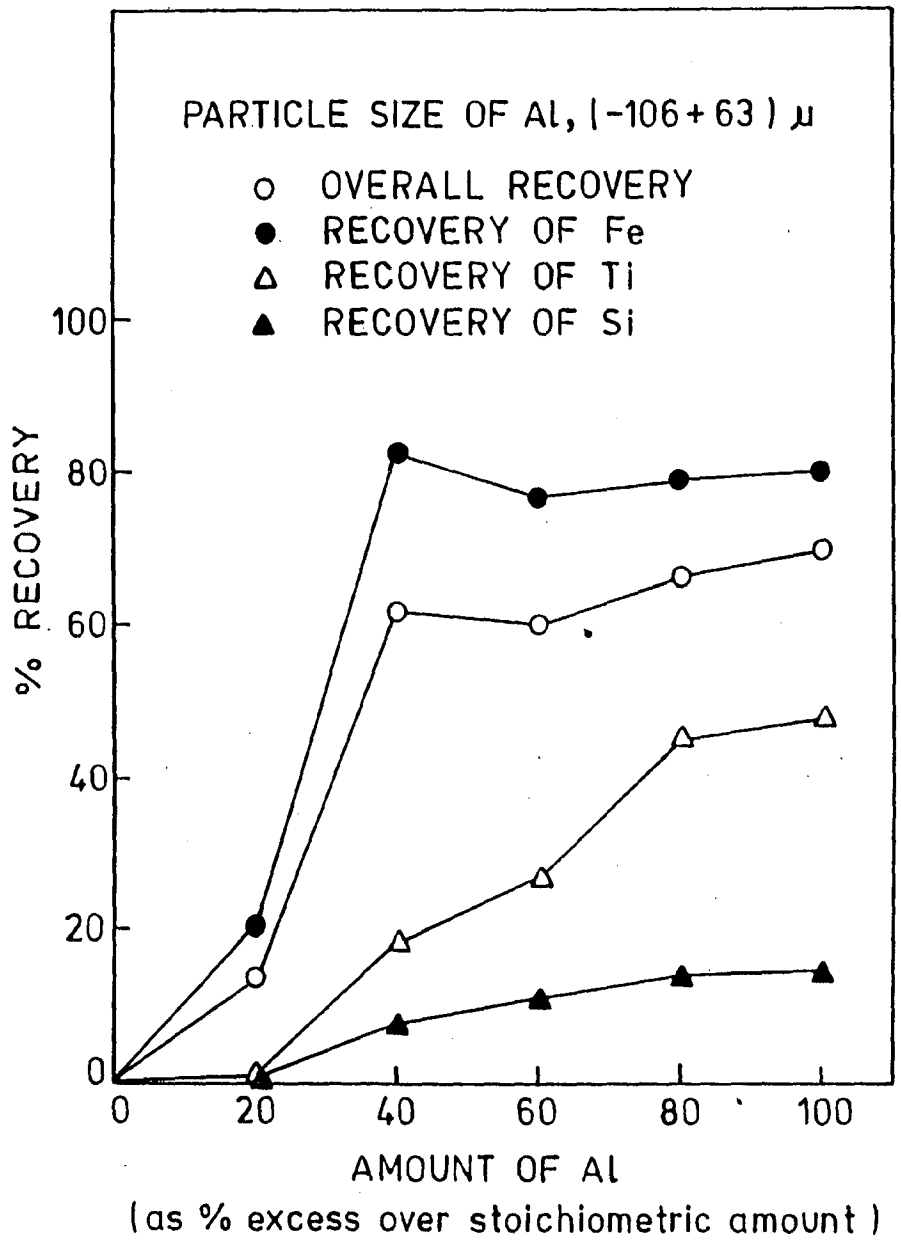

Fig.5.3 : Effect of amount of reductant (Al), on recovery values of the alloy (particle size of Al, -106+63 microns).

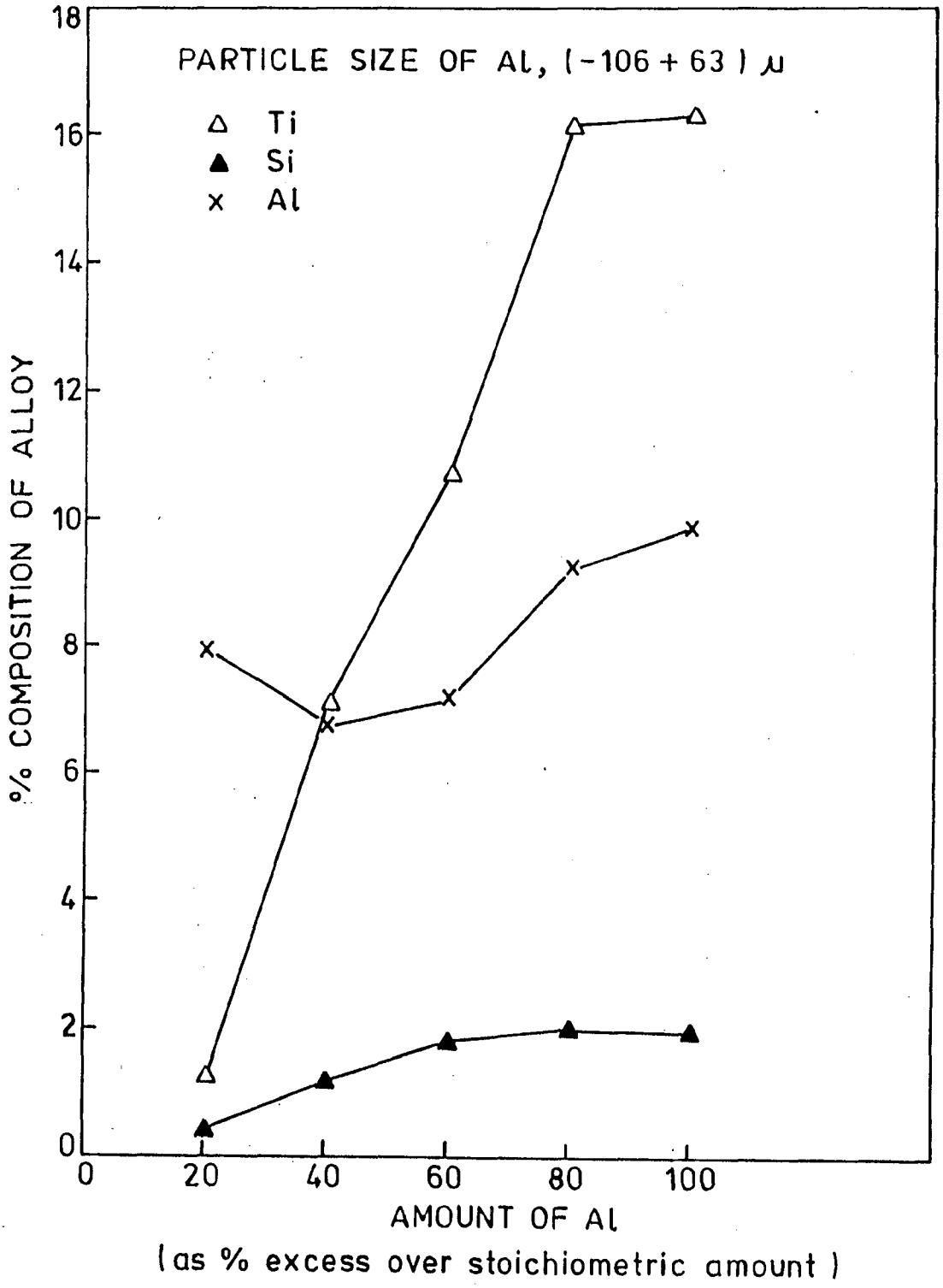

Fig.5.4 : Effect of amount of reductant on composition of the alloy (particle size of Al, -106+63 microns).

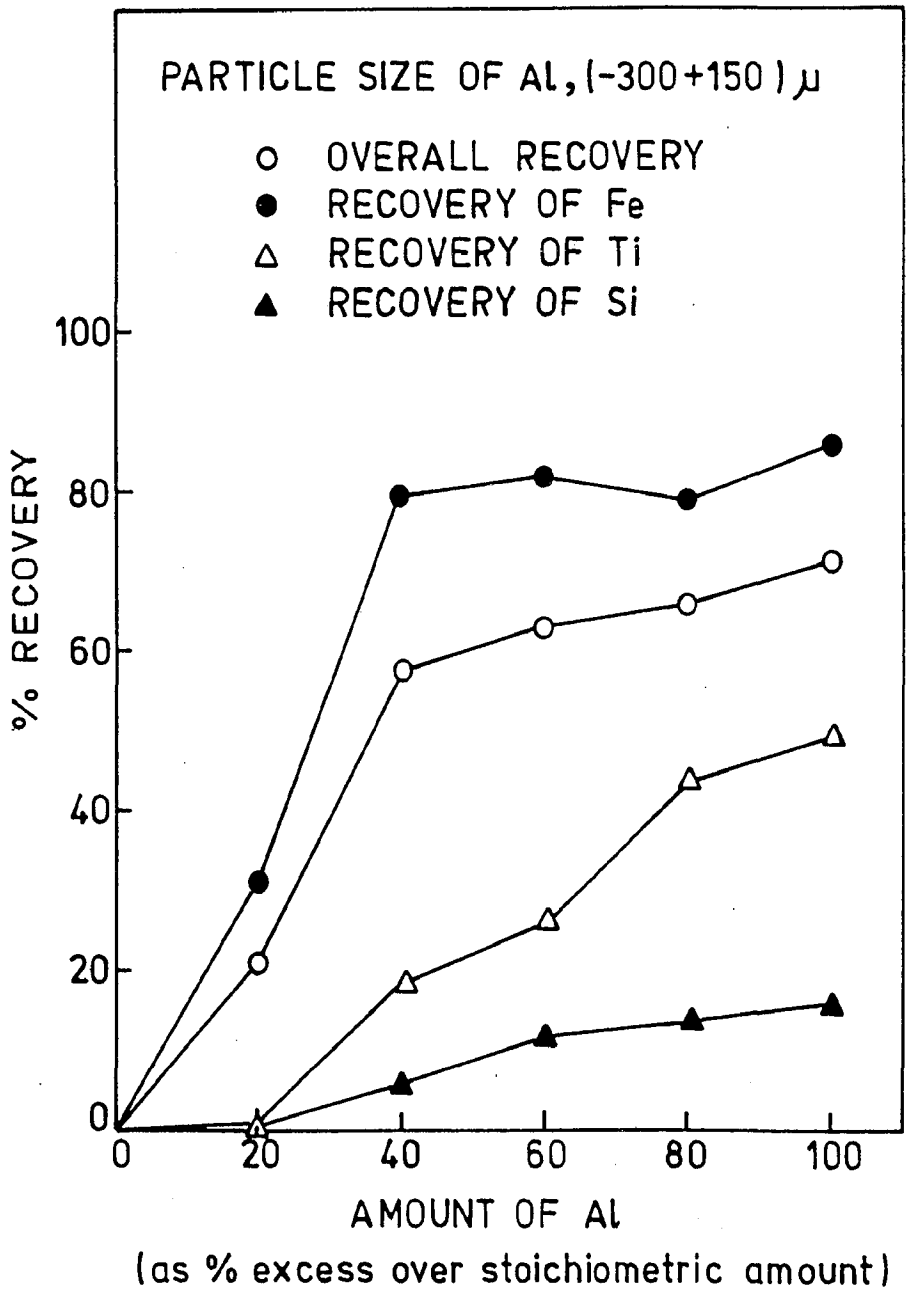

Fig.5.5 : Effect of amount of reductant (Al), on recovery values of the alloy (particle size of Al, -300+150 microns).

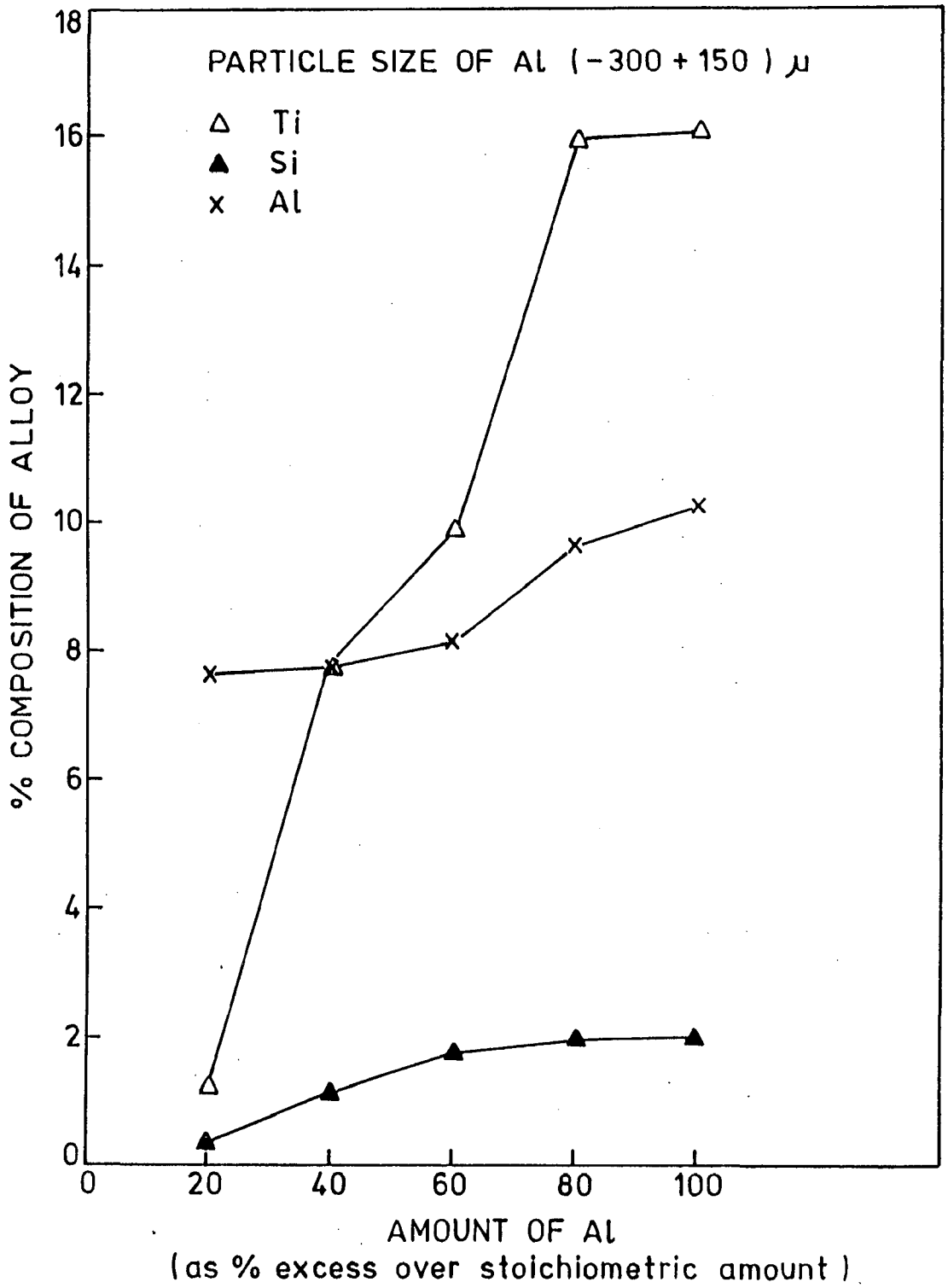

Fig.5.6 : Effect of amount of reductant on the composition of the alloy (particle size of Al, -300+150 microns).

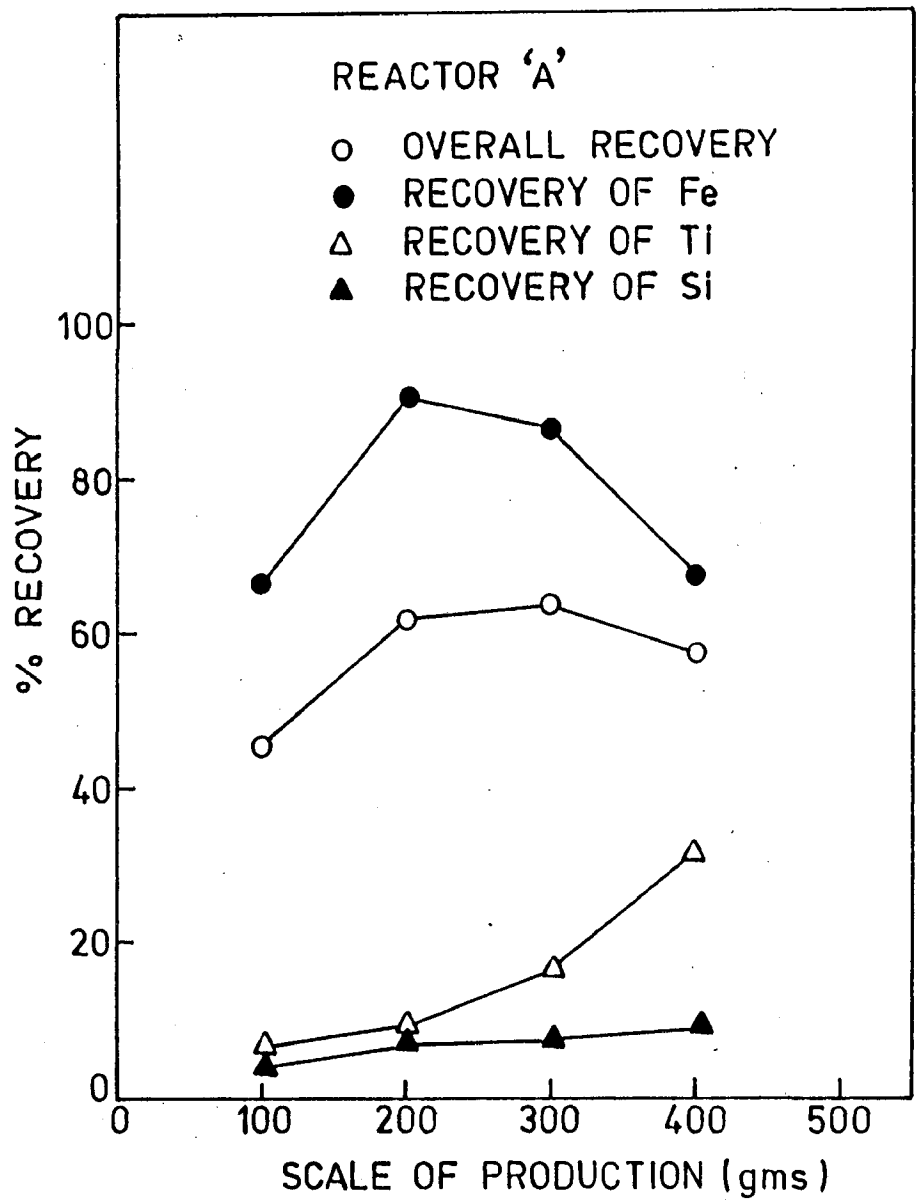

Fig.5.7 : Effect of scale of production on recovery values of the alloy in reactor 'A'.

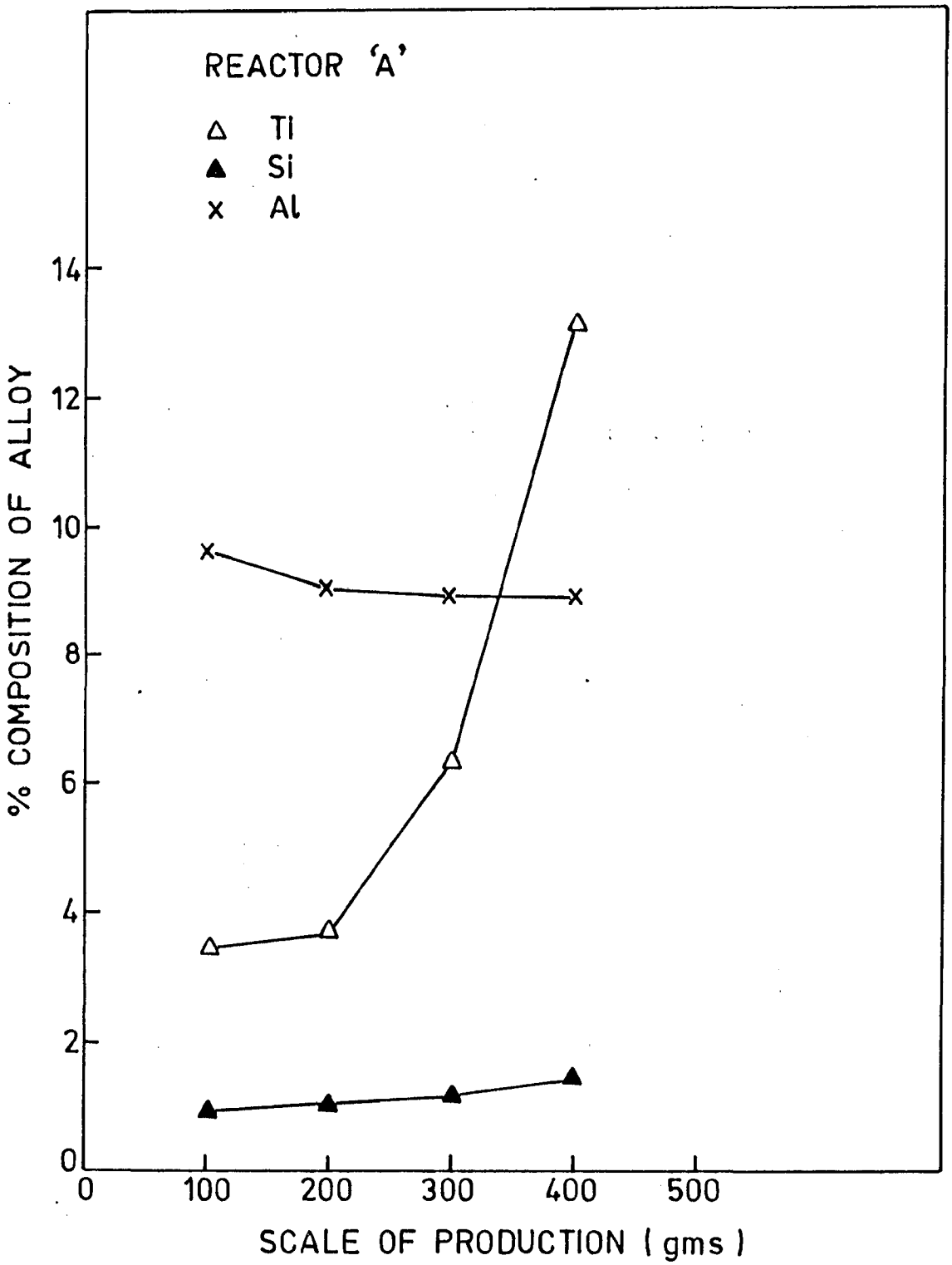

Fig.5.8 : Effect of scale of production on composition of the alloy in reactor 'A'.

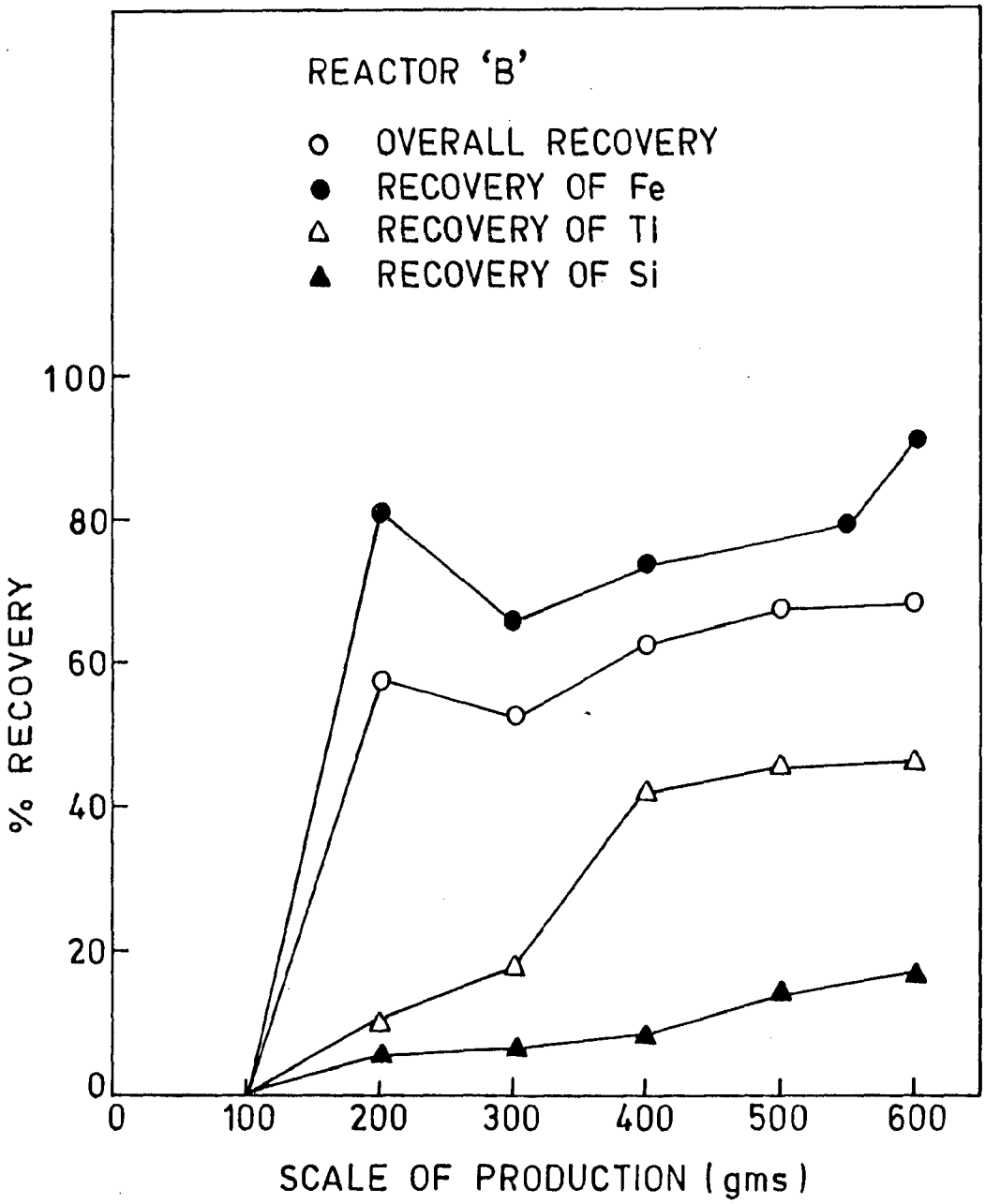

Fig.5.9 : Effect of scale of production on recovery values of the alloy in reactor 'B'.

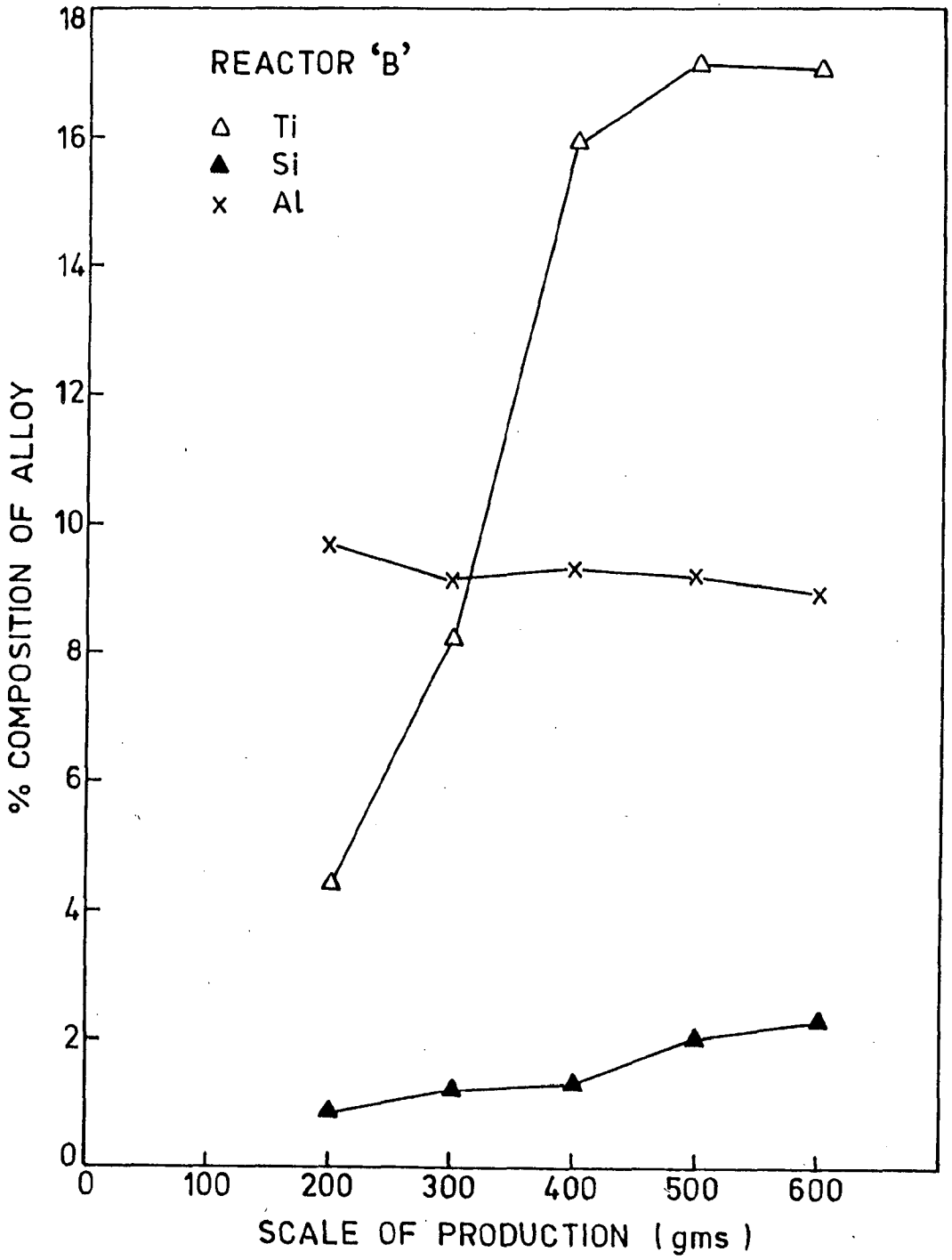

Fig.5.10 : Effect of scale of production on composition of the alloy in reactor 'B'.

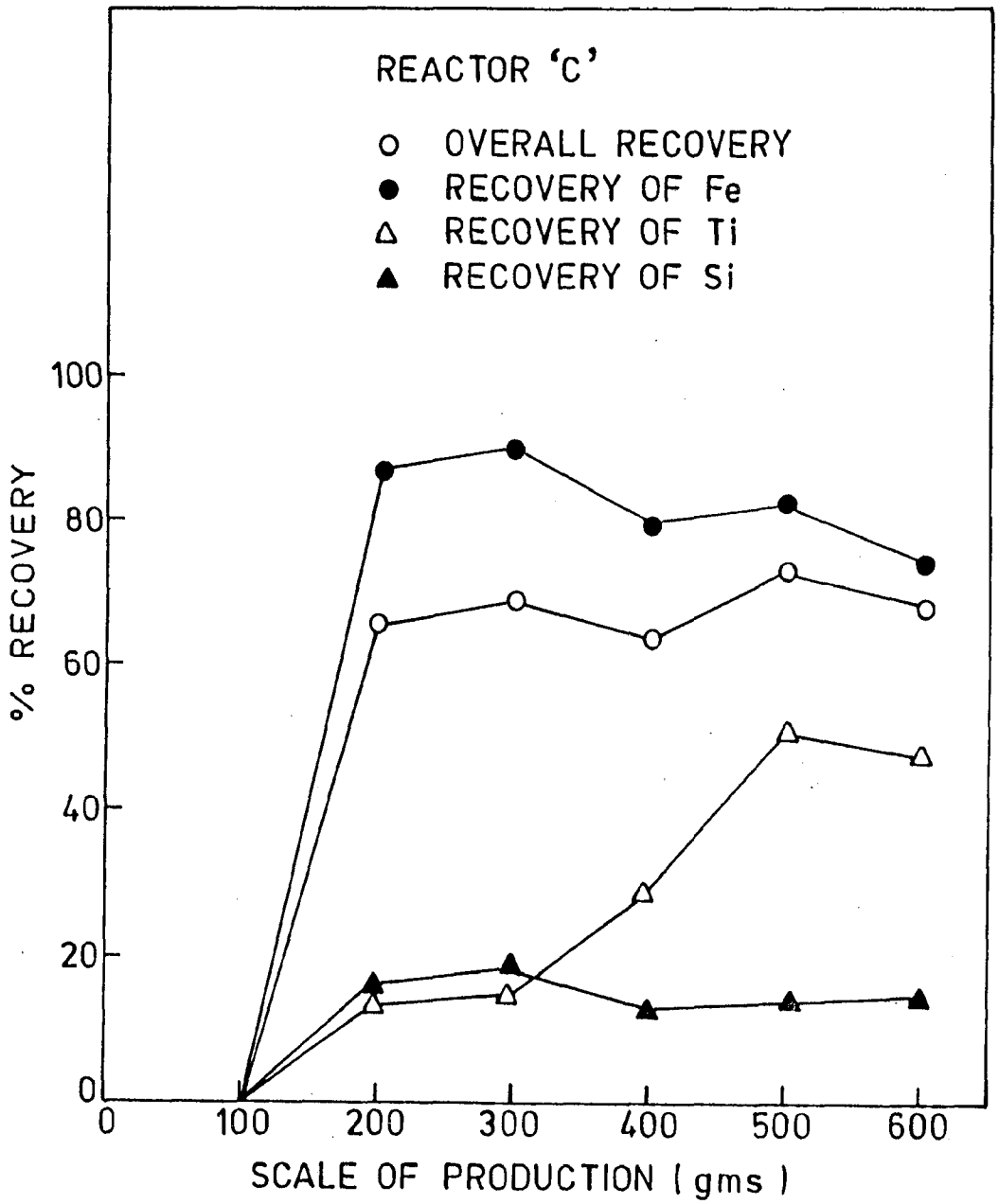

Fig. 5.11 : Effect of scale of production on recovery values of the alloy in reactor 'C'.

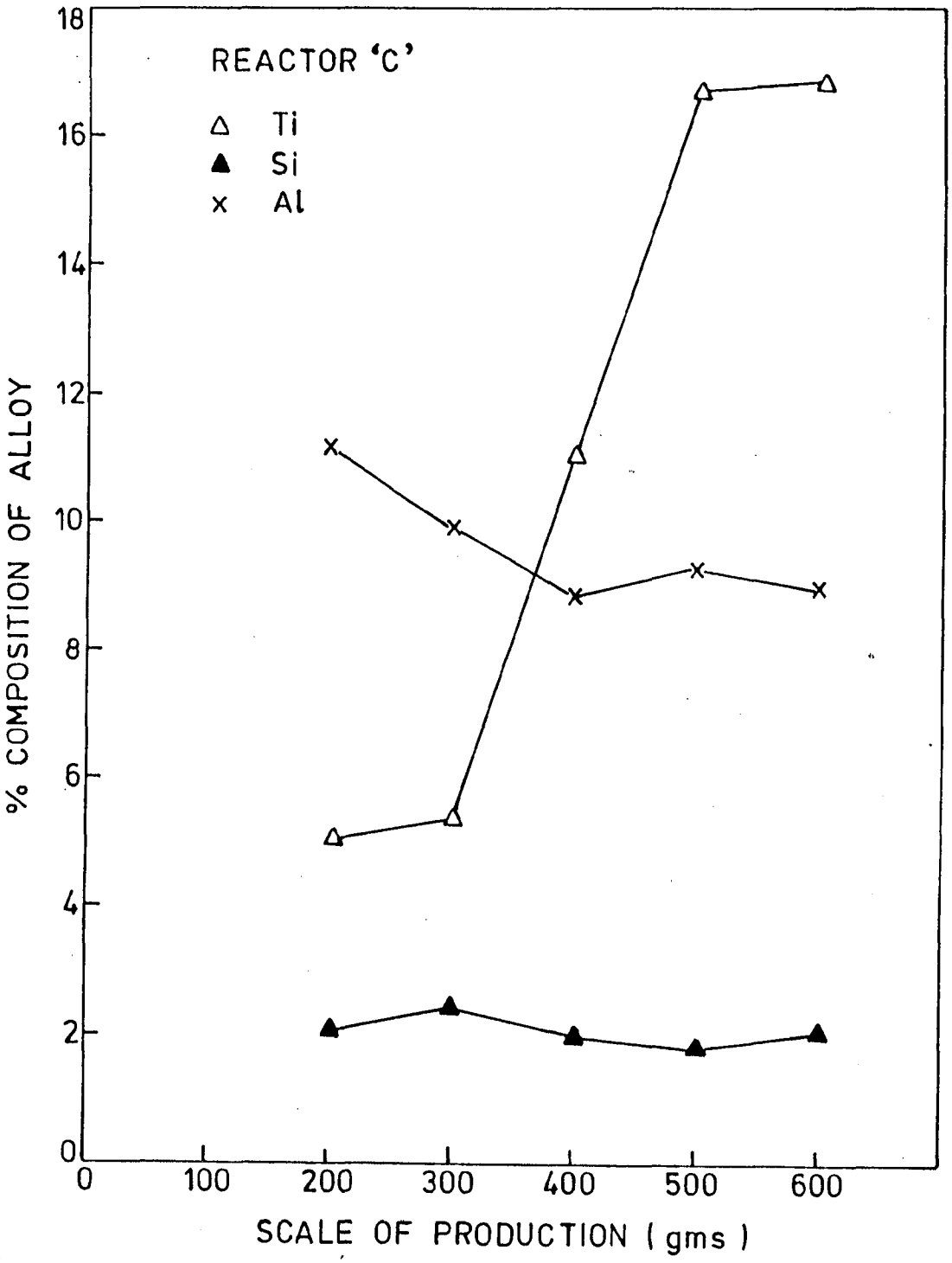

Fig.5.12 : Effect of scale of production on composition of the alloy in reactor 'C'.

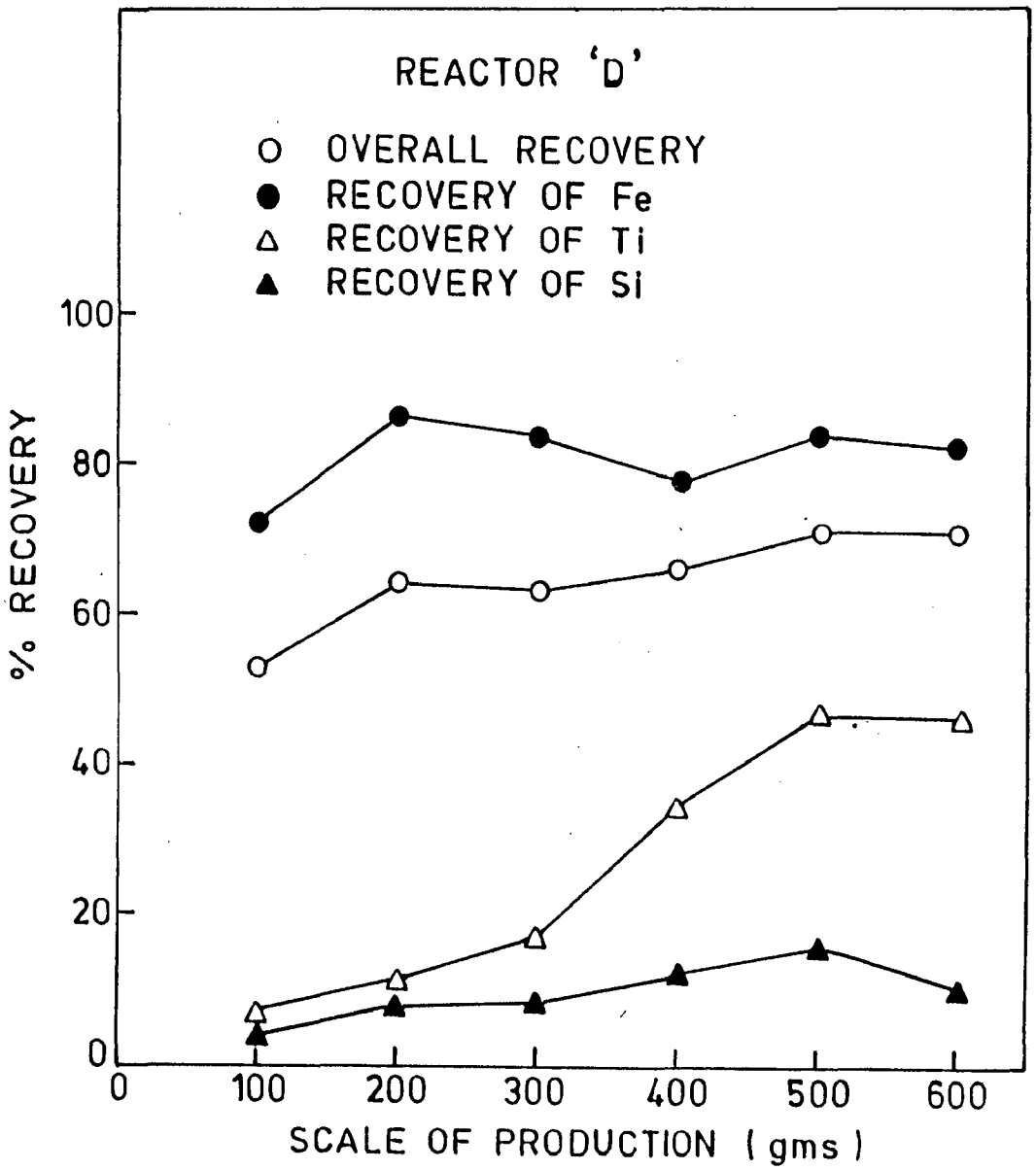

Fig.5.13 : Effect of scale of production on recovery values of the alloy in reactor 'D'.

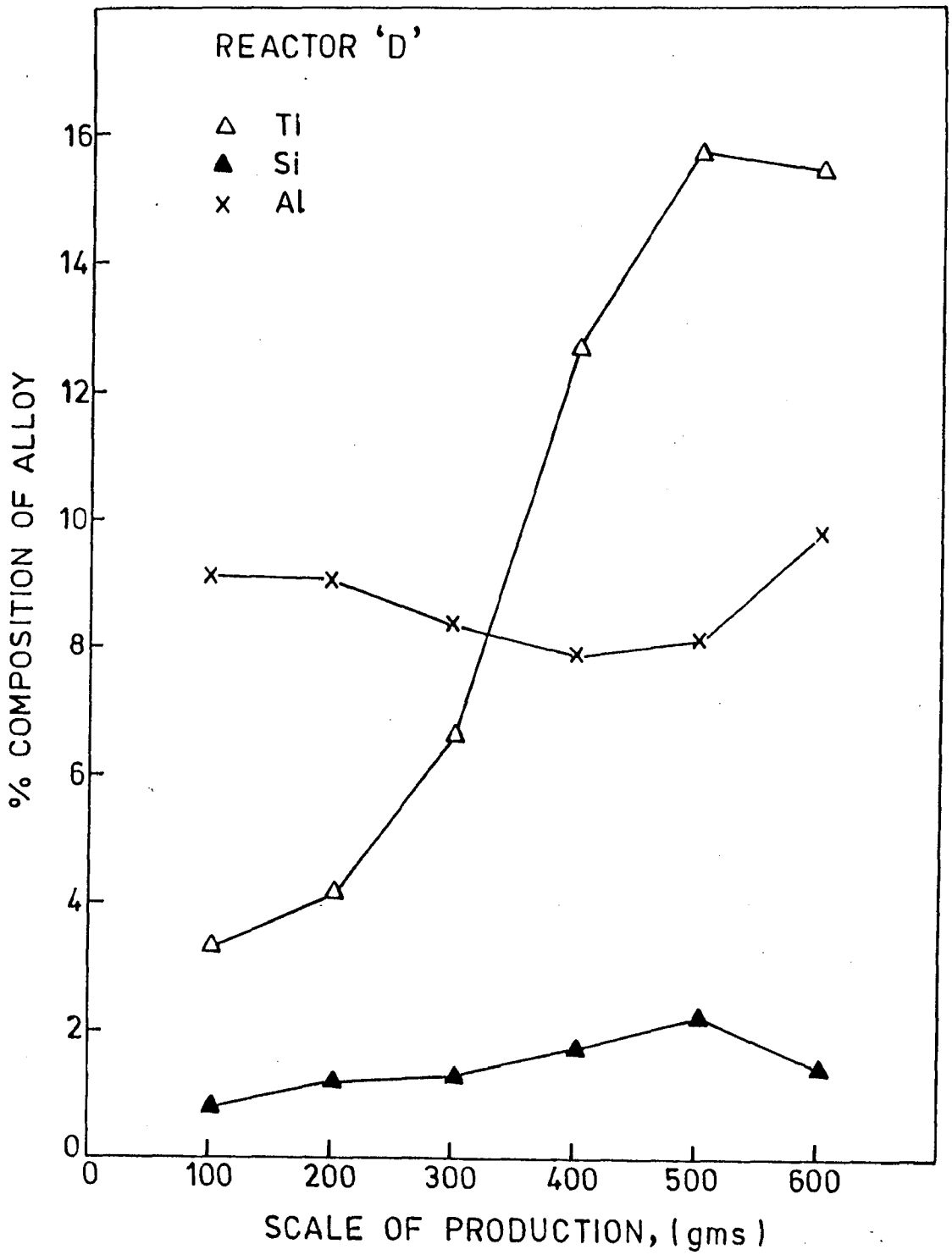

Fig.5.14 : Effect of scale of production on composition of the alloy in reactor 'D'.

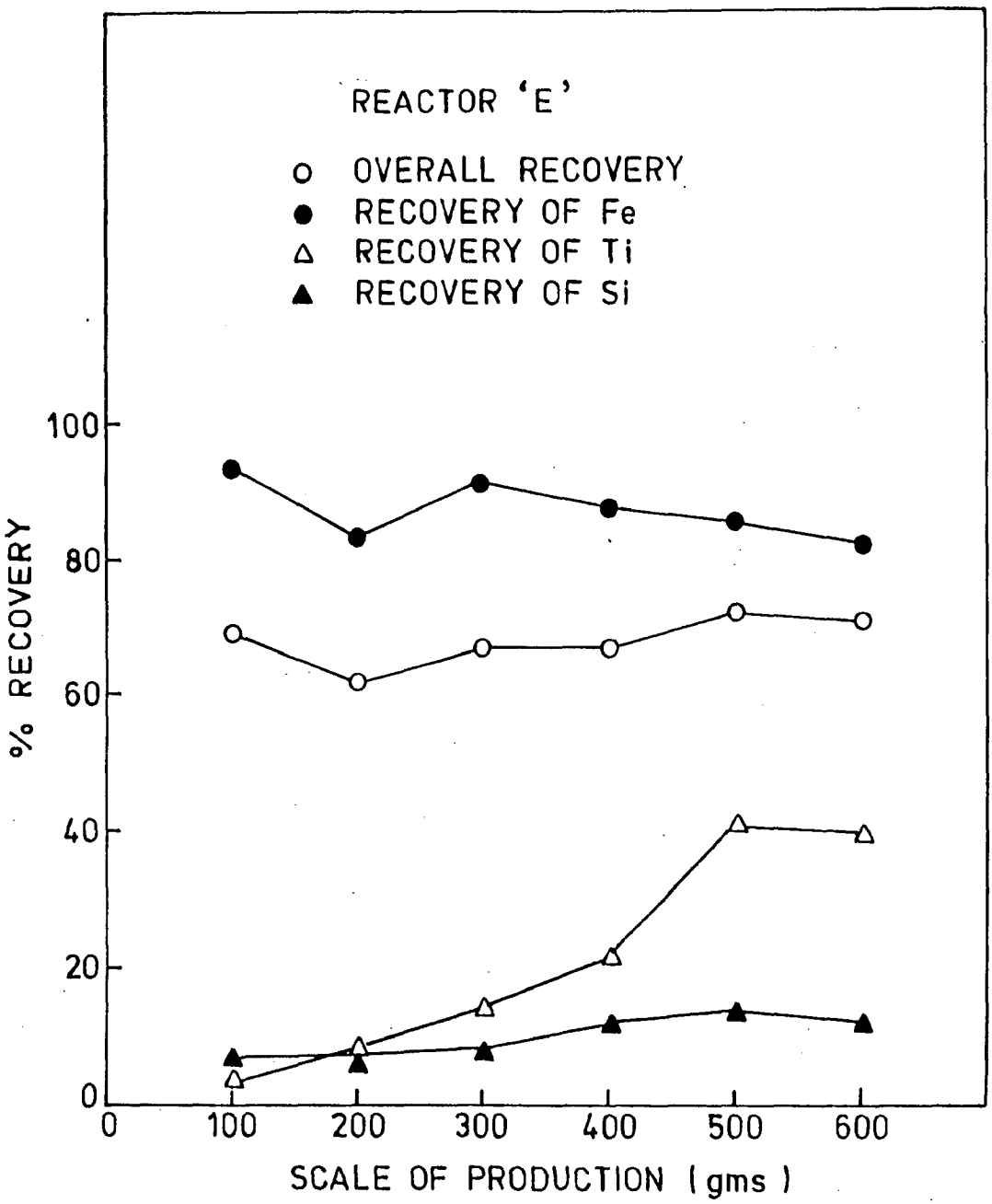

Fig.5.15 : Effect of scale of production on recovery values of the alloy in reactor 'E'.

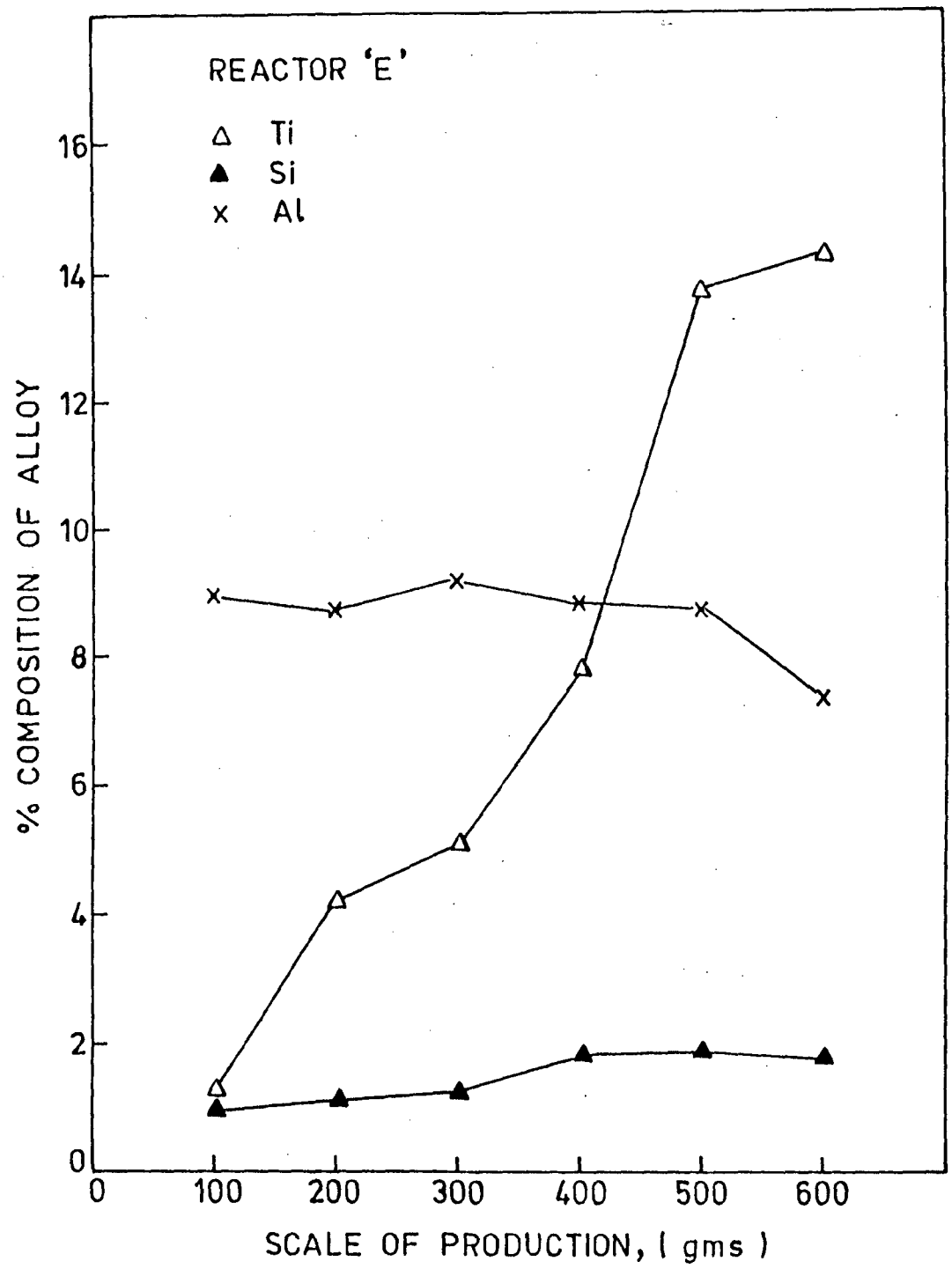

Fig.5.16 : Effect of scale of production on composition of the alloy in reactor 'E'.

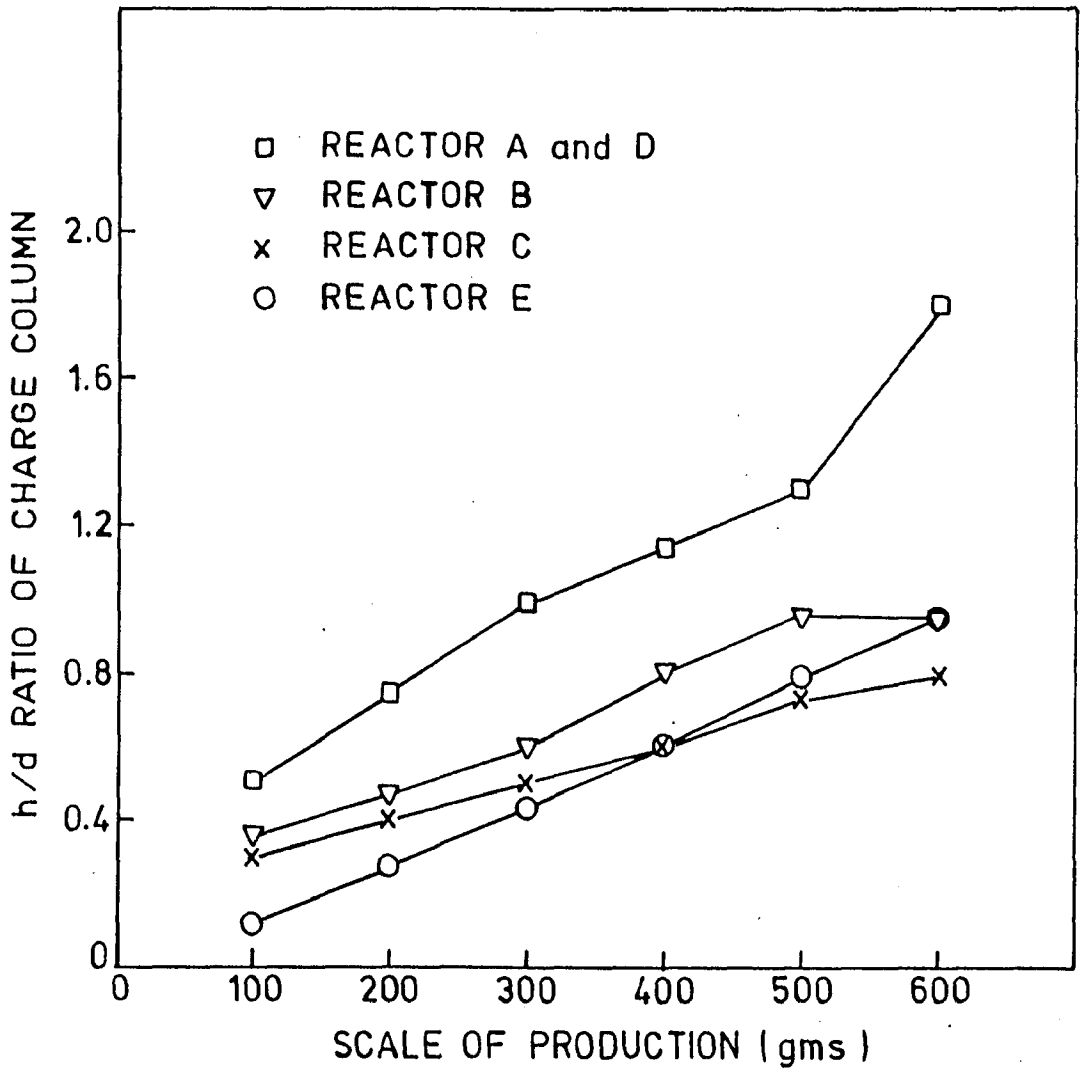

Fig.5.17 : Scale of production as a function of h/d ratio of the charge column in reactors.

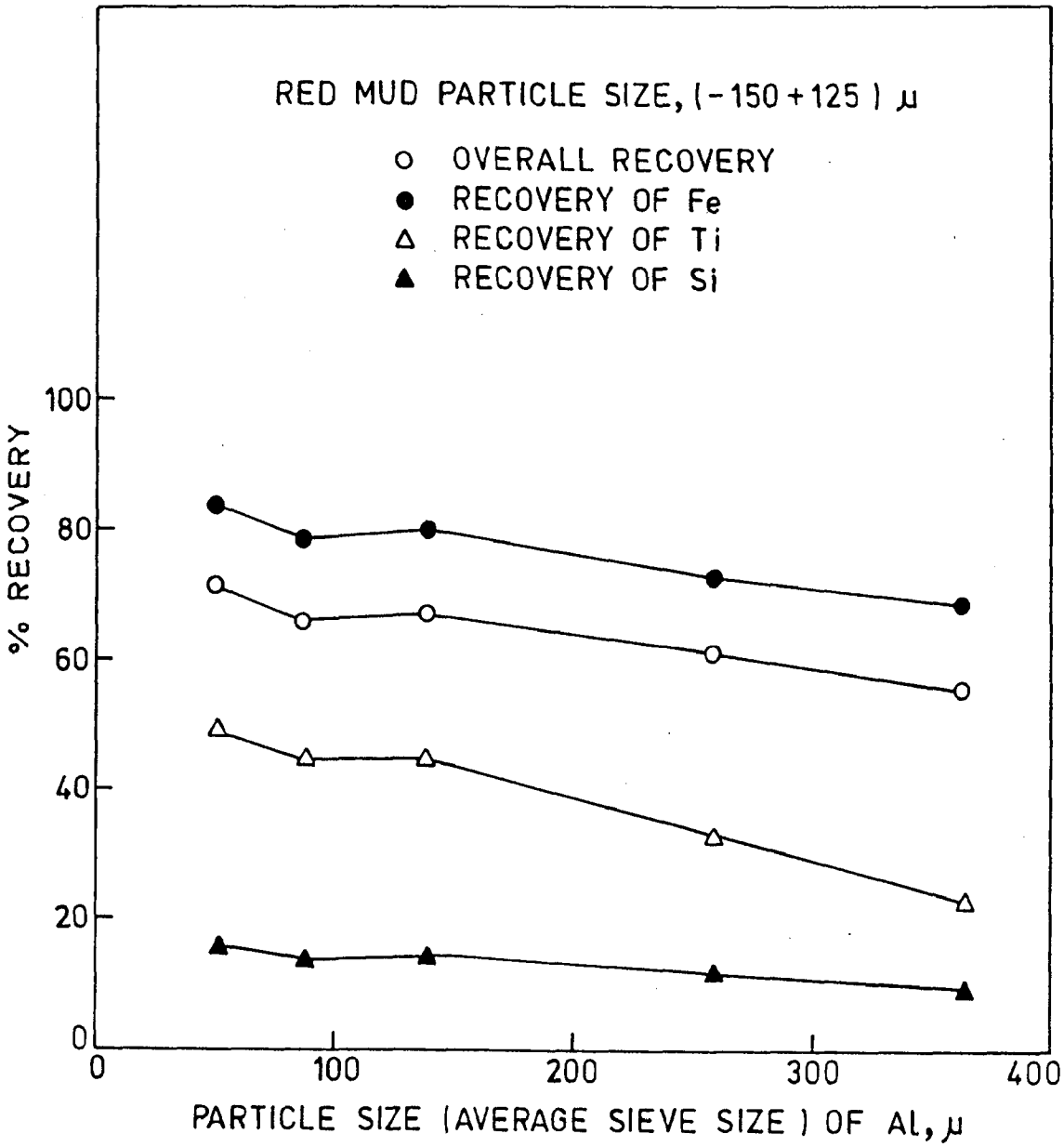

Fig.5.18 : Relationship between particle size of reductant (Al) and recovery values of the alloy for the red mud of particle size, -150+125 microns.

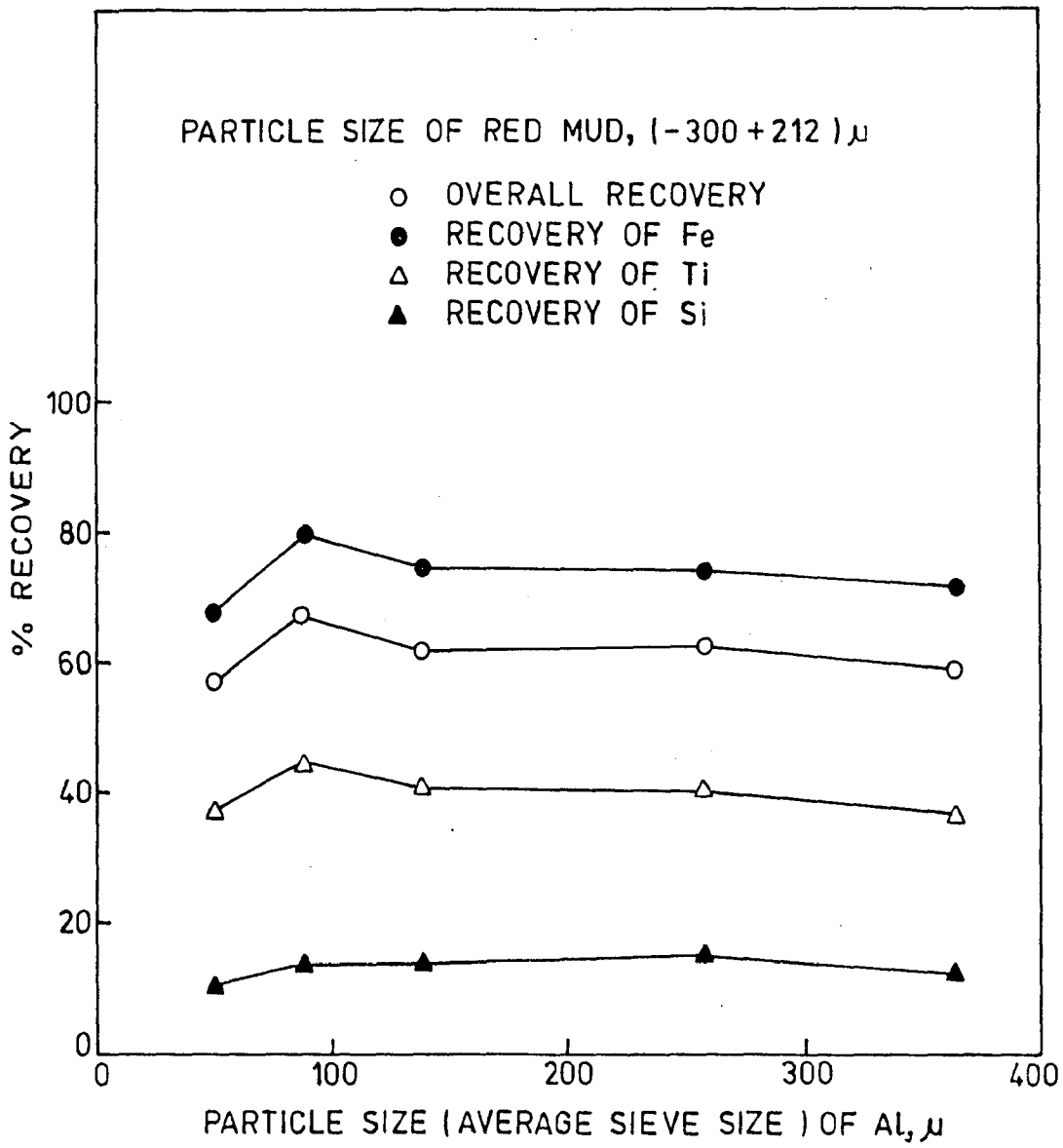

Fig.5.20 : Relationship between particle size of reductant (Al) and recovery values of the alloy for the red mud of particle size, -300+212 microns.

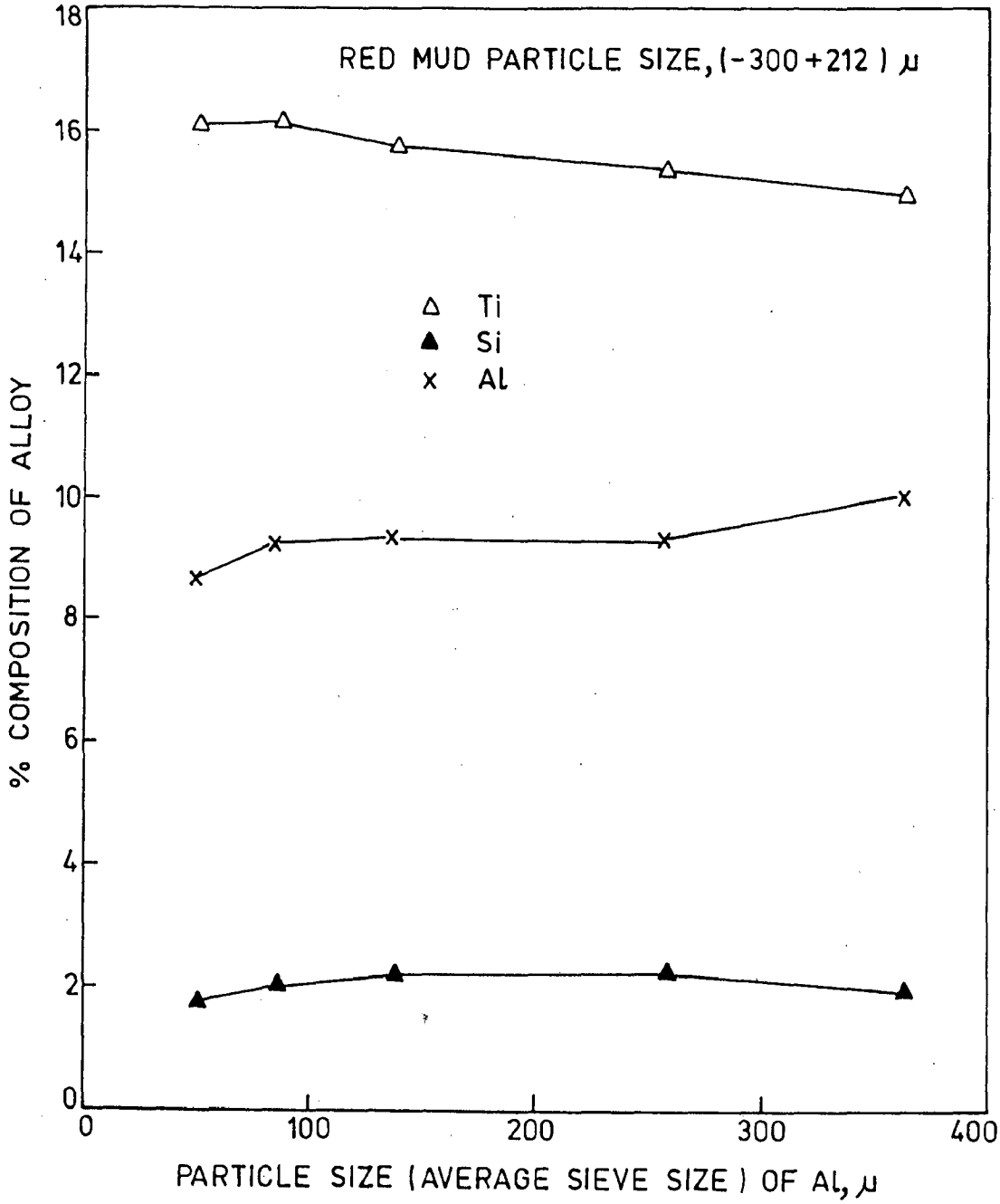

Fig.21 : Relationship between particle size of reductant (Al) and composition of the alloy for the red mud of particle size, -300+212 microns.

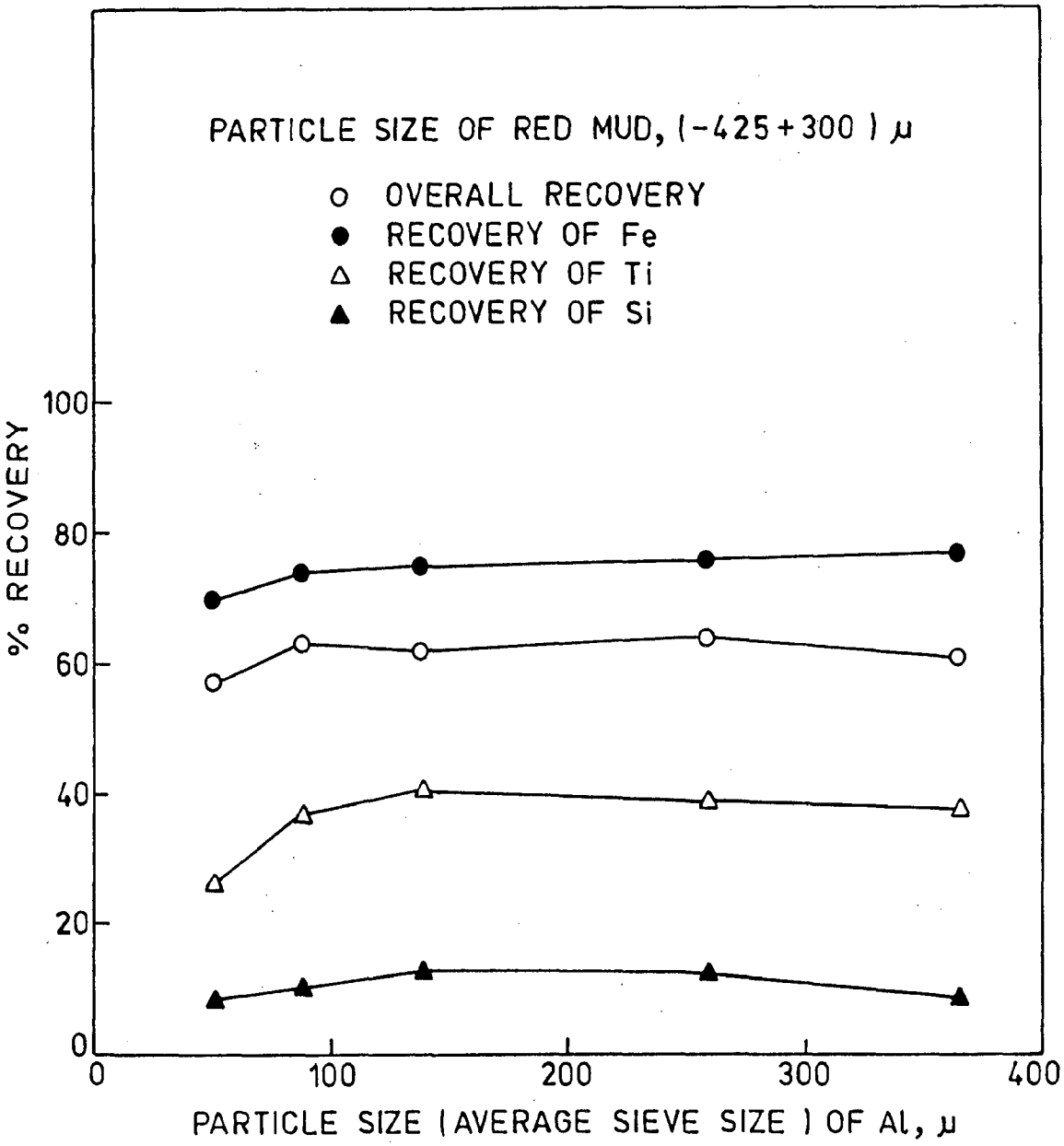

Fig.5.22 : Relationship between particle size of reductant (Al) and recovery values of the alloy for the red mud of particle size, -425+300 microns.

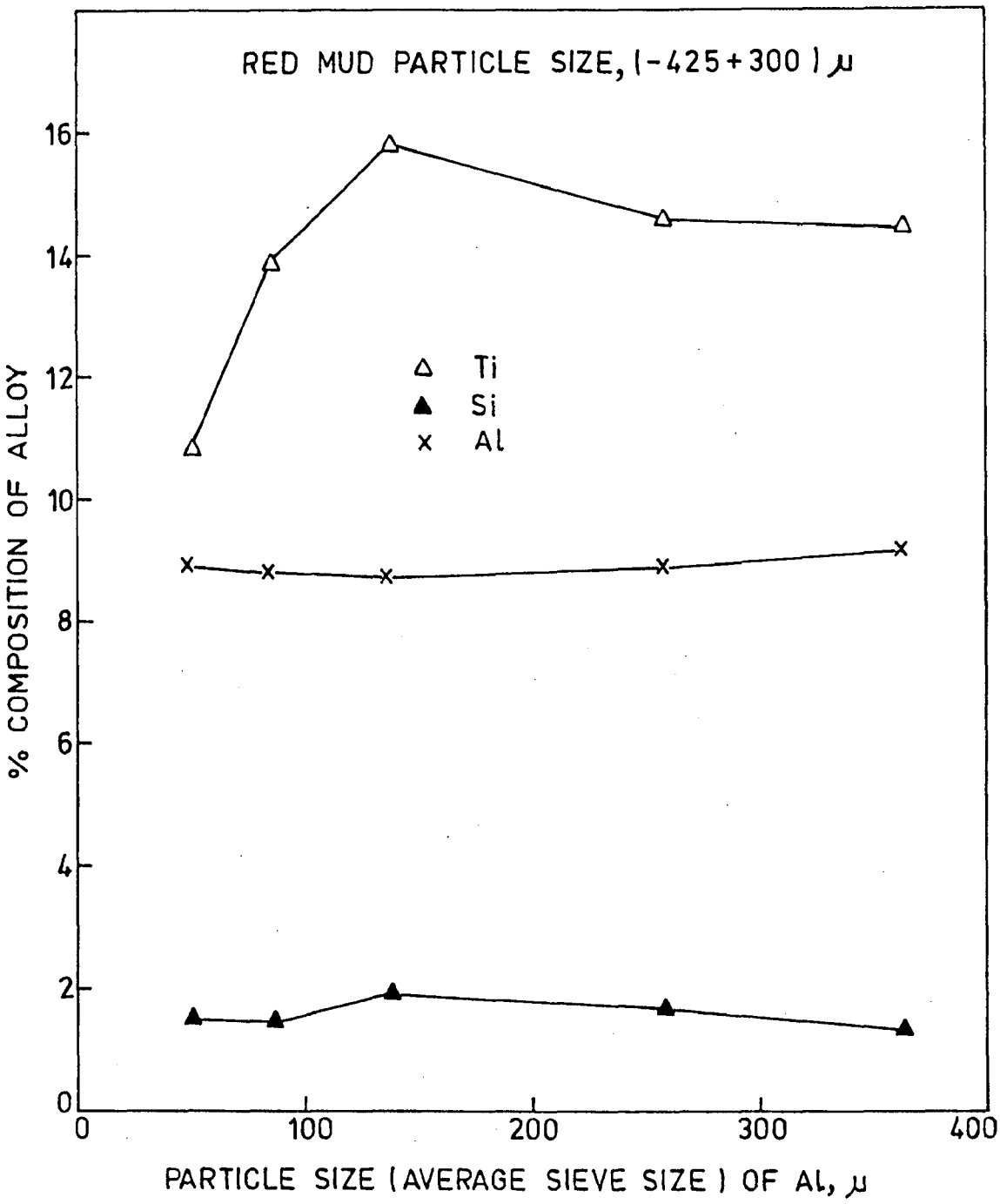

Fig.5.23 : Relationship between particle size of reductant (Al) and composition of the alloy for the red mud of particle size, -425+300 microns.

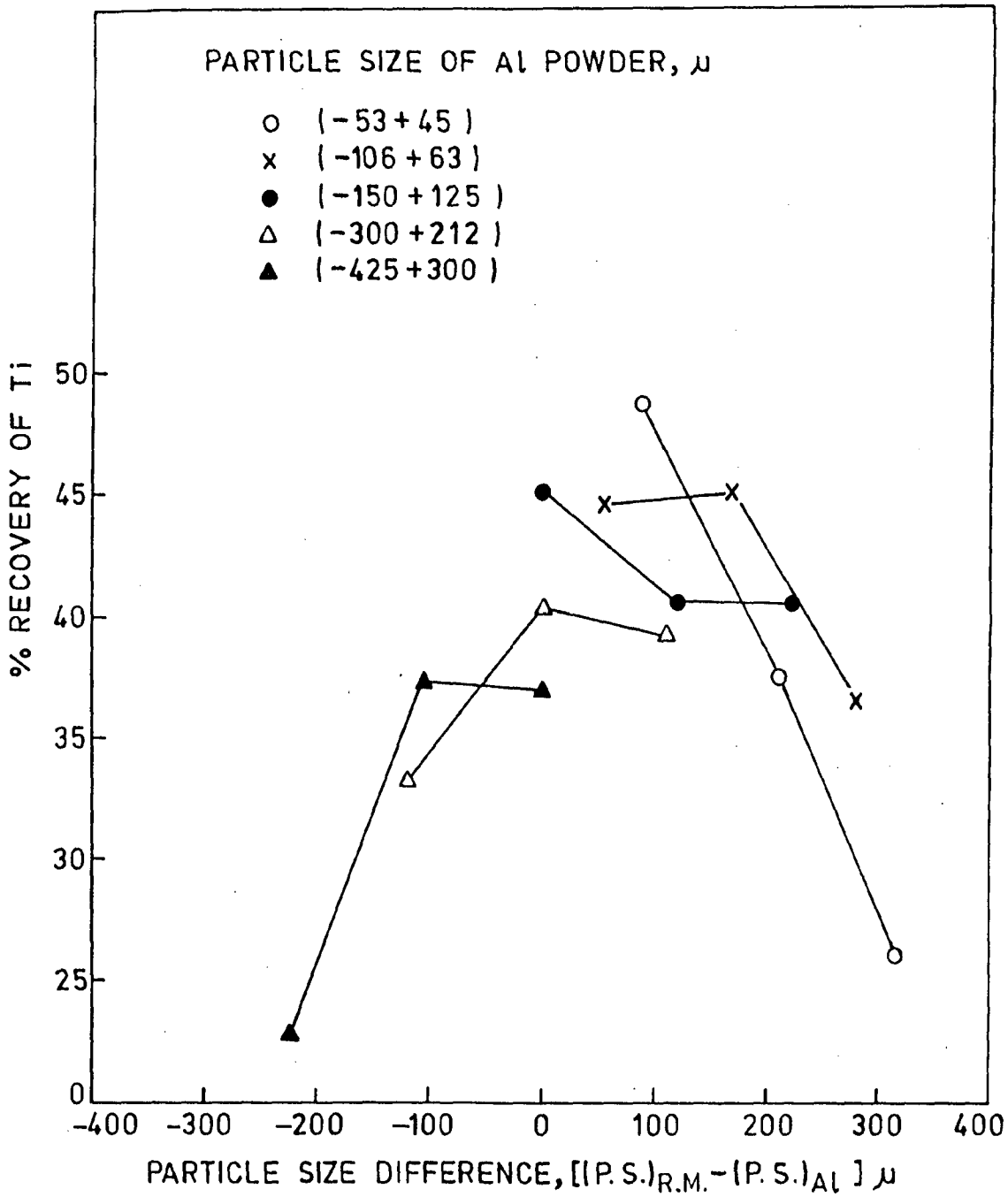

Fig.5.24 : Titanium recovery as a function of particle size difference of red mud and Al, power i.e. $(PS)_{RM} - (PS)_{Al}$.

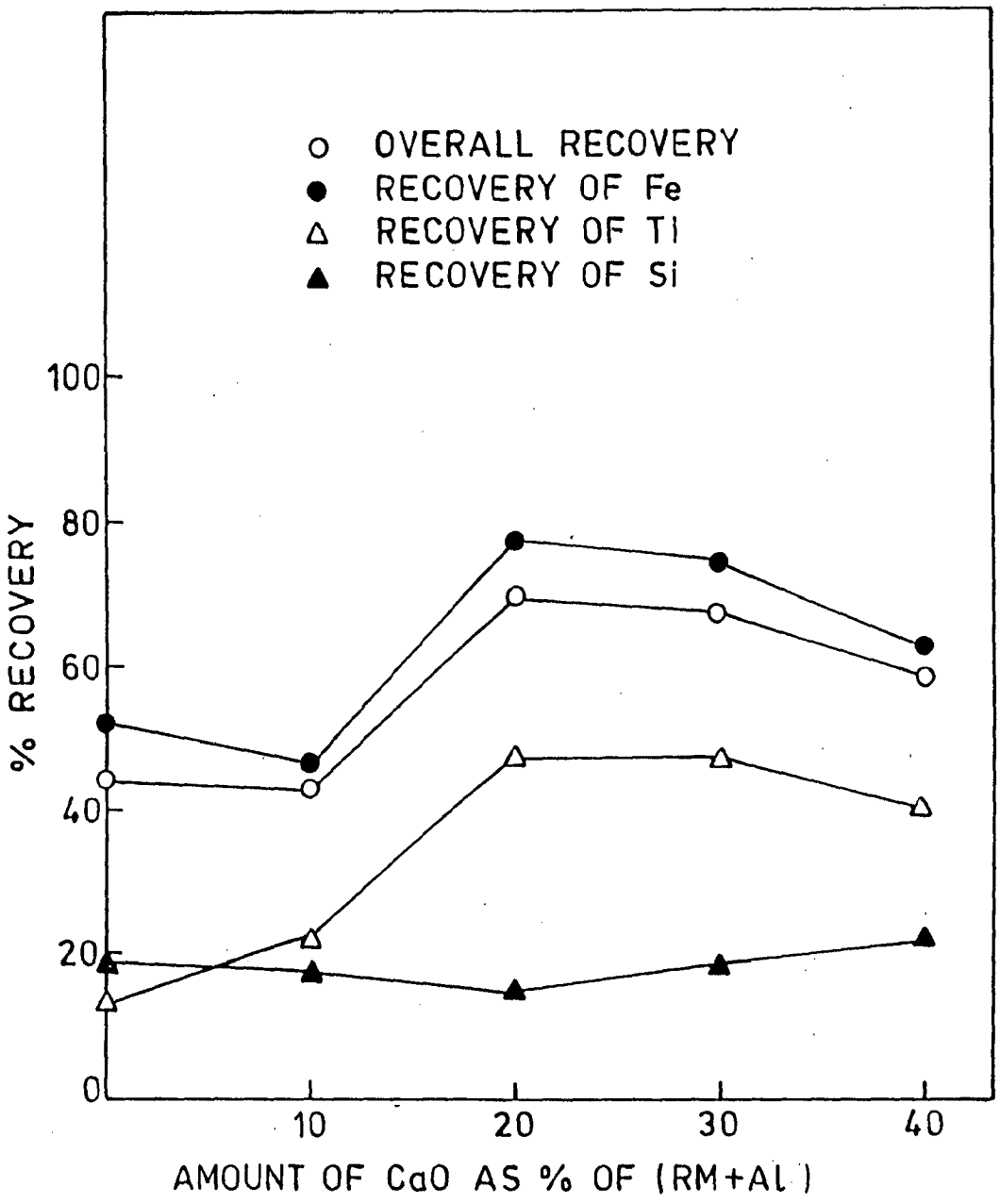

Fig.5.25 : Effect of Lime (CaO) addition on recovery values of the alloy.

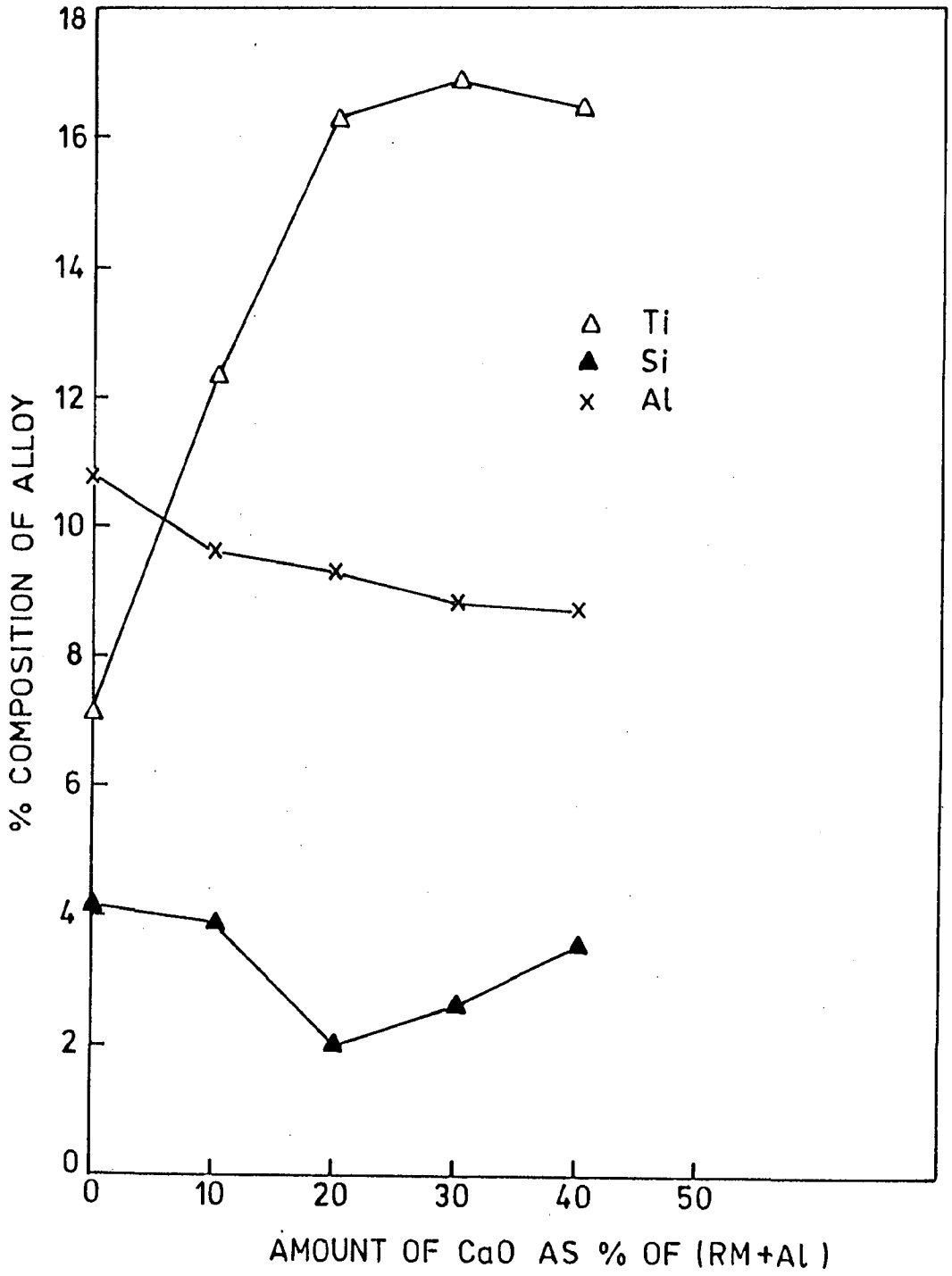

Fig.5.26 : Effect of Lime (CaO) addition on composition of the alloy.

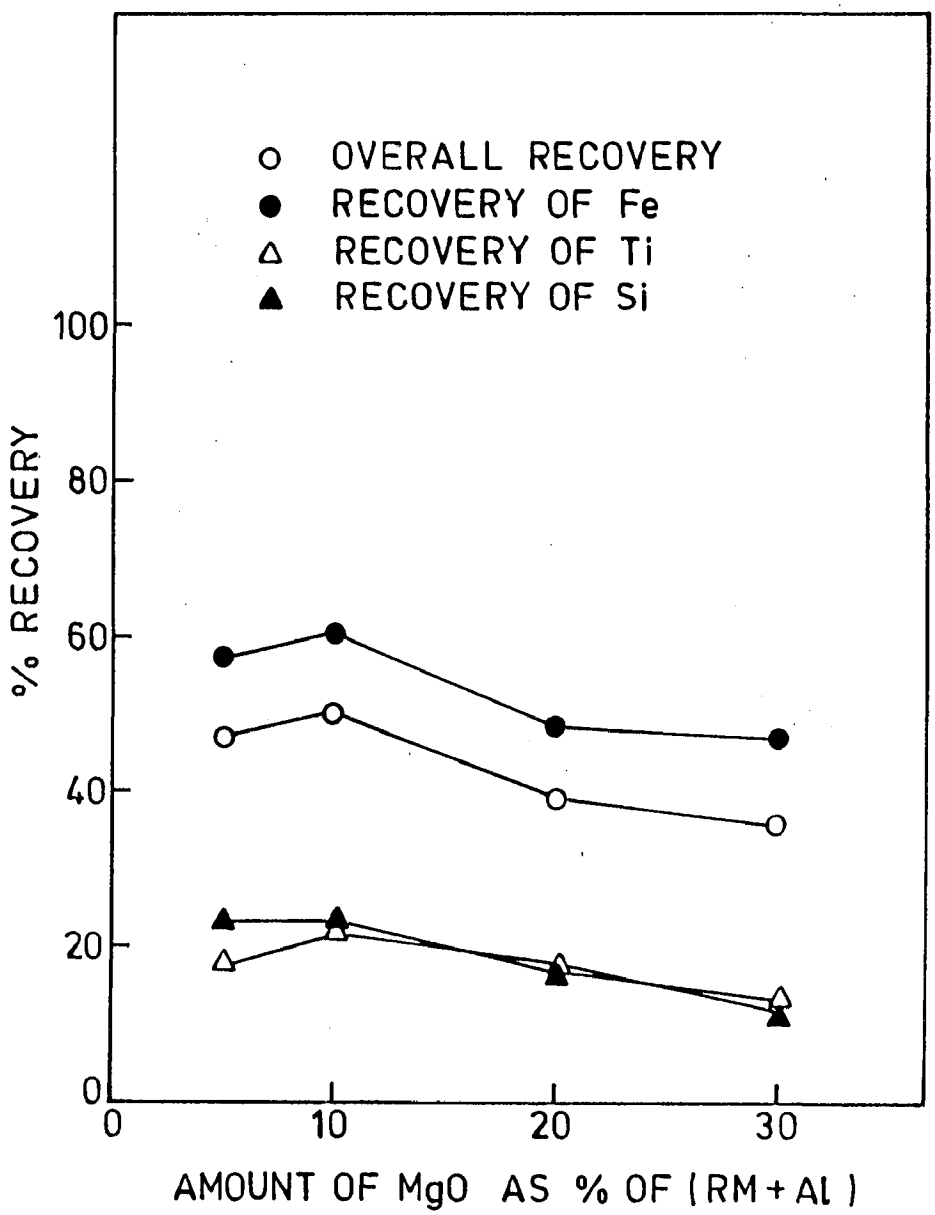

Fig.5.27 : Effect of Magnesia (MgO) addition on recovery values of the alloy.

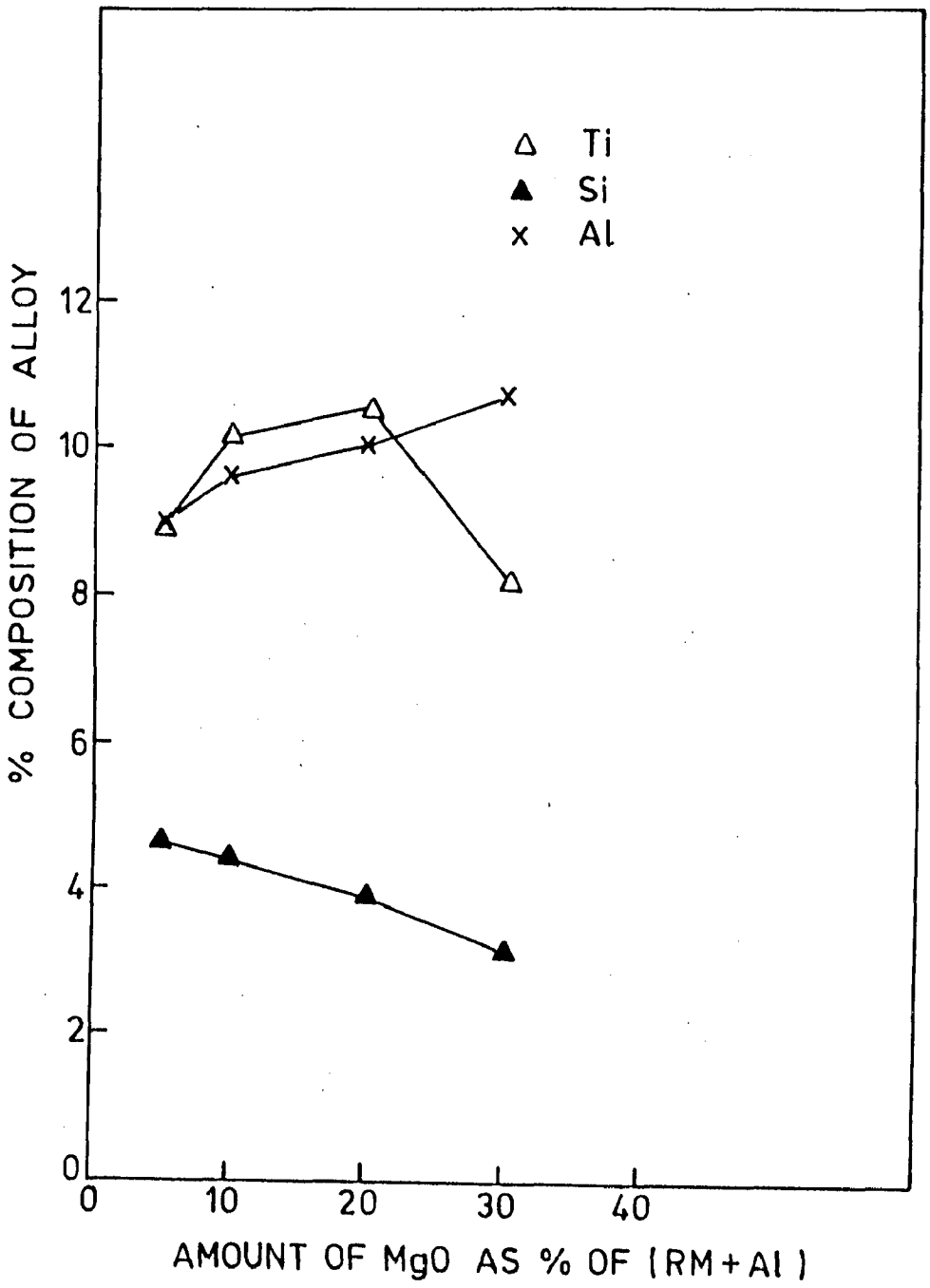

Fig.5.28 : Effect of Magnesia (MgO) addition on composition of the alloy.

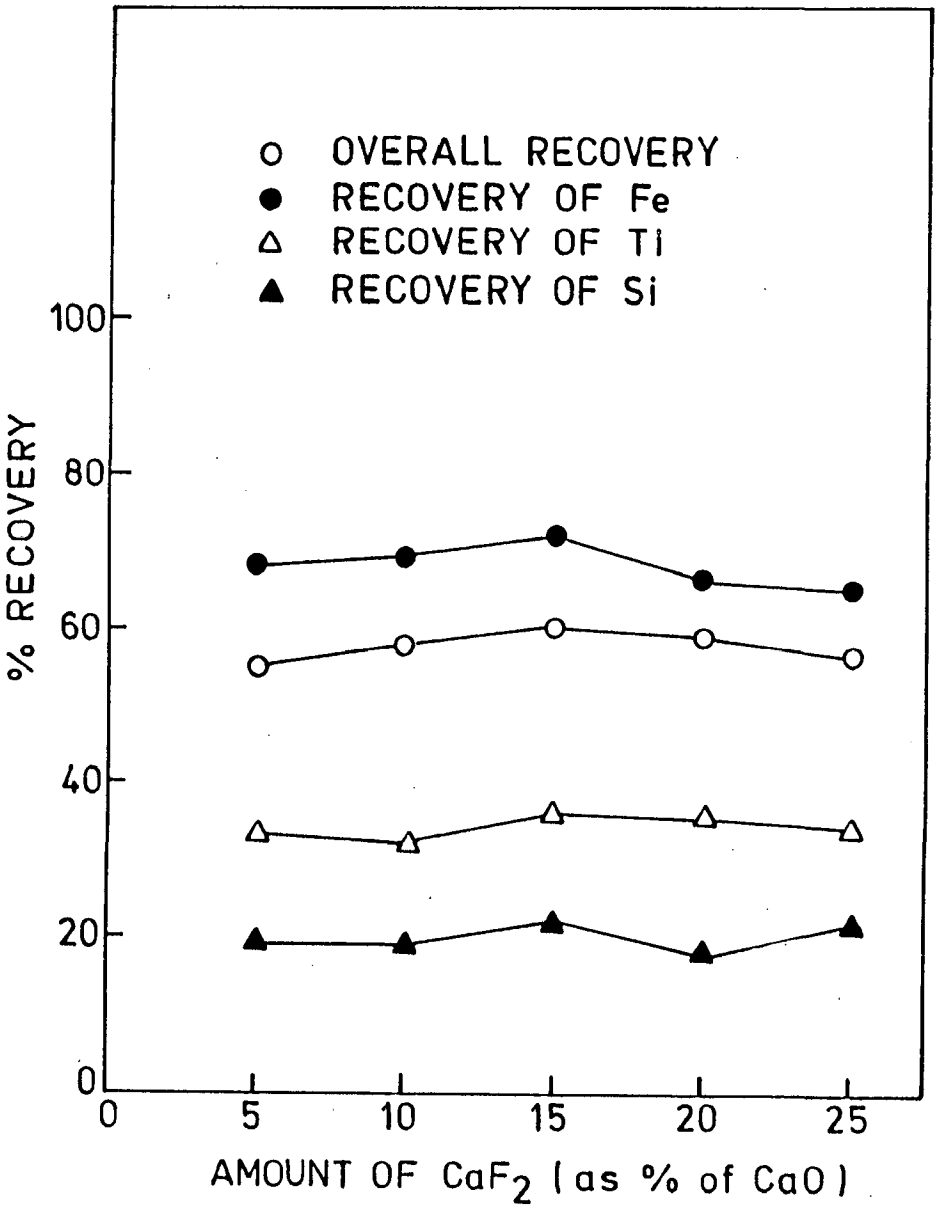

Fig.5.29 : Effect of Fluorspar (CaF_2) addition on recovery values of the alloy.

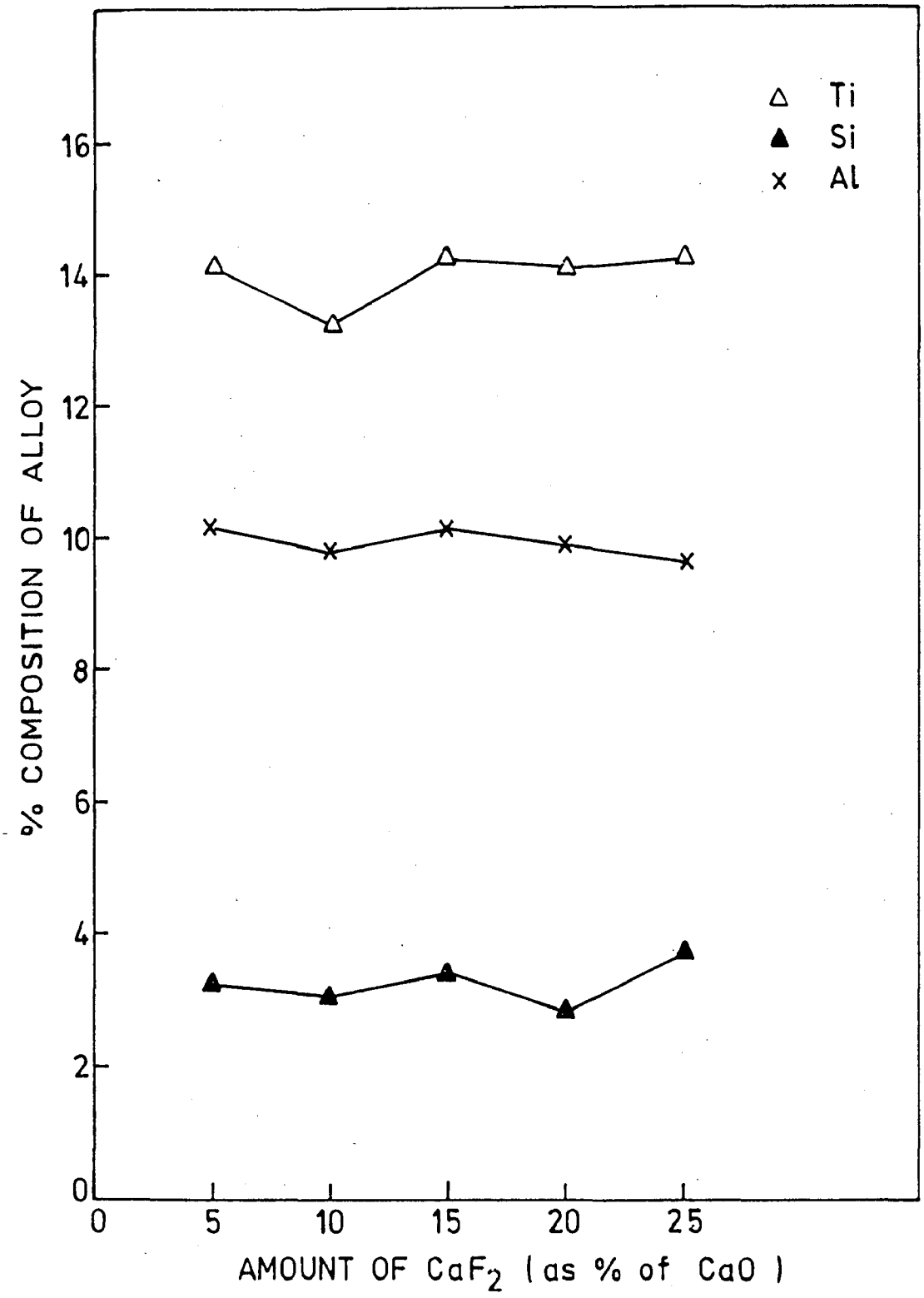

Fig.5.30 : Effect of Fluorspar (CaF_2) addition on composition of the alloy.

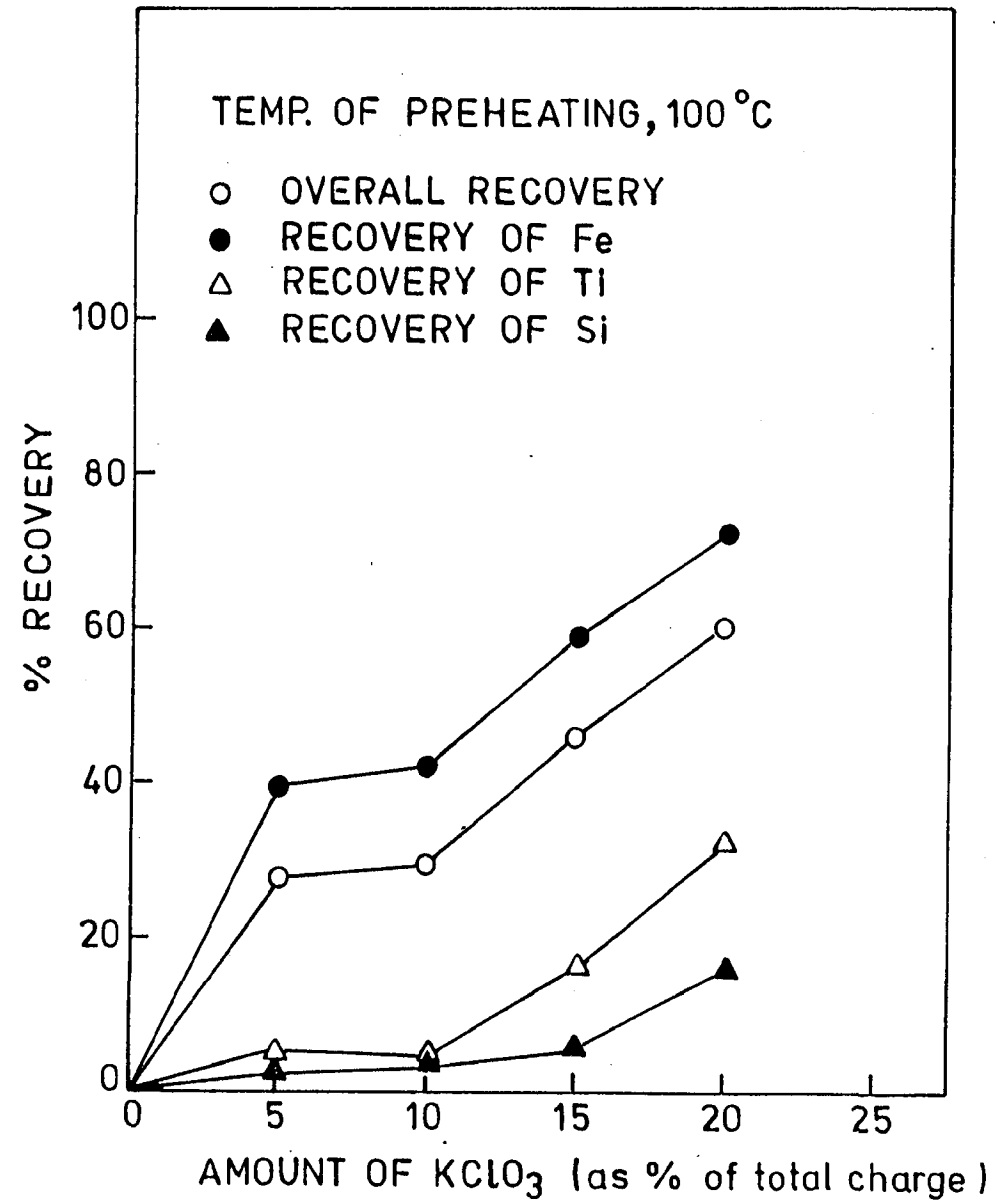

Fig.5.31 : Recovery values of the alloy as affected by $KClO_3$ addition at 100°C preheating.

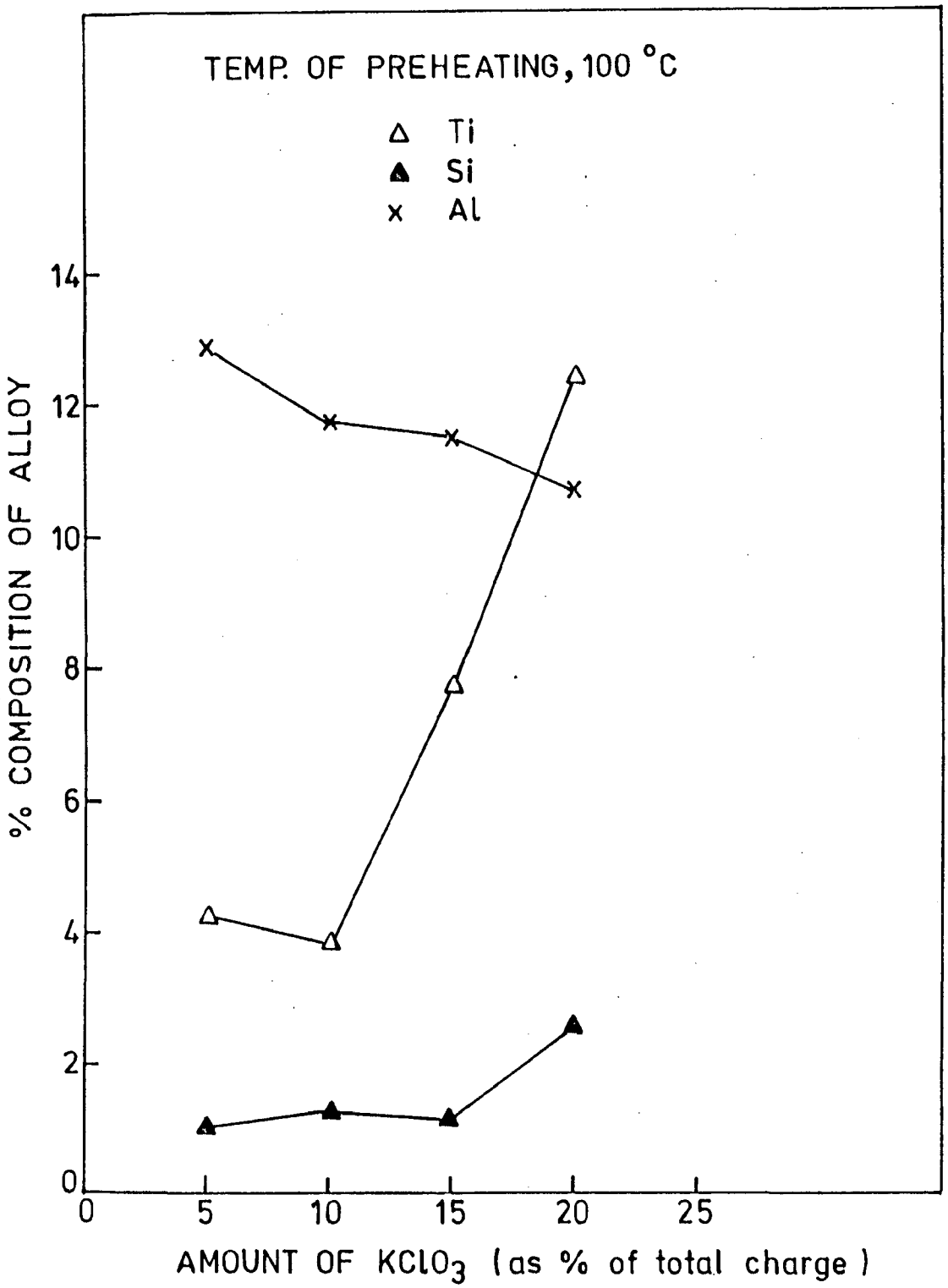

Fig.5.32 : Composition of the alloy as affected by $KClO_3$ addition at 100°C preheating.

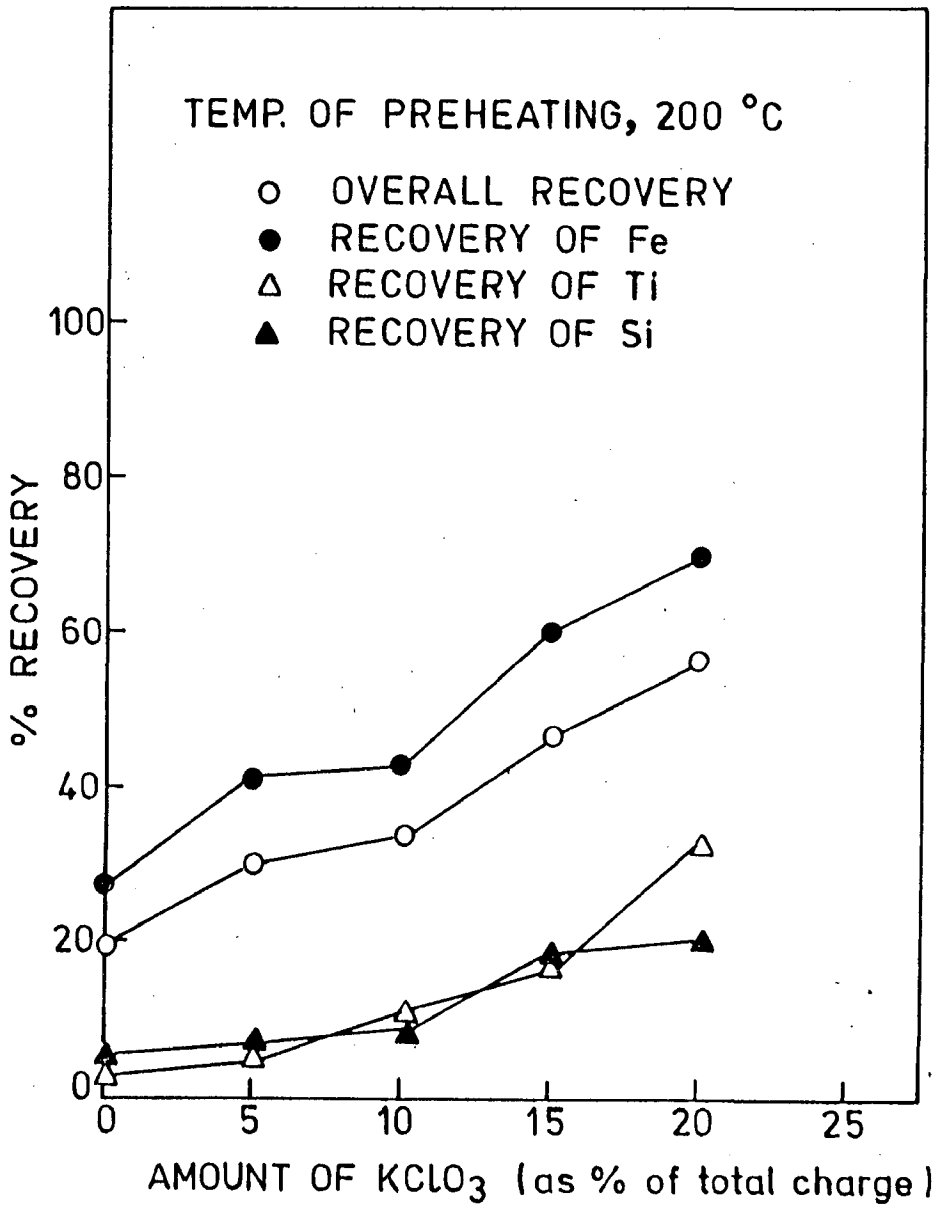

Fig.5.33 : Recovery values of the alloy as affected by $KClO_3$ addition at 200°C preheating.

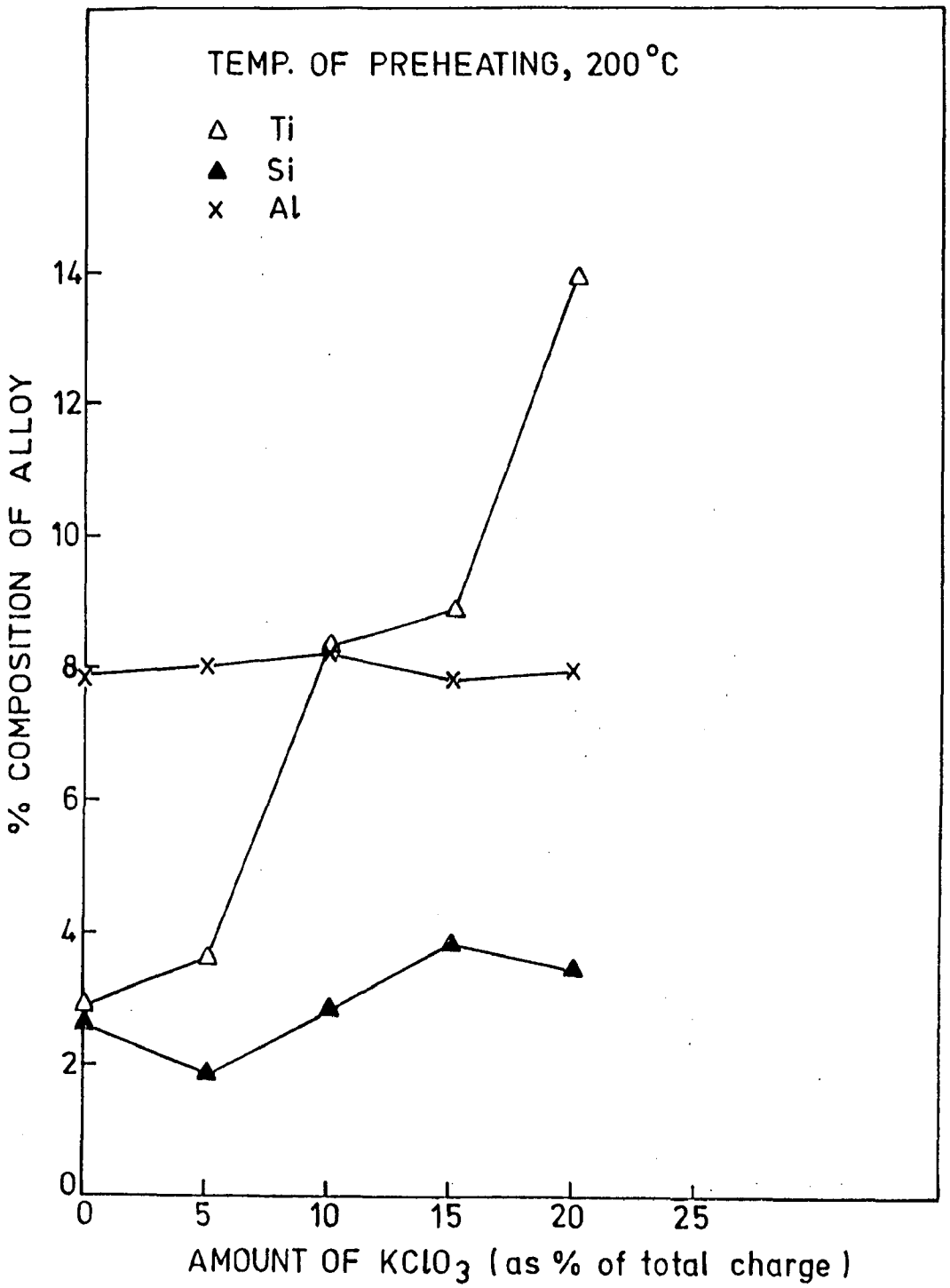

Fig.5.34 : Composition of the alloy as affected by $KClO_3$ addition at 200°C preheating.

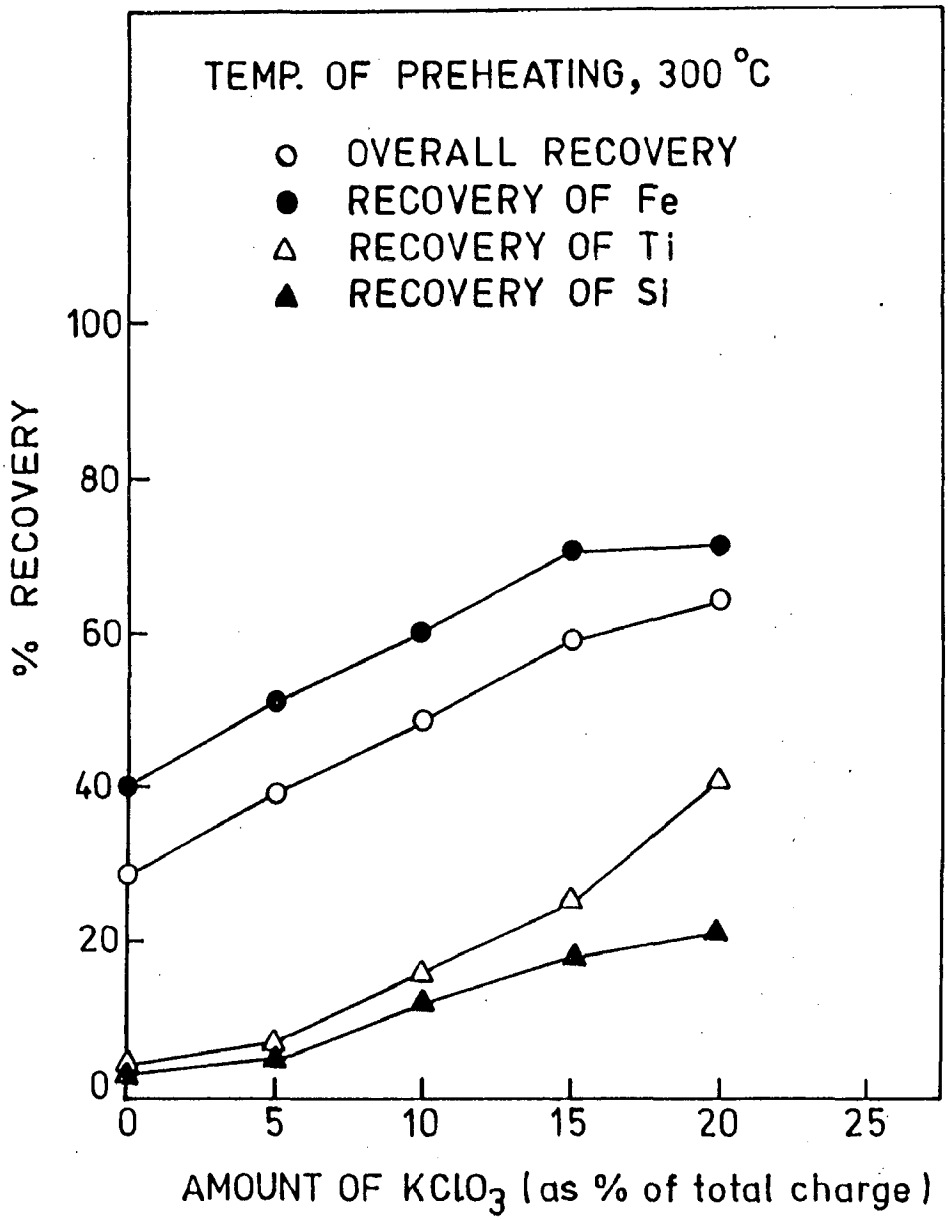

Fig.5.35 : Recovery values of the alloy as affected by $KClO_3$ addition at 300°C preheating.

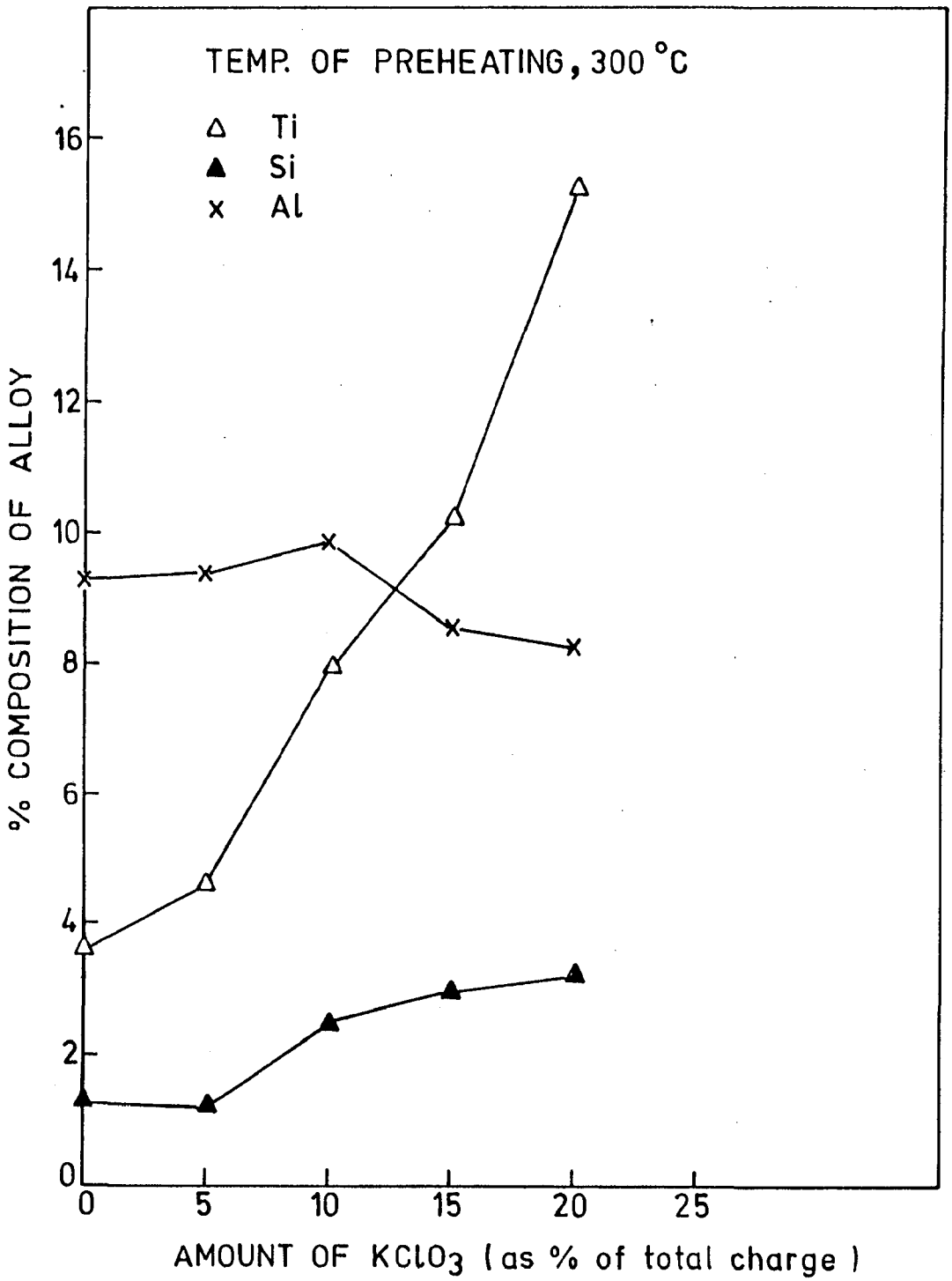

Fig.5.36 : Composition of the alloy as affected by $KClO_3$ addition at 300°C preheating.

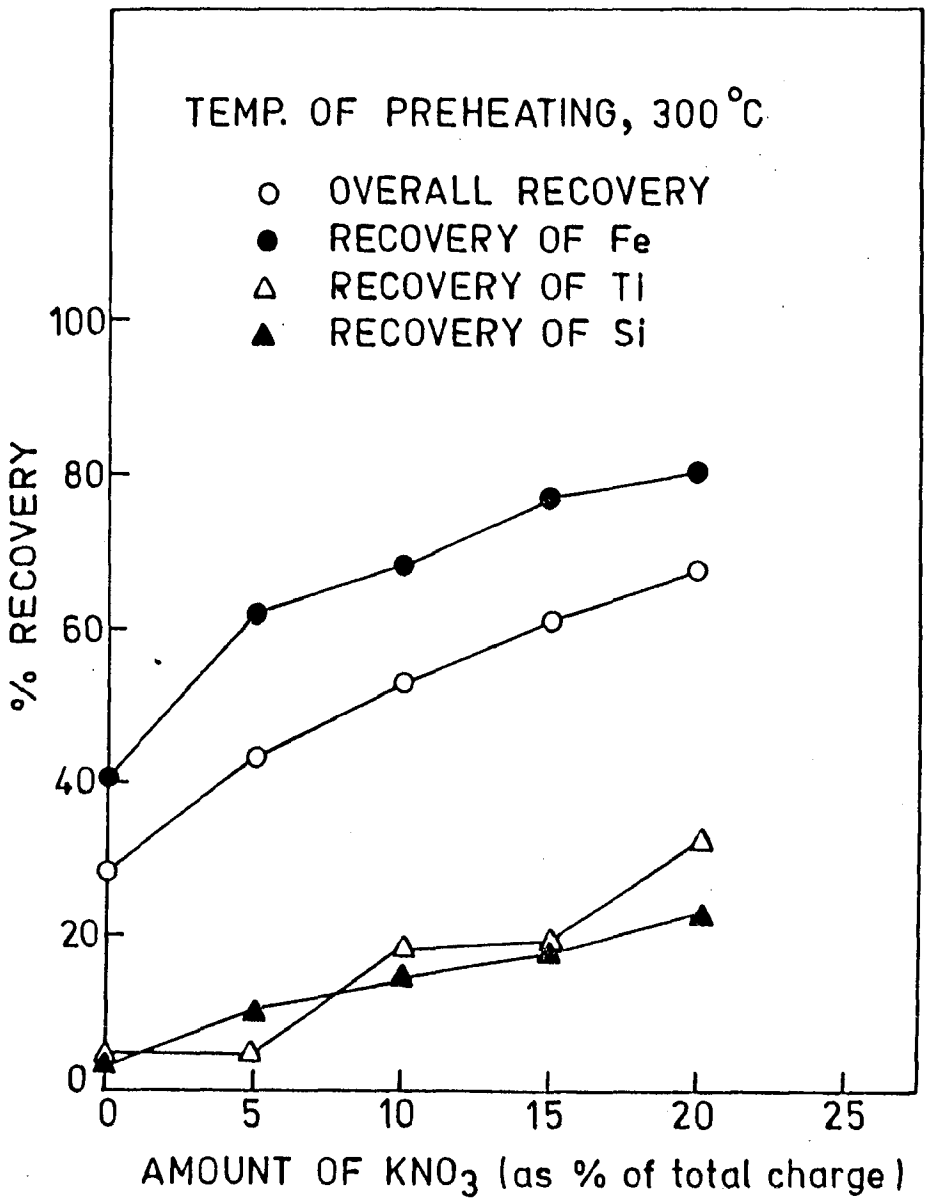

Fig.5.37 : Effect of KNO_3 addition on recovery values of the alloy at 300°C preheating.

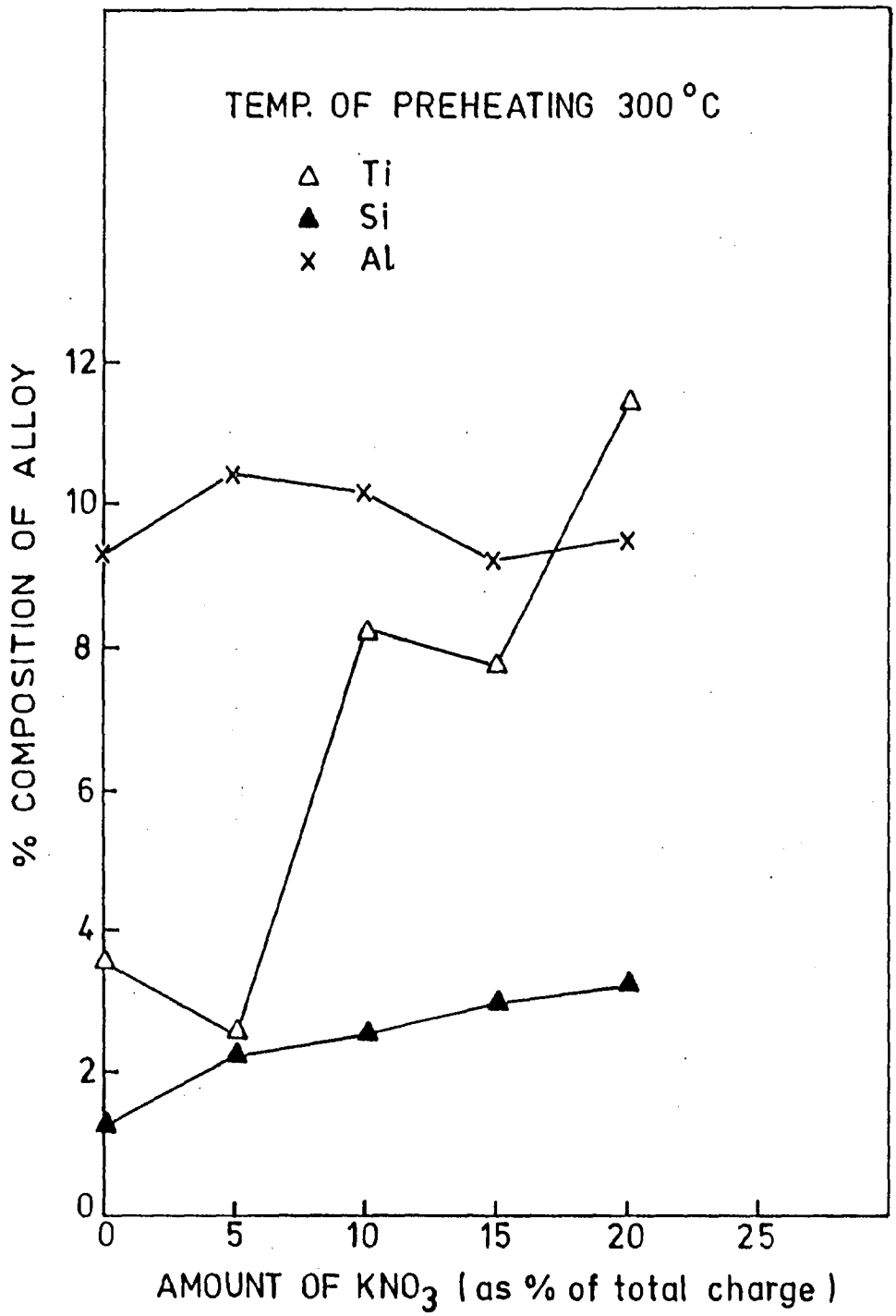

Fig.5.38 : Effect of KNO_3 addition on composition of the alloy at 300°C preheating.

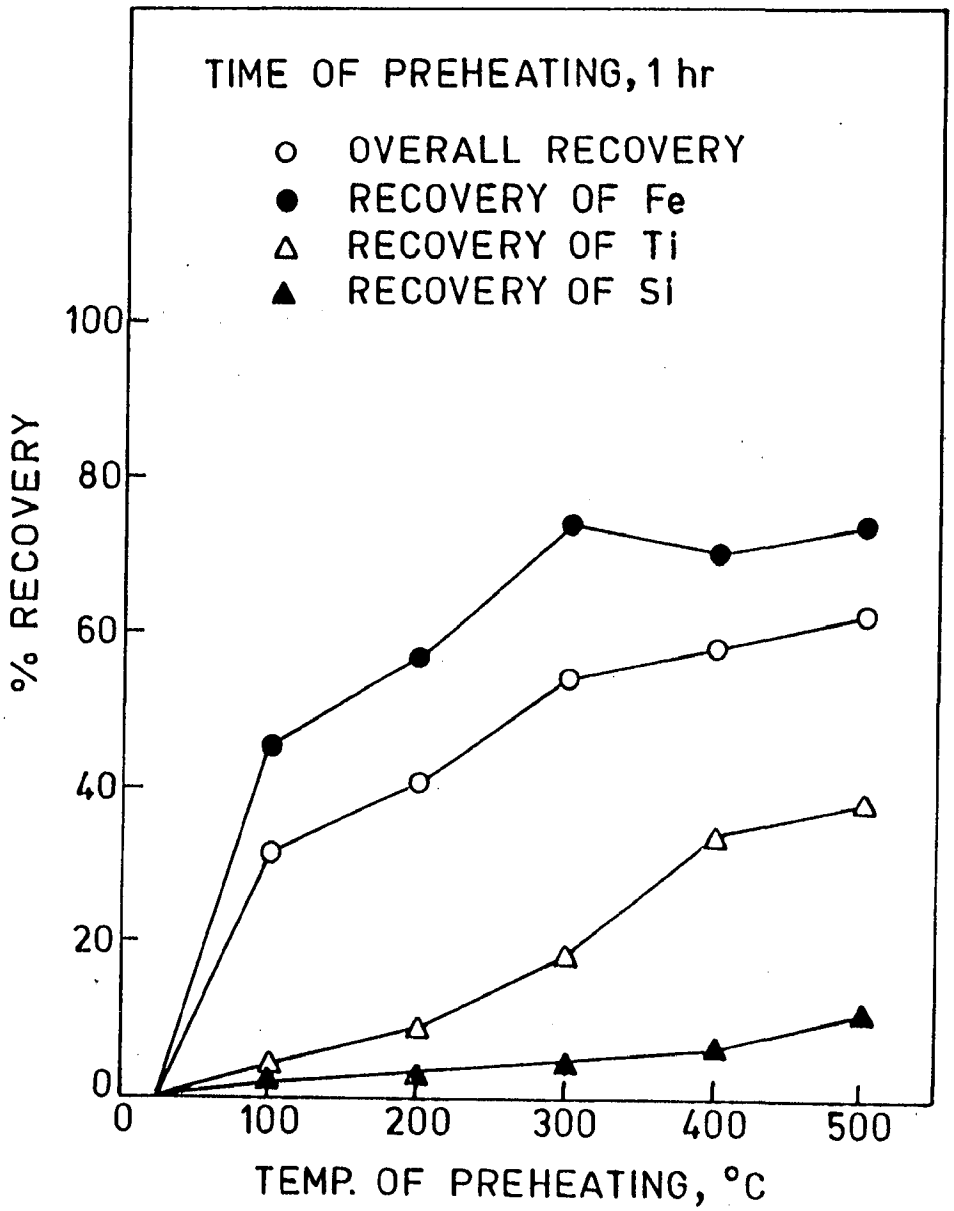

Fig.5.39 : Effect of preheating temperature on recovery values of the alloy (preheating time, 1 hr.).

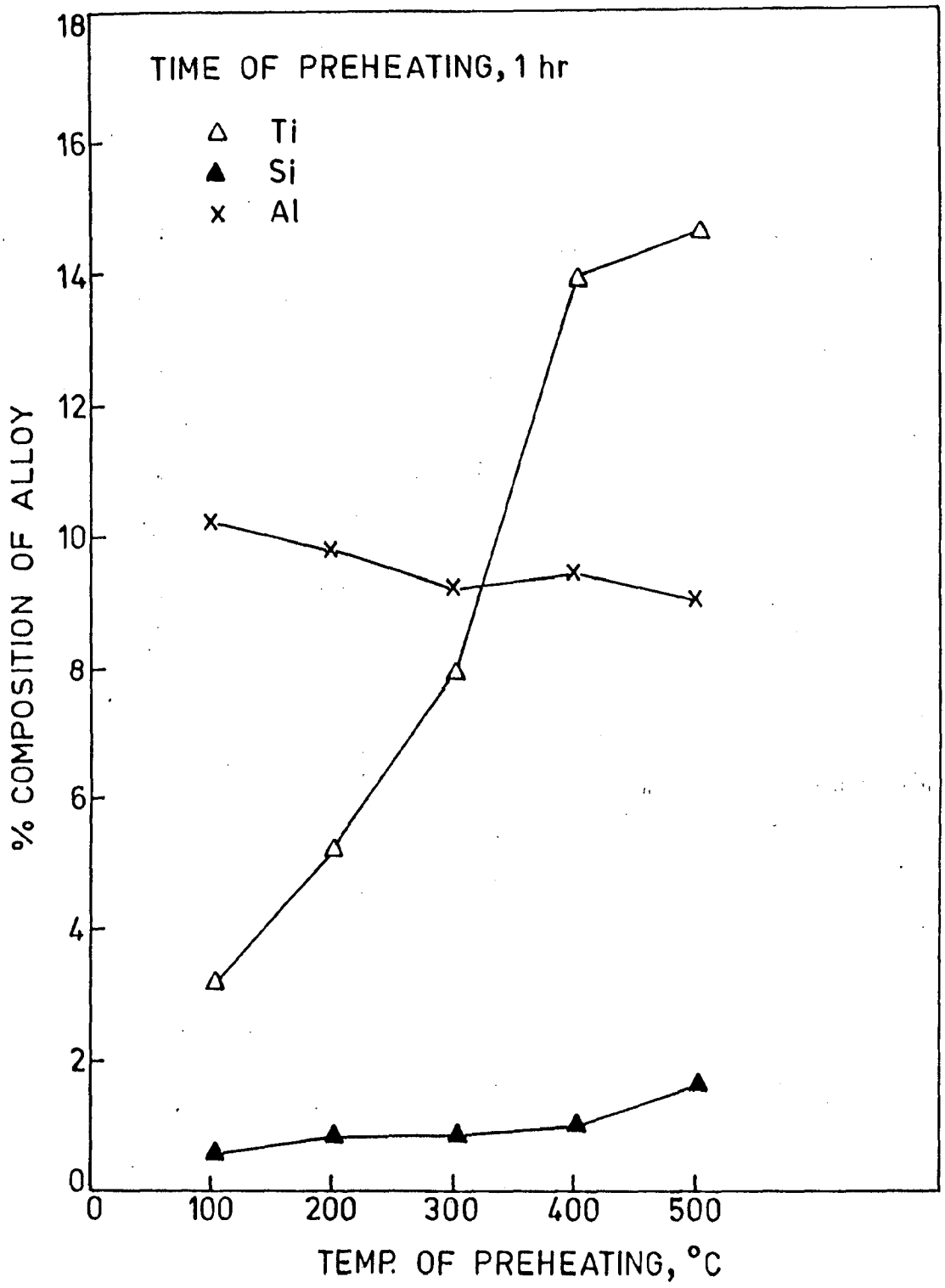

Fig.5.40 : Effect of preheating temperature on composition of the alloy (preheating time, 1 hr.).

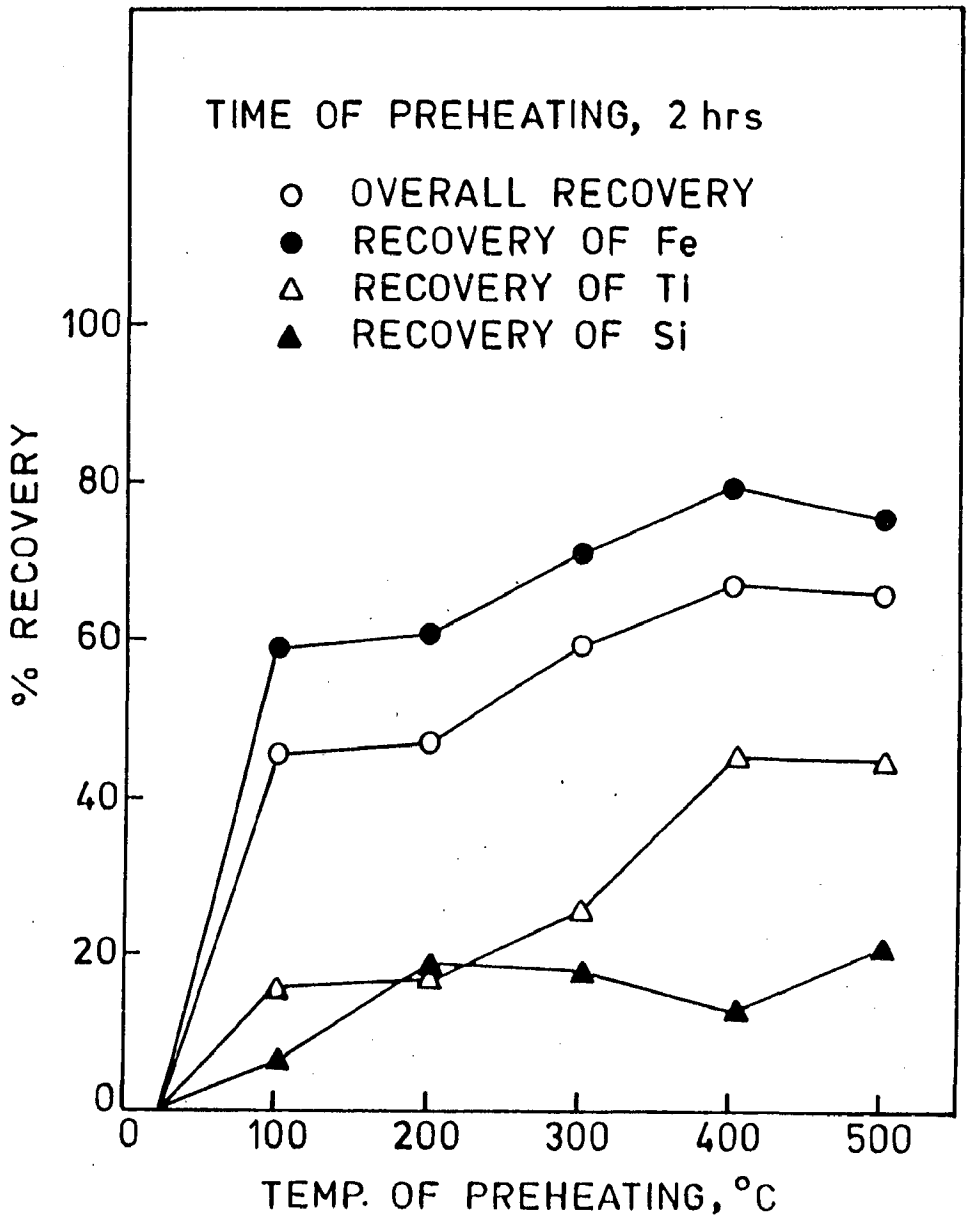

Fig.5.41 : Effect of preheating temperature on recovery values of the alloy (preheating time, 2 hr.).

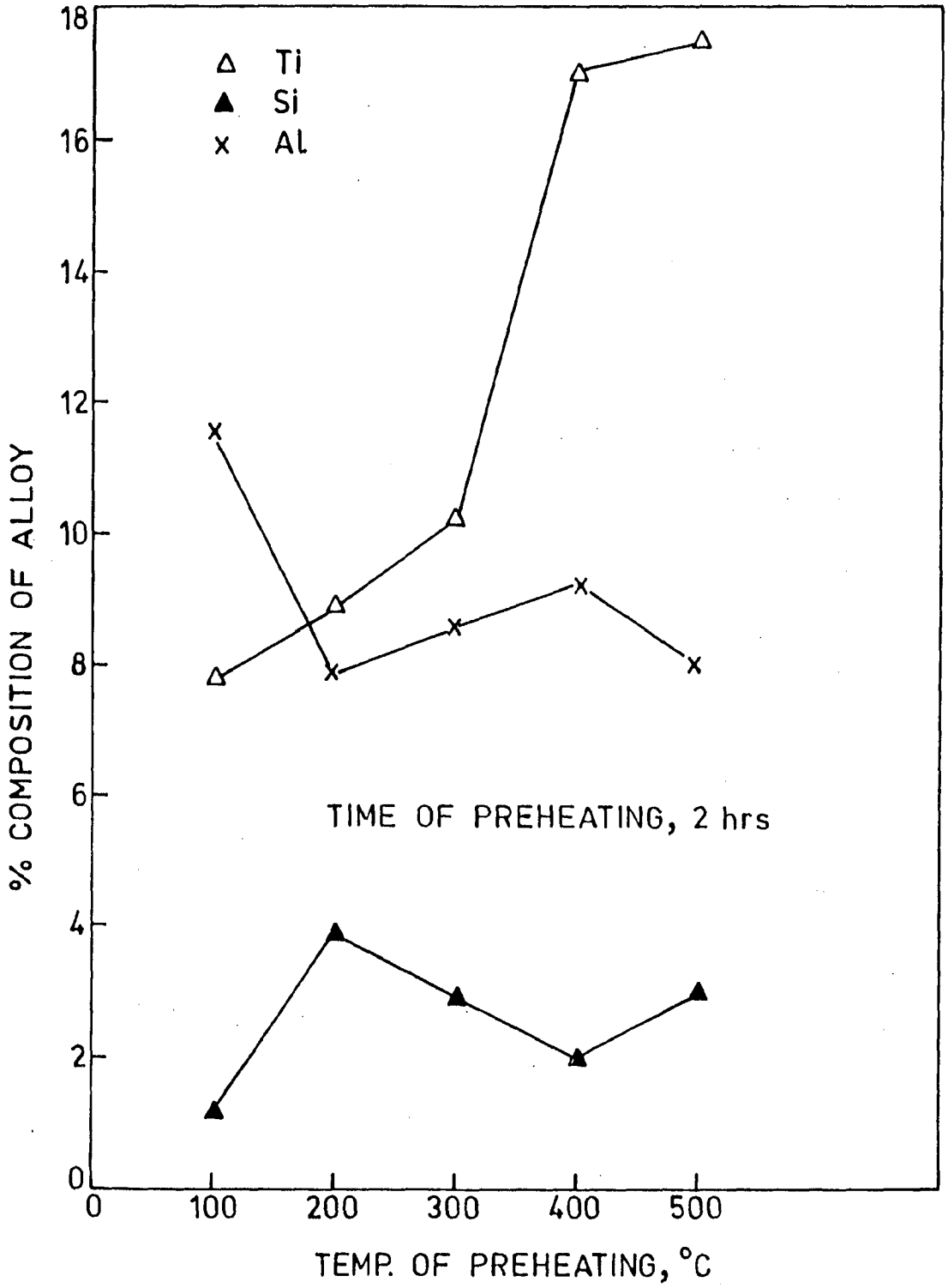

Fig. 5.42 : Effect of preheating temperature on composition of the alloy (preheating time, 2 hr.).

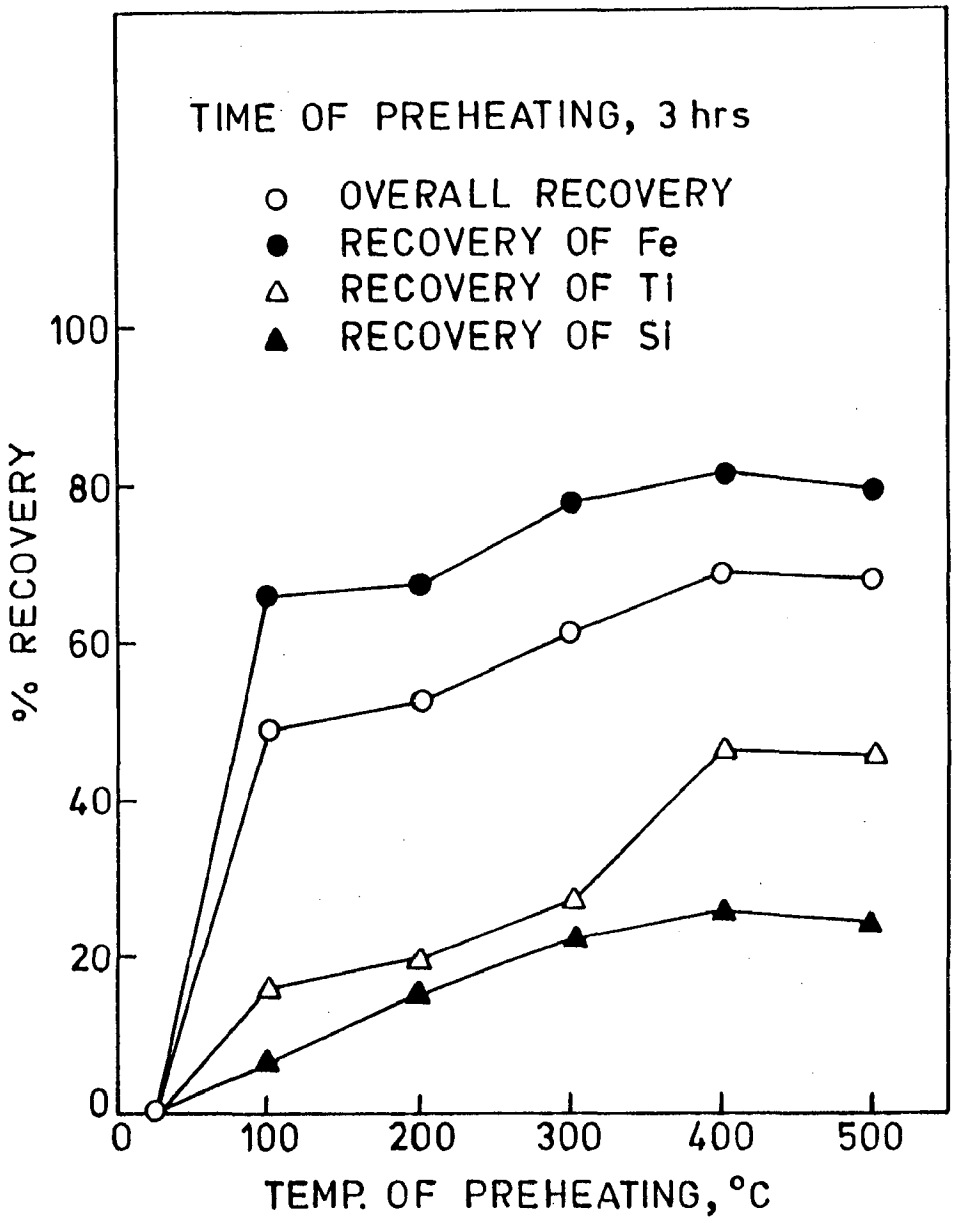

Fig.5.43 : Effect of preheating temperature on recovery values of the alloy (preheating time, 3 hr.).

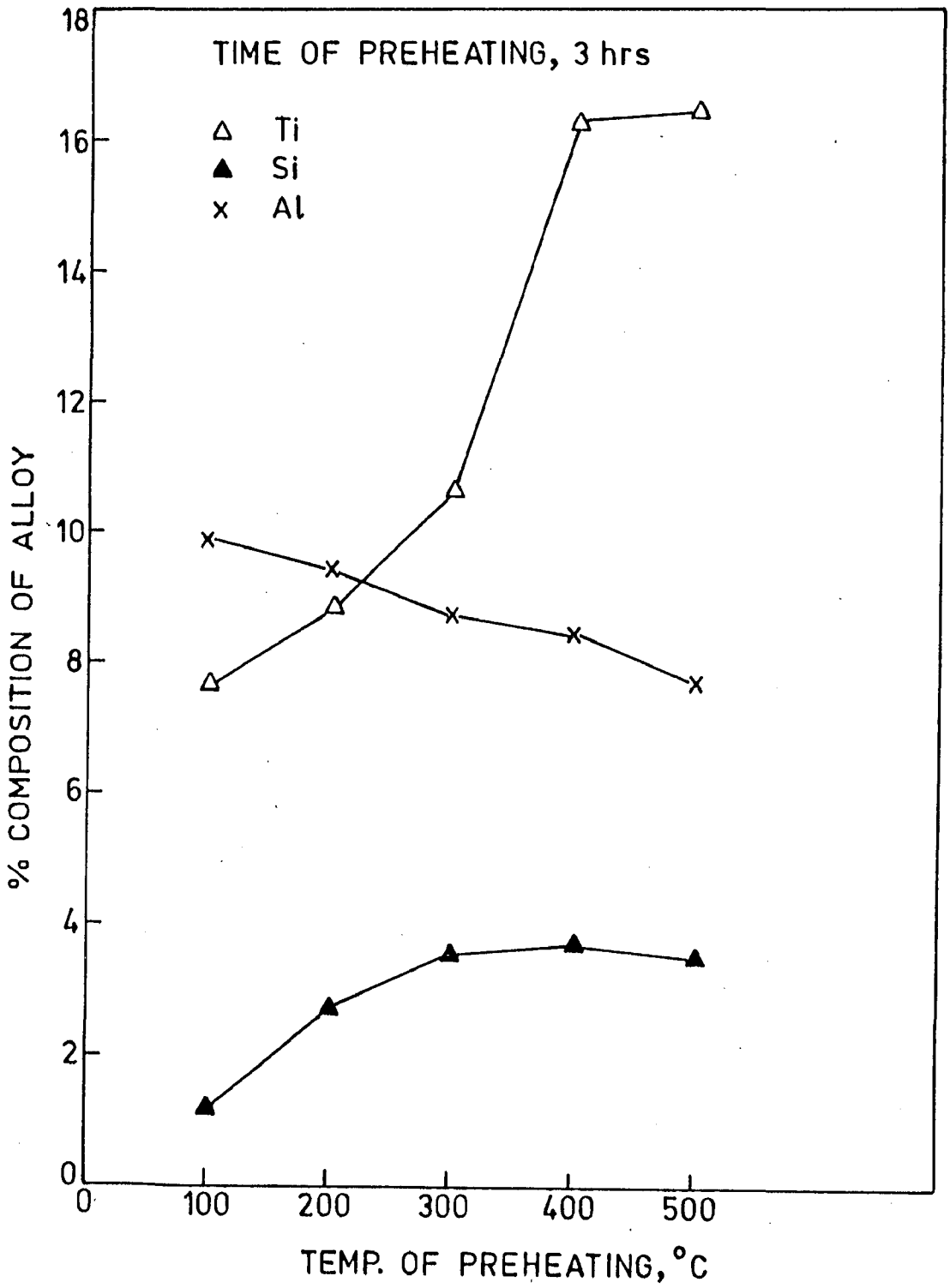

Fig.5.44 : Effect of preheating temperature on composition of the alloy (preheating time, 3 hr.).